

**Accelerating Polymer Degradation to Explore Potential Long Term Geotechnical  
Behaviour of Oil Sands Fine Tailings**

by

Kelsey Alissa Stienwand

A thesis submitted in partial fulfillment of the requirements for the degree of

Master of Science

in

Geoenvironmental Engineering

Department of Civil and Environmental Engineering  
University of Alberta

© Kelsey Alissa Stienwand, 2021

## Abstract

Many tailings' technologies used in the Athabasca oil sands require the use of chemical amendments such as synthetic flocculants to densify tailings by releasing water. It is anticipated that the synthetic flocculants will eventually degrade with time leaving only a mineral soil structure behind. The geotechnical properties following potential degradation of the amendments are unknown. This research provided the opportunity to further understand the long-term strength behavior of polymer amended tailings deposits. Specific objectives included: evaluation of potential polymer degradation methods to accelerate degradation of chemical amendments, compare impact of thermal polymer degradation on geotechnical behaviour on control samples, compare impact of polymer degradation on geotechnical behaviour on various chemically amended samples and finally to compare impact of polymer degradation on the geotechnical behaviour of various percent solids/ void ratios to reflect an in-situ tailings deposit.

Two degradation pathways were investigated: chemical/thermal degradation and biological degradation. The clay slurries and tailings samples used in the research were kaolinite, fluid fine tailings, flocculated fluid fine tailings, and centrifuge cake. Various techniques were employed to compare the impact of degradation, which included oscillatory rheometry, vane shear, and SEM imaging. Kaolinite and fluid fine tailings were used as control samples to determine if the thermal degradation pathway was altering the mineral structure of the polymer amended samples. Additionally, large strain consolidation (LSC) was utilized to consolidate centrifuge cake samples to simulate various void ratios that occur in in-situ tailings deposits.

In the control samples for the thermal degradation, the results showed changes to the rheological measurements and no changes to structure in the SEM images. Changes occurred from the heat treatment process; however, it is difficult to determine whether it was a result of the change in

percent solids that occurred during the heat treatment process or if the process was altering the mineral structure of the clay / tailings sample. The second polymer degradation method used was bacterial degradation. This pathway was explored using a commercially available bacterium. It is sold under the name 'Frac-Bac' and was provided for this research by Re-Nuu Production Optimization Inc. The results suggest impacts to the long-term strength behaviour of polymer amended tailings, however, many of these changes to the measured parameters were low to moderate in magnitude (average 20% decrease). When comparing the two polymer degradation methodologies, less error was introduced in the bacteria treated samples and consistent negative impacts were seen in all parameters.

The results suggest negative impacts to the long-term strength behaviour of polymer amended tailings; however, many of these changes were low to moderate in magnitude (average 30% change). Errors introduced from the limitations of the heat treatment process (change in percent solids) are known to have large effects on the measured shear strength in oil sands tailings and were difficult to control in the experiment. It appears that a change in structure occurred from the heat treatment process, however it is difficult to quantify whether it was a result of the change to percent solids or from degradation of the polymer itself. The results from the bacteria treated samples showed consistent negative impacts seen in all parameters.

Some suggestions for improving future work are additional research on the bacterial treatment process as the pathway showed consistent negative impacts to the samples and introduced fewer errors, quantifying error in the oscillatory rheology for each tailing sample, and improvements to the heat treatment process to ensure that moisture content / percent solids of the samples stay within defined parameters.

This research provided the opportunity to further understand the long-term strength behavior of polymer amended tailings deposits which found degradation of flocculants could have some negative impacts.

## Acknowledgements

I will be forever grateful to all the individuals at the University of Alberta that have supported and guided me throughout my program. Firstly, this project would not have been possible without the guidance or financial support of my supervisor, Dr. Nicholas Beier. I will cherish his enthusiasm for teaching and learning in my future endeavors.

I would also like to thank the staff at the Geotechnical Centre Laboratory. Mrs. Christine Hereygers for all her help and technical guidance – I would not have been able to setup the research without your innovative and out-of-the-box ideas. Dr. Louis Kabwe and Lucas Duerksen were also instrumental in helping me setup and troubleshoot the laboratory components of my research project. The staff of the UAlberta Geotechnical Centre, Mrs. Vivian Giang, Mrs. Sally Petaske, and Mrs. Jennifer Stogowski provided continuous support, and made a friendly and comfortable environment for all the graduate students. Without you, no one's research would be possible.

The Institute for Oil Sands Innovation (IOSI) Laboratory allowed me to use their equipment and a large portion of my research would not have been possible without the technical advice and support of Mrs. Lisa Brandt.

I would also to thank the Natural Sciences and Engineering Research Council of Canada (NSERC), Alberta Innovates Technology Futures (AITF), Canada's Oil Sands Innovation Alliance (COSIA), and the University of Alberta for financial support, which made this research possible.

I am extremely grateful for the wonderful friends and colleagues that I made during this program. I also need to thank the ladies of geotech, Rima, Haley, and Ahlam, that continue to amaze me with their intelligence, passion for the discipline and dedication to supporting women in STEM.

To my friends Jenna and Hilary, thank you. You have always been there to listen to my frustrations, setbacks, and the struggles of research. They were always there to provide a listening ear and encouragement to keep going.

I would not have made it this far without the love of my parents, Sharon and Lloyd. They have always been my biggest supporters and have believed in me even when I did not believe in myself. Thank you to my brother, sisters-in-law, and brothers-in-law for your love and support.

Thank you to my animals Brassy and Jax for their unconditional love. Finally, I need to thank my husband, Jesse. Thank you for supporting me, loving me, celebrating the small wins, and always encouraging me to pursue my dreams. Together we can conquer anything.

# Table of Contents

Abstract.....	ii
Acknowledgements.....	v
1 Introduction.....	1
1.1 Statement of the Problem.....	1
1.2 Objectives of Research.....	2
1.3 Organization of Thesis.....	3
2 Literature Review.....	4
2.1 Overview of the Oil Sands.....	4
2.1.1 Geological Background.....	4
2.1.2 Extraction Methods.....	5
2.2 Overview of Oil Sands Tailings.....	8
2.2.1 Oil Sands Tailings.....	8
2.2.2 Tailings Management.....	11
2.3 Chemically Amended Oil Sands Tailings.....	13
2.3.1 Diffuse Double Layer.....	14
2.3.2 Flocculation.....	17
2.3.3 Floc Characterization.....	19
2.3.4 Properties of Chemically Amended Tailings.....	20
2.3.5 Properties of Centrifuged Tailings.....	27
2.3.6 Effect of Shear on Flocculated Tailings.....	30
2.4 Polyacrylamide.....	33
2.4.1 PAM Degradation.....	37
2.5 Rheology in Tailings Management.....	41
2.5.1 Effect of Microstructure on Rheology.....	42
2.5.2 Shear Thinning and Thixotropy.....	44
3 Laboratory Methods.....	46
3.1 Materials Used in Laboratory Program.....	46
3.1.1 Flocculated Tailings Preparation.....	46
3.2 Tailings Characterization.....	49
3.3 Large Strain Consolidation Testing.....	50
3.3.1 LSC Setup and Sample Preparation.....	50
3.3.2 Criteria for End of Consolidation.....	53

3.3.3	Hydraulic Conductivity Measurement .....	53
3.4	Polymer Degradation Testing .....	54
3.4.1	Thermal Degradation Methodology .....	54
3.4.2	Bacterial Degradation Methodology .....	57
3.5	Rheology .....	58
3.5.1	Wall Depletion Effects .....	59
3.5.2	Flow Curve .....	60
3.5.3	Amplitude Sweep .....	61
3.6	Chemical Analysis .....	62
3.7	SEM Imaging .....	63
4	Experimental Results .....	65
4.1	Index Testing .....	65
4.2	Kaolin Results .....	68
4.2.1	Pore-water Chemistry .....	68
4.2.2	Rheology .....	69
4.2.3	SEM .....	71
4.3	Fluid Fine Tailings Results .....	73
4.3.1	Pore-water Chemistry .....	73
4.3.2	Rheology .....	73
4.4	Centrifuge Cake Results .....	75
4.4.1	Heat Treated Samples .....	75
4.4.2	Bacteria Treated Samples .....	77
4.5	Flocculated FFT Results .....	80
4.5.1	Heat Treated Samples .....	80
4.5.2	Bacteria Treated Samples .....	85
4.6	Consolidated Samples .....	89
4.6.1	Heat Treated Samples .....	90
5	Discussion .....	92
5.1	Pore Water Chemistry .....	92
5.1.1	Effect of Polymer Degradation on Pore Water Chemistry .....	92
5.2	Long Term Strength Behaviour .....	92
5.2.1	Effect of Heat Treatment on Strength Behaviour .....	94
5.2.2	Effect of Bacteria Treatment on Strength Behaviour .....	99



5.3	Microstructure.....	101
5.3.1	Effect of Heat Treatment on Microstructure.....	101
5.3.2	Effect of Bacterial Treatment on Microstructure.....	104
6	Conclusions and Recommendations.....	106
6.1	Conclusions.....	106
6.2	Recommendations.....	108
7	References.....	110
	Appendix A: Methods and Test Procedures.....	1
	Appendix B: Material Characterization Test Data.....	1
	Appendix C: Rheology Data.....	1
	Appendix D: Large Strain Consolidation Data.....	1

## List of Appendices

- Appendix A: Methods and Test Procedures
- Appendix B: Material Characterization Test Data
- Appendix C: Rheology Data
- Appendix D: Large Strain Consolidation Data

## List of Figures

Figure 1-1: Picture from Athabasca oil sands region.....	1
Figure 2-1: Oil Sands Project Areas .....	4
Figure 2-2: Geological formations (Source: TOTAL).....	5
Figure 2-3: Historical conveyor systems used at an oil sands mine.....	6
Figure 2-4: Schematic of Oil Sands Processing and Tailings Flow Diagram (Redrawn from Masliyah et al. 2004) .....	8
Figure 2-5: Shear strength versus solids content of oil sands fine tailings (Modified from McKenna et al. 2016) .....	10
Figure 2-6: Basic units of kaolinite.....	15
Figure 2-7: Distribution of cations and anions next to a clay particle .....	16
Figure 2-8: Backscattered environmental scanning electron of MFT for a magnification - 1000x, scale – 20 µm, view field - 150 µm (Mizani 2016).....	21
Figure 2-9: Backscattered environmental scanning electron of polymer amended MFT at a dose of 650 g/tonne for a magnification - 2000x, scale – 20 µm, view field - 75µm (Mizani 2016) .....	22
Figure 2-10: Compressibility of east pilot pond ILTT (Modified from Jeeravipoolvarn 2010) .....	24
Figure 2-11: Undrained shear strength of east pilot pond ILTT (Modified from Jeeravipoolvarn 2010) ..	24
Figure 2-12: Sensitivity of oil sands fine tailings (Modified from Beier et al. 2013).....	26
Figure 2-13: Centrifuge used at Albion's Jackpine Mine (Canada's Oil Sands Innovation Alliance 2021)	27
Figure 2-14: Void ratio versus effective stress of flocculated tailings (FTT) and flocculated centrifuged tailings (FCTC) (Modified from Kabwe et al. 2017).....	30
Figure 2-15: Shear strength versus effective stress of flocculated tailings (FTT) and flocculated centrifuged tailings (FCTC) (Modified from Kabwe et al. 2017).....	30
Figure 2-16: Comparison of Particle Size Distributions for ILTT (Jeeravipoolvarn 2010).....	32
Figure 2-17: Chemical structure of flocculants based on polyacrylamide. Clockwise from top left: anionic polyacrylamide (PAM), non-ionic PAM, and cationic PAM. ....	34
Figure 2-18: Viscosity versus shear rate for general polymers.....	35
Figure 2-19: SEM of A3338 Polymer (Mizani 2016).....	36
Figure 2-20: EOR980 acrylamide hydrolysis (modified from Andrews et al. 2016) .....	39
Figure 2-21: Polymer conformation that affect mechanical stability.....	40
Figure 2-22: Microstructures at rest and in flow (Modified from Chhabra and Richardsons 2008) .....	43
Figure 2-23: Agglomerate forms in kaolin suspensions (redrawn from Chhabra and Richardsons 2008) .	44
Figure 2-24: Illustration of thixotropic material (Modified from Mitchell and Soga 2005).....	45
Figure 3-1: Mixing apparatus.....	48
Figure 3-2: Tailings mixing .....	48
Figure 3-3: Flocculated tailings .....	48

Figure 3-4: Initial set up of the large strain consolidation test before loading sample .....	50
Figure 3-5: LSC cell 5 with dead loads acting on the piston .....	52
Figure 3-6: Schematic of cell 3 in loading frame and loaded up to 24 kPa .....	53
Figure 3-7: Schematic of heating bath .....	55
Figure 3-8: Time test on FFT .....	56
Figure 3-9: Qualitative - bacteria treated samples after 30 days of incubation at room temperature .....	58
Figure 3-10: Kinexus lab+ rheometer .....	59
Figure 3-11: Typical flow curves.....	61
Figure 3-12: Typical results of amplitude sweep tests.....	62
Figure 3-13: Pore water from heat treated sample, bacteria treated sample, and untreated FFT sample (L to R) .....	63
Figure 4-1: Grain Size Distribution .....	66
Figure 4-2: Bulk XRD analysis of centrifuged tailings .....	67
Figure 4-3: Bulk XRD analysis of FFT .....	68
Figure 4-4: Flow curve for lower %S kaolinite .....	69
Figure 4-5: Flow curve for higher %S kaolinite .....	70
Figure 4-6: Elastic shear modulus versus shear stress for kaolinite.....	71
Figure 4-7: Scanning electron microscopy of kaolinite before and after heat treatment .....	72
Figure 4-8: Flow curve for fluid fine tailings .....	74
Figure 4-9: Elastic modulus versus shear stress for fluid fine tailings.....	75
Figure 4-10: Flow curve for centrifuged tailings .....	76
Figure 4-11: Elastic modulus versus shear stress for centrifuged tailings .....	77
Figure 4-12: Shear rate ramp for bacteria treated centrifuged tailings .....	79
Figure 4-13: Elastic shear modulus versus shear stress for centrifuged tailings.....	80
Figure 4-14: Flow curve for heat treated flocculated tailings .....	82
Figure 4-15: Elastic modulus versus shear stress for heat treated flocculated tailings .....	83
Figure 4-16: Scanning electron microscopy of higher %S flocculated FFT before and after heat treatment .....	84
Figure 4-17: Shear rate ramp for bacteria treated flocculated tailings.....	86
Figure 4-18: Elastic modulus versus shear stress for bacteria treated flocculated tailings .....	87
Figure 4-19: Scanning electron microscopy of higher %S flocculated FFT before and after bacteria treatment .....	89
Figure 4-20: Compressibility curve for centrifuge cake .....	90
Figure 5-1: Annotated SEM of kaolinite at 20,000x magnification.....	102
Figure 5-2: Annotated SEM image of flocculated FFT before and after hear treatment at 20,000x magnification .....	103
Figure 5-3: Annotated SEM image of flocculated FFT before and after bacteria treatment at 20,000x magnification .....	105

## List of Tables

Table 2-1: Oil Sands Tailings Deposits (Fair and Beier 2012).....	13
Table 2-2: Classification of clay sensitivity values (Rosenqvist 1953).....	25
Table 2-3: Sensitivity data sets .....	26
Table 3-1: Moisture content results from time tests.....	57
Table 3-2: Shear rate ramp input parameters .....	61
Table 4-1: Geotechnical properties of materials used in the study .....	65
Table 4-2: MBI results for centrifuge cake and FFT .....	66
Table 4-3: pH and percent solids result for heat treated kaolinite .....	69
Table 4-4: Yield point, shear strength, $G'$ and $G''$ of kaolinite samples .....	70
Table 4-5: pH and percent solids result for FFT .....	73
Table 4-6: Yield point, shear strength, $G'$ and $G''$ of FFT samples .....	74
Table 4-7: pH and percent solids result for heat treated centrifuge cake.....	75
Table 4-8: Yield point, shear strength, $G'$ and $G''$ of heat-treated centrifuged tailings .....	77
Table 4-9: pH and percent solids result for bacteria treated centrifuge cake .....	78
Table 4-10: Yield point, shear strength, $G'$ and $G''$ of bacteria treated centrifuged tailings .....	79
Table 4-11: pH and percent solids results for heat treated flocculated tailings .....	81
Table 4-12: Yield point, shear strength, $G'$ and $G''$ of flocculated FFT samples .....	82
Table 4-13:pH and percent solids results for bacteria treated flocculated tailings .....	85
Table 4-14: Yield point, shear strength, $G'$ and $G''$ of flocculated FFT samples .....	87
Table 4-15: LSC Void Ratio Data.....	89
Table 4-16: pH and percent solids results for heat treated consolidated samples.....	90

# 1 Introduction

## 1.1 Statement of the Problem

Alberta's oil sands have the third largest reserve of oil in the world, after Venezuela and Saudi Arabia. The proven deposits contain approximately 26.3 billion cubic meters (165.4 billion barrels) of initial in-place reserves of crude bitumen (AER 2016). They underlie roughly 142,200 square kilometers (km) of land in the Athabasca, Cold Lake and Peace River regions on northern Alberta (Alberta Energy 2020).



*Figure 1-1: Picture from Athabasca oil sands region*

To produce oil, reserves are either extracted by surface mining or in-situ technologies. Mined oil sands are processed using large volumes of water and chemicals. This processing results in a slurry waste, which is managed using tailings impoundments.

The tailings slurry is composed of process-affected water, sand, fines, and a small amount of residual bitumen. The coarse solids settle rapidly and form a beach, and the remaining mineral solids accumulate in the pond. Over a few years, fine tails settle to approximately 30 wt% solids and were formerly referred to as mature fine tailing (MFT). The MFT will remain in a fluid state for decades because of its extremely slow consolidation rate (Chalaturnyk et al. 2002). Tailings streams that behave as fluids are collectively referred to as fluid fine tailings (FFT) (CTMC 2012). As of 2019 there was approximately 1,302.9 million cubic meters of fluid tailing (AER 2020). The FFT is considered non-trafficable with minimal shear strength, in the order of Pascals (Sorta et al. 2012). To reclaim the land, the tailings must show significant increases in strength or be sufficiently dewatered to develop enough shear strength to support equipment and reclamation activities (McKenna et al. 2016). One commonly used method is the addition of chemical amendments, which may improve the geotechnical properties of the tailings. These chemical amendments may include synthetic flocculants such as polyacrylamides (PAM). It is anticipated that the synthetic flocculants will eventually degrade with time leaving only a mineral soil structure behind (Sorbie 1991a). The geotechnical properties following potential degradation of the amendments is unknown. This research provides the opportunity to further understand the long-term strength behavior of amended tailings deposits.

## 1.2 Objectives of Research

Chemical amendments can enhance the undrained shear strength ( $S_u$ ) of flocculated FFT without a significant decrease in water content (Beier et al. 2013, Reid and Fourie 2016). This has led to their increased use in the industry; however, their use may present some long-term geotechnical challenges. It is anticipated that the synthetic flocculants will eventually degrade with time leaving only a mineral soil structure behind (Sorbie 1991b, Swiecinski et al. 2016). Meaning that there will be no bonding due to polymer flocculent. The overall objective of this research was to determine the influence of chemical amendments on the long-term geotechnical behaviour on oil sands tailings. Specific objectives include:

- Evaluation of potential polymer degradation methods to accelerate degradation of chemical amendments.
- Compare impact of thermal polymer degradation on geotechnical behaviour on control samples.

- Compare impact of polymer degradation on geotechnical behaviour on various chemically amended samples.

The research included a laboratory testing program where, using a variety of methods, samples were cured to degrade the flocculant. These cured samples provide a conservative representation of tailings that have undergone some level of degradation of the flocculants. The tailings sample was fully characterized before and after the polymer degradation process to assess any changes in the geotechnical behavior. Microstructure of the tailings before and after thermal or bacterial treatment was also assessed.

This research provides the opportunity to further understand the long-term strength behavior of amended tailings deposits. Current correlations of strength with material characteristics like clay to solids content or void ratio may not account for changes in strength with time. Understanding the transient nature of the deposit strength is required in the design of the capping and reclamation.

### 1.3 Organization of Thesis

Chapter 1 provides an overview of the problem statement, objective, and scope of this research.

Chapter 2 summarizes a review of literature related to this thesis. A general overview of the Athabasca Oil Sands region and oil sands tailings is provided. Following this, typical properties of tailings used in this research and the processes used to create them, including the diffuse double layer and flocculation are discussed in detail. Consideration is given to polyacrylamide (PAM) flocculants and what we currently know about PAM degradation in chemically amended tailings. Finally, rheology, a metric commonly used in this research is discussed.

Chapter 3 presents the methodology for the laboratory testing program. The methods used in the laboratory program are outlined and why they were selected for this research.

Results of the laboratory program and an interpretation of the results are presented in Chapter 4. The discussion and significance of the results are included in Chapter 5. Finally, the conclusion and recommendations are presented in Chapter 6.

## 2 Literature Review

### 2.1 Overview of the Oil Sands

#### 2.1.1 Geological Background

Alberta's oil sands have the third largest reserve of oil in the world, after Venezuela and Saudi Arabia. They underlie roughly 142,200 square kilometers (km) of land in the Athabasca, Cold Lake and Peace River regions on northern Alberta. These regions can be seen in Figure 2-1. With current technologies, mining is only feasible in about 3.4 percent of the total area as the accessible ore is located 50 to 200 meters from the surface (Natural Resources Canada 2013).

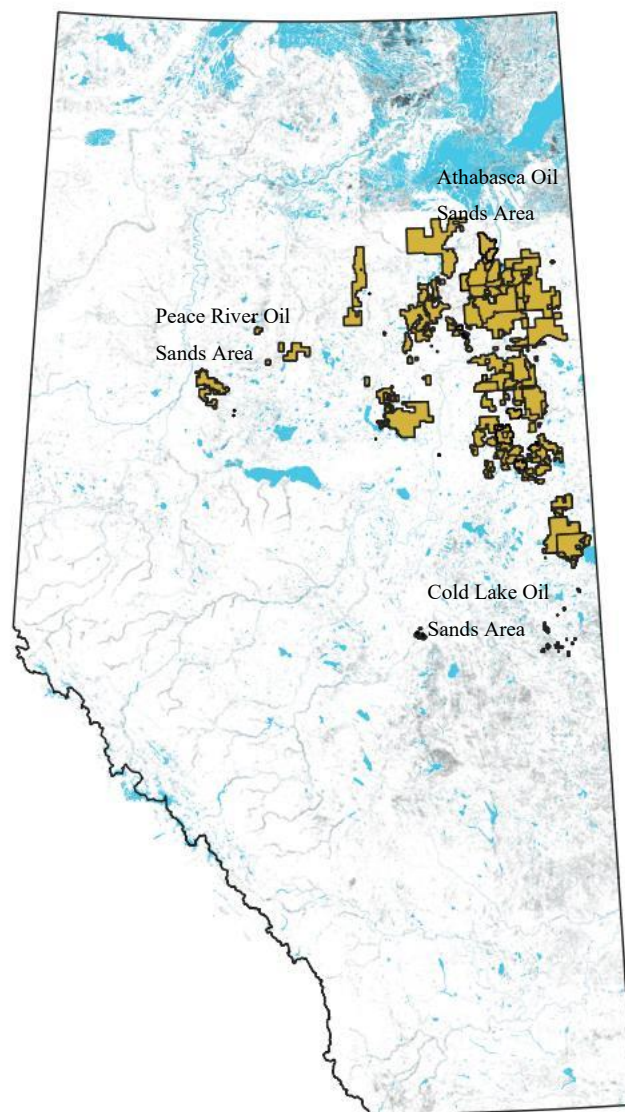


Figure 2-1: Oil Sands Project Areas



The origin of the oil sands remains largely undecided; however, many scientists believe that they were formed in the same way as other fossil fuels – organic matter died and was covered by layers of sediment that exerted sufficient pressures and temperatures to transform the matter into petroleum (Alberta Culture and Tourism 2018). As the Earth shifted, the oil migrated north where it became trapped in the quartz sand left behind from ancient rivers and seas.

The McMurray formation is a continuum of sedimentary environments. The lower section is fluvial deposits, with estuarine in the middle, and marine shoreface near the top. This leads to the informal use of the lower, middle and upper McMurray units (Gingras and Rokosh 2004, Broughton 2013). The formation varies from 45 to 60 m in thickness; however, data has shown a great amount of variation (Mellon et al. 1956). The oil sands deposits exist within the Lower Cretaceous McMurray Formation as seen in Figure 2-2.

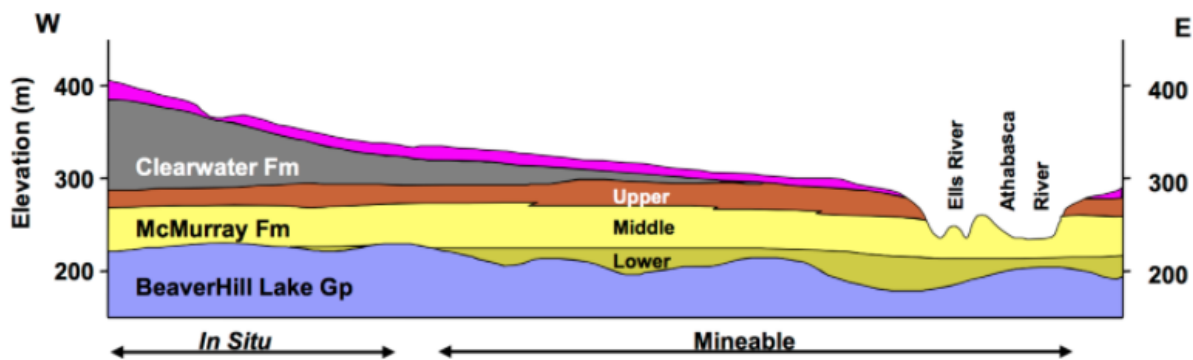


Figure 2-2: Geological formations (Source: TOTAL)

The oil sand ore is a mixture of 1 – 19 weight percent (wt%) bitumen, 84 – 86 wt% sand, silt and clay, and 3 – 6 wt% water (Chalaturnyk et al. 2002). The sand fraction consists almost entirely of quartz with small amounts of feldspar grains, mica flakes and clay minerals. The clay mineral composition of the clay size fraction consists of 0 – 7 wt% chlorite, 8 – 19 wt% kaolinite-smectite, 15 – 34 wt% kaolinite, 25 – 54 wt% illite-smectite, and 13 – 26 wt% illite (Kaminsky 2008).

### 2.1.2 Extraction Methods

Depending on the overburden depth, there are two main methods to recover the oil. Open pit mining is used for shallow resources, and steam assisted gravity drainage (SAGD) is used for resources more than 130 m deep (Natural Resources Canada 2013).

Surface mining begins by clearing the land and removing overburden, which is stored for later use in reclamation (Hartman and Mutmanský 2002). Following clearing, the ore is extracted from the ground using shovels and trucks (Birn and Khanna 2010). Historically, a bucketwheel, dragline, and conveyor system were used to extract the ore and transport it to be refined. One of the conveyor systems on display at Giants of Mining north of Fort McMurray is pictured in Figure 2-3. This system of removal was completely phased out by 2006 because the equipment was costly to maintain and difficult to move (Oil Sands Discovery Centre 2010). Today, hydraulic shovels dig into the oil sand ore and place it into heavy hauler trucks that range in size from 240 tons to 400 tons (Oil Sands Discovery Centre 2010). Shovels have the benefit of moving more easily to select the best quality ore. They also require less maintenance than equipment used previously. Trucks transport the oil sands from the pit face to the sizer or crusher, which breaks up large pieces of oil sand.



*Figure 2-3: Historical conveyor systems used at an oil sands mine.*

The ore is then crushed, and hot water is added so the ore can be pumped to the extraction plant (Birn and Khanna 2010, Masliyah et al. 2013). This process is typically referred to as conditioning. Hydro transport pipelines are used to transport the mixture to the extraction facilities. This step starts the separation of bitumen from the oil sand by breaking bonds between

the bitumen, water and sand. Once at the extraction plant, the bitumen is removed using a variation of the Clark Hot Water Extraction Process (CHWE). The CHWE process was patented in 1928 and was named after the creator, Dr. Karl Clark of the Alberta Research Council. During separation, additional hot water and sodium hydroxide (NaOH) is added to the slurry of sand, clay, bitumen and water in a large separation vessel (Chalaturnyk et al. 2002). Within the separation vessel, the mixture separates into three layers. The bitumen froth rises to the top, mineral sediments settle to the bottom, and a combination of bitumen, sand, clay, and water sits in the middle. The sand and water mixture are pumped from the bottom of the vessel into settling basins referred to as tailings ponds (Masliyah et al. 2004). The middle layer, referred to as middlings, are sent to secondary separation. In this process, air is injected into the slurry in floatation tanks. The injection of air encourages the creation of additional froth which is sent to froth treatment. The froth which normally contains 60% bitumen, 30% water, and 10% solids, is removed and further refined in this stage (Masliyah et al. 2004). The bitumen is diluted with naphtha to make it flow easily and then sent through a series of inclined plate settlers and centrifuges. The resulting bitumen has less than 5% water and only a small number of solids (0.5%). The tailings from froth treatment have trace amounts of solvent which is recovered in a stream-stripping column called a naphtha recovery unit (NRU). Once the tailings have passed through the NRU, they are discharged to tailings ponds. Typical commercial operations recover between 88 – 98% of the bitumen (Masliyah et al. 2004).

Each of the tailing's streams and management processes are discussed in further detail in Section 2.2.2. A schematic of the basic process is seen in Figure 2-4. Figure 2-4 was redrawn from (Masliyah et al. 2004) with data provided from Dr. Robert Tipman (Shell Canada Ltd.).

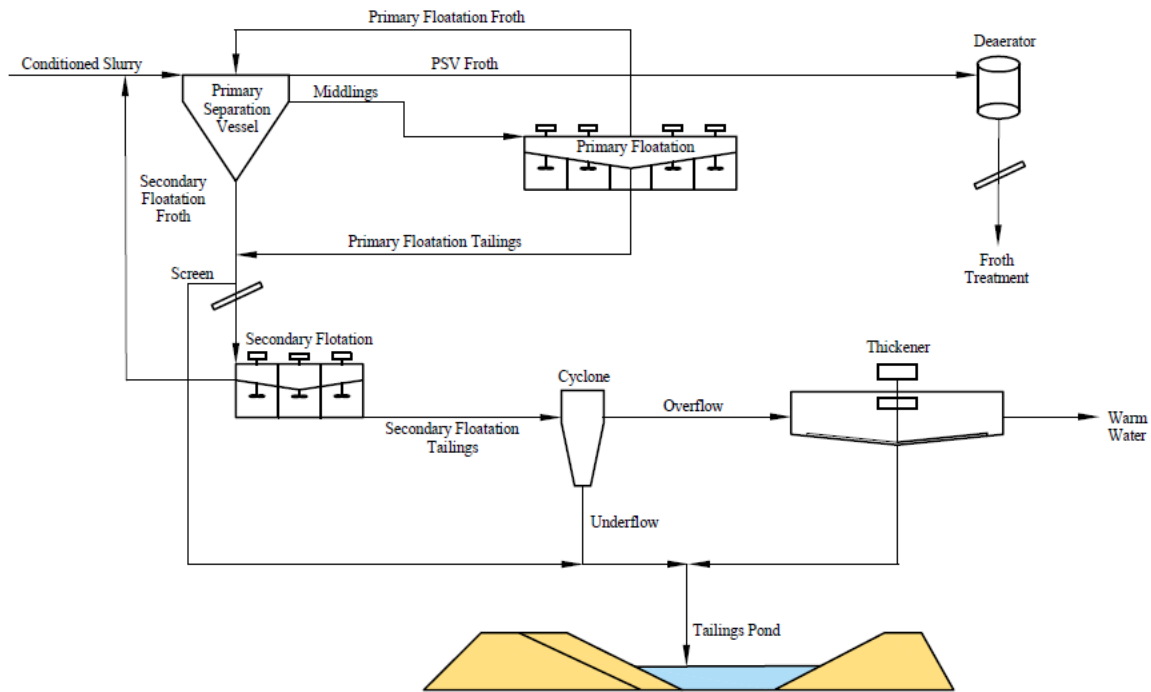


Figure 2-4: Schematic of Oil Sands Processing and Tailings Flow Diagram (Redrawn from Masliyah et al. 2004)

## 2.2 Overview of Oil Sands Tailings

### 2.2.1 Oil Sands Tailings

Tailings from the oil sands extraction process consist of water, sand, silt, clay, process chemicals, and small amounts of residual bitumen. The chemical composition of oil sands tailings is influenced greatly by the mineralogy and age of the oil sands ore, extraction techniques, and the types of additives used during bitumen processing (Small et al. 2015). Large volumes of tailings are produced when bitumen is extracted from the mined oil sands. The total volume of FFT reported by the mine operators in 2019 was 1270 Mm<sup>3</sup> (AER 2020).

Three main tailings streams exist in the surface mined oil sands: (1) coarse sand tailings (CST), (2) fluid fine tailings (FFT), and (3) froth-treatment tailings (Kasperski and Mikula 2011). Each stream is an aqueous slurry and vary in proportion of water, minerals, process chemicals, and residual bitumen. The Primary Separation Vessels in the extraction plant produce a tailings stream referred to as whole tailings (WT) (CTMC 2012). When whole tailings streams are sent to a hydrocyclone, two tailings' streams are created. Coarse tailings are separated as the underflow

and fines dominated tailings are collected from the overflow. The coarse tailing stream is largely composed of sand with a particle size greater than 44  $\mu\text{m}$  (Kasperski and Mikula 2011). The solids portion of fine tailings have an average particle size less than 44  $\mu\text{m}$ .

Once processed, WT or fine tailings streams are deposited in either man-made tailings ponds or in mined-out areas once mining has advanced. The coarse solids settle rapidly and form a beach, and the remaining fine fractions accumulate in the pond. Over a few years, fine tails settle to approximately 30 wt% solids and were historically referred to as mature fine tailings (MFT). MFT has a low sand to fines ratio (SFR) ( $<0.3$ ) and a nominal solids content greater than 30% and will remain in a fluid state for decades because of its extremely slow consolidation rate (Chalaturnyk et al. 2002). Tailings streams that behave as fluids are collectively referred to as fluid fine tailings (FFT) (OSTC and COSIA 2012, CTMC 2012). OSTC (2012) defines FFT as a liquid suspension of oil sands fines in water with a solids content greater than 2% but less than the solids content corresponding to the Liquid Limit.

As the tailings settle, water is released and rises to the surface of the pond. Oil sands tailings pond recycle water (RCW), is a very complex mixture of suspended solids, salts, inorganic compounds, organic compounds, and trace metals generated after the extraction of bitumen from the sands (Loganathan et al. 2015). All oil sands mines operate under a no-water release policy, meaning that companies must store RCW in tailing ponds to avoid its release into the receiving environment (Hwang et al. 2013).

Once the tailings reach a solids content of approximately 30 wt%, consolidation proceeds very slowly. To address the issue of growing volumes of FFT, the Energy Resources Conservation Board (ERCB) enacted Directive 074. The directive specified performance-based criteria to reduce fluid tailings and the formation of trafficable deposits. The directive had 3 specific targets: (1) at least 50% of the fines in the deposit were to be captured in dedicated disposal areas (DDAs); (2) within one year of being deposited, the DDA must have a undrained shear strength of 5 kPa; and (3) the DDA must be ready for reclamation within 5 years after active deposition stopped – the deposit had to meet strength, stability and structure necessary to establish trafficable surface, with a minimum shear strength of 10 kPa (AER 2009). In response to Directive 074, many methods have been researched and employed to dewater tailings and increase the undrained shear strength – with flocculation-based technologies being one. Figure

2-5 shows the typical shear strengths of oil sands fine tailings as a function of solids content. Shear strength and solids content/density are high correlated – typically as density increases, so too does shear strength. There is, however, a large amount of spread as a result of variability in the tailings deposits. In order to meet the requirements of Directive 074, oil sands fine tailings need to be dewatered to solids contents greater than 60%.

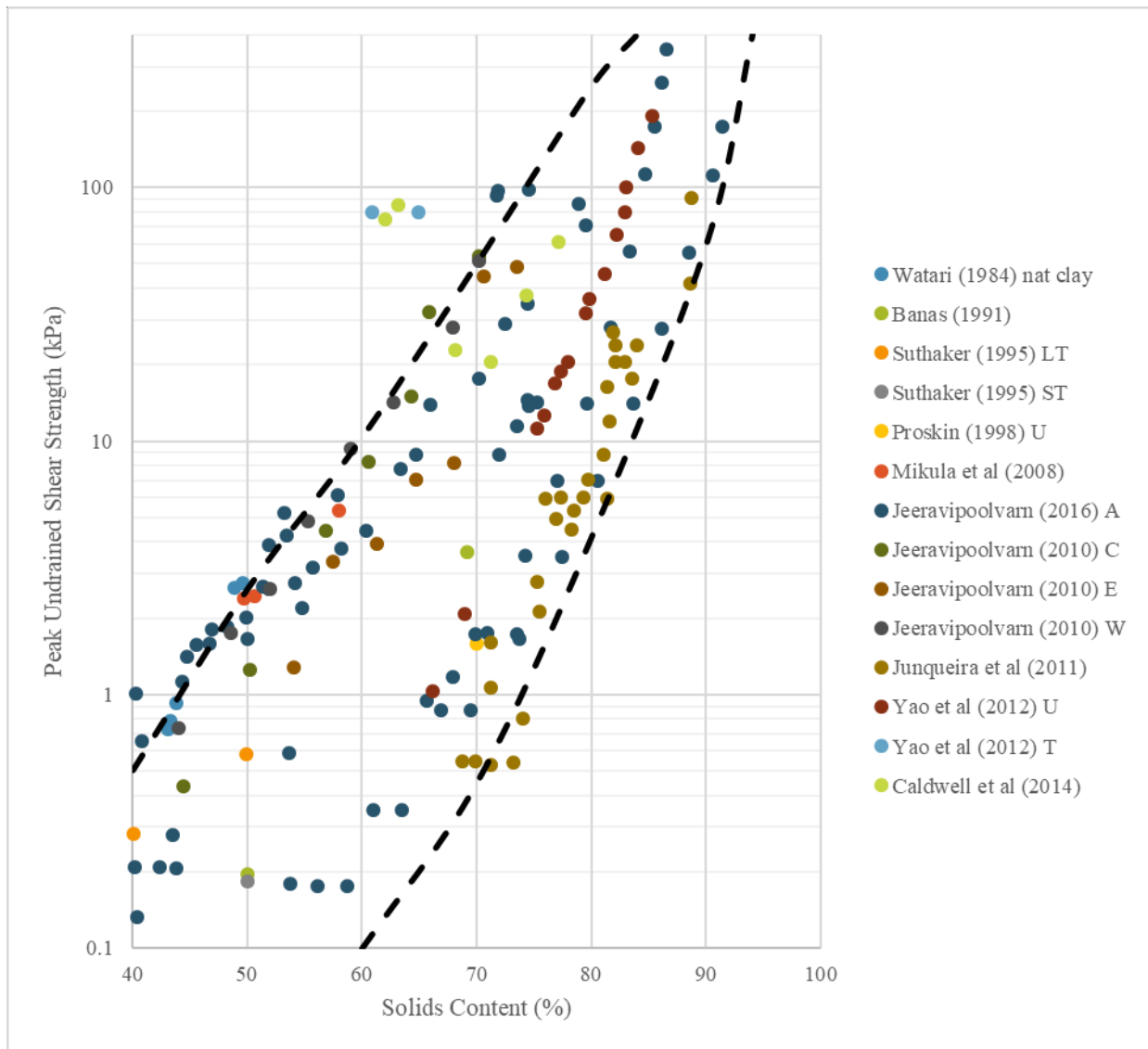


Figure 2-5: Shear strength versus solids content of oil sands fine tailings (Modified from McKenna et al. 2016)

In an effort to further improve management of tailings in the oil sands, AER suspended Directive 074 in March 2015 and replaced it with Directive 085. The directive aligns with the Lower Athabasca Regional Plan (LARP) and enabled the implementation of the Tailings Management

Framework for the Mineable Athabasca Oil Sands (TMF) (Government of Alberta 2015). The objective of the TMF is to minimize the accumulation of fluid tailings by ensuring that they are treated and reclaimed progressively during the life of a project and that all fluid tailings associated with a project are ready to reclaim (RTR) ten years after the end of mine life of that project.

### 2.2.2 Tailings Management

On March 1, 2012, representatives from developers of Canada's oil sands signed the COSIA charter. Canada's Oil Sands Innovation Alliance (COSIA) was created to "enable responsible and sustainable growth of Canada's Oil Sands while delivering accelerated improvement in environmental performance through collaborative action and innovation". COSIA's Tailings Environmental Priority Area (EPA), previously known as Oil Sands Tailings Consortium (OSTC) focuses specifically on improving the management of oil sands tailings. COSIA and OSTC have released a variety of guidance documents for the management of oil sands tailings.

One of the guidance documents released was the Oil Sands Tailings Technology Roadmap and Action Plan. The OSTC identified 8 technologies as part of the tailings technology roadmap that were commercially operated and/or commercially demonstrated to produce, treat, dispose of and reclaim tailings. These included: conventional hydraulic fill construction; water-capped MFT; composite tailings; conventional thickening; in-line thickening of tailings, with thin lift depositions/dewatering; in-line thickening of tailings, with thick lift deposition/accelerated dewatering; centrifuged MFT and coke capping.

In conventional hydraulic fill construction, whole tailings and/or cyclone underflow tailings are discharged as a single stream. The beached sand is either used for cell construction of containment dykes or beached to the interior of the pond. This method has been used extensively, however, the major issue with this management strategy is related to the FFT that segregates with time and eventually forms MFT. Water capping MFT involves placing MFT in a completed mine pit and capping the tailings with water. Research relating to water capping of MFT has been underway for decades, but operators still await the results of commercial scale demonstrations. Another method of dewatering is done by blending a sand slurry with FFT. Flocculants or coagulants are added to attain a non-segregating mix that used to promote fines capture (Fair and Beier 2012). When the fines are sourced as MFT, the resulting product is

referred to as composite or consolidating tailings (CT). If the fines are sourced as thickened tailing (TT), the resulting product is referred to as non-segregating tailings (NST). CT technology is being used at the Aurora North mine, and NST is being deployed at CNRL's Horizon Oil Sands (AER 2017a, AER 2018). A major limitation of CT and NST is that there is less sand available for dyke construction, beaching, or capping. TT is created by drawing FFT directly from the extraction process. It is then flocculated and thickened in a mechanical thickener. FFT enters the thickener at up to 20 wt.% solids. The resulting TT is densified up to 55 wt.% solids and the overflow water is extracted back to the extraction plant for re-use. This technology is being used at Imperial Oil Resources Limited's Kearl Mine. CT, TT and NST all have the potential to reach the goals of tailings management.

In-line thickening with thin lift dewatering uses an anionic polyacrylamide flocculent to densify the tailings. Rapid dewatering is accomplished by a combination of sedimentation, shear during beaching, and under drainage. Atmospheric conditions also result in further dewatering. In-line thickening with accelerated dewatering was developed by Syncrude. It uses in-line flocculation, and the tailings are discharged into deep in-pit deposits or shallow polders. In both deposition methods, water is expressed from the deposit and the expressed water and precipitation are decanted from the surface of the deposit (AER 2017b). It is currently in use at Suncor's oil sands operation (AER 2017). Centrifuged MFT involves pond dredging MFT, diluting it to a controlled wt.% solids, mixing it with a coagulant and/or polyacrylamide solution, and processing it through a solid bowl scroll centrifuge. The resulting cake has a solids content of about 55 to 60% (AER 2019).

As discussed above, over the past decades, many efforts have been made to develop viable dewatering technologies. The main goal of these technologies is to change the properties of the tailings by removing water. These included physical/mechanical processes, natural processes, chemical/biological amendments, mixtures/co-disposal, and permanent storage. Many have not been successful because of one or more of the following reasons: high operational cost, skilled labor shortage, long time commitment, low energy efficiency, low bitumen extraction, inconsistency due to tailing variability, difficulty removing supernatant liquid, detrimental effects to water quality, and low pumping efficiency (BGC Engineering Inc 2010, Cavanagh 2016).



### 2.2.2.1 Tailings Deposition Types

Deposition types were briefly discussed in the above section; however, they can have a great influence on the geotechnical properties of the final tailings deposit. The four deposit types that are being used commercially for fines management include:

1. Thin layered, fines dominated – It relies initially on dewatering by chemical and mechanical treatment, and later dewatering by drainage, atmospheric drying and freeze-thaw. A large surface area is needed for dewatering.
2. Deep, fines dominated – Initial water release is a result of polymer flocculant process, and additional dewatering occurs through self-weight consolidation and creep.
3. Fines-enriched sand deposits – Self-weight consolidation is relied upon for dewatering.
4. Water-capped fine deposits – FFT that has naturally densified to a solids content > 30% is placed into an engineered mine pit where a water cap is established to form a lake.

Table 2-1 shows a summary of relative cost, area, volume requirement, and energy intensity of each deposition type.

Table 2-1: Oil Sands Tailings Deposits (Fair and Beier 2012)

Deposit Type	Cost	Area	Volume Requirement	Energy Intensity
Thin-layered Fines Dominated	High to very high	Large to very large	Minimal to low	High to very high
Deep Fines Dominated	Moderate	Low-moderate	Low	Low
Fines Enriched Sand	Moderate	Moderate	High	Low
Water Capped In-pit Deposits	Low	Low-moderate	Medium	Low

The selection of a tailing’s management strategy should be a site-specific decision. Operators need to consider many factors; a few being land availability, site geology, containment availability, and geotechnical considerations.

## 2.3 Chemically Amended Oil Sands Tailings

As mentioned in Section 2.2.2, many tailings technologies used in the Athabasca oil sands require the use of flocculants to densify tailings by releasing water. They are used in many

industrial processes including water treatment, paper manufacturing, enhanced oil recovery, and brewing. There are three general groups of flocculants currently available: inorganic, natural, and synthetic. Inorganic flocculants are usually metal salts such as aluminum or iron. The most widely used are aluminum sulfate, iron sulfate, and iron chloride. Natural flocculants are becoming more widely used in some industries because of their environmental friendliness. Examples of natural flocculants include food grade polysaccharide, anionized nanocelluloses, and chitosan (Ajao et al. 2018). Synthetic flocculants are man-made and can be altered depending on the need. Conventional flocculants based on polymers and metal salts typically require a large amount of product, and they are difficult to store and handle. Even with the disadvantages, synthetic high molecular weight polymers are the most widely used in the oil sands industry.

The flocculation process is regarded as one of the most important processes in the treatment of fine particles from oil sands processing (Wang et al. 2014). This Section will describe the need for flocculation, the process, and the properties of the flocculated tailings.

### 2.3.1 Diffuse Double Layer

Fine-particle suspensions such as those present in oil sands tailings exhibit a significant degree of stability that resists aggregation. This stability is a result of the electrical charge on the particles dispersed in aqueous media and is further enhanced by the presence of protective adsorbed layers on the particle surface (Hogg 2000). This balance of charges is incorporated into the concept of the electrical double layer (EDL), also referred to as the diffuse double layer (DDL). The DDL is an ionic structure that is used to describe the variation of electric potential near a charged surface.

The main clay mineral present in oil sands fine tailings is kaolinite. Its chemical composition is  $\text{Al}_2\text{Si}_2\text{O}_5(\text{OH})_4$ . It is a layered silicate mineral with one tetrahedral sheet of silica linked with oxygen atoms to one sheet of alumina octahedra as seen in Figure 2-6.

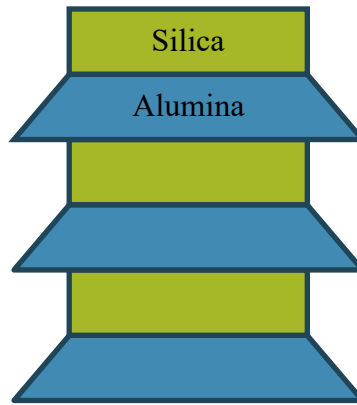


*Figure 2-6: Basic units of kaolinite*

Kaolinite is an aluminosilicate, meaning that some of the aluminum and silicon ions can be replaced by other elements of a different charge. For example, if aluminum ( $\text{Al}^{3+}$ ) were to be replaced with iron ( $\text{Fe}^{2+}$ ), the net charge would be negative. When the clays are suspended in solution, a hydrosphere of adsorbed water and cations forms around the clay particles. Outside of this layer, ions of opposite polarities create an electrically neutral diffuse layer. The ions present in the adsorbed layer are influenced by electrostatic attraction. The ions present in the diffuse layer are influenced by two equal and opposite forces – electrostatic attraction and diffusive forces. This leads to the significant degree of stability.

There are multiple models that are used to explain the phenomenon. The Helmholtz, Gouy–Chapman, and Gouy–Chapman–Stern models are commonly used. The Helmholtz model predicts a linear dissipation of the surface charge potential from the surface to the cations, however, it does not consider factors such as diffusion of ions in solution, possibility of adsorption onto the surface, and the interaction between solvent dipole moments and the electrode (Mojid 2011). The Gouy-Chapman model made significant improvements to the Helmholtz model. The assumption of this model allows loosely held cations to diffuse into the liquid phase until the counter potential restricts the process. It allows Maxwell-Boltzmann statistics to be applied, and the electric potential decreases exponentially away from the surface of the bulk fluid. It does however treat ions as point charges (Mojid 2011). The third model assumes that ions have finite size, and the first layer of ions are at a distance equal to the radius of the ion from the surface. It also assumes that some of the ions are adsorbed by the surface in the plane – called the Stern Layer. Figure 2-7 shows the configuration of the DDL.

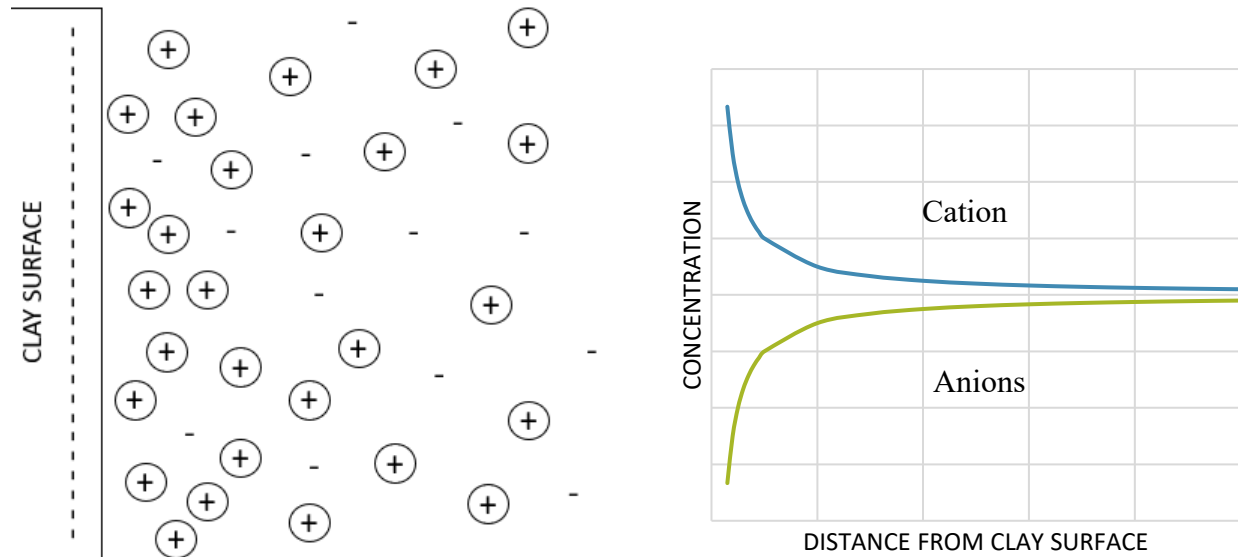


Figure 2-7: Distribution of cations and anions next to a clay particle

To bring two particles closer together, energy is required to overcome the energy barrier. One effective method to lower the energy barrier is to change the electrolyte concentration; this will be discussed further in Section 2.3.2. The compression of DDL by electrolyte concentration can be explained through the Gouy-Chapman theory as shown in Equation 1.

$$\frac{1}{K} = \sqrt{\frac{DkT}{8\pi n_0 \varepsilon^2 v^2}} \quad (1)$$

Where  $1/K$  is the electric double layer thickness,  $D$  is the dielectric constant of the medium,  $k$  is the Boltzman constant,  $T$  is temperature,  $n_0$  is the ion concentration,  $\varepsilon$  is unit electronic charge, and  $v$  is the ionic valence.

The DDL concept is thought of as the underlying mechanism for the engineering behavior of kaolinite clays present in the oil sand tailings (Wang and Siu 2006). The face charge is always negative and slightly pH dependent; and the edge charge can be either negative or positive, depending on the pH (Wang and Siu 2006). This negative surface charge yields the formation of the DDL.

### 2.3.2 Flocculation

The purpose of flocculation is to form aggregates or flocs from finely divided particles and from chemically destabilized particles. The act of flocculation is a transport step that brings together destabilized particles to form larger particles that can be readily removed by settling or filtration. Flocculation can occur in separate tanks or basins specifically designed to the purpose or in in-line facilities such as pipes or conduits.

There are two types of flocculation: microflocculation, and macroflocculation. Microflocculation is the aggregation of particles brought about by the random thermal motion of fluid molecules. The random motion is typically referred to as Brownian motion. It is significant for particles that range in size from 0.001 to 1  $\mu\text{m}$ . Macroflocculation refers to the aggregation of particles greater than 1 or 2  $\mu\text{m}$ . It is brought about by induced velocity gradients and differential settling. Velocity gradients involve faster moving particles overtaking slower-moving particles in a velocity field. If the particles collide and stick together, a larger particle will be formed. During differential settling large particles overtake smaller particles. When they collide, they stick together and settle at a rate that is faster than the initial larger particle (Jarvis, Jefferson and Parsons 2005).

It involves three primary steps:

1. Destabilization of the suspended fine particles by processes such as the elimination of interparticle repulsion;
2. Floc formation and growth; and
3. Floc degradation from chemical, mechanical or biological.

Step three is often thought of as detrimental, but it plays a helpful role in the redistribution of particles as flocs develop and grow (Hogg 2000).

#### 2.3.2.1 Destabilization

Destabilization is accomplished by eliminating or shielding the charges. Electrical charges between the particle and the water and can usually be controlled by pH. At a certain pH, the iso-electric point occurs (no net charge), and the particles become unstable. If the iso-electric point is at a practical pH, it is the most desirable method of destabilization (Hogg 2000). An alternative to altering the pH is to shield the charge from one particle to another. This is done by using a high concentration of a specific ion in the water to compress the diffuse double layer (DDL) surrounding the particles. Once the DDL is compressed, the particles become close enough that

attractive forces dominate. Reagents such as lime and alum are used frequently in practice. Polymeric substances are also effective for destabilization (Hogg 2000).

#### *2.3.2.2 Flocculation*

Once the particles become destabilized, flocs grow because of collisions between particles due to Brownian motion, velocity gradients, and differential settling of individual particles or flocs. Polymer dosage, mixing time, and agitation intensity are optimized for peak flocculant performance. In practice, settling rate, supernatant turbidity, and compressibility are used to indirectly measure flocculant performance (Hogg 2000). The effectiveness of the system is dependent of several parameters involving the solid, polymer, and the solution chemistry conditions. The forces responsible for adsorption of polymers on mineral surfaces are primarily a result of three types of bonds: (1) electrostatic, (2) hydrogen, and (3) covalent bonding. The solution chemistry, rheology of the solid suspension, and the polymer properties dictate the nature of the interactions between the polymer and the mineral.

Polymer adsorption onto the particle is an important step in flocculation. Adsorption of non-ionic polymers can occur due to the formation of hydrogen bonding between the hydrogen atoms of the polymer and the oxygen atoms on the surface of the particles. Hydrogen bonding may account for some of the adsorption experienced when using cationic and anionic polymers, however, electrostatic attraction and salt linkage are the main driving forces behind adsorption of these polymers. When surfaces of opposite charge encounter each other, electrostatic attraction happens. During the flocculation process, this typically occurs between positively charged groups of the cationic flocculant and negative groups on the surface of a clay particles. Salt linkage is the covalent bond that is formed between anionic flocculants and negative mineral particles (Williams 2007).

Adsorption and flocculation typically occur simultaneously. Long chain polymers used in flocculation adsorb onto the surface of multiple particles at the same time. When this occurs, they begin to form a three-dimensional network, creating large flocs that settle rapidly (Vedoy and Soares 2015). It has been determined that molecular weight is the most important polymer property affecting PAM flocculation (Vedoy and Soares 2015). Typically, flocculants with higher average molecular weights have longer polymer chains, and therefore can adsorb onto the

surface of more particles at the same time. Chemical amendments have proven to be quite successful in terms of dewatering (Vedoy and Soares 2015).

### 2.3.3 Floc Characterization

Multiple studies have been undertaken in recent years to characterize flocs (Jarvis et al. 2005, Jarvis, Jefferson, Gregory et al. 2005, Liang et al. 2015). A recent review by Liang et al. (2015) reviewed the modern techniques to characterize floc size, floc shape and structure, and floc strength.

There are two main types of floc size characterization techniques – in-situ and ex-situ (Liang et al. 2015). In-situ techniques include photography and video using image analysis software, focused beam reflectance measurement, and particle vision measurement (PVM). Ex-situ techniques include dynamic image analysis (DIA), light scattering, light transmission and microscopy. Ex-situ techniques are not ideal as they may result in flocs being sheared or diluted resulting in measurement errors (Liang et al. 2015). When referring to a floc size, an equivalent diameter is typically used as a simple measurement is limited as it only gives an indication of floc size in one direction (Jarvis et al. 2005). There are multiple ways to represent equivalent diameter, so it is critical to be consistent when comparing equivalent diameters.

Floc shape and structure are characterized through imaging techniques discussed above. Using imaging, parameters such as perimeter, area, length, and width can be extracted. Commonly used indicators include convexity, circularity, roundness, aspect ratio, area fractal dimension, and mass fractal dimension (Liang et al. 2015).

Finally, floc strength can be characterized using multiple techniques. It is important to note that only relative strengths are achievable under certain conditions and all methods have drawbacks (Jarvis et al. 2005). In this context, floc strength is defined as the ability of the floc to resist breakage when external forces are applied (Jarvis et al. 2005). Floc strength characterization techniques can be broken into two categories:

- Shear resistance capacity
  - Comparison before and after shearing
  - Shear yield point
- Direct measurement of interaction forces

- Surface forces apparatuses
- Atomic force microscopy
- Forces between particle and particle

One of the most used approaches to measuring floc strength is to measure observed changes in floc size as different applied shear rates using an impeller-based system (Jarvis et al. 2005).

#### 2.3.4 Properties of Chemically Amended Tailings

Chemically amended/ flocculated tailings are evaluated on dewaterability potential and yield stress (Mizani 2016). The dewaterability potential is important because operators want to maximize the flocculation efficiency. Operators are also interested in yield stress to determine flow and beaching behavior. These basic properties allow engineers and operators to design and optimize tailings impoundments.

##### 2.3.4.1 Pore Water Chemistry

The pore water chemistry of polymer amended tailings tend to be comparable to untreated tailings. Bajwa (2015) found that metal parameters remained the same, except for calcium ( $\text{Ca}^{2+}$ ) which decreased approximately 1.9 times following polymer treatment. Higher concentrations of sodium ( $\text{Na}^+$ ) were also found in treated tailings – representative of higher levels of soluble salts. There were no major changes in the concentration of nutrients after the addition of a polymer flocculant. Changes to pH were also investigated in this study. It was found that the pH was higher in polymer amended tailings (7.56, 7.65, 7.59) as compared to unamended tailings (7.45) (Bajwa 2015). After the addition of a polymer solution, there is an immediate increase in the water content. When the tailings begin draining off water, there is an increase in the percent solids by mass (or decrease in water content). The sand to fines ratio (SFR) of tailings also changes drastically with the addition of a polymer.

##### 2.3.4.2 Shear Strength & Fabric

Unamended FFT behaves like a flowing liquid when water contents are greater than 84%. Yield stresses are typically in the order of 1 Pa. The addition of a polymer flocculant leads to changes of the fabric and water content of tailings. These changes result in increases to the observed yield stress (Jeeravipoolvarn 2010).



The microstructure of raw MFT shows edge-to-face and edge-to-edge structure (commonly referred to as card house structure), whereas in-line thickened tailings (polymer amended) microstructure appears to be random without the distinct card-house like structure (Jeeravipoolvarn 2010). It is known that polymer amended tailings at the same density as raw MFT have much higher moduli and higher yield stress because of structural changes from the addition of polymer (Mizani 2016). As seen in Figure 2-8 and Figure 2-9, flocculation improves the aggregation of particles and forms larger void spaces. The larger voids form possible water channels, increasing the hydraulic conductivity and improving the dewaterability potential (Mizani 2016).

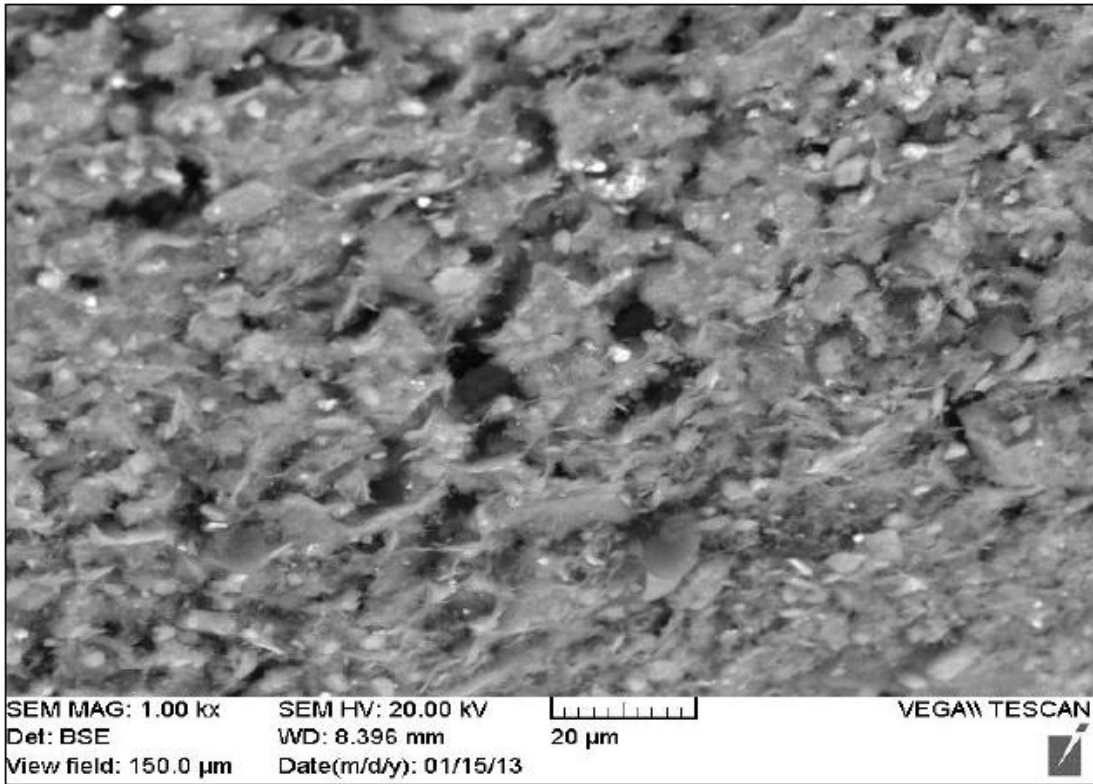


Figure 2-8: Backscattered environmental scanning electron of MFT for a magnification - 1000x, scale – 20 μm, view field - 150 μm (Mizani 2016)

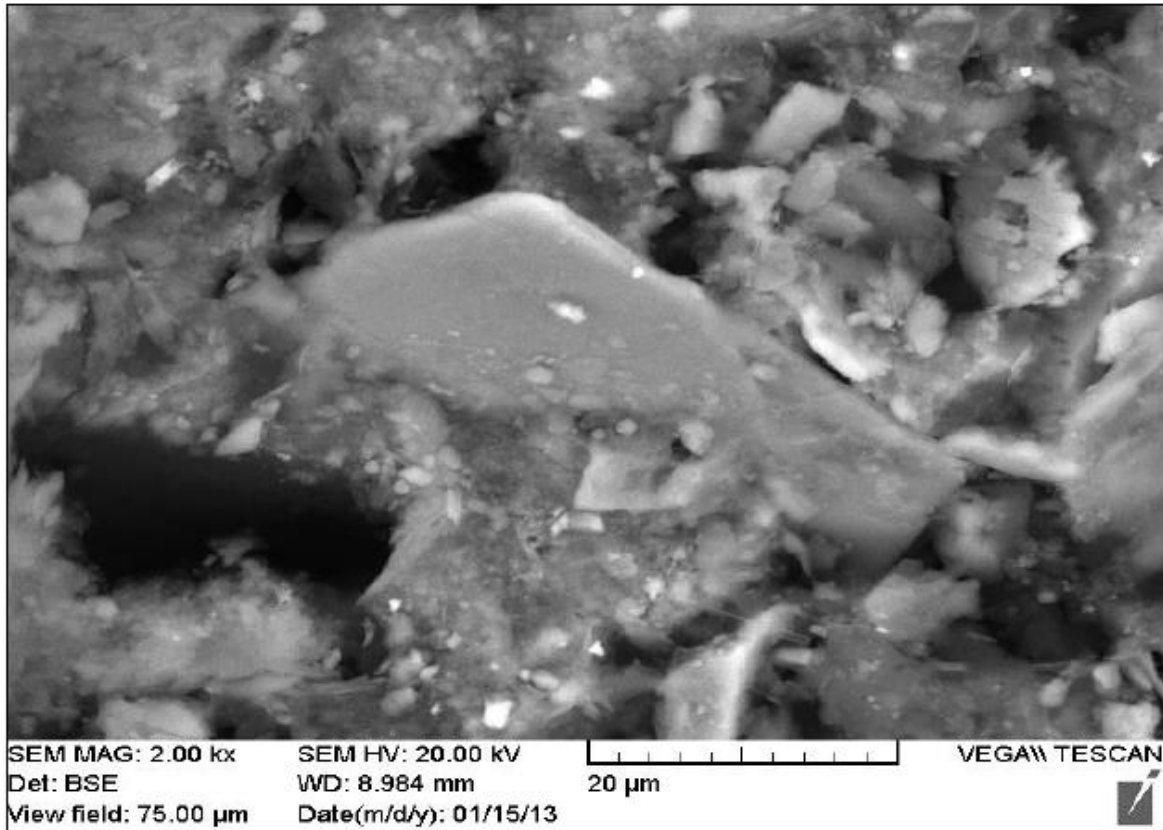


Figure 2-9: Backscattered environmental scanning electron of polymer amended MFT at a dose of 650 g/tonne for a magnification - 2000x, scale – 20 μm, view field - 75μm (Mizani 2016)

It is assumed that the small cages seen in Figure 2-8 that are formed by fine particles in raw FFT are the main reason for the inability of FFT to dewater. As discussed above, the addition of PAM bridges the particles, forming larger voids. After the polymer amended tailings are deposited, the yield stress increases rapidly because of dewatering, consolidation, and thixotropic behavior of the tailings.

#### 2.3.4.3 Consolidation Behavior

Consolidation is the process by which soil changes in volume in response to changes in pressure. It is caused by the deformation and reorientation of soil particles, and the expulsion of water from the pore spaces (Das and Sivakugan 2017). Multiple consolidation theories exist to model and predict consolidation behaviour. One of the first theories was Terzaghi's theory of one-dimensional consolidation. In Terzaghi's theory, it is assumed that both the permeability and compressibility of the clay remain constant during consolidation under a particular increment of

load which in practice are only approximately satisfied. Over time, improvements were made to Terzaghi's model; however, they were all based on small strain consolidation.

Today, one dimensional finite strain consolidation theory introduced by Gibson et al. (1967) is used to model the consolidation phenomenon of oil sands tailings as the derivation removes the imitation of small strains and changes in soil compressibility and permeability were considered. The theory has three formulations: (1) void ratio, (2) excess pore pressure, and (3) porosity. The governing equation in terms of void ratio is presented in Equation 2.

$$\pm \left( \frac{\rho_s}{\rho_f} - 1 \right) \frac{d}{de} \left[ \frac{k(e)}{(1+e)} \right] \frac{\partial e}{\partial z} + \frac{\partial}{\partial z} \left[ \frac{k(e)}{\rho_f} \frac{d\sigma'}{de} \frac{\partial e}{\partial z} \right] + \frac{\partial e}{\partial t} = 0 \quad (2)$$

Where  $\rho_s$  is solids density,  $\rho_f$  is fluid density,  $e$  is void ratio,  $k$  is hydraulic conductivity,  $\sigma'$  is effective stress,  $t$  is time and  $z$  is the volume of solids in a prism of unit (bulk) cross-sectional area lying between the datum plane and the point (reduced or material coordinate).

The governing equation in terms of excess pore pressure,  $u$  is shown in Equation 3, where Somogyi (1980) used Koppula's (1970) rearrangement of continuity and fluid flow relationships.

$$\frac{\partial}{\partial z} \left[ \frac{k(e)}{\gamma_w(1+e)} \right] \frac{\partial u}{\partial z} + \frac{k(e)}{\gamma_w(1+e)} \frac{\partial^2 u}{\partial z^2} + \frac{\partial e}{\partial \sigma'} \frac{\partial u}{\partial t} - \left[ (G_s - 1) \cdot \gamma_w \frac{d(\Delta Z)}{dt} \right] = 0 \quad (3)$$

The formulation in terms of porosity was presented by Lee (1979) shown in Equation 4.

$$-\frac{\partial}{\partial x} \left[ \frac{k(1+e)}{\rho_f} \frac{d\sigma'}{de} \frac{\partial n}{\partial x} \right] - \left\{ (G_s - 1) \frac{d[k(1-n)^2]}{dn} - \frac{\partial q}{\partial n} \frac{d}{dn} \left[ \frac{k}{\rho_f} (1-n) \right] \right\} \frac{\partial n}{\partial x} + \frac{k}{\rho_f} \frac{\partial^2 q}{\partial x^2} (1-n) = \frac{\partial n}{\partial t} \quad (4)$$

Where  $n$  is porosity,  $q$  is the applied stress and  $x$  is the convective vertical coordinate. All the above formulations are identical; however, different formations will result in different initial boundary conditions to solve the governing equations.

The consolidation behavior of oil sands fine tailings has been studied extensively (Jeeravipoolvarn 2005, Jeeravipoolvarn 2010, Kabwe et al. 2017). The change in compressibility occurs at a higher void ratio in in-line flocculated tailings and is more gradual as compared to cyclone overflow (Jeeravipoolvarn 2010). Jeeravipoolvarn (2010) found that the in-line

thickened tailings compressibility behavior withstands higher effective stresses at void ratios of 8 and below.

Typical results from in-line thickened tailings are shown in Figure 2-10 and Figure 2-11 modified from Jeeravipoolvarn (2010).

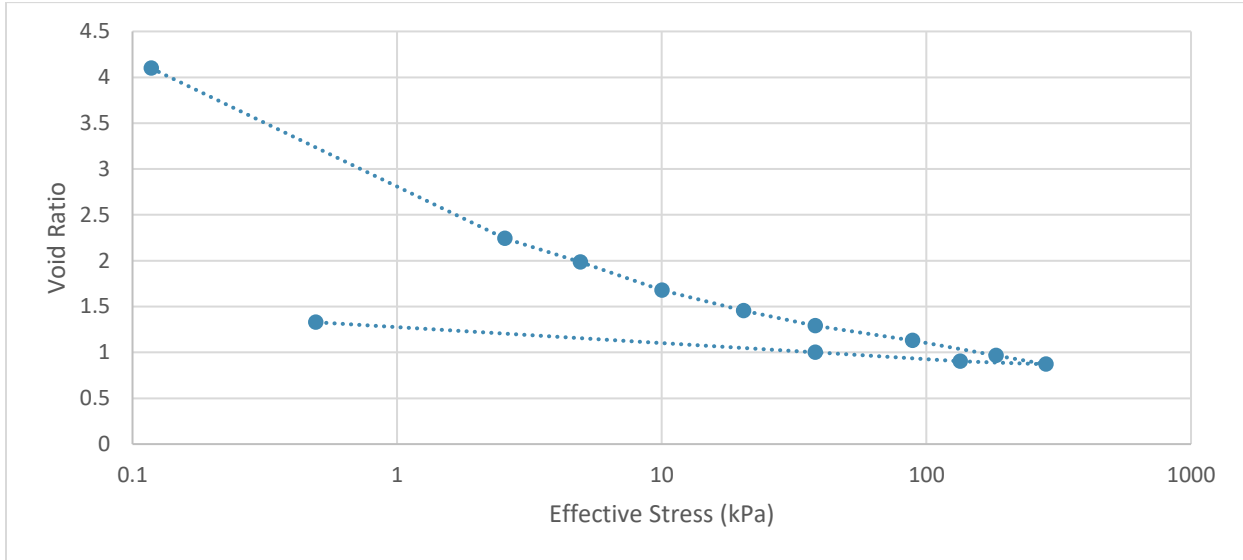


Figure 2-10: Compressibility of east pilot pond ILTT (Modified from Jeeravipoolvarn 2010)

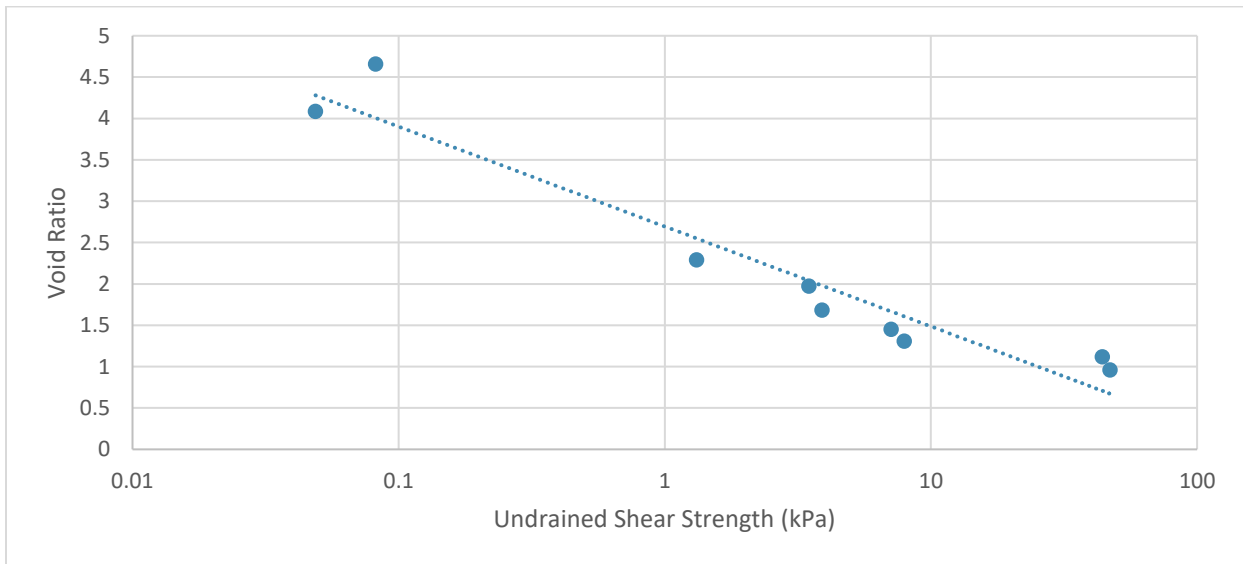


Figure 2-11: Undrained shear strength of east pilot pond ILTT (Modified from Jeeravipoolvarn 2010)

#### 2.3.4.4 Sensitivity

The sensitivity of chemically amended fine tailings deposits is also a parameter of interest. Sensitivity ( $S_t$ ) is defined as the ratio of the undisturbed ( $S_u$ ) to fully remolded strength ( $S_{ur}$ ) at the same water content (Mitchell and Soga 2005). Soft sensitive clays are of concern because they can have a drastic reduction in shear resistance. They can be triggered by local overloading and typically escalate in a retrogressive manner where potentially large volumes of clay liquefy.

$$S_t = \frac{S_u}{S_{ur}}$$

Many different phenomena may contribute to the development of sensitivity, including metastable fabric, cementation, weathering, thixotropic hardening, leaching, ion exchange, and change in the monovalent/divalent cation ratio, and formation or addition of dispersing agents (Mitchell and Soga 2005). Sensitive clays were classified by Roseqvist (1953) from insensitive to extra quick clays, Table 2-2.

Table 2-2: Classification of clay sensitivity values (Roseqvist 1953)

Classification	$S_t$
<b>Insensitive</b>	~1.0
<b>Slightly sensitive clays</b>	1 – 2
<b>Medium sensitive clays</b>	2 – 4
<b>Very sensitive clays</b>	4 – 8
<b>Slightly quick clays</b>	8 – 16
<b>Medium quick clays</b>	16 – 32
<b>Very quick clays</b>	32 – 64
<b>Extra quick clays</b>	> 64

It has been inferred that chemically amended fine tailings deposits may exhibit shear-sensitive behavior based on their reported strengths (Beier et al. 2013). Beier et al. (2013) collected and analyzed three publicly available data sets shown in Table 2-3 below.

Table 2-3: Sensitivity data sets

Data	Source
Shell PT 1	Masala and Matthews (2010)
Shell PT 2	Masala and Matthews (2010)
Syncrude ILTT	Jeeravipoolvarn (2010)

The relationship between residual/remolded shear strength ( $S_{ur}$ ) and liquidity index ( $I_L$ ) calculated by Locat and Demers (1988) provides a good overall fit for typical MFT and was used to represent various values of sensitivity in Figure 2-12 (Beier et al. 2013).

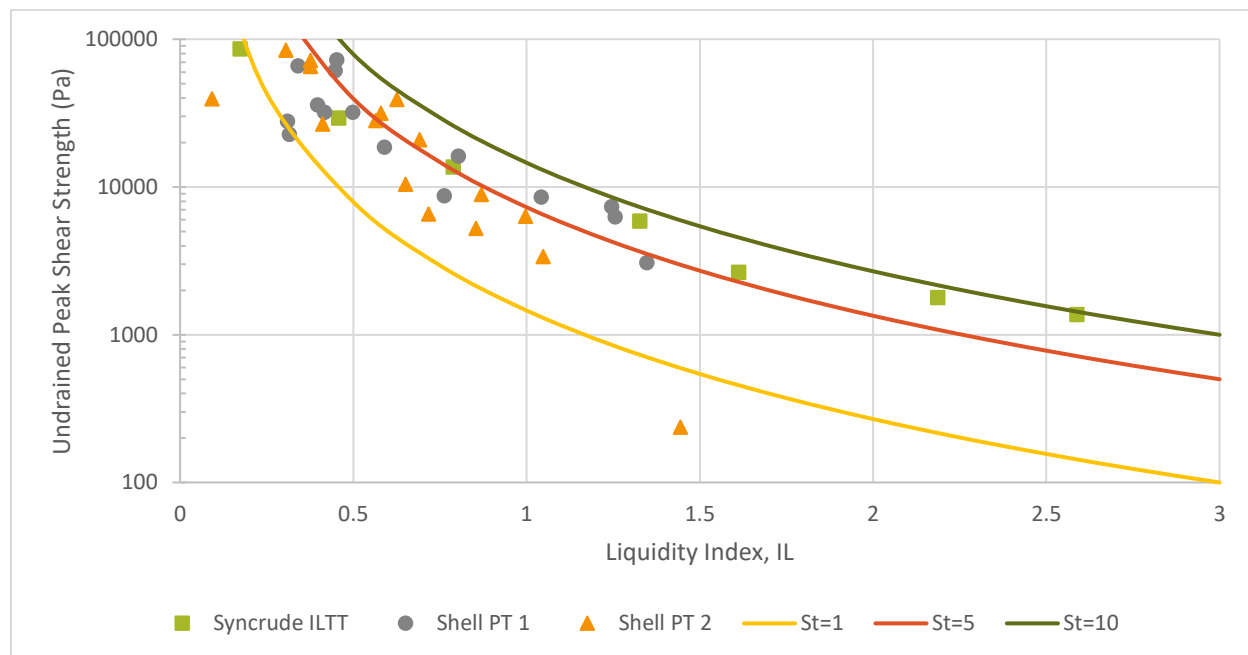


Figure 2-12: Sensitivity of oil sands fine tailings (Modified from Beier et al. 2013)

Deposits with sensitivities in the range of 9-10 (slightly quick clays) were reported in these data sets (Beier et al. 2013). Most samples, however, exhibited sensitivities in the range of 2-3 (medium sensitive clays). As the deposits began to dewater, the sensitivity of the deposits appeared to decrease to values consistently below 5. Chemically amended oil sands fine tailings were shown to reach undrained shear strengths at much lower solid's contents than unamended fine tailings (Beier et al. 2013). This means that chemically amended tailings deposit can hold significantly more water than unamended deposits. These findings suggest that chemically amended deposits may exhibit sensitive, metastable behavior upon deposition (Beier et al. 2013).

#### 2.3.4.5 Shear Thinning & Thixotropy

The rheological behavior becomes dependent on shear thinning and thixotropic behavior as the tailings age. It has also been found that the elastic shear modulus of polymer amended tailings is recovered almost entirely after a high shear event (Mizani 2016). This implies that the de-structuration is not permanent under high shear and the benefit of the polymer will be retained under nearly all deposition scenarios (Mizani 2016). This behavior is further discussed in Section 2.5.2.

#### 2.3.5 Properties of Centrifuged Tailings

The development of the centrifuge technology for treating oil sands tailings began over 13 years ago. Laboratory scale technologies were developed in the early 2000's and pilot scale testing began in 2007. The process used for oil sands fine tailings is a two-step process (Owolagba 2013). The first step is dewatering, which involves conditioning the FFT with flocculent aids using large industrial centrifuges. The process results in two streams. One stream is referred to as centrate and contains about 0.5 – 1% solids. The second stream is referred to as cake and is about 60% solids (Owolagba 2013) .



Figure 2-13: Centrifuge used at Albian's Jackpine Mine (Canada's Oil Sands Innovation Alliance 2021)

The second step involves natural processes after deposition. These processes include consolidation, desiccation and freeze-thaw. The centrifuge cake has a volume of about 50% of the original FFT, and therefore seen as a potential solution to the oil sands tailings challenges.

Early results from the laboratory scale testing showed that the use of a polymer flocculant was key to the process. The flocculant ensured that clays remained a part of the cake product and did not become entrained with the centrifuge centrate. The process of polymer injection was refined during the pilot scale tests. In the 2010 tests, polymer was injected, and some form of in-line static mixing was used to disperse the flocculant. A dynamic mixer was also evaluated as part of the test program. In addition to polymer flocculant addition, gypsum was added as a strategy to increase the strength of the centrifuge cake. Results showed a significant increase in throughput, and cake strength (as measured by laboratory vane) when gypsum was used to pretreat the MFT feed.

In the test programs, the minimum fines or solids capture parameter was greater than 95% and when acceptable performance was maintained, 97%. Performance was found to be controlled by a variety of parameters such as bowl speed, working volume (pool depth), cake discharge, and polymer flocculant and MFT mixing.

#### *2.3.5.1 Geotechnical Index Properties*

Owolagba (2013) tested the geotechnical index properties of centrifuged tailings before and after centrifugation. They found that the gravimetric water content ( $w$ ) went from 240% to 63%; solids content ( $s$ ) increased from 29% to 61%; void ratio ( $e$ ) decreased from 6.1 to 1.5; and the degree of saturation remained at 100%. Rima and Beier (2018) tested similar index properties with slightly different results. The resulting centrifuge cake has a gravimetric water content of 89% and a solids content of 53%.

#### *2.3.5.2 Pore Water Chemistry*

$\text{Na}^+$  and  $\text{HCO}_3^-$  have been found to be the dominant ions in centrifuge cake, measuring 780 mg/L and 1207 mg/L (Rima and Beier 2018). Elevated levels of  $\text{Na}^+$  can be attributed to the addition of sodium hydroxide during the extraction process, and  $\text{HCO}_3^-$  is related to  $\text{CO}_2$  adsorption during aeration for bitumen extraction (Jeeravipoolvarn 2005). It should be noted that these



results only apply to samples received by the authors and may not be the same for all centrifuged tailings.

#### *2.3.5.3 Shear Strength*

The initial measured shear strength of centrifuge cake is typically below 1 kPa (Kabwe et al. 2017, Rima and Beier 2018). Early centrifuge performance data for Athabasca fine tailings showed vane shear yield points between 2 kPa and 6 kPa; results varied based on the grams of polymer per tonne of dry solids, solids percentage in feed and centrifuge feed rate (Mikula et al. 2009).

#### *2.3.5.4 Consolidation Behavior*

Large strain consolidation (LSC) tests are commonly used to test the consolidation behavior of soil slurries. They provide the consolidation characteristics of the tailings such as the compressibility and shear strength relationships. The relationships are used to guide numerical modelling efforts of oil sands fine tailings ponds. To determine shear strength, a vane shear apparatus is used (Kabwe et al. 2017). Typical results from LSC tests are shown in Figure 2-14 and Figure 2-15. Kabwe (2017) found that flocculated tailings (FTT) were slightly more compressible than centrifuged tailings (FCTC) at effective stresses between 1 kPa and 100 kPa. At stresses greater than 100 kPa, the compressibility's were the same. They also found that at fines void ratios less than 2, FCTC had a greater shear strength.

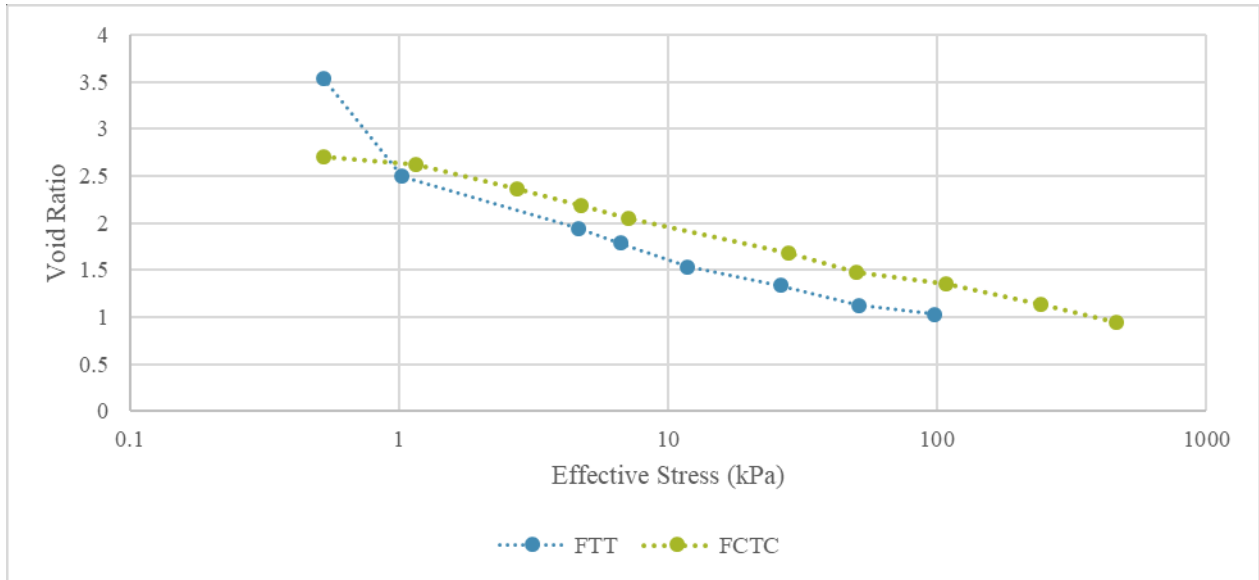


Figure 2-14: Void ratio versus effective stress of flocculated tailings (FTT) and flocculated centrifuged tailings (FCTC) (Modified from Kabwe et al. 2017)

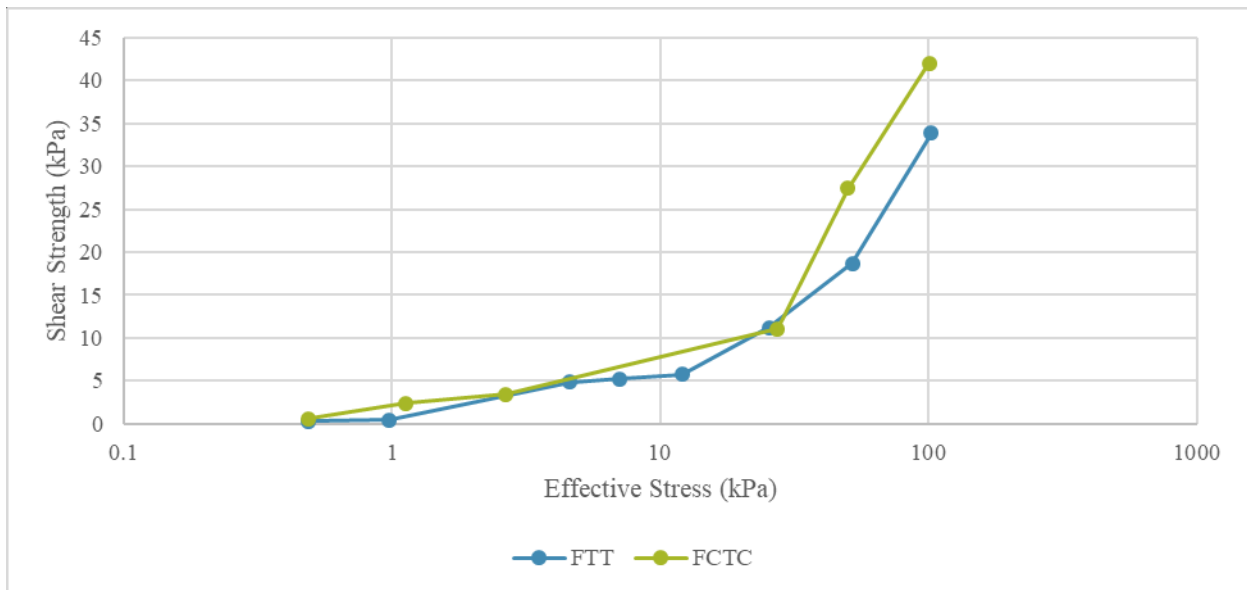


Figure 2-15: Shear strength versus effective stress of flocculated tailings (FTT) and flocculated centrifuged tailings (FCTC) (Modified from Kabwe et al. 2017)

### 2.3.6 Effect of Shear on Flocculated Tailings

The following studies have been previously completed and relate to the direct or indirect measurement of the effect of shear on flocculated tailings.

### *2.3.6.1 Geotechnical Behaviour of In-Line Thickened Oil Sands Tailings*

This study was completed by Jeeravipoolvarn (2010) in partial fulfillment of a Ph.D. thesis at the University of Alberta. The study involves the geotechnical behaviour of in-line thickened oil sands tailings. In-line thickened tailings (ILTT) is a process in which coagulants and flocculants are added to and mixed with waste streams and discharged simultaneously. This process is used to increase hydraulic conductivity, shear strength, and floc size of thin fine tailings. Early work on ILTT was undertaken by Syncrude to achieve rapid sedimentation and high solids content deposits (Shaw and Wang 2005).

ILTT were subjected to testing before and after shearing to represent non-disturbed tailing and remolded in-line thickened tailings. Three sub tests – a hindered sedimentation test, a compressibility test and a large strain consolidation test were also completed to fully understand the sedimentation and consolidation characteristics of cyclone overflow, in-line thickened, and sheared in-line thickened tailings.

Most notably, the study showed that shearing ILTT reduced the floc size, changing the fines fraction ( $<45\ \mu\text{m}$ ) from 5% to 77% as seen in Figure 2-16 (Jeeravipoolvarn 2010).

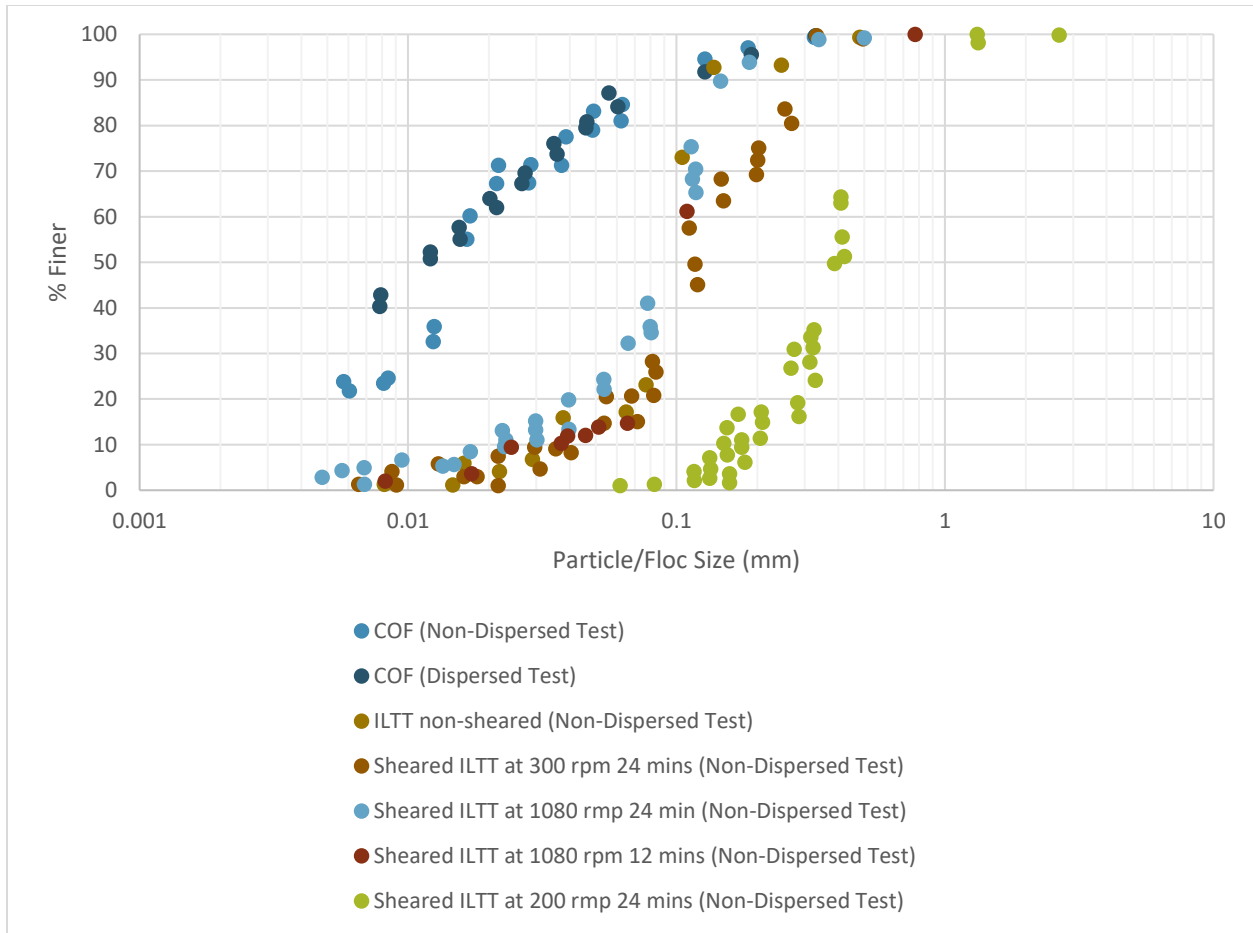


Figure 2-16: Comparison of Particle Size Distributions for ILTT (Jeeravipoolvarn 2010)

### 2.3.6.2 Influence of Dewatering and Desiccation on Microstructure and Vane Strength of Polymer Amended Oil Sand Mature Fine Tailings

Bajwa and Simms (2013) presented research on the microstructure and undrained shear strength of polymer amended FFT. As anticipated, the results showed that apparent grain size distribution is influenced by polymer dosage.

They measured the apparent grain size distribution through wet sieving and hydrometer. Additionally, they measured the vane shear strength and used scanning electron microscopy (SEM) for additional information.

### *2.3.6.3 Effects of Shearing and Shearing Time on Dewatering and Yield Characteristics of Oil Sands Flocculated Fine Tailings*

This work presented at IOSTC 2016 was a modelling study on the effects of pipeline shearing on dewatering and yield characteristics of MFT flocculated with different polymers (Derakhshandeh et al. 2016). The study used three flocculants: a partially hydrolyzed polyacrylamide, a polyethylene, and a Ca-polyacrylamide. To model pipeline shearing, a Couette device was used for controlled shearing of the flocculated tailings. Dewatering and yield characteristics were measured before and after shearing by capillary suction time, permeability index, peak yield stress and 7-day water release tests to quantify the effect of shearing.

The results of the study showed that shearing increased the long-term water release while having a negative impact on the short-term water release and yield characteristics. Additionally, it was found that yield stress decreased with shearing.

## **2.4 Polyacrylamide**

Polyacrylamides (PAMs) are high molecular weight synthetic polymers produced through copolymerization of acrylamide with alternate functional groups. The polymers can be nonionic, cationic, or anionic, resulting in a versatile chemical (Lipp and Kozakiewicz 1993). Anionic PAM has many industrial applications, including water treatment, paper manufacturing, and enhanced oil recovery. It is produced by copolymerization of acrylamide and acrylic acid. Cationic PAMs are copolymers of acrylamide and quaternary esters, or amines and they are the most soluble in water. In the oil sands industry, anionic polymers are most commonly used (Hripko et al. 2018). For non-ionic HPAM, adsorption occurs from the formation of hydrogen bonding between the hydrogen atoms on the acrylamide groups (shown in Figure 2-17) and the oxygen atoms on the surface of the particles (Vedoy and Soares 2015). Electrostatic attraction and salt linkage are the main forces behind adsorption of cationic and anionic HPAM polymers, respectively. Hydrogen bonding also influences adsorption of cationic and anionic HPAM polymers.

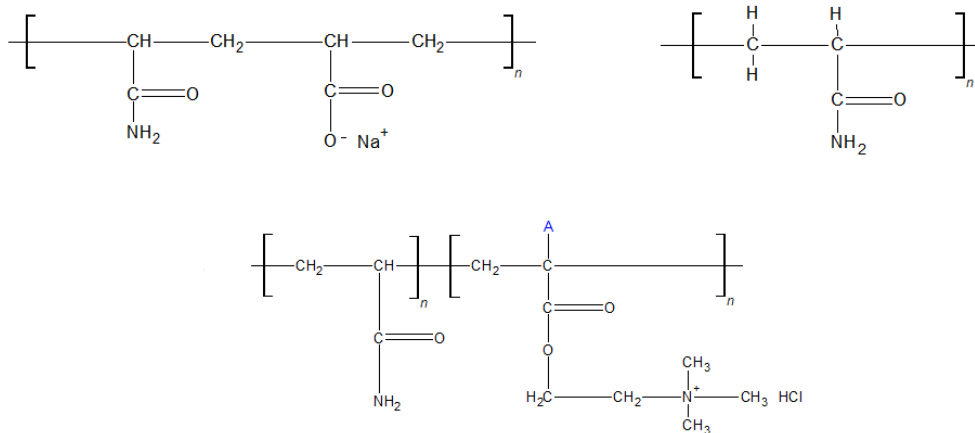


Figure 2-17: Chemical structure of flocculants based on polyacrylamide. Clockwise from top left: anionic polyacrylamide (PAM), non-ionic PAM, and cationic PAM.

Anionic flocculants can have molecular weights of 3 to 30 million (Vedoy and Soares 2015). This ranges from medium molecular weight (MMW) to very high molecular weight (VHMW). Viscosity is commonly used to classify and select proper PAM flocculants for the given application. Viscosity  $\eta$  is the coefficient of proportionality between the applied shear stress  $\sigma$  and the shear rate  $\gamma$ .

$$\eta = \sigma/\gamma \quad (5)$$

The viscosity of polymers generally depends on the shear applied as seen in Figure 2-18. Viscosity is a common design parameter in industrial applications based on the shear rates they may have to endure.

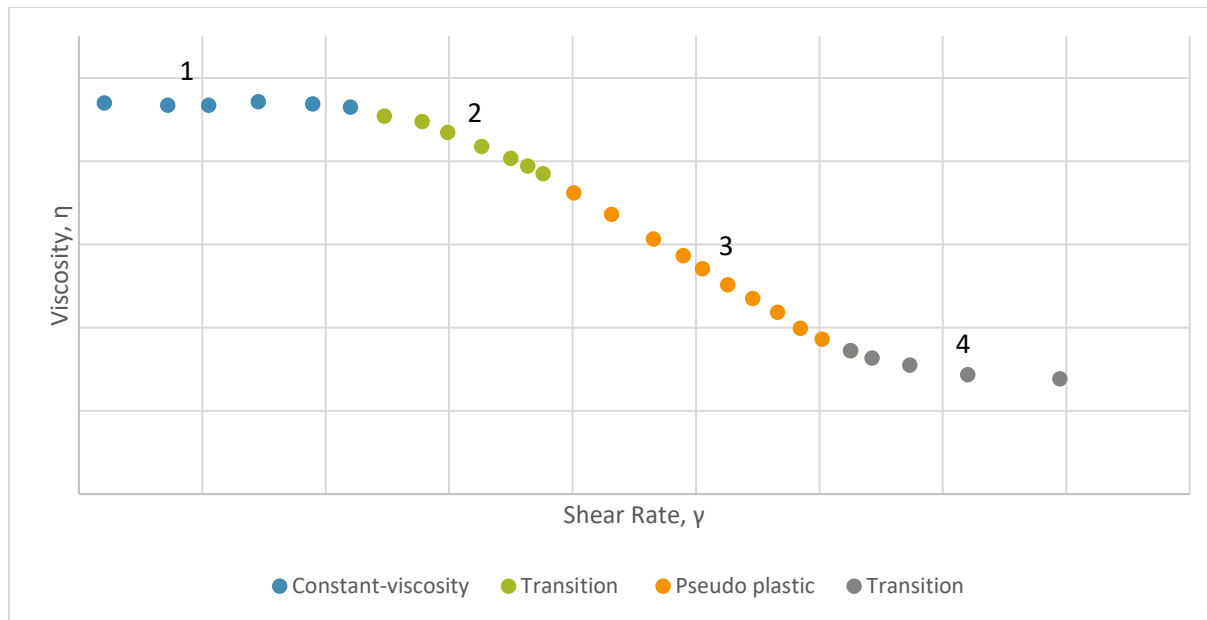


Figure 2-18: Viscosity versus shear rate for general polymers

There are four distinguishable regions in the viscosity-shear rate plot:

1. Constant-viscosity region – the polymers behave as a Newtonian fluid. This region is associated with low shear rates or low concentrations.
2. Transition region – this area corresponds to polymer molecules undergoing deformations.
3. Pseudo plastic region – this region corresponds to an area where the viscosity decreases with increasing shear rates. As the shear increases, more polymers chains orient in the direction of flow.
4. Transition region – the area corresponds to high degrees of shear.

Polymer concentration also affects the viscosity behavior. A critical concentration is determined by plotting viscosity versus concentration on a log-log scale. At low concentrations, the polymers curl up like balls of string; separated by the solvent molecules (most commonly water). The critical concentration is defined by the point at which the polymer balls are in contact with each other and have just started interpenetration (SNF Floerger 2018).

When considering flocculation, the efficiency is dependent on the molecular weight, molecular weight configuration, chain length, and the spatial configuration of the molecule (Vedoy and Soares 2015). As the chain length increases, the greater the possibility of creating bridging. In addition to the bridging effect, high molecular weight polymers can trap unflocculated particles in the floc mesh. Finally, the configuration/structure of the polymer plays an important role.

Common structures include linear, branched, and crosslinked. Linear polymers have a chain in which all the carbon-carbon bonds exist in a single straight line. Branched polymers occur when group of units branch off from the long polymer chain. These branches can also be long repeating groups. They are advantageous because they form more structured and stable flocs (Mpofu et al. 2003). Cross-linked polymers form long chains that are either branched or linear. The long chains can form covalent bonds between the polymer molecules. Cross-linked polymers are commonly found in materials such as rubber. Polymer microstructure such as charge type, density and topology are import factors in flocculation efficiency; however, they are rarely studied regarding flocculation of oil sands tailings (Vedoy and Soares 2015).

Charge type and density are important because they can control the adsorption of the polymer onto the mineral surface. There is an optimum point that exists based on the slurry being flocculated. Low to medium charge densities will increase the length of the polymer chains during adsorption by promoting the repulsion of charged polymers.

A high molecular weight anionic polymer, A3338, was used as a flocculant for this research. It is a branched polymer, with an average molecular weight of  $18 \times 10^6$  g/mol (Mizani et al. 2017).

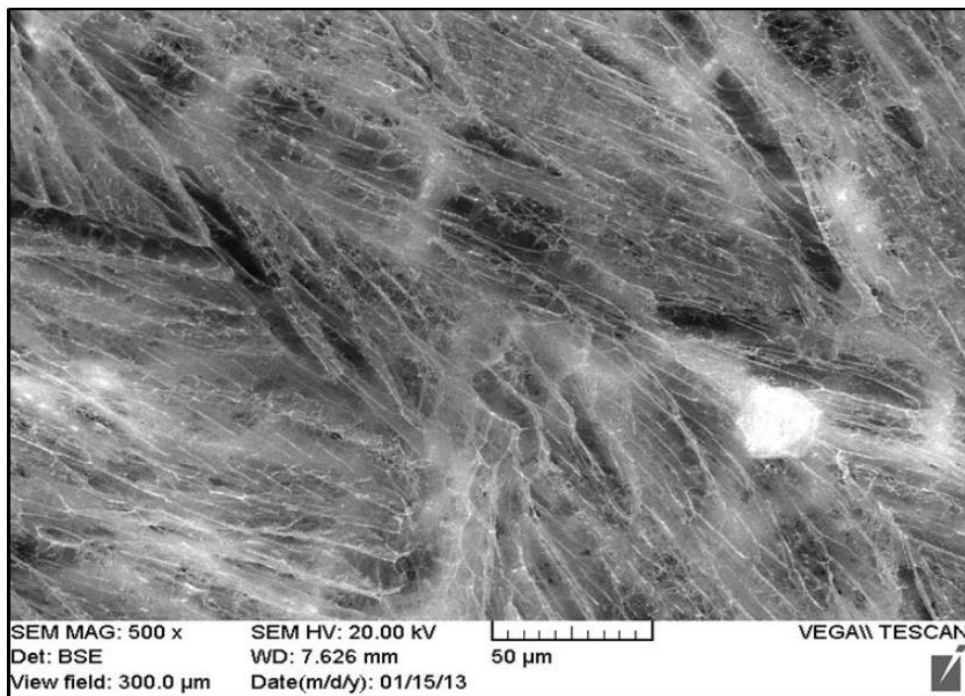


Figure 2-19: SEM of A3338 Polymer (Mizani 2016)



### 2.4.1 PAM Degradation

The degradation of commercially available polymers has been largely studied because of their use in enhanced oil recovery. Three degradation mechanisms were identified in literature: main chain scission, depolymerization to monomer or other low molecular weight fragments, or it may degrade by loss of its ionic functionality (Gurkaynak et al. 1996).

The main degradation pathways are:

1. Chemical degradation – the breakdown of the polymer molecules, either through short-term attack by contaminants, such as oxygen, or long-term attack of the molecular backbone by processes such as hydrolysis.
2. Mechanical degradation – the breakdown of the molecule as a result of high mechanical stresses.
3. Biological degradation – the microbial breakdown of macromolecules.

To accelerate the degradation of the polyacrylamide polymer, the chemical and biological degradation pathways were selected for this research. The most straightforward method to accelerate the chemical degradation via hydrolysis of the polymer is subjecting it to elevated temperatures (Swiecinski et al. 2016).

#### 2.4.1.1 Chemical and Thermal Degradation

Significant research was conducted in the 1980s to understand the mechanism of the hydrolysis of polyacrylamide and the resulting polymer structures (Truong et al. 1986, Yasuda et al. 1988). The primary degradation pathway of polyacrylamides is the hydrolysis of the acrylamide and other hydrolysable groups on the polymer backbone (Swiecinski et al. 2016). Chemical methods such as ozonation (Kaiser and Lawrence 1977, Soponkanaporn and Gehr 1989) and chlorination (Suzuki et al. 1979, Soponkanaporn and Gehr 1989) reduce the size of high molecular weight PAMs. The reactions of ozone with polymers are first order. However, the reaction rate of polyacrylamide was found to be almost zero, except in presence of a base and/or UV light (Suzuki et al. 1979). Chlorination can result in the production of organic halides from the reaction between PAM and the chlorine (Soponkanaporn and Gehr 1989). Degradation rates have been shown to in (Soponkanaporn and Gehr 1989) crease with decreasing polyelectrolyte concentration, increasing pH and increasing temperature. It was found that the polymer degraded faster at a pH of 9 than a pH of 6 or 3 (Soponkanaporn and Gehr 1989).

Thermal stability of the acrylic backbone can be observed viscometrically (Levitt and Pope 2008). Meaning, that at room temperature, any change in viscosity can be attributed to change in molecular weight distribution of the polymer. Andrews et al. (2016) illustrated that the monomer sequencing of the hydrolyzed polymers with the same level of hydrolysis will be the same regardless of the temperature of hydrolysis; proving that accelerated aging of polymers at high temperatures yields the same results as long-term aging at lower temperatures. Extensive research has been completed to investigate the thermal stability of polyacrylamides because of their use in the enhanced oil recovery industry. A variety of temperatures have been employed, ranging from 60 to 500 degrees Celsius (e Silva et al. 2000, Swiecinski et al. 2016). One study showed that the hydrolysis rate progressed slowly once the acrylate content of the polymer reached 45%. A 3.5% sea salt deuterium oxide solution was pipetted over the polymer to create a mixture of about 4% polymer solids. It took over 675 days at 60°C for the mole percent of acrylamide to decrease from 70% to 45%. Faster degradation results were obtained at 91°C, where the mole percent of acrylamide decreased from 70 to 20 in 510 days. The mole percent of acrylamide decreased significantly in the first 21 days of heating at a temperature of 91°C. It is important to note that the concentration of polymer used in this study is significantly higher than those used in the oil sands industry (4% polymer solids versus 0.085% in flocculated FFT). Results from the above study are shown in Figure 2-20. While results are not directly comparable to the thermal degradation of polymers in oil sands tailings, they do show the ability to simulate aging through rapid thermal degradation of polyacrylamide.

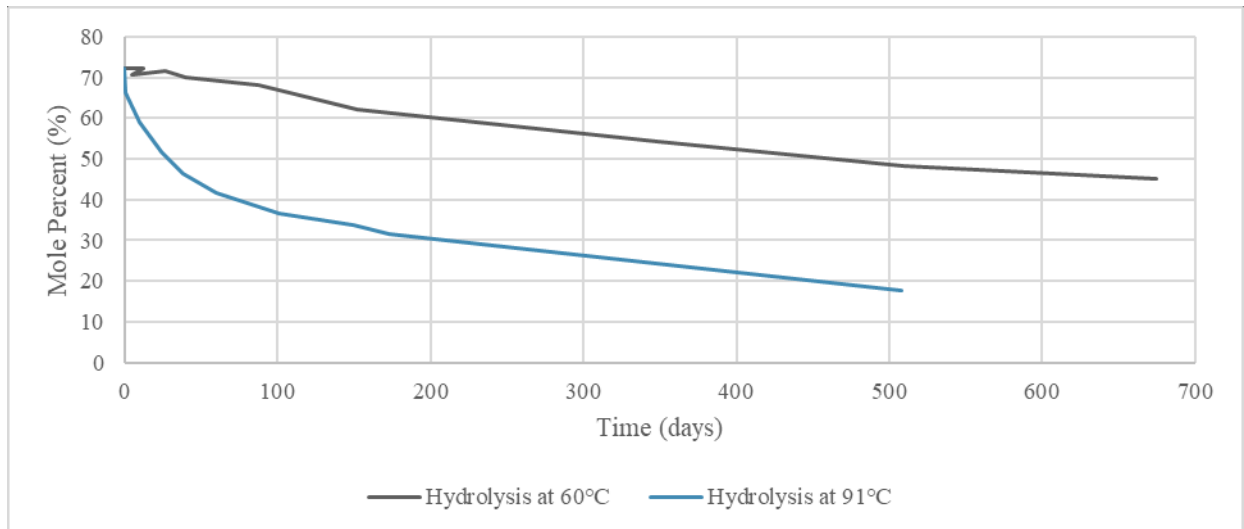


Figure 2-20: EOR980 acrylamide hydrolysis (modified from Andrews et al. 2016)

A method was developed to reconstitute an aragonite soil using synthetic flocculants by (Mao and Fahey 1999). This study used synthetic flocculants to achieve higher void ratios that were more representative of in-situ void ratios of 100 m deep calcareous soil deposits. When samples were reconstituted by sedimentation and reconsolidation, they were unable to reach the same void ratios at equivalent effective stress levels. The process involved sedimenting the soil in water containing a synthetic flocculant. The result was a soil with void ratios equivalent to those of the undisturbed samples at corresponding effective stress levels. After the samples were ‘locked into place’, they cured the samples using a heat treatment to remove the flocculant from the sample. It was inferred that the flocculant was no longer required for maintaining the soil structure once the structure had been ‘locked into place’ by consolidation, and that removing it in some way might reduce the strength back to that of the natural soil. In this study, various methods were considered to either leach out the flocculant, or break it down, without affecting the structure of the soil. Experiments with flocculant-water mixtures were undertaken and it was found that a temperature just under boiling point appeared to achieve full breakdown in a very short time. The samples were immersed in water and then the water was gradually increased to between 80°C and 90°C using an electric immersion heater. The water was maintained at this temperature for at least 12 hours and then gradually decreased back to room temperature. As anticipated, Mao and Fahey (1999) found that the untreated flocculated sample had additional strength in both monotonic and cyclic tests, however, the polymer degradation process appeared to remove the strengthening effect.

### 2.4.1.2 Mechanical Degradation

Mechanical/physical degradation is frequently called shear degradation in literature. Synthetic polymers, like polyacrylamide, have shown to be very sensitive to shear degradation. The process typically occurs rapidly in a high flow rate region (Sorbie 1991). Degradation is much more severe at higher flow rates, and longer flow distances. The degradation process breaks the large molecules up into smaller fragments and thus changes the molecular weight distribution of the polymer. The main factor that affects a polymers mechanical stability is the molecular type in terms of whether it is a flexible coil molecule or a structure with a more rigid molecular backbone, shown in Figure 2-21.

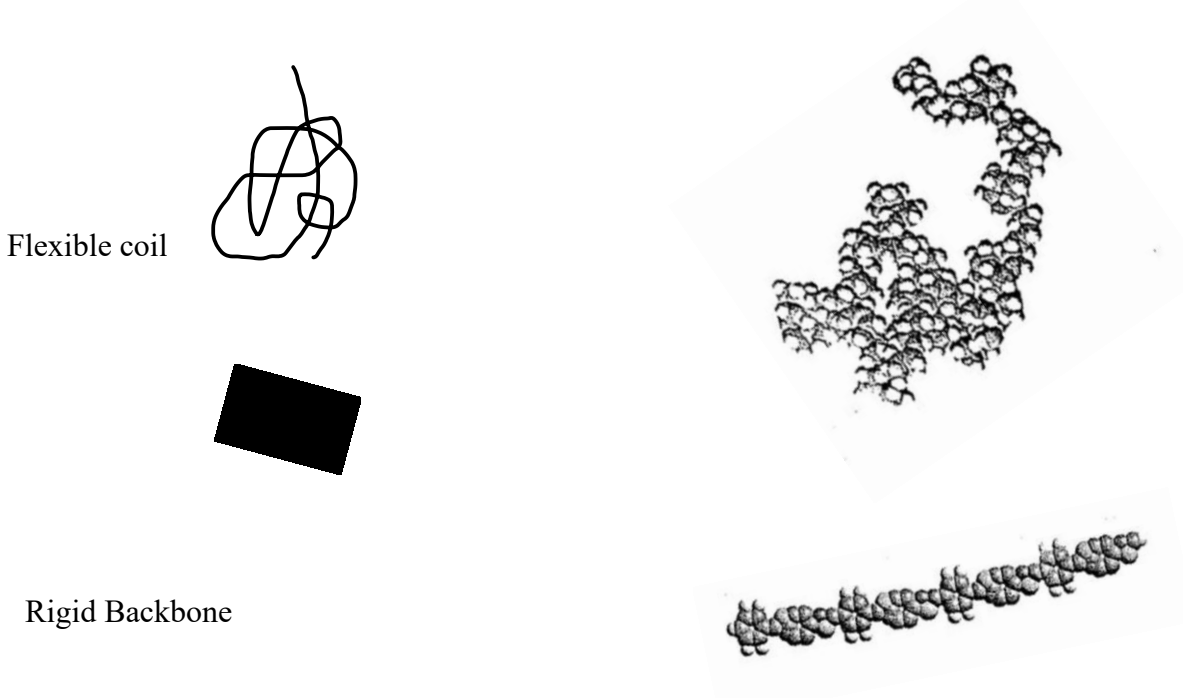


Figure 2-21: Polymer conformation that affect mechanical stability

Synthetic polymers such as polyacrylamide, are known to be very sensitive to shear degradation (Sorbie 1991). Significant research has been undertaken in the oil sands industry to understand mechanical degradation of polymer amended oil sands tailings. Mizani (2016) studied the behavior of the microstructure of polymer amended oil sands tailings during deposition and focused on the arresting behavior. It was found that the arresting yield stress was much smaller than the initial yield stress, due to the destruction of structure under shear. Despite the tailings

experiencing significant structural degradation, they recovered substantially under lower stress levels and over time (Mizani 2016). De-structuration was found to be reversible, and therefore, the benefit of the polymer was retained under most deposition scenarios. Due to the apparent reversible nature of mechanical degradation of polymer amended tailings, this method was not selected.

#### *2.4.1.3 Biological Degradation*

Early research involving the biological degradation of polymers by microorganisms was limited in terms of the degradation process because the objective was to simply prevent damage by adding a biocide. Unlike the other degradation pathways, the biological pathway has not been fully characterized under aerobic or anaerobic conditions (Haveroen et al. 2005). By the 1980s, researchers knew that aging of aqueous solutions of polyacrylamide was probably the result of microorganisms when the addition of a small amount of an antimicrobial agent halted the process (Chmelir et al. 1980).

More recent studies have investigated polyacrylamide as an organic nitrogen source for soil microorganisms. It was found that PAM was utilized as sole nitrogen (N) source, but not as sole carbon (C) source (Kay-Shoemake et al. 1998). This indicated that that PAM may be converted into long chain polyacrylate. Other studies have suggested that PAM may be metabolized into propionate, and finally CO<sub>2</sub> and ammonium (Haveroen 2005). A study was undertaken to investigate the activities of oil sands microbial consortia in the presence of polyacrylamide or acrylamide under sulfate-reducing, methanogenic, and simulated environmental conditions by several environmental microbial consortia (Haveroen 2005). Results showed that when supplied as a nitrogen source, polyacrylamide significantly enhanced methanogenesis, but under sulfate-reducing conditions, no conclusions could be drawn (Haveroen 2005). Viscosity is commonly used to measure PAM degradation, so attempts were made to determine if viscosity was reduced in the viable culture when compared to the killed control in this same study. It was found that the viscosity of the viable culture was significantly less than that of the killed control, indicating that some degree of polymer degradation has occurred (Haveroen et al. 2005).

## **2.5 Rheology in Tailings Management**

Rheology is a branch of the natural sciences that emerged more than 80 years ago (Malkin and Isayev 2006). It is traditionally defined as the study of deformations and flow of matter;

however, rheological studies are not focused on “deformation and flow”, but rather the properties that determine its behavior (Malkin and Isayev 2006). In practice, oil sands tailings are characterized by yield stress (Mizani 2016). Yield stress is the stress that must be exceeded for the fluid to flow. From previous studies it has been found that the yield stress that characterizes when gold tailings start flowing, can be drastically different from the yield stress that characterizes when those same tailings will stop flowing (Mizani et al. 2013). This distinction is also relevant for yield stress of oil sands tailings and is an important design parameter (Mizani 2016).

The rheological behavior of polymer amended oil sands tailings can explain the microstructure under shearing and resting conditions. For this study, it is important to understand the possible changes to the microstructure when the polymer degrades.

#### 2.5.1 Effect of Microstructure on Rheology

Materials are naturally oriented in a state that is a function of its minimum energy. When an external force is applied to a system, it will resist deformation by showing resistance as a form of viscosity or yield stress (Chhabra and Richardson 2008). As the external force is applied to a system, the microstructure will change to; align in the direction of flow, stretch, deform, or disintegrate. Disintegration occurs when aggregates return to primary particles. These changes are illustrated in Figure 2-22 as it goes from a state of rest, to one of motion.

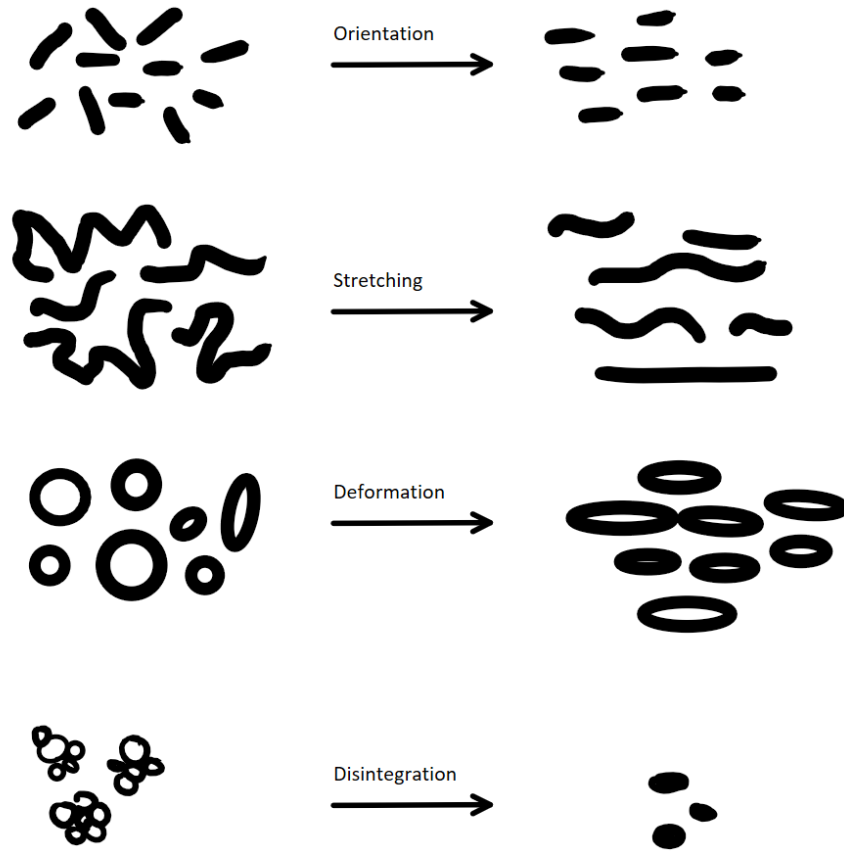


Figure 2-22: Microstructures at rest and in flow (Modified from Chhabra and Richardson 2008)

Each of these microstructures will result in different rheological behaviors. Microstructures and therefore the observed behavior can oftentimes be modified for different purposes. In the case of kaolin clay, it is easy adjusted by changing the pH or adding a flocculant. Adjusting parameters such as the additive or mixing conditions can result in aggregates of many forms, as seen in Figure 2-23. These different forms will have drastically different rheological behaviors. For example, a dispersed form will have a much lower viscosity and yield stress than the face-face or edge-face form.

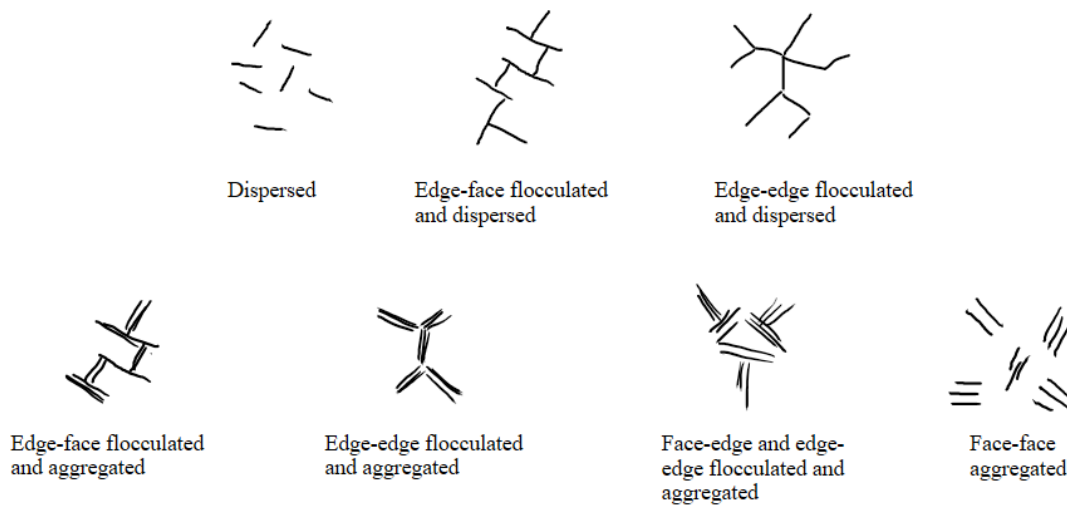


Figure 2-23: Agglomerate forms in kaolin suspensions (redrawn from Chhabra and Richardson 2008)

Like kaolin, the rheological behavior of oil sands fine tailings is altered by adjusting the pH or adding a flocculant. Typically, gypsum and/or polymeric flocculants are used in the industry, as discussed in Section 2.3 to change the rheological behavior. Naturally, oil sands tailings have a dispersed form and become edge-face flocculated and dispersed with the addition of a polymer (Jeeravipoolvarn 2010).

Polymeric systems exhibit complex rheological characteristics. These systems have special properties such as visco-elastic, shear-thinning, strain hardening, and time-dependence (thixotropy). These properties stem from the ability of macromolecules to interact, to entangle, and to knot up with their neighbor (Chhabra and Richardson 2008). These properties in have been studied extensively (Mewis and Spaul 1976, Mizani 2016). Mizani (2016) found that the rheology of polymer amended tailings is dependent on shear thinning and thixotropic behavior.

### 2.5.2 Shear Thinning and Thixotropy

Shear thinning is used to describe fluids whose viscosity decreases under shear strain. This behavior is often seen in polymer solutions and complex fluids.

Thixotropy is a time-dependent shear thinning property. These types of materials will experience a decrease in viscosity under shear strain and then will return to a more viscous state in a fixed time. The material loses structure when subjected to shear, and then rebuilds itself under low or no shear (Mitchell and Soga 2005). Mitchell and Soga (2005) use a ratio of the aging strength



( $S_A$ ) to the remolded strength ( $S_R$ ) to describe thixotropic strength. Thixotropy can be simplified into a process of aging and remolding, shown in Figure 2-24.

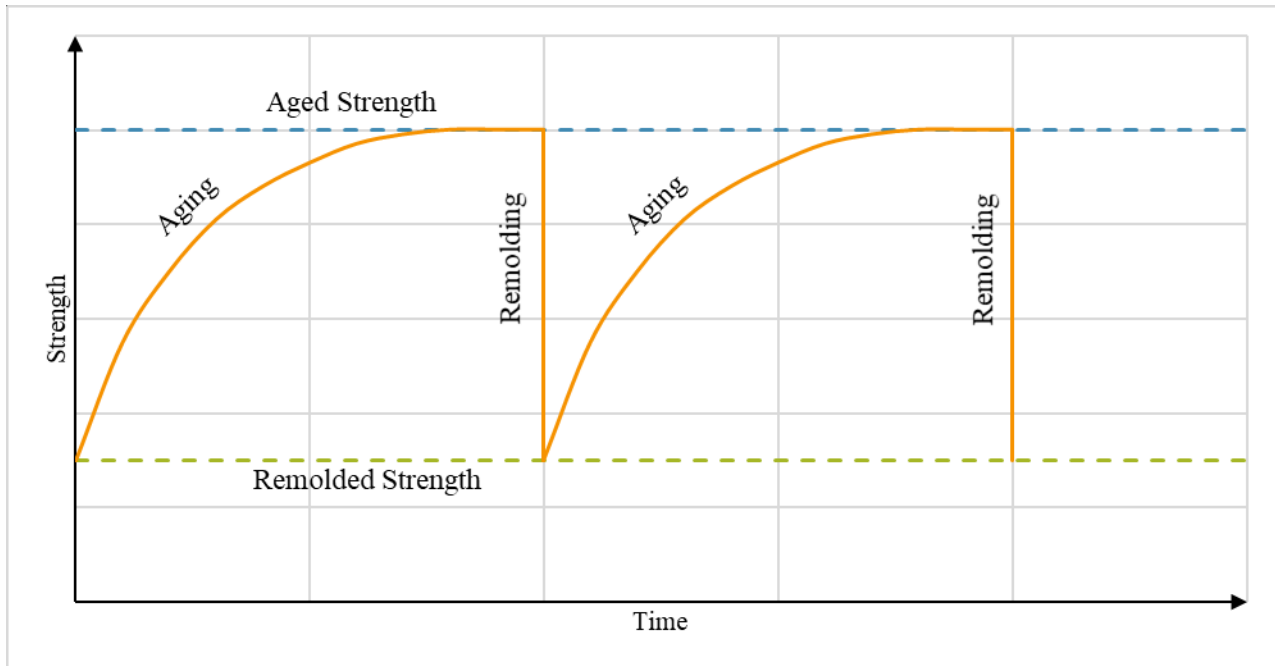


Figure 2-24: Illustration of thixotropic material (Modified from Mitchell and Soga 2005)

Oil sands fine tailings are comprised of mostly kaolinite, and smaller amounts of illite. Kaolinite is known to show no thixotropy, and illite shows only moderate recovery of strength – it is therefore expected that tailings would not be thixotropic (Skempton and Northey 1952). As discussed in Section 2.5.1, extensive laboratory programs have shown that the rheology of polymer amended tailings is dependent on shear thinning and thixotropic behavior (Mizani 2016).

### 3 Laboratory Methods

This chapter describes the methods used in the laboratory program. Two main methods were used to cure the polymer amended tailings. The first method was based largely on research by Mao and Fahey (1999) and involves the use of heat to degrade the polymer. Tailings were placed in a water bath at approximately 90°C for approximately 48 hours. The second method explored the use of a commercially available bacterium to degrade the polymer within the amended tailings. Multiple doses and retention times were explored.

#### 3.1 Materials Used in Laboratory Program

The materials used in this study are Edgar Plastic Kaolin (EPK) clay, flocculated centrifuged tailings product (centrifuge cake) and flocculated FFT.

The clay-sized fraction of FFT consist of mainly kaolinite, with small amounts of illite, montmorillonite, chlorite, and mixed-layer clays. Kaolinite and FFT were selected to determine if the heating process was changing the structure of the clay mineral in the centrifuge cake and FFT. Kaolinite was also selected because it has been found to exhibit almost no thixotropy (Skempton and Northey 1952).

The centrifuge cake used in the laboratory program was provided by an oil sands mine operator. It was treated with a flocculant and gypsum ( $\text{CaSO}_4$ ) on site prior to centrifugation and then shipped to the University of Alberta Geotechnical Center. All tests were undertaken on as-received tailings. Untreated FFT was also provided by the Oil Sands Tailings Research Facility (OSTRF). These tailings were selected to keep the polymer type and dose consistent throughout testing.

##### 3.1.1 Flocculated Tailings Preparation

In order to prepare flocculated tailings, the first step is to condition the polymers at the right concentration so that they become readily miscible with the tailings. For this research, 0.4% w/w was selected based on previous research (Fisseha 2020). The A3338 flocculant solution was prepared by dissolving 4 g of dry flocculant in 996 g of distilled water. The solution was prepared at least 24 hours before use and was not used if it was more than 2 weeks old.

To prepare the flocculated FFT, a homogenous mixture of FFT was mixed using as-received tailings and reclaim water, to not alter the chemistry. Mixing times and speeds were selected to ensure floc structure was not disturbed.

It is important to note that the polymer dosage is calculated based on the tailings solids and not the total tailings mass. For a predetermined mass of FFT, the required mass of polymer solids for tailings treatment was calculated based on the tailings solids content and the respective dosage. For this research, the tailings mixed at a dose of 850 g per tonne based on published data from Salam et al. (2018).

$$M_{floculant\ solution} = \frac{M_{FFT} * \% solids * 850\ g/tonne}{0.4\% w/w\ polymer} \quad (6)$$

Where:

- $M_{floculant\ solution}$  is the mass of the flocculant solution to be added;
- $M_{FFT}$  is the total mass of the FFT; and
- $\% Solids$  is the solids content of the FFT.

The flocculant was incorporated into the FFT using the following procedure (Fisseha 2020): (1) a known mass of 35.5% solids FFT was placed in a 5-gallon pail; (2) a 4-blade impeller was submerged into the tailings (Figure 3-1); (3) the FFT was mixed at a speed of 250 rpm to homogenize the mixture; (4) the desired mass of flocculant solution was added and directed near the impeller during mixing; (5) the mixture was mixed for 10 seconds; (6) the impeller was removed and the sample was left to rest for 30 minutes; and (7) the released water was decanted using a plastic syringe.

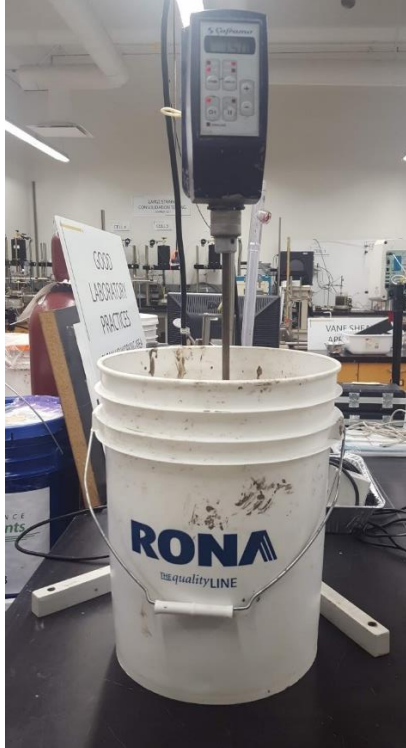


Figure 3-1: Mixing apparatus



Figure 3-2: Tailings mixing



Figure 3-3: Flocculated tailings

Figure 3-3 shows the initial condition and fabric of the flocculated tailings. The flocculated tailings had medium sized flocs with a jelly appearance similar to that of cottage cheese. The release water is mainly due to the increased hydraulic conductivity of the FFT.

### 3.2 Tailings Characterization

The following geotechnical index properties were measured where applicable to help classify material behavior:

- Bitumen content;
- Water content;
- Specific gravity;
- Particle size distribution;
- Atterberg limits;
- Mineralogy;
- Methylene blue index (MBI); and
- Scanning electron microscopy.

Bitumen content was determined using the Dean Stark analysis method and completed by AGAT Laboratories Ltd on untreated FFT and centrifuge tailings samples to determine the bitumen, mineral solids and water contents of the tailings. The laboratory technicians followed ASTM standards and accepted lab practices. A detailed procedure is given in Appendix A.

Water content is also referred to as moisture content and is defined as the ratio of the weight of water to the weight of solids in a given volume of soil. It was determined according to the ASTM D2216-10, where it was dried at 110°C for 24 hours.

Specific gravity is defined as the ratio of the unit weight of a given material to the unit weight of water. It is a vital parameter when determining other geotechnical parameters such as void ratio and dry density. It was determined according to ASTM D854-14 using vacuum deairing. A detailed procedure is included in Appendix A.

A hydrometer test was performed according to ASTM D422-63. This was used to determine the particle size distribution of the sample. A detailed procedure is included in Appendix A.

Atterberg limits are the basic measure of the critical water contents of a fine-grained soil. The plastic and liquid limits of the untreated and amended FFT (including bitumen) were analyzed by AGAT Laboratories Ltd. The liquid limit was determined using the Casagrande cup method. The ASTM D4318-17e1 outlines the procedure for determining the liquid and plastic limit of tailings.

X-ray diffraction (XRD) is a nondestructive analytical technique that was used to quickly obtain the mineralogical composition of tailings. The analysis was completed by AGAT Laboratories Ltd on untreated FFT samples. The laboratory technicians followed ASTM standards and accepted lab practices.

MBI is a relatively simple index test that provides an indication of clay content and activity. The test has been used in the oil sands for over 30 years (Kaminsky 2014). The test measures how much methylene blue dye can be absorbed by a sample as determined by a titration test. Tests were completed at AGAT Laboratories Ltd.

### 3.3 Large Strain Consolidation Testing

Large strain consolidation (LSC) was used to consolidate the tailings to a variety of void ratios to simulate tailings at different depths in a deposit.

#### 3.3.1 LSC Setup and Sample Preparation

LSC was performed in a standard consolidation apparatus (150 mm dia. X 150 mm height). The initial setup of the sample can be seen in Figure 3-4 and was based on previous works (Suthaker and Scott 1994, Scott et al. 2008, Jeeravipoolvarn 2010).

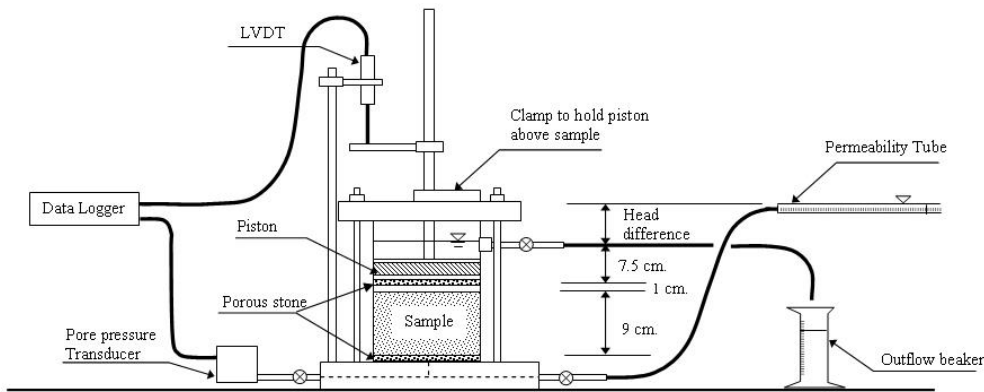
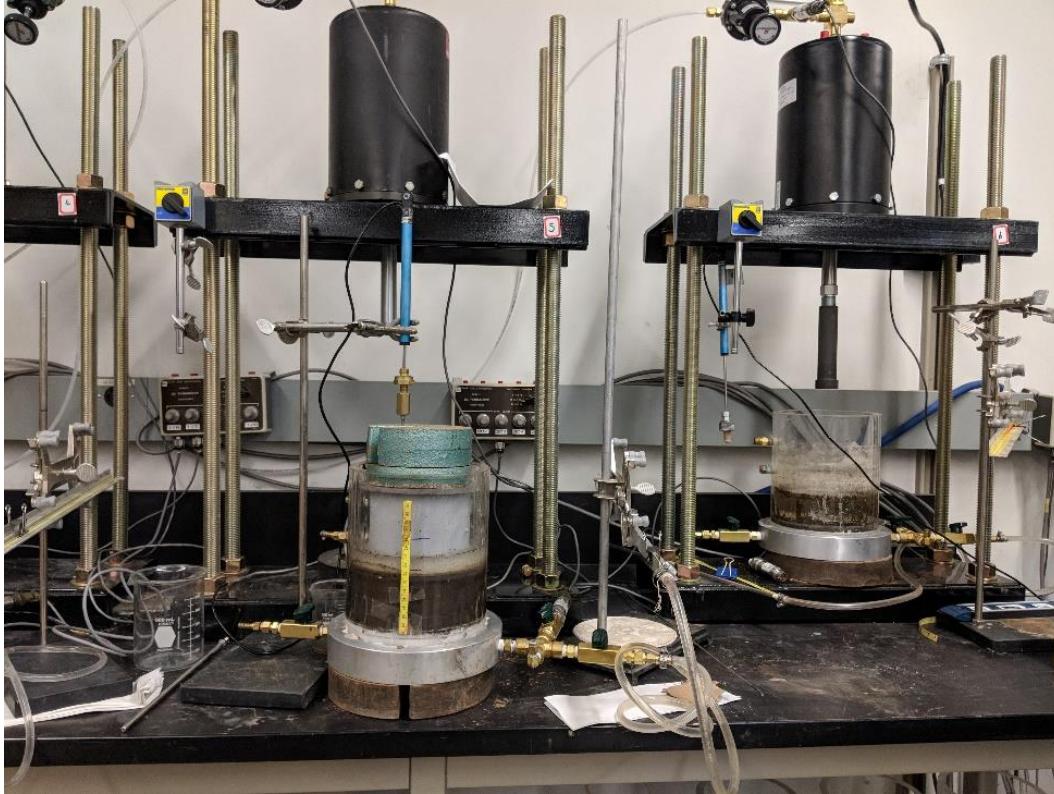


Figure 3-4: Initial set up of the large strain consolidation test before loading sample

The metal base is fitted with three valves for the purpose of pore pressure measurement, hydraulic conductivity measurement, and the third for deairing. A fourth outlet is located at the top of the cell to ensure a constant head is provided above the sample. A porous stone as shown in Figure 3-4, was placed at the bottom of the cell to control and evenly distribute water flow through the bottom of the sample. For the purpose of sample separation and filtration, a 0.22-micron pore size filter paper is placed atop the porous stone. The cells are then flushed with distilled water and filled with the tailings sample. Another porous stone is placed on top of the sample. The total pore pressure is measured with a pressure transducer connected to an electronic data logger.

The apparatus consists of a regulated pressurized air bellofram seated on a loading frame. The cell is placed within the apparatus and effective stresses are applied to the sample in the cell. Settlement is measured with a linear variable differential transformer (LVDT) and pore pressures are measured with pore pressure transducers.

The apparatus used in the laboratory program confines the slurried material, so it can be tested at any water content. The centrifuge cake was placed in the cell and monitored until pore pressure was dissipated - known as self-weight consolidation. The first applied stress was about 0.1 kPa. Subsequent dead loads were approximately doubled for each load step, up to 6.6 kPa on cells 4 and 5 seen in Figure 3-5.



*Figure 3-5: LSC cell 5 with dead loads acting on the piston*

Effective stresses over 12 kPa were applied in a loading frame by an air pressure Bellofram. Subsequent loads on cell 3 were doubled with the loading frame for each load step, between 12 and 24 kPa. The Bellofram setup can be seen in Figure 3-6.



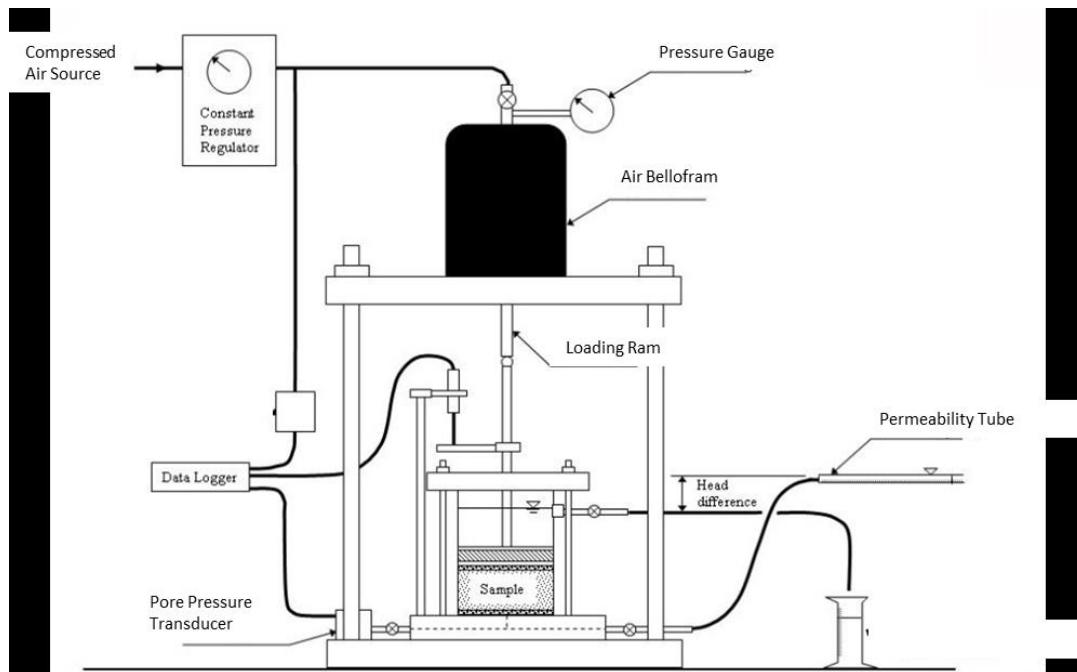


Figure 3-6: Schematic of cell 3 in loading frame and loaded up to 24 kPa

When a load was applied, the progression of consolidation was evaluated by monitoring the change in height of the sample using a LVDT and by measuring pore pressure dissipation at the bottom of the sample.

### 3.3.2 Criteria for End of Consolidation

In this research, the end of consolidation for each load step was determined by the following indicators:

1. Vertical deformation under the applied load was infinitesimal; and
2. Excess pore pressure as a result of the applied load was entirely dissipated.

### 3.3.3 Hydraulic Conductivity Measurement

At the beginning of the experiment, the saturated hydraulic conductivity was approximated from the following equation (Scott et al. 2008):

$$v_s = -\left(\frac{\gamma_s}{\gamma_w} - 1\right) \frac{k}{1 + e} \quad (7)$$

where:

$v_s$  = initial settling velocity,  
 $\gamma_s$  = unit weigh of solids,  
 $\gamma_w$  = unit weight of water,  
 $k$  = hydraulic conductivity, and  
 $e$  = initial void ratio.

During consolidation, the constant head permeability setup was used to calculate the saturated hydraulic conductivity of the sample. The setup consisted of a 4 mm glass tube connected to the bottom outlet of the cell with a transparent flexible tube. A measuring tape was placed under the horizontal tube. The glass tube was clamped horizontally at a height above the LCS cell to establish a constant head between the glass tube and the water surface level in the cell. The saturated hydraulic conductivity was experimentally determined using the follow process:

1. the port and tubes were deaired by allowing downward seepage through the cell;
2. the glass tube was filled with distilled water and clamped horizontally;
3. it was insured that the water level in the cell was at the level of the constant head port;
4. the height of the glass tube was adjusted until an upward flow through the sample was observed;
5. once the flow rate steadied, the height of the glass tube, water level in the cell, and measurement along the glass tube were taken at two time intervals.

Using the collected data, Darcy's law was used to calculate the saturated hydraulic conductivity. It was insured that the hydraulic gradient was kept small enough to avoid creating a seepage failure.

## 3.4 Polymer Degradation Testing

### 3.4.1 Thermal Degradation Methodology

As discussed in Section 2.4.1, polymer degradation can be caused by chemical and thermal processes, mechanical shear and/or biological attack. The thermal degradation pathway was selected for this research, as it is the most straightforward (Swiecinski et al. 2016). Previous research suggested that accelerated aging of a polymer at elevated temperatures will result in a polymer with structure similar to an extended aging process at lower temperatures (Swiecinski et

al. 2016). Therefore, an elevated temperature below the boiling point of water was selected to heat the tailings samples.

A water bath was constructed for heat treatment. It consisted of:

- A large, glass tub;
- 2 flexible silicone rubber heaters;
- 1 Omega iSeries temperature control box;
- 1 thermistor; and,
- 1 mechanical stirrer.

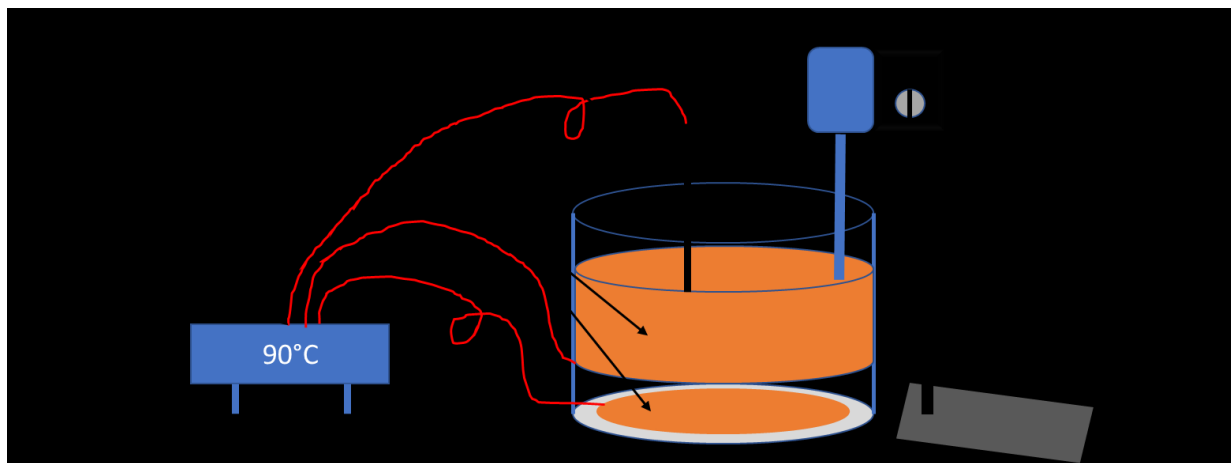


*Figure 3-7: Schematic of heating bath*

The glass tub had a diameter of approximately 40 cm and a height of 30 cm. Water levels were maintained at approximately 20 cm from the base.

Andrews et al. (2016) found that the hydrolysis rate begins to decrease when the acrylate content of the polymer reaches about 45% as seen in Figure 2-20. Due to time restraints, complete hydrolysis could not be accomplished as it could have taken more than 600 days. Therefore, samples were aged at between 85°C and 95°C for 30 days – where we expected about 50% degradation. Complete hydrolysis was also not necessary to reduce the effects of the polymer in the tailing's samples. Several problems were encountered with the heating period of 30 days. It was difficult to keep the moisture content of the tailing samples constant which has a great impact on the undrained shear strength as seen in Figure 2-5.

Since we were unable to keep the moisture content constant, a shorter method of degrading the polymer was investigated. A method of reconstituting an aragonite soil using a synthetic flocculant was developed by Mao and Fahey (1999). They created the structured soil and then degraded the polymer using a heat treatment. After a multitude of trials, researchers selected a temperature just under boiling. This was selected as it reduced the viscosity of the polymer mixture back to that of water. Their soil-polymer samples were consolidated and then extruded into a larger-diameter tube and immersed in water. The temperature of the water was then gradually increased to between 80°C and 90°C using an electric immersion heater. The samples were kept in water maintained at that temperature for at least 12 hours. The temperature was then gradually decreased back to room temperature. The remaining samples were heat treated using the methodology of (Mao and Fahey 1999).

In this research, tailings samples had a larger diameter, so the heating time was increased from 12 hours to 48 hours after several trials. Results from the timed test are displayed below in Figure 3-8. Changes in moisture content were a concern in this laboratory program because oil sands fine tailing experience large changes to shear strength, with small changes in moisture content. To determine the optimum time to heat the tailings, a series of tests were completed on FFT (not polymer treated).

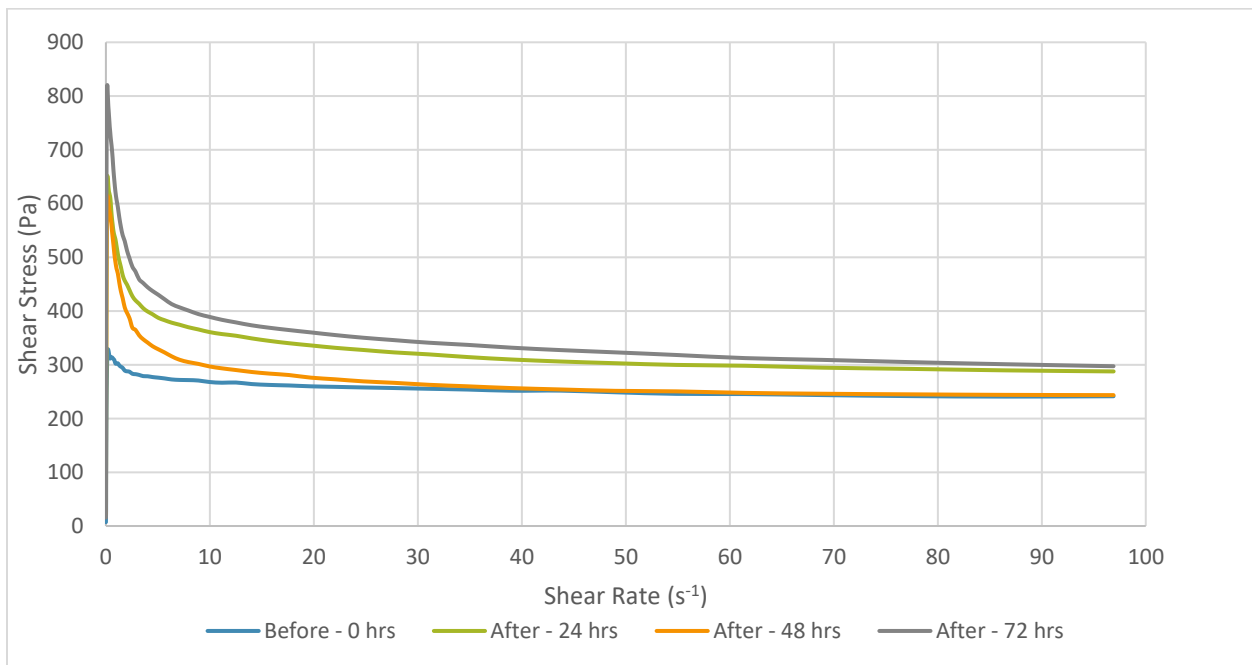


Figure 3-8: Time test on FFT

All the samples experienced a reduction in moisture content between 5 to 13% as seen in Table 3-1. This change in moisture content likely explains the increase in peak shear stress in the heat-treated samples. The sample heat treated for 48 hours showed a decrease in strength at shear rates greater than  $4 \text{ s}^{-1}$  even though the moisture content dropped from 90% to 85%. Based on these tests, 48 hours was selected for heat-treatment.

*Table 3-1: Moisture content results from time tests*

Heat-treatment Time	Initial Moisture Content	Final Moisture Content	Change in Moisture Content
<b>24 hr.</b>	90%	84%	6%
<b>48 hr.</b>	90%	85%	5%
<b>72 hr.</b>	90%	77%	13%

### 3.4.2 Bacterial Degradation Methodology

Bacterial degradation pathway was explored using a commercially available bacterium. It is sold under the name ‘Frac-Bac’ and was provided for this research by Re-Nuu Production Optimization Inc. This bacterium was selected as it is known to degrade polyacrylamide polymers. A natural bacterium was not selected at this time as the objective of the research was to rapidly degrade the PAM.

As instructed by the supplier, the bacteria were mixed in with the tailings sample at a dose of 10000 ppm by volume. Additional doses were tested at 5000, 10000, 15000 and 50000 ppm. The samples were incubated at room temperature for 30 days before testing.

A limited amount of bacterium was provided, so smaller, qualitative samples were prepared for the first round of testing to best determine a good dose for the remaining tests. The highest dose was selected as it appeared to have the greatest degradation.



Figure 3-9: Qualitative - bacteria treated samples after 30 days of incubation at room temperature

The final round of testing included four samples for each tailings type. Three of the tailing's samples were treated with Frac-Bac, and one was left untreated. All samples were incubated at room temperature for 30 days.

### 3.5 Rheology

For all materials with strengths below 1 kPa, the Malvern Kinexus Lab+ rheometer was used to determine rheological parameters, shown in Figure 3-10. This rheometer was able to measure both viscosity and viscoelastic parameters of the given materials. Viscosity is defined as a material's resistance to deformation and is a function of shear rate, with time and temperature dependence. The shear ramp tests in this study were completed with shear rates between 0.1 and 100  $\text{s}^{-1}$  over the span of 5 minutes. Viscoelasticity is a property of a material that exhibits both viscous and elastic characteristics. Measurements of the shear modulus,  $G'$ , and  $G''$  were also collected as they are important for characterization.



Figure 3-10: Kinexus lab+ rheometer

### 3.5.1 Wall Depletion Effects

Wall depletion effects, commonly referred to as “slip” occurs in two-phase or multi-phase liquids (ex. Solid-liquid) when they are being studied in viscometers and rheometers. It occurs because of the displacement of the disperse phase away from solid boundaries; resulting in a layer of lower-viscosity, liquid depleted material (Barnes 1995). When the low-viscosity layer forms at the boundary, any flow of liquid over the boundary is easier because of the lubrication effect, where is effectively “slips” over. The layer forms as a result of, steric, hydrodynamic, viscoelastic, chemical, and gravitational forces acting on the disperse phase immediately adjacent to the solid boundary. Slip is usually greatest at low shear rates. The effects are commonly experienced when you are using rheometers but often not appreciated in industry or

research. Strange breaks in flow-curves and differing viscosities from different-sized geometries are common indicators of slip. Oftentimes, yield stresses that are reported in literature are artifacts of slip that are not properly assessed.

Flocculated suspensions have been found to be particularly vulnerable to this phenomenon due to their complex nature (Barnes 1995). At rest and at low shear stresses, flocculated suspensions experience static and dynamic depletion effects. As shear rates are increased, and higher stresses are experienced, flocs begin to breakdown. As the floc size decreases, the static and dynamic effects causing the low-viscosity layer to form, decreases. Meaning that what was a large depletion effect at low shear rates, decreases to virtually nothing at high shear rates.

Vane-type geometries can lessen, or in some cases, eliminate the wall depletion effects. However, slip is an important phenomenon to consider when reviewing rheological data from a rheometer or viscometer.

### 3.5.2 Flow Curve

A shear rate ramp or flow curve is a graphical representation of how the shear viscosity changes when it is subjected to different shear rates or shear stresses. In this experiment, a stress was incrementally stepped logarithmically from a minimum value up to a value where the tailings start to flow. Each stress was held for an amount of time as determined by the accompanied software. A data point was taken when the shear rate reaches an equilibrium. Flow curves for all samples with peak shear stress less than 1 kPa were completed. Flow curves are typically undertaken on non-Newtonian fluids – i.e., viscosity is dependent on the applied stress. Figure 3-11 graphically displays the comparison between bingham, plastic, pseudoplastic, Newtonian, and dilatant fluids. Mineral tailings often display non-Newtonian flow behavior. They also possess a yield stress that must be exceeded before irreversible deformation and flow can occur (Boger et al. 2006). Oil-sands fine tailings typically follow the behavior of a Bingham fluid (Mizani 2016).



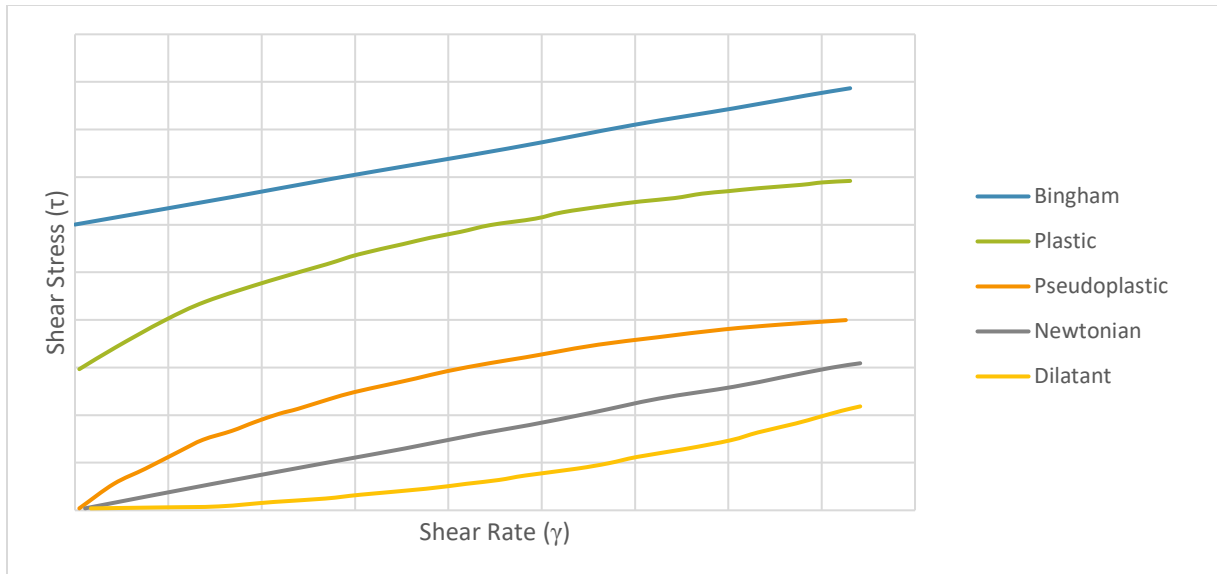


Figure 3-11: Typical flow curves

Undisturbed samples were loaded into the rheometer with a standard gap of  $1 \text{ mm} \pm 1 \text{ }\mu\text{m}$ . All tests were undertaken at room temperature with a Kinexus vane geometry to decrease wall depletion effects. The vane had a 14 mm diameter and a 21 mm blade length. The shear ramp range was selected based on the experience of the lab manager. Input parameters for the shear ramp tests are displayed in Table 3-2.

Table 3-2: Shear rate ramp input parameters

Parameter	Input
Shear rate range	$0.01 \text{ s}^{-1}$ to $400 \text{ s}^{-1}$
Run time	5 minutes
Samples per decade	20

The accuracy of the yield stress measured is dependent on the number of points per decade chosen. Collecting more data points per decade in a logarithmic test provides a more accurate yield stress if the material remains stable over the duration of the test. The number of samples chosen per decade was selected based on experience of the IOSI Lab Manager.

### 3.5.3 Amplitude Sweep

The dynamic oscillation strain sweep is an alternative method to analyze the yield behavior of oil sands fine tailings. In this experiment, the deflection of the measuring system is increased

stepwise from one measuring point to the next while keeping the frequency at a constant value. The results are presented as a figure with shear stress plotted on the x-axis and storage modulus  $G'$  plotted on the y-axis; both axes on a logarithmic scale as seen in Figure 3-12. The linear viscoelastic region (LVE region) indicates the range in which the test can be carried out without destroying the structure of the sample. The tests were undertaken at a frequency of 1 Hz. The strain was increased from 0.1% to 400%. This range was selected based on the results presented by Mizani (2016). Like the flow curve measurements, undisturbed samples were loaded into the rheometer with a standard gap of  $1 \text{ mm} \pm 1 \text{ } \mu\text{m}$ . All tests were undertaken at room temperature with a Kinexus vane geometry.

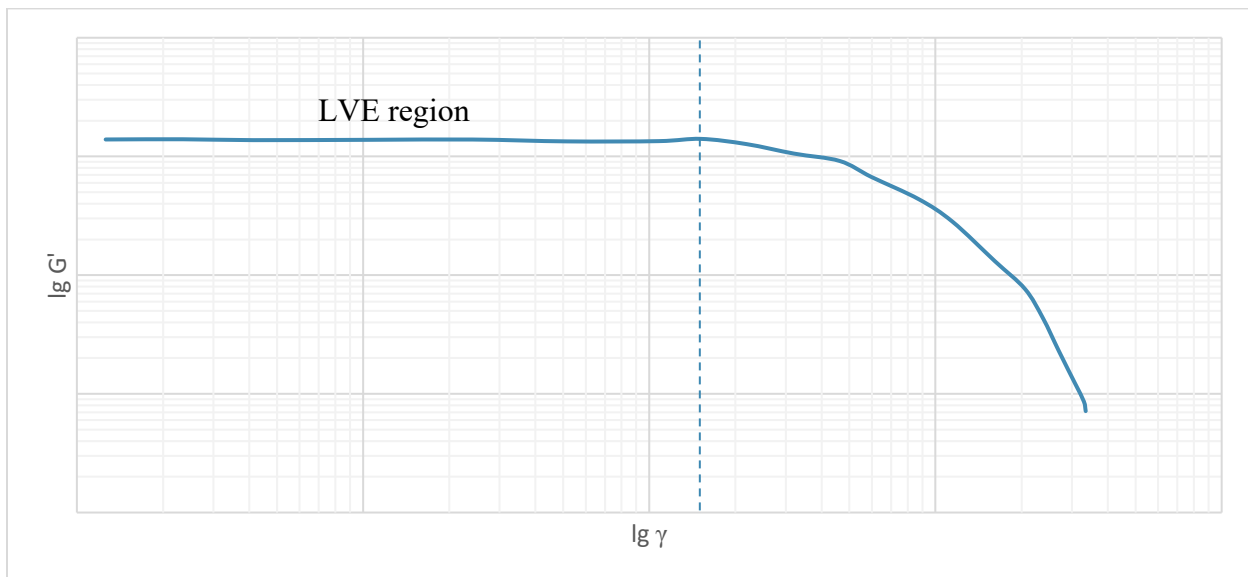
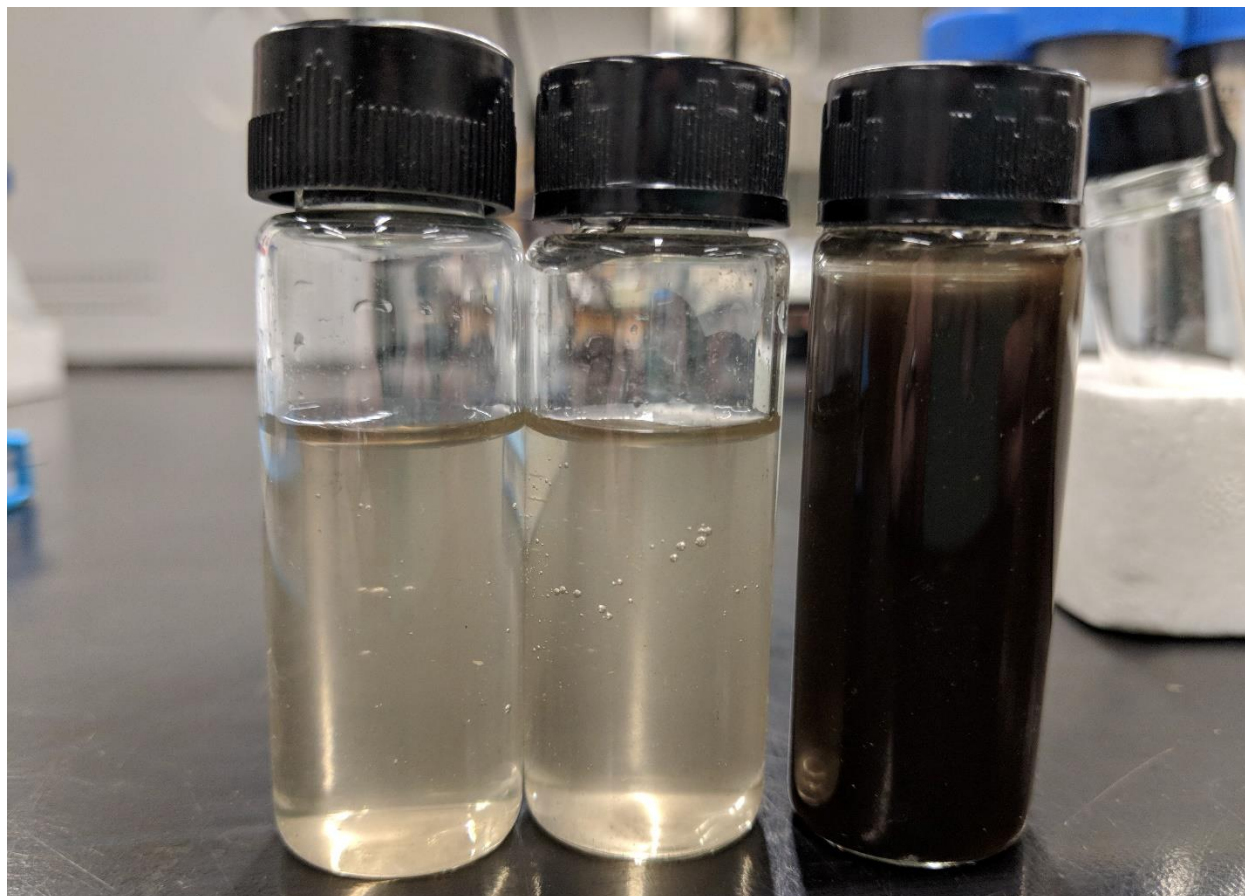


Figure 3-12: Typical results of amplitude sweep tests

### 3.6 Chemical Analysis

The hydrolysis of the polyacrylamide was of interest in this study over a range of temperatures. Taylor and Nasr-El-Din (1994) investigated a variety of techniques and found that  $^{13}\text{C}$  NMR was the most reliable method for determining the degree of hydrolysis of concentrated polymers. NMR was completed at the Nuclear Magnetic Resonance Spectroscopy (NMR) Facility in the Department of Chemistry at the University of Alberta. Before submission, samples of treated and untreated tailings were spun in a centrifuge to release the pore water within the samples. The pore water was then collected and sent for NMR analysis (Figure 3-13). Samples were submitted,

and experienced NMR facility staff prepared the samples, optimized the spectrometer, and completed the analysis.



*Figure 3-13: Pore water from heat treated sample, bacteria treated sample, and untreated FFT sample (L to R)*

The polymer concentrations were below detection limits in all the samples sent to the NMR facility, so no data was obtained.

### 3.7 SEM Imaging

Wet samples of untreated and heat-treated samples were sent to nanoFAB Fabrication and Characterization Facility for scanning electron microscopy (SEM) imaging of the tailings microstructure. The main purposes were to: (1) to determine if heat treatment effects the structure of the clay particles, and (2) to determine if and/or how degradation of polymer affects the morphology and arrangement of flocs in flocculated FFT.

The freeze-drying technique was conducted to preserve the original internal structure of the clay/FFT as opposed to the standard drying method. The samples were dried in a Savant

SuperModulyo Freeze Dryer. Using the Zeiss Sigma FESEM imaging tool, in-lens Field Emission SEM (FESEM) images of the freeze-dried samples were obtained at magnifications of 500x, 8,000x, and 20,000x.

## 4 Experimental Results

### 4.1 Index Testing

The following geotechnical index properties were completed where applicable to help classify material behavior:

- Atterberg limits;
- Bitumen content (mass bitumen/total mass);
- Methylene blue index (MBI)
- Mineralogy;
- Particle size distribution;
- Scanning electron microscopy;
- Specific gravity; and
- Water content.

Atterberg limits, bitumen content, and specific gravity of the kaolinite, centrifuge cake and FFT are presented in Table 4-1.

*Table 4-1: Geotechnical properties of materials used in the study*

Material	Specific Gravity	Bitumen (%)	Liquid Limit (%)	Plastic Limit (%)	Fines (%)	Clay (%)
<b>Kaolinite</b>	-	0.0	52	31	98	61
<b>Centrifuge Cake</b>	2.24	5.7	57	26	87	52
<b>FFT</b>	2.15	3.9	52	32	94	40

The grain size distribution of the kaolinite, centrifuge cake, and FFT are shown in Figure 4-1. Grain size was determined using wet sieves and hydrometer analysis.

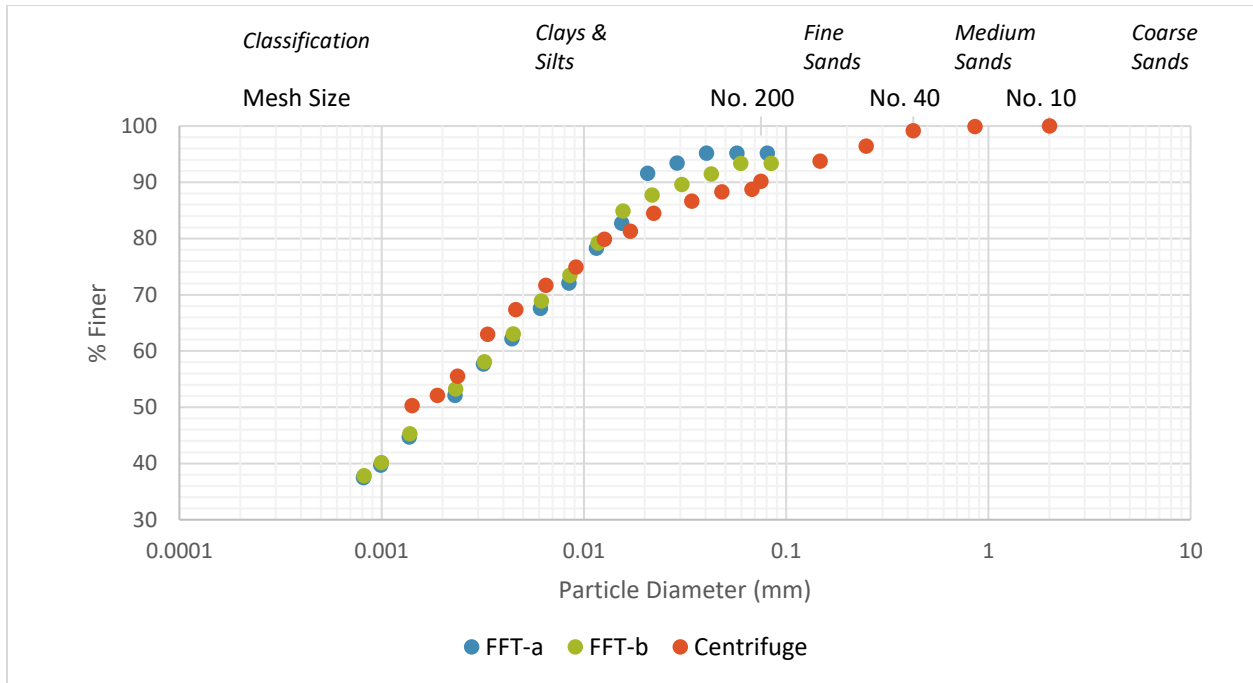


Figure 4-1: Grain Size Distribution

The MBI was determined for a sample of FFT and a centrifuge cake sample. The results are presented in Table 4-2.

The percent clay can also be estimated from the MBI using the following formula (Kaminsky 2014):

$$\% \text{ Clay} = \frac{MBI \left( \frac{meq}{100g} \right) + 0.04}{0.14} \quad (8)$$

Table 4-2: MBI results for centrifuge cake and FFT

Sample ID	Weight (g)		Methylene Blue	meq/100g	Estimated % Clay
	Recommended	Actual	Volume (mL)		
<b>Centrifuge Cake</b>	2.00	2.14	10.50	4.91	35.4
<b>FFT</b>	2.00	2.00	25.00	7.50	53.8

A sample of centrifuge cake was analyzed by AGAT Laboratories Ltd. for bulk and clay XRD mineralogy to determine the mineralogical composition. The clay fraction indicated that the sample consisted mainly of kaolinite (80%), with lesser amounts of illite (18%). Minor amounts of quartz and siderite were also present. Bulk XRD results showed that the sample consisted mainly of quartz (43%) and kaolinite (32%), with lesser amounts of illite (15%) and potassium feldspar (2%) as seen in Figure 4-2.

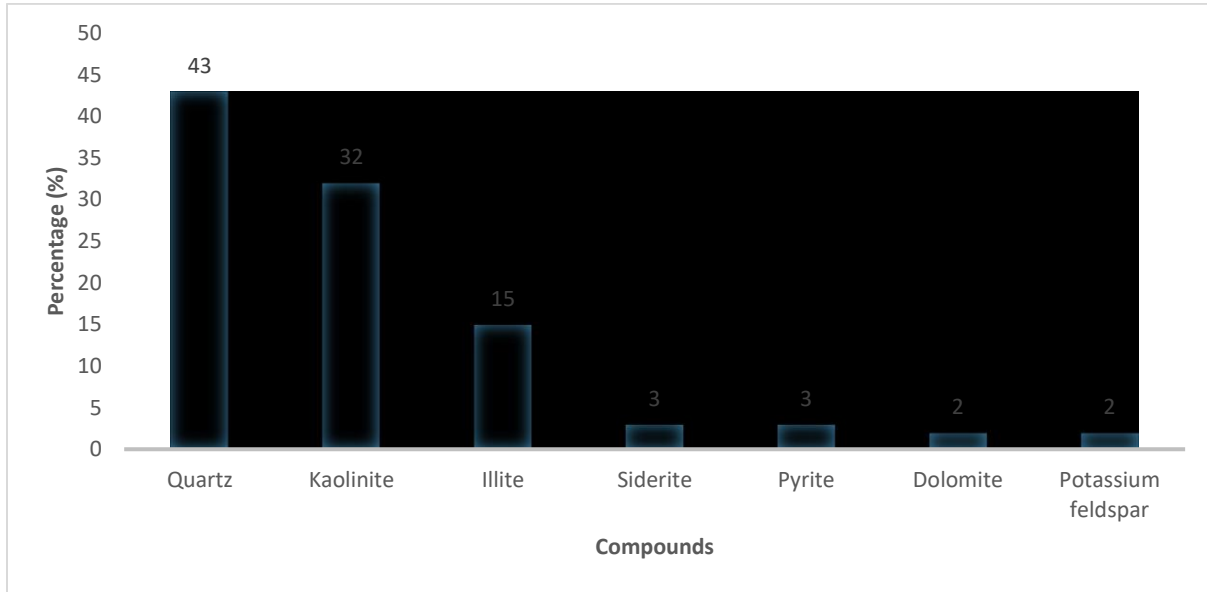


Figure 4-2: Bulk XRD analysis of centrifuged tailings

Bulk XRD analysis of the FFT sample indicated that the sample consisted mainly of kaolinite (58%) with lesser amounts of quartz (24%) and illite (9%) as seen in Figure 4-3. Minor amounts of muscovite, potassium feldspar and pyrite, plus trace amounts of plagioclase feldspar, silicate, and rutile were also present in the sample.

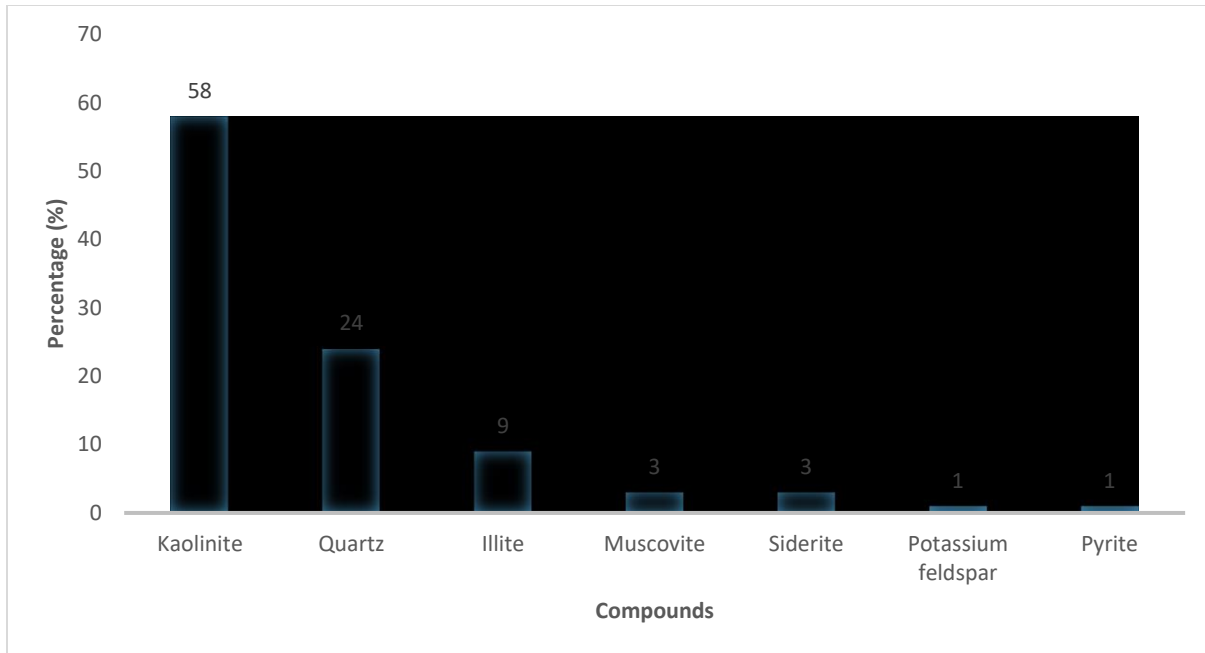


Figure 4-3: Bulk XRD analysis of FFT

As described in Section 3.1, kaolinite was selected as a control to determine if the heating process altered the structure of the clay minerals based on the results of XRD analysis.

## 4.2 Kaolin Results

The clay-sized fraction of FFT consist of mainly kaolinite, with small amounts of illite, montmorillonite, chlorite, and mixed-layer clays. Kaolinite was selected to ensure that the heating process was not changing the structure of the clay mineral. Kaolinite was also selected because it has been found to exhibit almost no thixotropy (Skempton and Northey 1952). Four samples of kaolinite were prepared. Two treated samples were cured in the water bath for 48 hours and two untreated samples and two samples were kept in sealed containers for the same period in a moisture and temperature-controlled room.

### 4.2.1 Pore-water Chemistry

Samples were weighed before and after heat-treatment. Percent solid and pH data were collected, and results are shown in Table 4-3.



Table 4-3: pH and percent solids result for heat treated kaolinite

Sample ID	Percent Solids			pH	
	Initial	Final	% Difference	Initial	Final
<b>Treated – lower %S</b>	34.0%	44.7%	23.80%	8.09	8.00
<b>Untreated – lower %S</b>	34.3%	34.9%	1.76%	6.56	6.66
<b>Treated – higher %S</b>	53.8%	54.5%	1.18%	5.92	5.94
<b>Untreated – higher %S</b>	54.2%	54.7%	0.90%	5.52	5.44

The measured pH remained relatively constant in all kaolinite samples.

#### 4.2.2 Rheology

Using the Kinexus Rheometer, a flow curve was generated for the kaolinite samples as seen in Figure 4-4 and Figure 4-5. The kaolinite samples show an initial spike in shear stress at the start of the test and rapidly decreased with increasing shear rate.

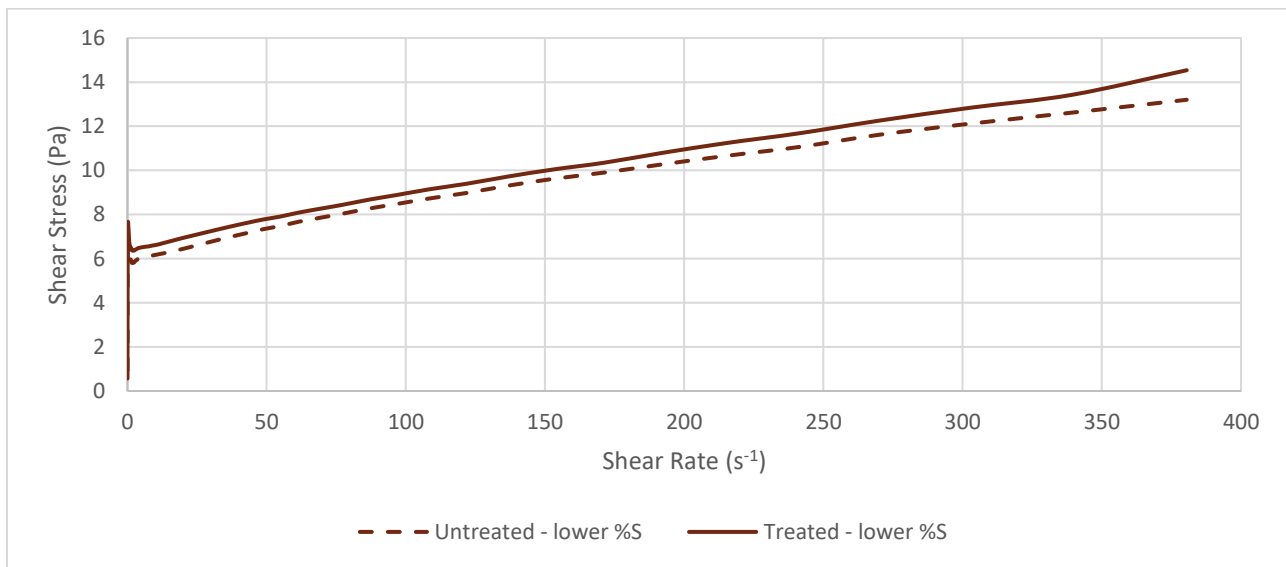


Figure 4-4: Flow curve for lower %S kaolinite

Shear stress measured in the higher %S treated kaolinite sample was approximately 50 Pa lower than the untreated sample.

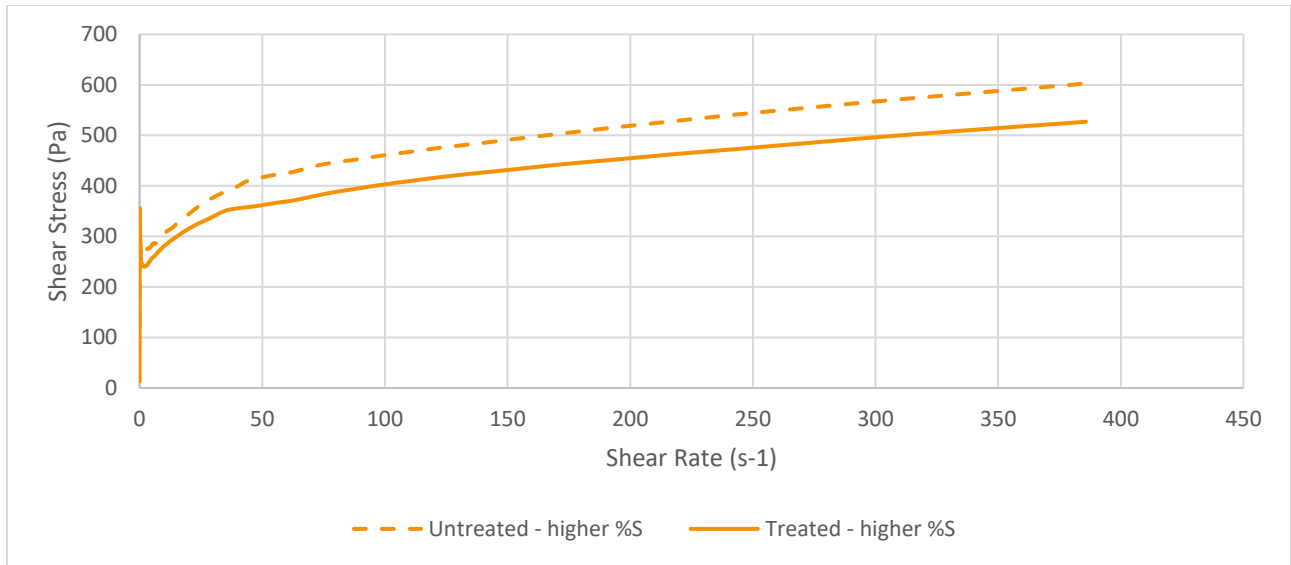


Figure 4-5: Flow curve for higher %S kaolinite

The yield point was determined using a set shear rate of  $0.01 \text{ s}^{-1}$  to approximate the state of rest. The peak shear strength was defined as the peak stress. The elastic modulus versus shear stress for kaolinite is presented in Figure 4-6. The loss/viscous modulus ( $G''$ ) versus shear stress for kaolinite is presented in Appendix D. The findings are summarized below in Table 4-4.

Table 4-4: Yield point, shear strength,  $G'$  and  $G''$  of kaolinite samples

Sample ID	Yield Point (Pa)	Shear Strength (Pa)	LVE Region	
			$G'$ (Pa)	$G''$ (Pa)
<b>Treated – lower %S</b>	0.81	15	162	24
<b>Untreated – lower %S</b>	1.38	13	228	38
<b>Treated – higher %S</b>	79	527	16,719	2,393
<b>Untreated – higher %S</b>	168	603	31,451	4,447

The yield point of the lower percent solids sample decreased very slightly after heat treatment. The yield point of the higher percent solids samples also decreased after heat treatment.

The linear viscoelastic region (LVE) of untreated samples extends slightly further than the treated tailings for both the high percent solids and low percent solids samples. The yield point of the treated samples was decreased in both the high percent solids and low percent solids samples.

The  $G'$  value in the LVE region represents the stiffness of the sample. As we are seeing a decrease in this value, it may imply an impact to structure. A decrease in the  $G''$  value was also observed.

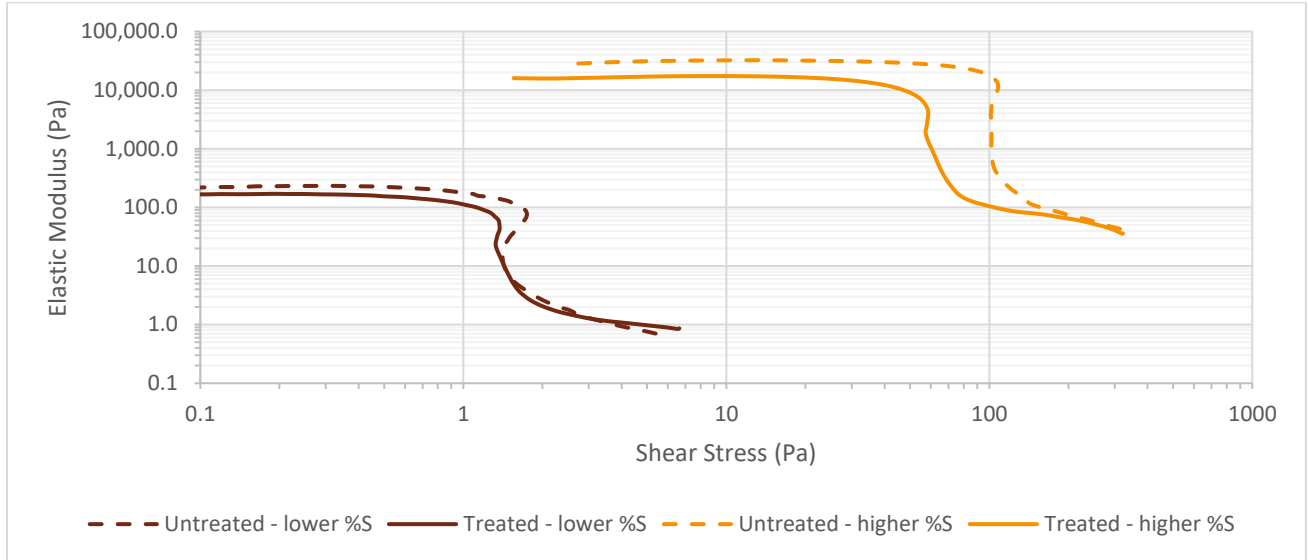
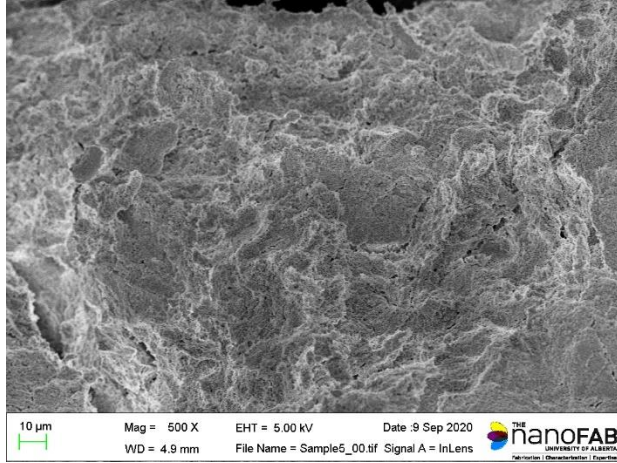


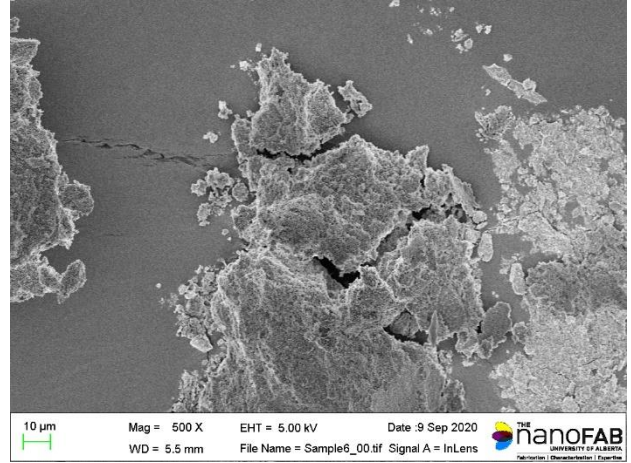
Figure 4-6: Elastic shear modulus versus shear stress for kaolinite

### 4.2.3 SEM

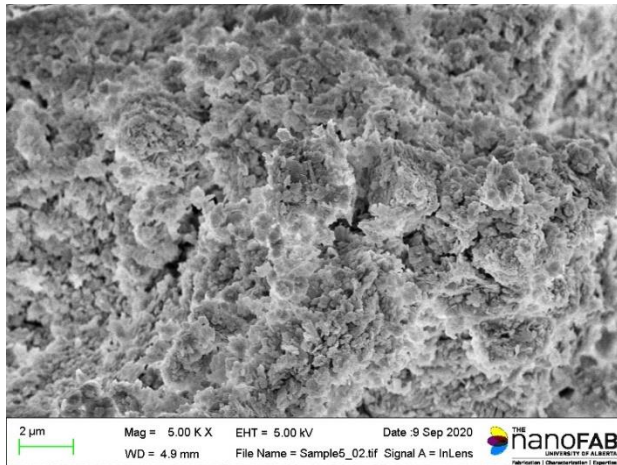
Scanning electron microscopy observations were completed on kaolinite before and after heat treatment to determine if there was any change in structure of the clay as a result of the heating process. The following Figure 4-7 shows a micrograph of kaolinite at its liquidity index prior to and after heat treatment. Significant changes to the structure of the kaolinite sample were not observed after heat treatment.



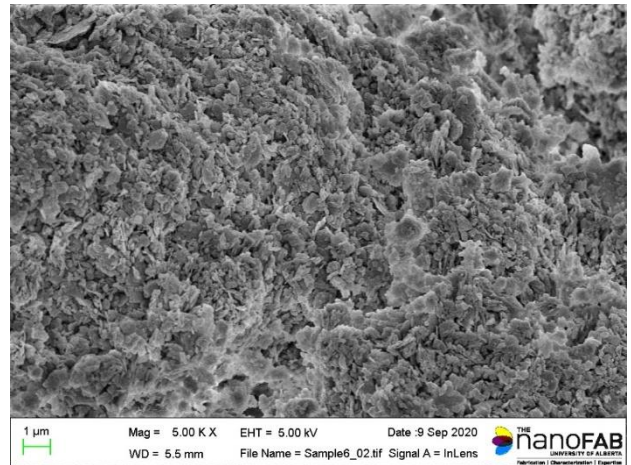
(a) 500x magnification; untreated



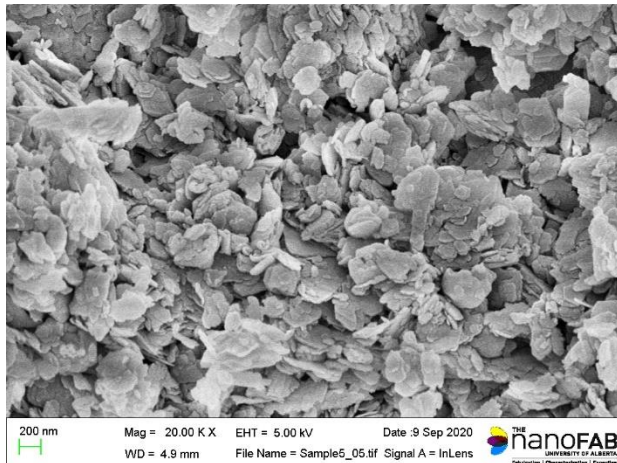
(b) 500x magnification; heat treated



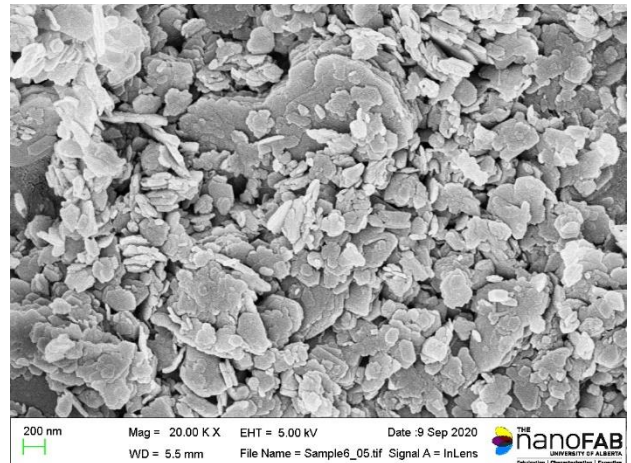
(c) 5,000 x magnification; untreated



(d) 5,000x magnification; heat treated



(e) 20,000x magnification; untreated



(f) 20,000x magnification; heat treated

Figure 4-7: Scanning electron microscopy of kaolinite before and after heat treatment

### 4.3 Fluid Fine Tailings Results

#### 4.3.1 Pore-water Chemistry

Four samples of unamended FFT were prepared in containers for this part of the experiment. Two samples were cured in the water bath for 48 hours and two samples were kept in sealed containers for the same period in a moisture and temperature-controlled room. Samples were weighed before and after heat treatment. Additionally, moisture contents were measured before and after testing. Results are shown in Table 4-5.

Table 4-5: pH and percent solids result for FFT

Sample ID	Percent Solids			pH	
	Initial	Final	% Difference	Initial	Final
<b>Treated – lower %S</b>	33.5%	32.7%	2.2%	7.49	7.51
<b>Untreated – lower %S</b>	33.3%	33.1%	0.7%	7.41	7.36
<b>Treated – higher %S</b>	56.7%	55.6%	2.1%	7.12	7.08
<b>Untreated – higher %S</b>	55.2%	56.2%	-1.7%	7.04	7.1

#### 4.3.2 Rheology

Using the Kinexus Rheometer, a flow curve was generated as seen in Figure 4-8. The tailings show an initial spike in shear stress at the start of the test similar to what was observed in other research (Mizani 2016). Other investigations on clay suspensions have found an initial yield stress that was significantly higher than the Bingham stress. Previous studies have distinguished the high static yield stress from the lower dynamic yield stress. An explanation for the occurrence of the static yield stress is unknown in kaolinite suspensions, however, a secondary structure that breaks down rapidly and recovers very slowly or only under specific ambient conditions has been observed in bentonite suspensions (Toorman 1997). The measured shear stress in the higher percent solids untreated tailings were slightly greater than the treated tailings. The untreated tailings also have a higher percent solid which may explain the greater shear stress. The lower percent solid samples had similar measured shear stresses throughout the test.

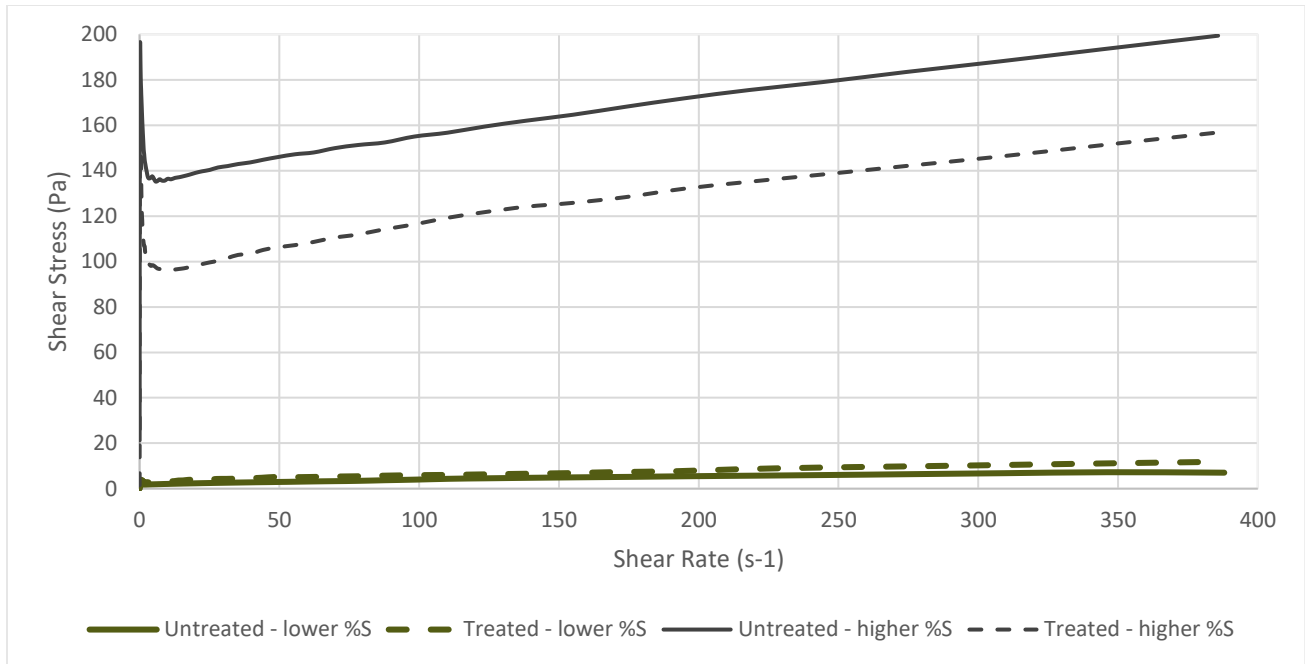


Figure 4-8: Flow curve for fluid fine tailings

The yield point was determined using a set shear rate of  $0.01 \text{ s}^{-1}$  to approximate the state of rest and the peak shear strength was defined as the maximum stress. The findings are shown below in Table 4-6.

Table 4-6: Yield point, shear strength,  $G'$  and  $G''$  of FFT samples

Sample ID	Yield Point (Pa)	Shear Strength (Pa)	LVE Region	
			$G'$ (Pa)	$G''$ (Pa)
<b>Treated - lower %S</b>	0.27	12	4	0.62
<b>Untreated - lower %S</b>	0.22	20	11	1
<b>Treated - higher %S</b>	15	172	1,013	145
<b>Untreated - higher %S</b>	33	199	782	121

The yield point of the lower percent solids sample increased after treatment and the yield point of the higher percent solids sample decreased after treatment.

The elastic modulus versus shear stress for centrifuged tailings is presented in Figure 4-9. The linear viscoelastic region (LVE) of untreated tailings extends slightly further than the treated tailings.

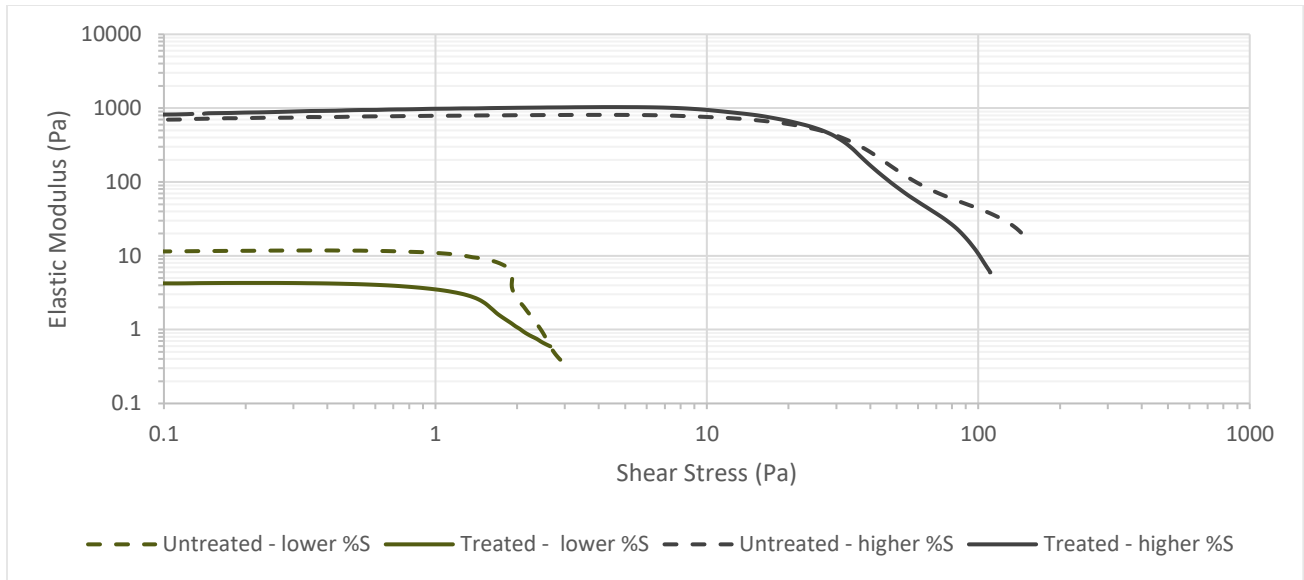


Figure 4-9: Elastic modulus versus shear stress for fluid fine tailings

## 4.4 Centrifuge Cake Results

### 4.4.1 Heat Treated Samples

#### 4.4.1.1 Pore-water Chemistry

The percent solids of each sample were measured at the beginning of the experiment and the end of the experiment to better compare the rheology results. All samples remained relatively constant over the period of the experiment. The pH of all samples was measured before and after treatment. The pH of one of the heat-treated samples increased and the other sample decreased over the time of treatment. The pH of the untreated samples decreased over the 48-hour period.

Table 4-7: pH and percent solids result for heat treated centrifuge cake

Sample ID	Percent Solid			pH	
	Initial	Final	% Difference	Initial	Final
<b>Treated 1</b>	51.6%	52.5%	-1.7%	7.70	8.40
<b>Untreated 1</b>	51.5%	52.3%	-1.6%	7.71	7.45
<b>Treated 2</b>	50.0%	49.6%	0.8%	8.00	7.67
<b>Untreated 2</b>	49.8%	50.7%	-1.8%	7.92	7.40

#### 4.4.1.2 Rheology

Four identical samples of as-received centrifuged tailings were prepared. Two samples were cured in the water bath for 48 hours and two samples were kept in sealed containers for the same period in a moisture and temperature-controlled room. Samples were weighed before and after heat treatment.

Using the Kinexus Rheometer, a flow curve was generated as seen in Figure 4-10. The centrifuged tailings show an initial spike in shear stress at the start of the test and gradually decreased with increasing shear rate. On average, shear stress measured in the treated tailings were between 25 – 50 Pa lower than the untreated tailings.

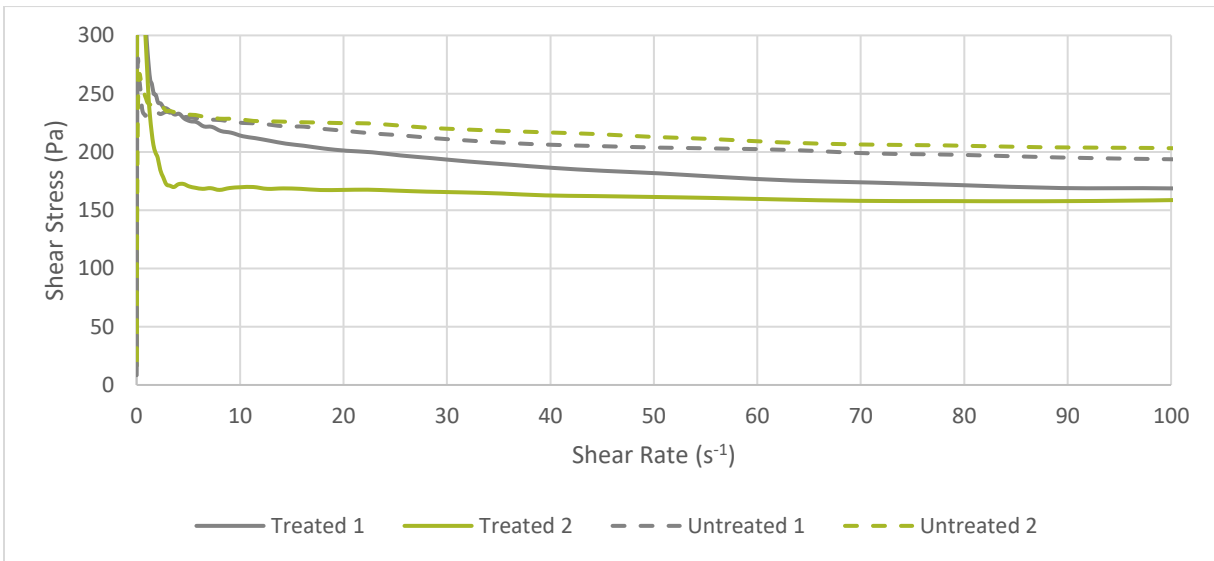


Figure 4-10: Flow curve for centrifuged tailings

The yield point was determined using a set shear rate of 0.01 s<sup>-1</sup> to approximate the state of rest and the peak shear strength was defined as the maximum measured value. The findings are shown below in Table 4-8. The yield point of the heat-treated centrifuged tailings increased in both samples.



Table 4-8: Yield point, shear strength,  $G'$  and  $G''$  of heat-treated centrifuged tailings

Sample ID	Yield Point (Pa)	Shear Strength (Pa)	LVE Region	
			$G'$ (Pa)	$G''$ (Pa)
Treated 1	48	705	262	40
Untreated 1	16	280	261	31
Treated 2	35	456	-	-
Untreated 2	27	267	382	47

The elastic modulus versus shear stress for centrifuged tailings is presented in Figure 4-11. The data collected from the Untreated 1 sample was not usable and therefore not included. The linear viscoelastic region (LVE) of untreated tailings extends slightly further than the treated tailings.

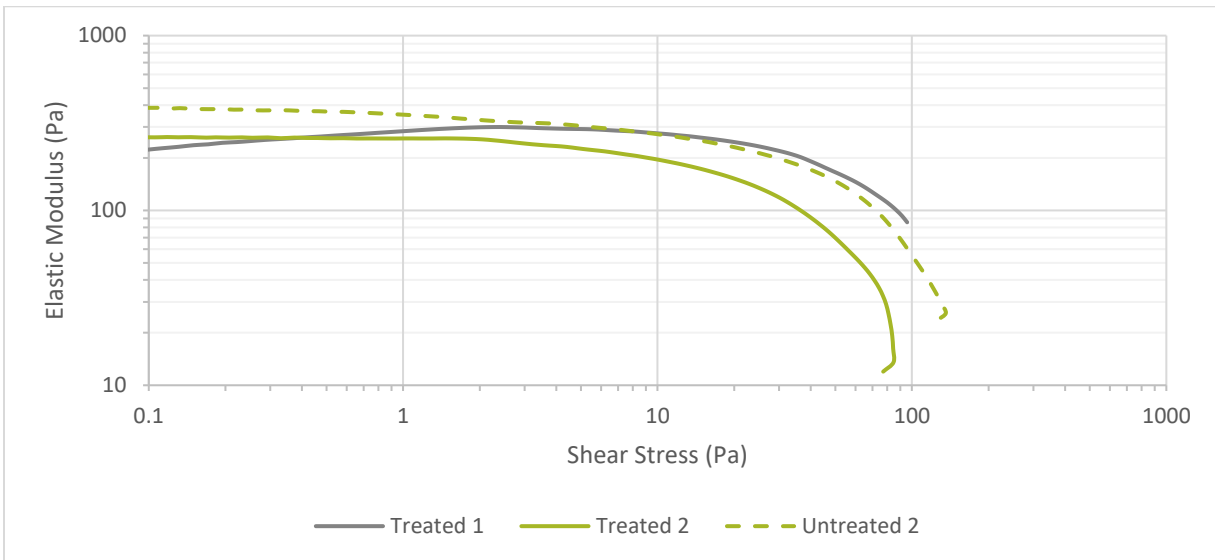


Figure 4-11: Elastic modulus versus shear stress for centrifuged tailings

#### 4.4.2 Bacteria Treated Samples

Four samples of centrifuged tailing were inoculated with bacteria at a dose of 50,000 ppm and one control (untreated) sample was prepared.

##### 4.4.2.1 Pore-water Chemistry

The pH of all samples was measured before and after treatment. The pH of bacteria treated samples decreased over the time of treatment, becoming slightly more acidic. The untreated sample also decreased slightly.

Percent solids of all samples were measured before and after treatment to comparison. All samples increased in percent solids, indicating potential evaporation over the course of the incubation period. Evaporation was minimal with the exception of Treated 2.

*Table 4-9: pH and percent solids result for bacteria treated centrifuge cake*

Sample ID	Percent Solids			pH	
	Initial	Final	% Difference	Initial	Final
<b>Treated 1</b>	48.9%	49.9%	2.0%	7.92	7.43
<b>Treated 2</b>	48.6%	54.8%	12.7%	7.67	7.17
<b>Treated 3</b>	49.0%	50.6%	3.3%	7.61	7.19
<b>Treated 4</b>	48.9%	50.1%	2.6%	7.61	7.23
<b>Untreated</b>	50.5%	51.3%	1.6%	7.47	7.21

#### *4.4.2.2 Rheology*

Using the Kinexus Rheometer, a flow curve was generated as seen in Figure 4-12. The centrifuged tailings show an initial spike in shear stress at the start of the test and decreased with increasing shear rate. Results varied between treated and untreated tailings. Treated 2 had the highest final percent solids, significantly greater than the control sample, so it is not considered. Treated 4 and the control sample have the most comparable percent solids; results show decreases in shear stress of approximately 25 Pa.

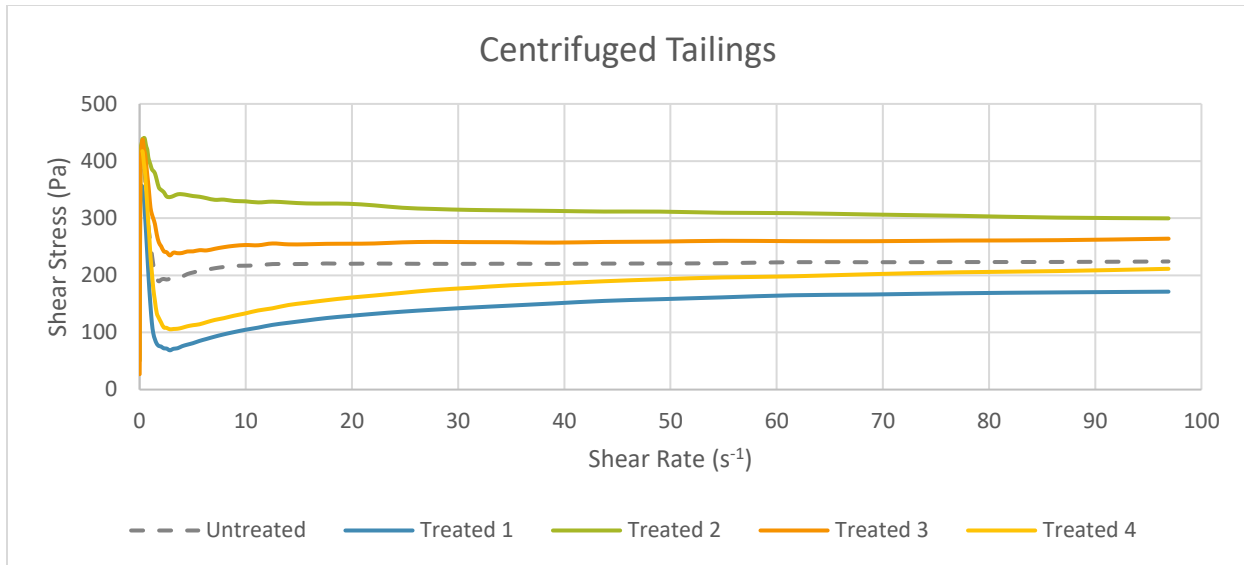


Figure 4-12: Shear rate ramp for bacteria treated centrifuged tailings

The yield point was determined using a set shear rate of  $0.01 \text{ s}^{-1}$  to approximate the state of rest. The peak shear strength was defined as the maximum measured value. The findings are shown below in Table 4-10. The yield point of the bacteria treated centrifuged tailings decreased in all samples as compared to the untreated sample.

Table 4-10: Yield point, shear strength,  $G'$  and  $G''$  of bacteria treated centrifuged tailings

Sample ID	Yield Point (Pa)	Shear Strength (Pa)	LVE Region	
			$G'$ (Pa)	$G''$ (Pa)
<b>Treated 1</b>	47	357	497	86
<b>Treated 2</b>	58	440	558	92
<b>Treated 3</b>	44	438	1,591	250
<b>Treated 4</b>	43	417	1,198	1,163
<b>Untreated</b>	80	428	1,961	292

The elastic modulus versus shear stress for centrifuged tailings is presented in Figure 4-13. The linear viscoelastic region (LVE) of untreated tailings extends slightly further than the treated tailings.

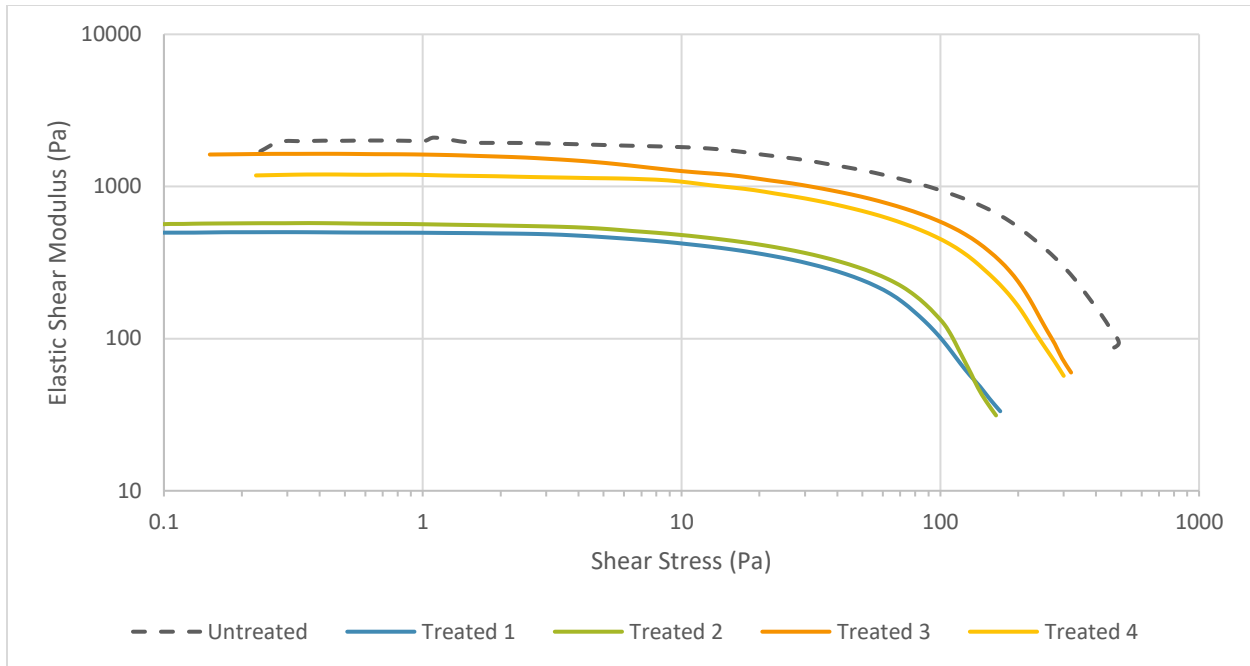


Figure 4-13: Elastic shear modulus versus shear stress for centrifuged tailings

## 4.5 Flocculated FFT Results

### 4.5.1 Heat Treated Samples

A total of eight flocculated tailings samples were prepared as described in Section 3.1.1. Four samples were prepared with a lower percent solid (approximately 32%) and four were prepared with a higher percent solid (approximately 51%). Half of the samples were cured in the water bath for 48 hours and the other half were kept in sealed containers for the same period in a moisture and temperature-controlled room. Samples were weighed before and after heat-treatment.

#### 4.5.1.1 Pore-water Chemistry

The pH of all samples was measured before and after treatment. The pH of heat-treated samples decreased over the time of treatment, becoming slightly more acidic. The untreated samples decreased.

Percent solids of all samples were measured before and after treatment for comparison. All samples increased in percent solids, indicating potential evaporation over the course of the treatment period.

Table 4-11: pH and percent solids results for heat treated flocculated tailings

Sample ID		Percent Solids			pH	
		Initial	Final	% Difference	Initial	Final
Lower % Solids	Untreated 1	31.9%	32.1%	0.6%	8.04	7.87
	Untreated 2	32.0%	32.0%	0.1%	7.55	7.29
	Treated 1	31.7%	33.8%	6.5%	7.59	7.20
	Treated 2	32.0%	36.5%	14.0%	7.53	7.20
Higher % Solids	Untreated 1	51.1%	51.7%	1.2%	7.34	7.22
	Untreated 2	50.0%	50.7%	1.4%	7.46	7.33
	Treated 1	51.2%	52.5%	2.6%	7.47	7.00
	Treated 2	49.6%	58.3%	17.6%	7.40	7.20

#### 4.5.1.2 Rheology

Using the Kinexus Rheometer, a flow curve was generated for all FFT samples seen in Figure 4-14: Flow curve for heat treated flocculated tailings is shown in Figure 4-14. The centrifuged tailings show an initial spike in shear stress at the start of the test and rapidly decreased with increasing shear rate to a minimum. The tailings then showed a gradual increase in shear stress with increasing shear rate.

The higher initial percent solids tailings had an average decrease in measured shear stress of 300 Pa whereas the lower initial percent solids tailings had an average decrease in measured shear stress of 70 Pa.

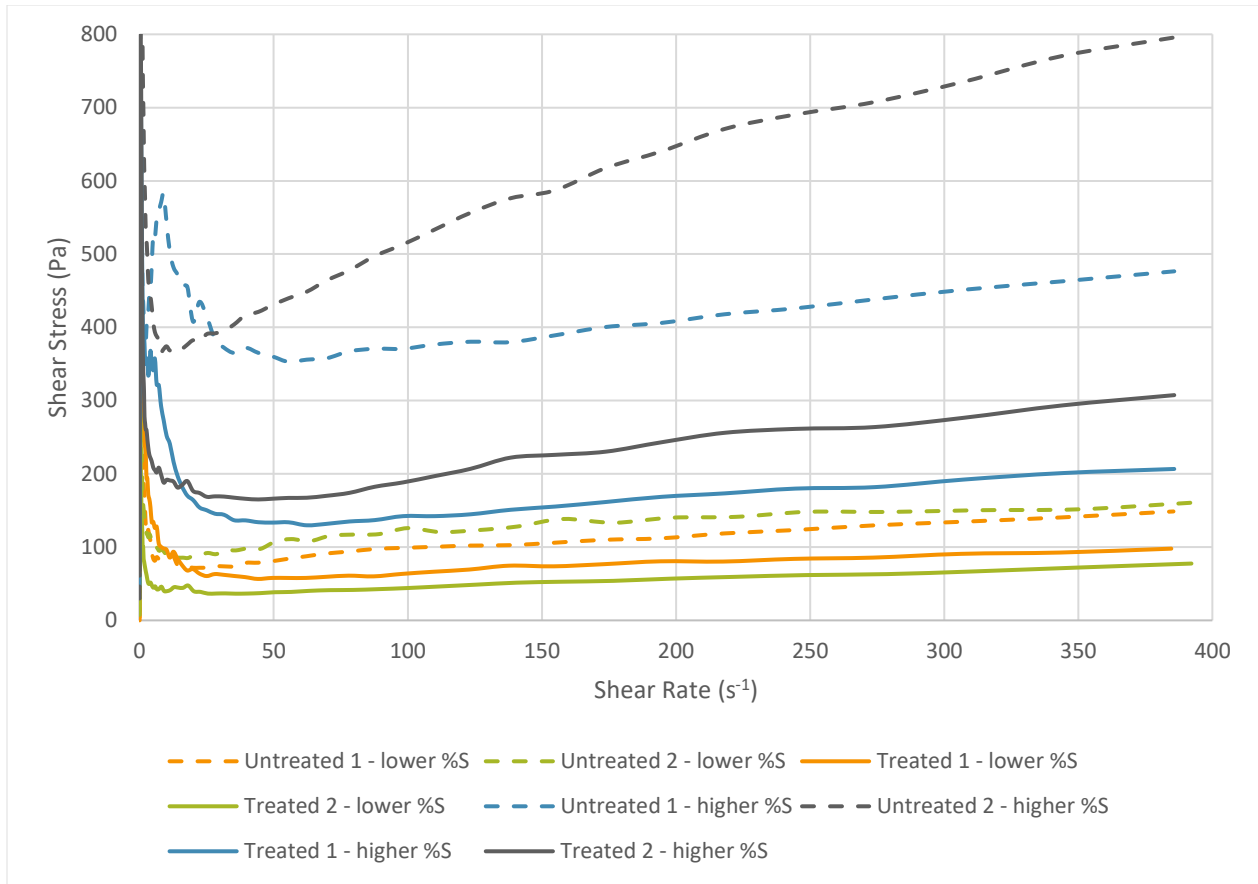


Figure 4-14: Flow curve for heat treated flocculated tailings

The yield point was determined using a set shear rate of  $0.01 \text{ s}^{-1}$  to approximate the state of rest and the peak shear strength was defined as the maximum measured value. The findings are shown below in Table 4-12. The yield point of the lower percent solids increased after heat treatment and remained approximately the same in the other sample. The yield point of the higher percent solids sample increased in both samples after heat treatment.

Table 4-12: Yield point, shear strength,  $G'$  and  $G''$  of flocculated FFT samples

Sample ID	Yield Point (Pa)	Shear Strength (Pa)	LVE Region	
			$G'$ (Pa)	$G''$ (Pa)
Treated 1 – lower %S	15	380	125	17
Untreated 1 – lower %S	7	303	150	21
Treated 2 – lower %S	15	284	104	14
Untreated 2 – lower %S	15	296	130	19
Treated 1 – higher %S	87	763	466	71

Sample ID	Yield Point (Pa)	Shear Strength (Pa)	LVE Region	
			G' (Pa)	G'' (Pa)
Untreated 1 – higher %S	56	642	748	134
Treated 2 – higher %S	77	850	820	125
Untreated 2 – higher %S	73	980	1300	230

The elastic modulus versus shear stress for centrifuged tailings is presented in Figure 4-15. The linear viscoelastic region (LVE) of untreated tailings extends slightly further than the treated tailings.

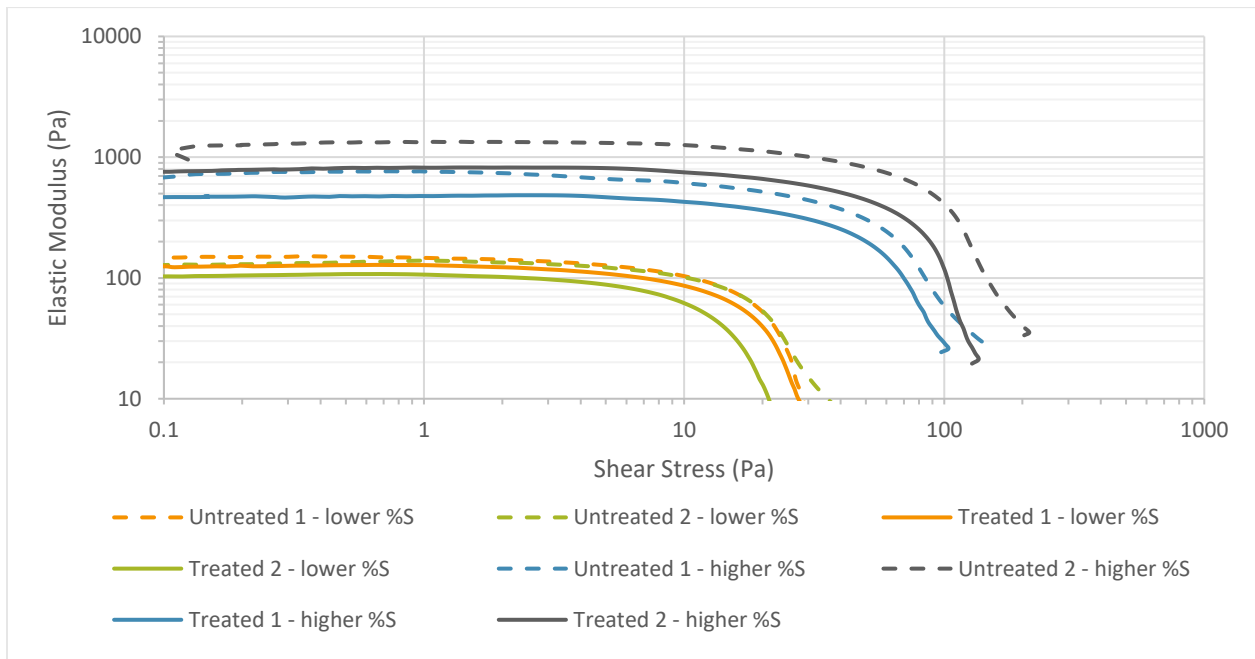
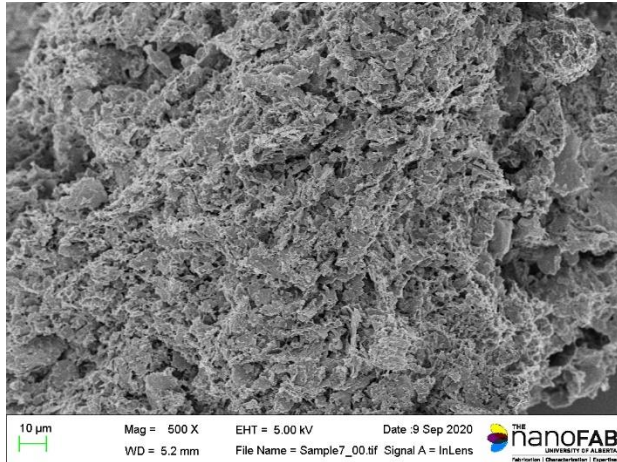


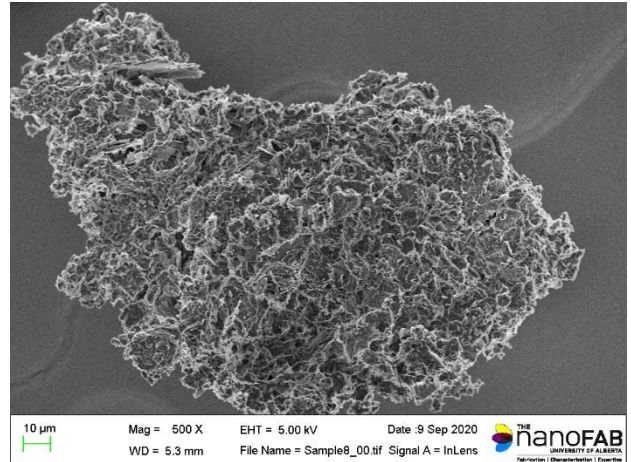
Figure 4-15: Elastic modulus versus shear stress for heat treated flocculated tailings

#### 4.5.1.3 SEM

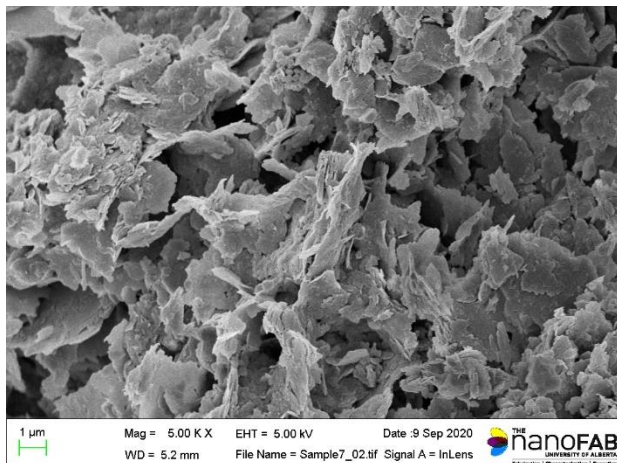
The following shows a SEM of flocculated FFT prior to and after heat treatment. The clay card-house like structure of the untreated flocculated FFT is visible at 5,000x and 20,000x magnification. At 5,000x, there appears to be fewer pore spaces visible in the heat-treated sample. In addition, the flocculated structure seen in the untreated 20,000x magnification sample is not visible in the heat-treated sample.



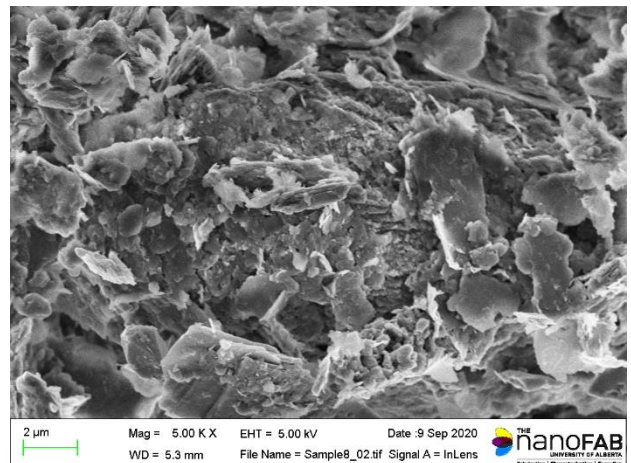
(a) 500x magnification; untreated



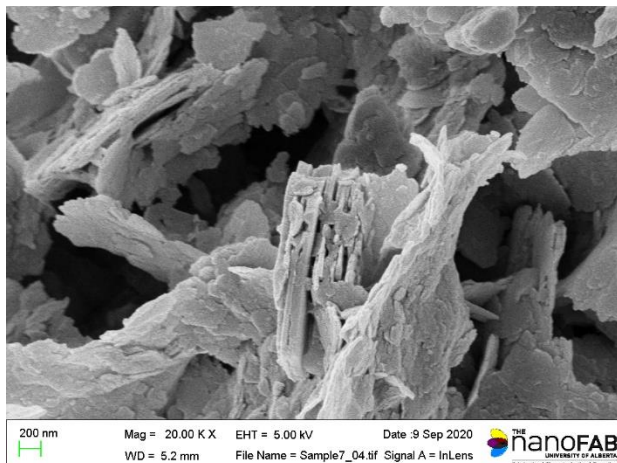
(b) 500x magnification; heat treated



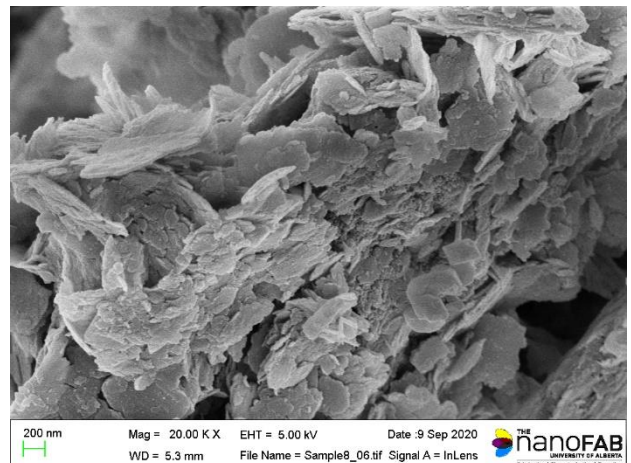
(c) 5,000x magnification; untreated



(d) 5,000x magnification; heat treated



(e) 20,000x magnification; untreated



(f) 20,000x magnification; heat treated

Figure 4-16: Scanning electron microscopy of higher %S flocculated FFT before and after heat treatment



## 4.5.2 Bacteria Treated Samples

### 4.5.2.1 Pore-water Chemistry

The pH of all samples was measured before and after treatment. The pH of heat-treated samples decreased over the time of treatment, becoming slightly more acidic. The untreated samples decreased.

Percent solids of all samples were measured before and after treatment to compare. All samples increased in percent solids, indicating potential evaporation over the course of the treatment period.

Table 4-13: pH and percent solids results for bacteria treated flocculated tailings

Sample ID		Percent Solids			pH	
		Initial	Final	% Difference	Initial	Final
Lower % Solids	Treated 1	29.8%	37.1%	24.5%	8.04	7.66
	Treated 2	31.1%	38.0%	22.1%	7.75	7.48
	Treated 3	30.1%	37.0%	22.7%	7.62	7.36
	Untreated	30.4%	37.8%	24.5%	7.65	7.58
Higher % Solids	Treated 1	48.3%	50.4%	4.4%	7.34	7.10
	Treated 2	48.9%	49.9%	2.0%	7.46	7.08
	Treated 3	48.9%	49.9%	1.9%	7.46	7.04
	Untreated	51.9%	51.3%	1.2%	7.52	7.41

### 4.5.2.2 Rheology

Using the Kinexus Rheometer, a flow curve was generated for all FFT samples seen in Figure 4-17. The flocculated tailings show an initial spike in shear stress at the start of the test and rapidly decreased with increasing shear rate to a minimum. The tailings then showed a gradual increase in shear stress with increasing shear rate.

The higher initial percent solids tailings had an average decrease in measured shear stress of approximately 200 Pa after treatment whereas the lower initial percent solids tailings had an insignificant decrease in measured shear stress after treatment.

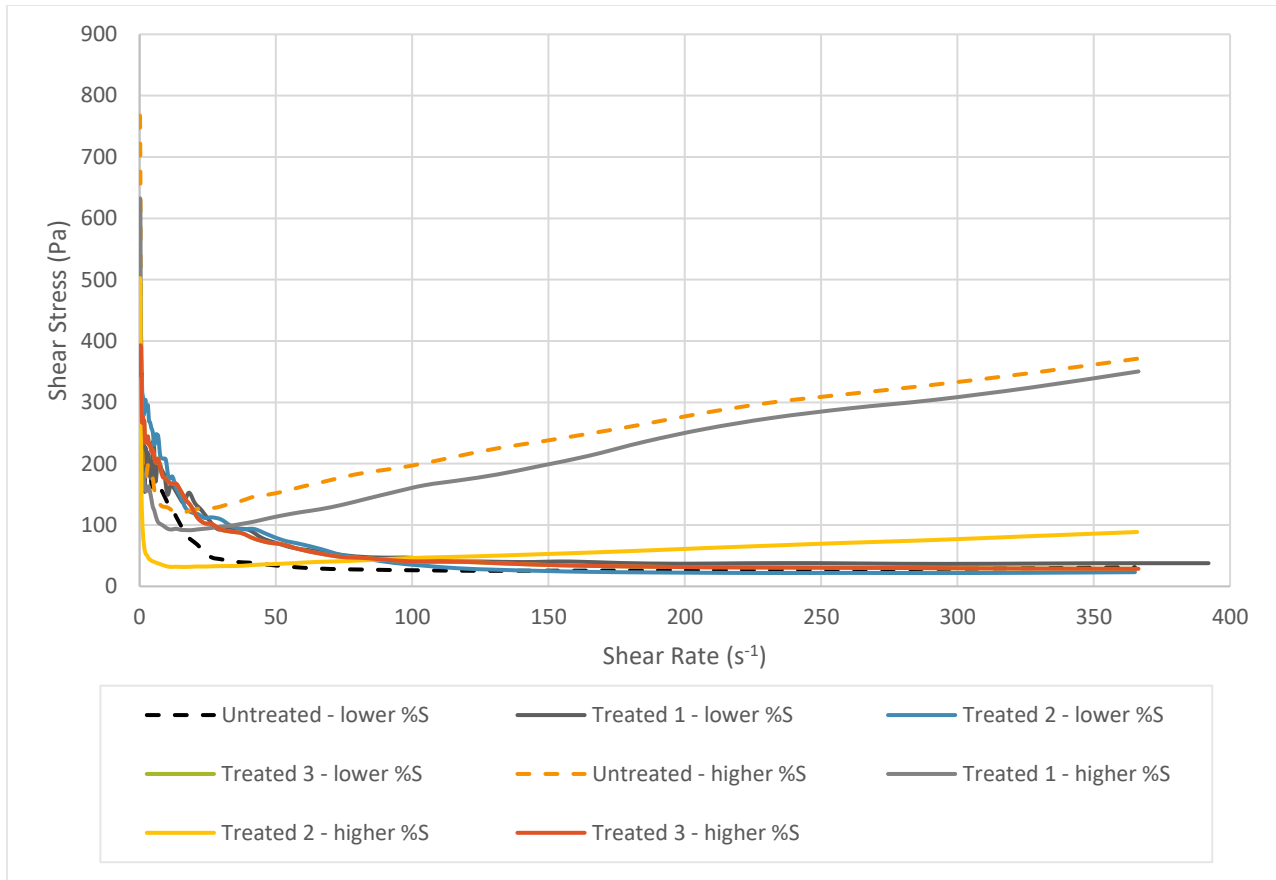


Figure 4-17: Shear rate ramp for bacteria treated flocculated tailings

The yield point was determined using a set shear rate of 0.01 s<sup>-1</sup> to approximate the state of rest and the peak shear strength was defined as the maximum measured value. The findings are shown below in Table 4-14. The yield point of the bacteria treated flocculated tailings decreased in all samples as compared to the untreated sample.

Table 4-14: Yield point, shear strength,  $G'$  and  $G''$  of flocculated FFT samples

	Sample ID	Yield Point (Pa)	Shear Strength	LVE Region	
			(Pa)	$G'$ (Pa)	$G''$ (Pa)
<b>Lower % Solids</b>	Treated 1 – lower %S	16	402	1,308	263
	Treated 2 – lower %S	8	466	1,886	396
	Treated 3 – lower %S	18	393	1,429	273
	Untreated – lower %S	26	422	1,725	330
<b>Higher % Solids</b>	Treated 1 – higher %S	48	633	3,547	650
	Treated 2 – higher %S	35	503	4,248	784
	Treated 3 – higher %S	100	659	3,830	689
	Untreated – higher %S	103	768	5,592	1,016

The elastic modulus versus shear stress for centrifuged tailings is presented in Figure 4-18. The linear viscoelastic region (LVE) of untreated tailings extends slightly further than the treated tailings.

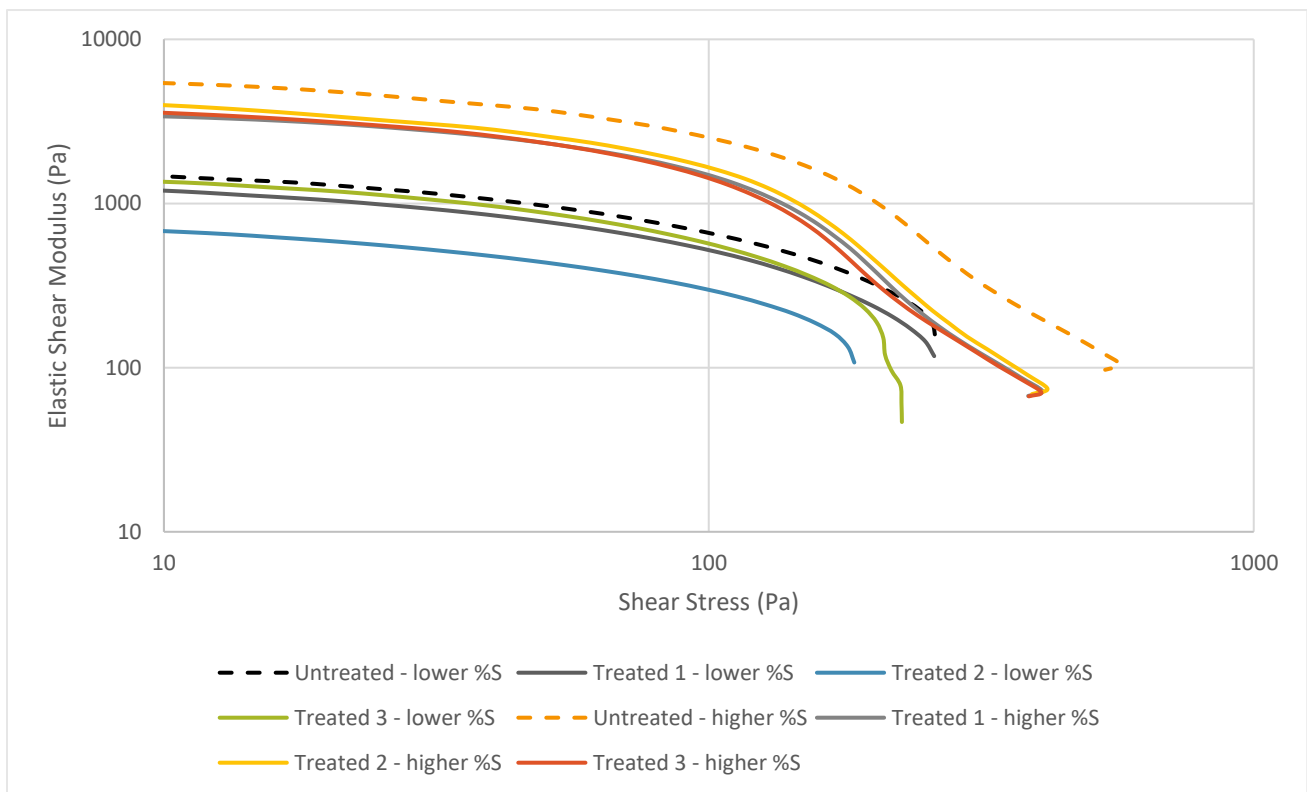
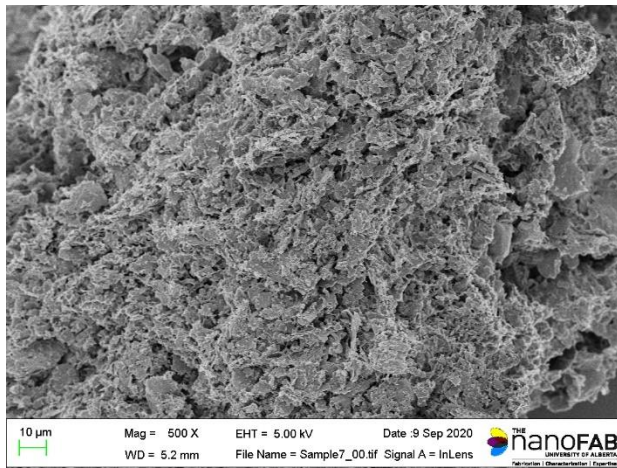


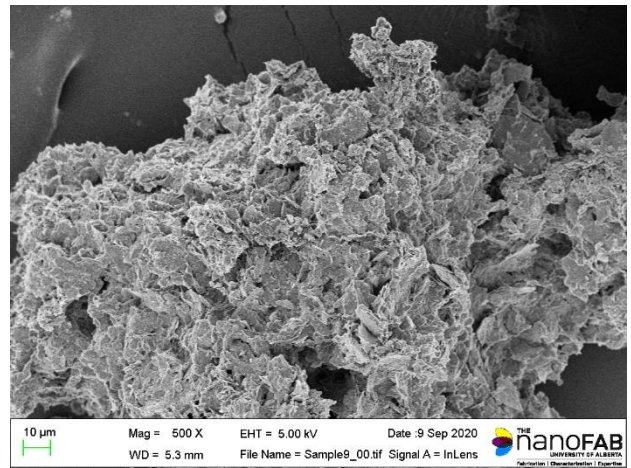
Figure 4-18: Elastic modulus versus shear stress for bacteria treated flocculated tailings

### 4.5.2.3 SEM

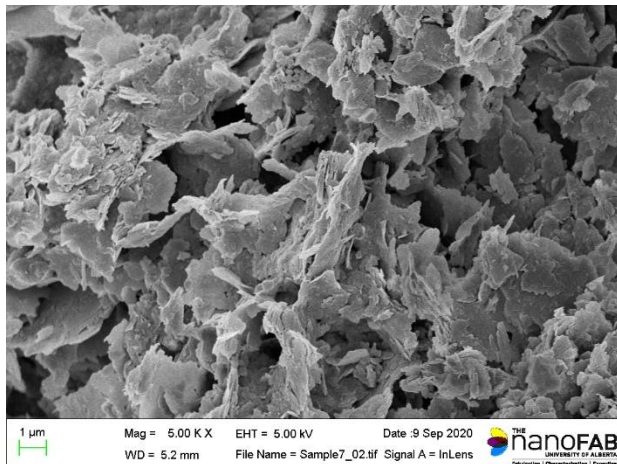
The following shows SEM images of flocculated FFT prior to and after bacterial treatment at magnifications of 500, 5,000, and 20,000x. More voids are visible, and the spaces appear to be larger in the untreated sample than in the bacteria treated sample. Floccs are still visible in the bacteria treated sample at all magnifications.



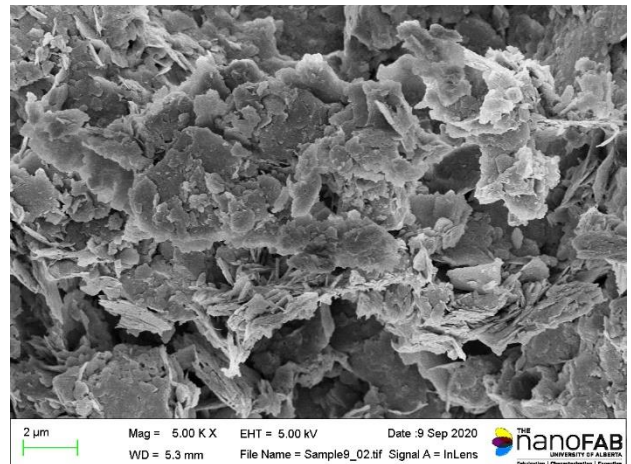
(a) 500x magnification; untreated



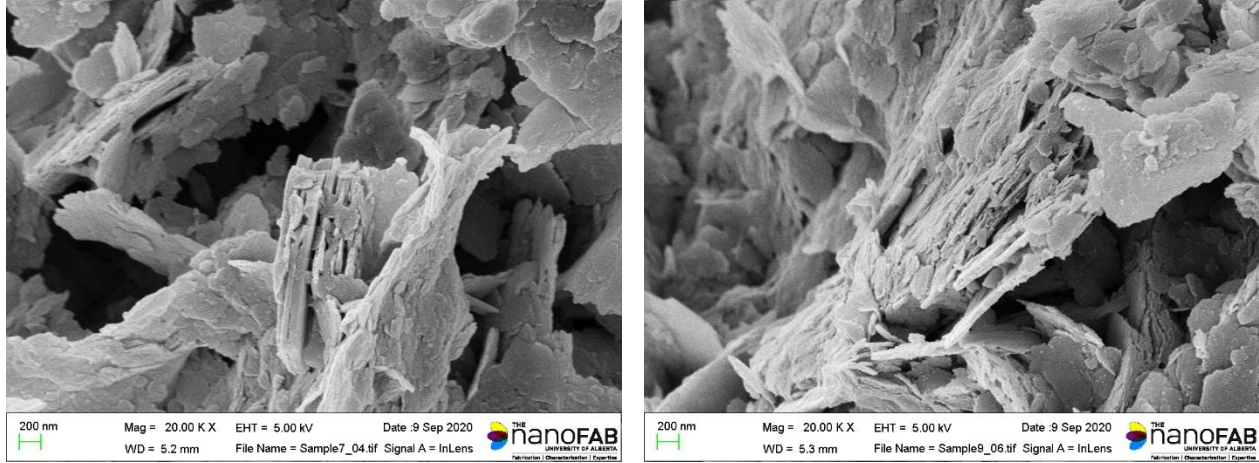
(b) 500x magnification; bacteria treated



(c) 5,000x magnification; untreated



(d) 5,000x magnification; bacteria treated



(e) 20,000x magnification; untreated

(f) 20,000x magnification; bacteria treated

Figure 4-19: Scanning electron microscopy of higher %S flocculated FFT before and after bacteria treatment

#### 4.6 Consolidated Samples

Three samples of the same centrifuge cake were used for the LSC tests. The samples had an initial void ratio of 2.07. The test was completed as described in Section 3.3. The consolidation test results are presented in Figure 4-20. This shows the sample compressibility (void ratio versus effective stress). One sample was consolidated to a void ratio of 1 and two others were consolidated to a void ratio of 1.5 (Table 4-15). Void ratio was calculated as follows:

$$e_1 = \frac{h_{1*}(1 + e_0)}{h_0} - 1 \quad (9)$$

The first increment was self weight consolidation. The cell was monitored until the pore pressure dissipated to zero. The next load was then added and again monitored until pore pressure was dissipated. The change in height was monitored using a LVDT and the results from each cell are plotted in Appendix C.

Table 4-15: LSC Void Ratio Data

Cell	Initial Void Ratio	Final Void Ratio	Increments to Final Void Ratio
3	2.07	1.04	7
4	2.07	1.53	5
5	2.07	1.56	5

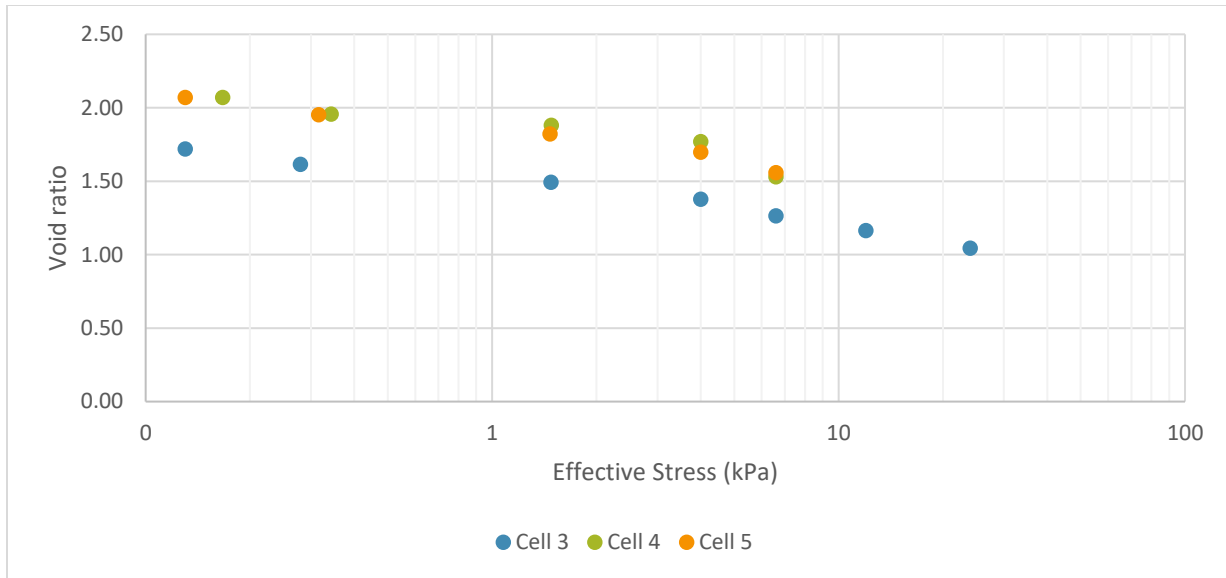


Figure 4-20: Compressibility curve for centrifuge cake

#### 4.6.1 Heat Treated Samples

##### 4.6.1.1 Pore-water Chemistry

The pH of samples was measured before and after treatment. The pH of samples decreased over the time of treatment, becoming slightly more acidic.

Percent solids of all samples were measured before and after treatment for comparison. All samples increased in percent solids, indicating potential evaporation over the course of the treatment period.

Table 4-16: pH and percent solids results for heat treated consolidated samples

Sample ID	Percent Solids			pH	
	Initial	Final	% Difference	Initial	Final
<b>e=1.5</b>	68.1%	69.1%	1.4%	7.04	6.99
<b>e=1</b>	75.3%	76.4%	1.5%	7.36	7.20

##### 4.6.1.2 Rheology

A vane shear test was conducted on the consolidated samples to determine the undrained shear strength of the material using the motorized vane shear apparatus as the samples were no longer acting as complex fluids or soft solids. Standard vane sizes and torque springs (for vane tester)

were employed in the shear strength measurement. Three measurements were taken, and the average was reported.

Minimal strength losses were seen in the consolidated samples.

Sample ID	Shear Strength (kPa)		
	Initial	Final	% Difference
<b>e=1.5</b>	14.8	14.5	2.03%
<b>e=1</b>	27.7	26.7	3.61%

## 5 Discussion

### 5.1 Pore Water Chemistry

#### 5.1.1 Effect of Polymer Degradation on Pore Water Chemistry

The effect of polymer degradation on pore water chemistry was of interest in this study as it may suggest a change in physiochemical properties because of polymer degradation. As a baseline, previous research has shown that the pH was higher in polymer amended tailings (7.56, 7.65, 7.59) as compared to unamended tailings (7.45) (Bajwa 2015). Based on this observation, it was expected that pH may decrease after treatment and the degradation of polymers.

The pH of samples was taken before and after heat or bacteria treatment and on control samples at the same time intervals. In all but one polymer amended tailings sample that was heat treated, it was found that the pH decreased. The largest decrease was seen in the high percent solids flocculated FFT sample, where pH decreased from 7.47 to 7.00 after heat treatment. This sample also showed the largest decrease in strength. Two of the four control samples also showed a decrease in pH; however, the decrease was considerably smaller. All the polymer amended tailings samples that were bacteria treated showed a decrease in pH after treatment. Similar to the heat-treated samples, the largest decrease in pH was in the high percent solids flocculated FFT sample. Additionally, the samples with the largest decreases in pH also had large decreases in shear strength.

The decrease in pH may correspond to an increase in positive counter-ions / change in the concentration of metals because of polymer degradation. It also appears that the largest decreases in pH correspond to the largest decreases in shear strength.

### 5.2 Long Term Strength Behaviour

In geotechnical engineering, the most used parameter when discussing strength behaviour is undrained shear strength. For very soft soils, the vane apparatus has become very common when measuring soils which are too soft for triaxial testing.

The other commonly used parameter when considering the geotechnical behavior of oil sands tailings is the yield point. While yield point measurements may provide the opportunity to further understand the long-term strength behavior of amended tailings deposits, performing them on thixotropic material is inherently challenging. The choice of a representative technique



is important and depends greatly on the application. The time scale of the employed technique greatly alters the results and thus the use of other terms such as the elastic modulus ( $G'$ ) in the LVE region may be a more reliable technique as it is independent of time. As shown in Section 4.0, multiple techniques were employed to compare strength behaviour before and after treatment, including the use of the elastic modulus.

Multiple factors from the experiment design complicated the measurements of long-term strength behaviour. It is known that water content has a large effect on the undrained shear strength of oil sands tailings. The samples were treated for 48 hours as it resulted in the least amount of evaporation but longest heating cycle. The process was based on the Mao and Fahey (1999) study where 12 hours of heating could result in change to the floc structure; however, the samples were much smaller in their study. Due to safety reasons, it was not possible to seal the samples in this experiment as there were concerns that they would become pressurized. Over the duration of the heat treatment process, it was nearly impossible to complete without altering the water content of the samples, leading to potentially unreliable measurements of strength behaviour. It is important to consider the changes to water content when interpreting the results of the strength behaviour tests.

Multiple studies have been completed comparing the water content or percent solids versus the undrained shear strength on kaolin, FFT, centrifuge cake, and flocculated FFT. The following relationships were used to calculate the effect of percent solids or water content on the measured shear strength in Pa:

Material	Relationship	Reference
<b>Kaolinite</b>	$S_u = \left(\frac{w}{64.058}\right)^{-6.73}$	Dolinar and Trauner (2007)
<b>Centrifuge Cake</b>	Upper Bound: $S_u = 3 \times 10^{-5} e^{0.2396\%S}$ Lower Bound: $S_u = 1.2 e^{0.1524\%S}$	(McKenna et al. 2016)
<b>FFT</b>	Upper Bound: $S_u = 3 \times 10^{-5} e^{0.2396\%S}$ Lower Bound: $S_u = 1.2 e^{0.1524\%S}$	(McKenna et al. 2016)
<b>Flocculated FFT</b>	$S_u = 1.9503 e^{0.1569(\%S)}$	Abdulnabi et al. (2021)

Additionally, errors in measurement can originate from the use of the rheometer and the material itself. Errors in the rheological measurements can also occur from thermal expansion, torque resolution, and environmental factors. Errors stemming from the samples themselves may include uneven thermal degradation, nonlinear shear deformation, and centrifugal forces. Measured error in the yield point and shear strength measurements were determined to be an average of  $\pm 7.5\%$ . No error on the elastic modulus ( $G'$ ), and loss/viscous modulus ( $G''$ ) measurements were reported from the manufacture or in literature. As large variation exists in the measured strength measurement values of oil sands tailings, the reported values should not be considered as representative of absolute values, but rather, relative compared to the other samples.

As discussed in Section 3.5.1, errors originating from slip occur because of the displacement of the disperse phase away from solid boundaries; resulting in a layer of lower-viscosity, liquid depleted material. The vane-type geometries used in this research can lessen, or in some cases, eliminate the wall depletion effects. However, slip is an important phenomenon to consider when reviewing rheological data from a rheometer or viscometer. No breaks that were indicative of slip or slip artefacts were identified in flow curves.

## 5.2.1 Effect of Heat Treatment on Strength Behaviour

### 5.2.1.1 Control Samples

Samples of kaolinite and FFT were heat treated and the results were used to assess whether the heat treatment process was altering the structure of the samples. If structural changes occurred, it would be expected that changes to the yield point and shear strength would be observed outside of the margin of error of  $\pm 7.5\%$ .

The yield point of the lower percent solids kaolinite sample decreased from 1.38 to 0.81 Pa (41% decrease), and the shear strength increased from 13.2 to 14.5 Pa (10% increase) after treatment. The  $G'$  decreased from 228 Pa to 162 Pa (29% decrease) and the  $G''$  decreased from 38 to 24 Pa (37% decrease) (Table 4-4). It is important to note that the heat treatment process increased the percent solids of the sample from approximately 34% to 45% over the course of the heat treatment process. The increase in percent solids from 34 to 45% could have increased the reported shear strength of the kaolinite by up to 70% (Dolinar and Trauner 2007). As expected, the measured yield points and shear strengths of the low percent solids sample were very low and

the differences between the treated and untreated samples exceeded the margin of error of  $\pm 7.5\%$ , however, the increase in shear strength may be explained by the increase in percent solids after heat treatment. The decrease in yield point and increase in shear strength was an unexpected result. Within the LVE region, both the  $G'$  and  $G''$  decreased after treatment. When  $G' < G''$ , it indicates a fluid structure and when  $G' > G''$ , this indicates a gel or solid like structure. The difference between the  $G'$  and  $G''$  in the untreated sample was 190 Pa. In the treated sample, this difference decreased to 138 Pa suggesting that the treated sample is acting more like a fluid compared to the untreated sample.

In the higher percent solids kaolinite sample, the yield point and the shear strength decreased from 168 to 79 Pa (53% decrease) and 603 to 527 Pa (13% decrease), respectively, after treatment. The  $G'$  decreased from 31,451 Pa to 16,719 Pa (47% decrease) and the  $G''$  decreased from 4,447 to 2,393 Pa (46% decrease) (Table 4-4). The heat treatment process did not have a large effect on the percent solids of the higher percent solids sample in comparison to the lower percent solids sample, however the increase in percent solids could have increased the reported shear strength of the kaolinite by up to 6% (Dolinar and Trauner 2007). Accounting for the effect of the difference in percent solids, the decrease in measured shear strength of the higher percent solids sample was within the margin of error of  $\pm 7.5\%$ . The difference between the  $G'$  and  $G''$  in the untreated sample was 27,004 Pa. In the treated sample, this difference decreased to 14,326 Pa suggesting that the treated sample is acting more like a fluid compared to the untreated sample.

The yield point of the lower percent solids FFT sample increased from 0.22 to 0.27 Pa (23% increase) and the shear strength decreased from 20 to 12 Pa (40% decrease) after treatment. The  $G'$  decreased from 11 Pa to 4 Pa (64% decrease) and the  $G''$  decreased from 1 to 0.62 (38% decrease) (Table 4-6). The heat treatment process did not have a large effect on the percent solids of the sample, however the decrease in percent solids could have decreased the reported shear strength of the FFT by up to 10.8%. Accounting for the effect of the difference in percent solids, the decrease in measured shear strength of the higher percent solids sample exceeded the margin of error of  $\pm 7.5\%$ . The difference between the  $G'$  and  $G''$  in the untreated sample was 10 Pa. In the treated sample, this difference decreased to 3.38 Pa suggesting that the treated sample is acting more like a fluid compared to the untreated sample.

In the higher percent solids sample, the yield point and the shear strength decreased from 33 to 15 Pa (55% decrease) and 199 to 172 Pa (14% decrease), respectively, after treatment. The  $G'$  increased from 782 to 1,013 Pa (30% increase) and the  $G''$  increased from 121 to 145 (20% increase) (Table 4-6). The heat treatment process did not have a large effect on the percent solids of the sample, however the decrease in percent solids could have decreased the reported shear strength of the FFT by up to 13%. Accounting for the effect of the difference in percent solids, the decrease in measured shear strength of the higher percent solids sample exceeded the margin of error of  $\pm 7.5\%$ . The difference between the  $G'$  and  $G''$  in the untreated sample was 661 Pa. In the treated sample, this difference increased to 868 Pa suggesting that the treated sample is acting more like a solid compared to the untreated sample.

Based on the results of the shear ramp and oscillatory tests on the kaolinite and FFT samples, results appeared to be heavily correlated to the changes in percent solids. The observed results in the shear strength were within the margin of error in the higher percent solids kaolinite sample, whereas the decreases in the FFT samples and the lower percent solids were greater than the margin of error.

The results suggest that there are likely changes to the structure of the kaolinite and FFT because of the heat treatment process, however it is difficult to quantify if it is a result of the change to percent solids or if it may be attributed to a change to the clay / mineral structure.

#### *5.2.1.2 Centrifuge Cake Samples*

Based on the results of the shear ramp and oscillatory tests on centrifuge cake samples, results showed an increase in the strength behaviour and a transition to a more “solid-like” structure after treatment. Duplicate samples were prepared, and similar results were observed in both samples. The yield point of the untreated samples was determined to be 16 and 27 Pa and the yield point of the treated samples were 48 and 35 Pa. Similar increases were observed in the measured shear strength values where the shear strength of the treated samples was determined to be 705 and 456 Pa and the untreated sample was 280 and 267 Pa. The average yield point increased from 22 to 43 Pa (50% increase) and the average shear strength increased from 274 to 481 Pa (76% increase). The average  $G'$  decreased from 322 Pa to 262 Pa (19% decrease) and the average  $G''$  increased from 39 to 40 Pa (3% increase) (Table 4-8). The heat treatment process did not have a large effect on the percent solids of the sample, however the change in percent solids

could have affected the reported shear strength of the centrifuge cake by up to 25%. The increase in measured shear strength and yield point of the higher percent solids sample exceeded the margin of error of  $\pm 7.5\%$ . Within the LVE region, both the  $G'$  and  $G''$  decreased after treatment. When  $G' < G''$ , it indicates a fluid structure and when  $G' > G''$ , this indicates a gel or solid like structure. The average difference between the  $G'$  and  $G''$  in the untreated sample was 226 Pa. In the treated sample, this difference increased to 335 Pa suggesting that the treated sample is acting more like a solid.

Significant increases to the measured yield point and shear strength were observed, whereas low to moderate changes to the  $G'$  and  $G''$  occurred. These results were unexpected from the heat treatment process and show a positive change to the strength behaviour of the centrifuge cake samples.

#### *5.2.1.3 Flocculated FFT Samples*

The average yield point of the lower percent solids flocculated FFT sample increased from 11 to 15 Pa (36% increase), and the average shear strength increased from 300 to 332 Pa (11% increase) after treatment. The average  $G'$  decreased from 140 Pa to 115 Pa (18% decrease) and the average  $G''$  decreased from 20 to 16 Pa (20% decrease) (Table 4-12). It is important to note that the heat treatment process increased the percent solids of the samples from approximately 32% to up to 37% over the course of the heat treatment process. The increase in percent solids could have increased the reported shear strength of the flocculated FFT by up to 119% (Abdulnabi et al. 2021). The increase in shear strength may be explained by the increase in percent solids after heat treatment. Within the LVE region, both the  $G'$  and  $G''$  decreased after treatment. When  $G' < G''$ , it indicates a fluid structure and when  $G' > G''$ , this indicates a gel or solid like structure. The average difference between the  $G'$  and  $G''$  in the untreated sample was 120 Pa. In the treated sample, this difference decreased to 99 Pa suggesting that the treated sample is acting more like a fluid compared to the untreated sample.

The average yield point of the higher percent solids flocculated FFT sample increased from 65 to 82 Pa (26% increase), and the average shear strength decreased from 811 to 807 Pa (0.5% decrease) after treatment. The average  $G'$  decreased from 1,024 Pa to 643 Pa (37% decrease) and the average  $G''$  decreased from 182 to 98 Pa (46% decrease) (Table 4-12). It is important to note that the heat treatment process increased the percent solids of the samples from approximately

51% to up to 58% over the course of the heat treatment process. The yield point of the higher percent solids flocculated FFT saw moderate increases and minimal changes to the shear strength, even with significant changes to the percent solids of the sample. The increase in percent solids could have increased the reported shear strength of the flocculated FFT by up to 200%. Within the LVE region, both the  $G'$  and  $G''$  decreased after treatment. When  $G' < G''$ , it indicates a fluid structure and when  $G' > G''$ , this indicates a gel or solid like structure. The average difference between the  $G'$  and  $G''$  in the untreated sample was 824 Pa. In the treated sample, this difference decreased to 545 Pa suggesting that the treated sample is acting more like a fluid compared to the untreated sample.

When comparing the lower percent solids flocculated FFT results to the control FFT results, decreases to  $G'$  and  $G''$  were seen in both samples, however larger decreases were observed in the control samples. When comparing the high percent solids flocculated FFT results to the control FFT results, the  $G'$  and  $G''$  values saw significant decreases after heat treatment in the flocculated samples, implying the addition of the polymer may result in more dramatic changes to the structure of the sample after heat treatment for higher percent solids tailings.

Moderate to low increases to both the yield point and the shear strength were observed, however, decreases in the  $G'$  and  $G''$  values were reported. Additionally, there was a transition of the samples to a more “fluid-like” material when comparing  $G'$  and  $G''$  in the LVE region. Moderate changes were seen in all measured parameters and overall may indicate a negative change to the long-term strength behaviour of the centrifuge cake samples.

#### *5.2.1.4 Consolidated Samples*

The only method used to evaluate strength behaviour in the consolidated samples was the peak strength using the vane shear apparatus. Both the  $e=1$  and the  $e=1.5$  samples decreased in strength slightly after heat treatment. The shear strength decreased from 14.8 to 14.5 kPa (2% decrease) in the  $e=1.5$  sample and from 27.7 to 26.7 kPa (4% decrease).

It is important to note that the heat treatment process increased the percent solids of the samples from approximately 68 to 69% in the  $e=1.5$  sample and 75 to 76% in the  $e=1$  sample over the course of the heat treatment process. The increase in percent solids could have increased the reported shear strength of the consolidated centrifuge cake by up to 70%.

These results likely suggest a change to the shear strength behaviour after treatment. A decrease in shear strength was observed even though an increase in percent solids was recorded over the treatment process. In the centrifuge cake samples at the natural void ratio, a 76% increase in shear strength and the treated sample transitioned to behave more like a solid whereas the consolidated samples observed decreases in measured shear strength values. Moderate changes were seen in the measured parameters and overall may indicate a negative change to the long-term strength behaviour of the consolidated centrifuge cake samples.

## 5.2.2 Effect of Bacteria Treatment on Strength Behaviour

### 5.2.2.1 *Centrifuge Cake Samples*

Based on the results of the shear ramp and oscillatory tests on centrifuge cake samples, results showed an increase in the strength behaviour and a transition to a more “fluid-like” structure after treatment. Duplicate treated samples were prepared, and similar results were observed in all treated samples. The average yield point decreased from 80 to 48 Pa (40% decrease) and the average shear strength decreased from 428 to 413 Pa (3.5% decrease). The decrease in measured shear strength and yield point of the centrifuge cake sample was within the margin of error of  $\pm 7.5\%$ . The average  $G'$  decreased from 1,961 Pa to 961 Pa (51% decrease) and the average  $G''$  increased from 292 to 398 Pa (36% increase) (Table 4-12).

Within the LVE region, the  $G'$  decreased and the  $G''$  increased after treatment. When  $G' < G''$ , it indicates a fluid structure and when  $G' > G''$ , this indicates a gel or solid like structure. The average difference between the  $G'$  and  $G''$  in the untreated sample was 1,669 Pa. In the treated sample, this difference decreased to 563 Pa suggesting that the treated sample is acting more like a fluid.

The results in the bacteria treated samples were expected based on the hypothesis. Decreases in the yield point and shear strength were observed and the treated sample transitioned to a more “fluid-like” structure. Overall, the results may indicate a negative change to the long-term strength behaviour of the bacteria treated centrifuge cake samples.

### 5.2.2.2 *Flocculated FFT Samples*

Based on the results of the shear ramp and oscillatory tests on the flocculated FFT samples, results showed decreased in the strength behavior, resulting in a less elastic structure.

For the lower percent solids samples, the average yield point decreased from 26 to 14 Pa (46% decrease), and the shear strength decreased slightly from 422 to 420 Pa after treatment (0.5% decrease). The average  $G'$  decreased from 1,725 Pa to 1,541 Pa (11% decrease) and the average  $G''$  decreased from 330 to 310 Pa (6% decrease) (Table 4-14). The decrease in yield point exceeds the margin of error of  $\pm 7.5\%$ , whereas the decrease in shear strength is within the margin of error of  $\pm 7.5\%$ . Within the LVE region, both the  $G'$  and  $G''$  decreased after treatment. When  $G' < G''$ , it indicates a fluid structure and when  $G' > G''$ , this indicates a gel or solid like structure. The average difference between the  $G'$  and  $G''$  in the untreated sample was 1,395 Pa. In the treated sample, this difference decreased to 1,231 Pa suggesting that the treated sample is acting more like a fluid compared to the untreated sample.

For the higher percent solids samples, the average yield point decreased from 103 to 61 Pa (41% decrease), and the shear strength decreased from 768 to 598 Pa (22% decrease) after treatment. The average  $G'$  decreased from 5,592 to 3,875 Pa (31% decrease) and the average  $G''$  decreased from 1,016 to 708 Pa (30% decrease) (Table 4-14). Within the LVE region, both the  $G'$  and  $G''$  decreased after treatment. When  $G' < G''$ , it indicates a fluid structure and when  $G' > G''$ , this indicates a gel or solid like structure. The average difference between the  $G'$  and  $G''$  in the untreated sample was 4,576 Pa. In the treated sample, this difference decreased to 3,167 Pa suggesting that the treated sample is acting more like a fluid compared to the untreated sample.

When comparing the lower percent solids flocculated FFT results to the control FFT results, decreases to  $G'$  and  $G''$  were seen in both samples, however larger decreases were observed in the control samples. When comparing the high percent solids flocculated FFT results to the control FFT results, the  $G'$  and  $G''$  values saw significant decreases after bacteria treatment in the flocculated samples, implying the addition of the polymer may result in more dramatic changes to the structure of the sample after bacteria treatment for higher percent solids tailings.

The results in the bacteria treated flocculated FFT samples were expected based on the hypothesis. Decreases in the yield point and shear strength were observed and the treated sample transitioned to a more “fluid-like” structure, however, similar to the centrifuge cake these results were moderate. The results for the bacteria treated samples were much more consistent and decreases in strength behavior were observed, indicating a negative impact to the long-term strength behaviour of the bacterial treated FFT samples.



### 5.3 Microstructure

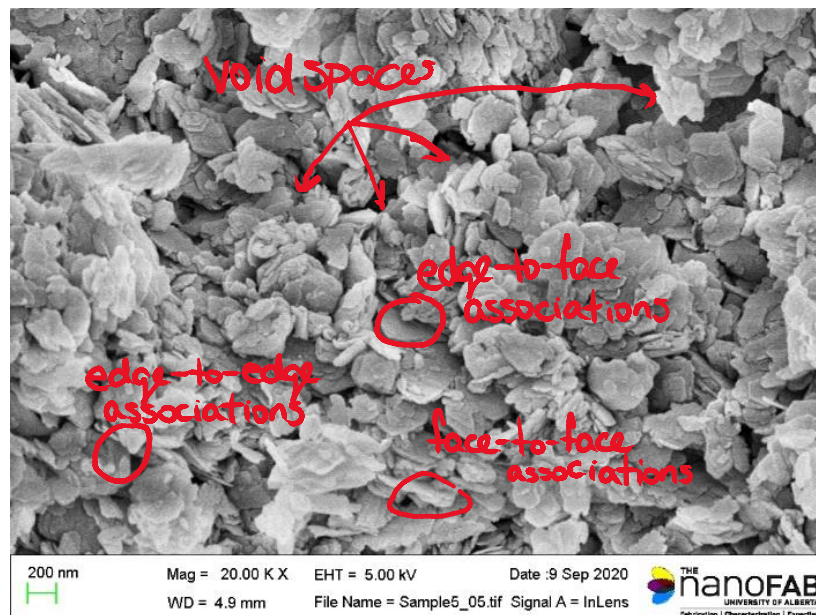
Quantitative measurements of fabric were completed on the SEM images using Image J software through the gray pixel analysis (Ferreira and Rasband 2012). Image analysis consisted of:

1. optimizing the micrograph to adjust the threshold between 0 and 255, where zero represented black and 255 represented white;
2. run the particle analyzer to extract the features such as size range and circularity; and
3. trace particle on the image by flood filling (including holes checkbox).

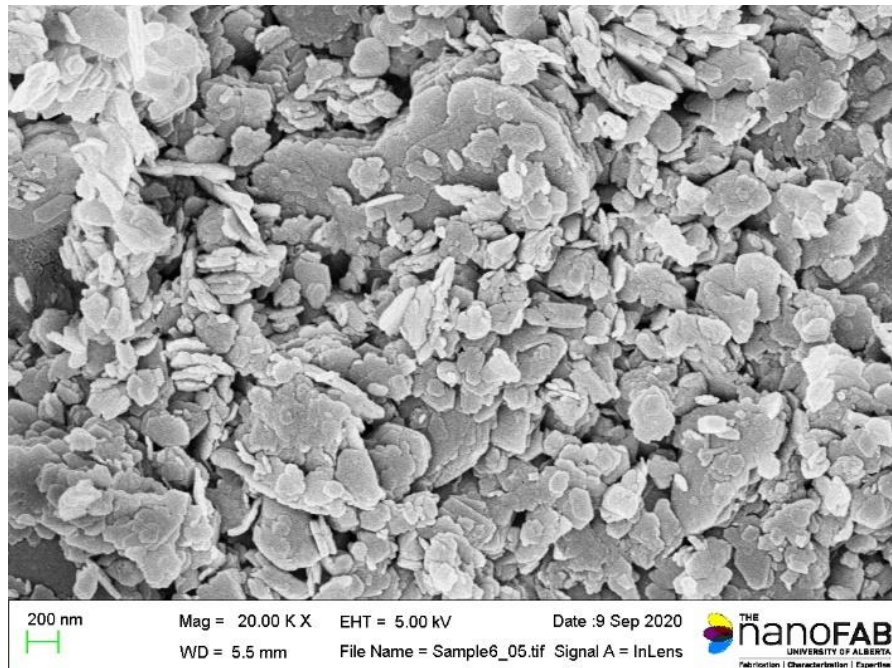
Histograms of the results were compared from before and after treatment. Results are discussed below.

#### 5.3.1 Effect of Heat Treatment on Microstructure

Figure 4-7 shows micro and nano scale images of the kaolinite sample before and after heat treatment at three different magnifications. No significant changes are visible between the untreated and heat-treated samples. At a magnification of 20,000x, edge-to-edge and edge-to-face associations between clay mineral surfaces are observed in both samples, shown in Figure 5-1. The average pore size is similar between the untreated and the heat-treated sample. From the imageJ analysis, the distribution from the grey image analysis at a magnification of 500 was similar before and after heat treatment.



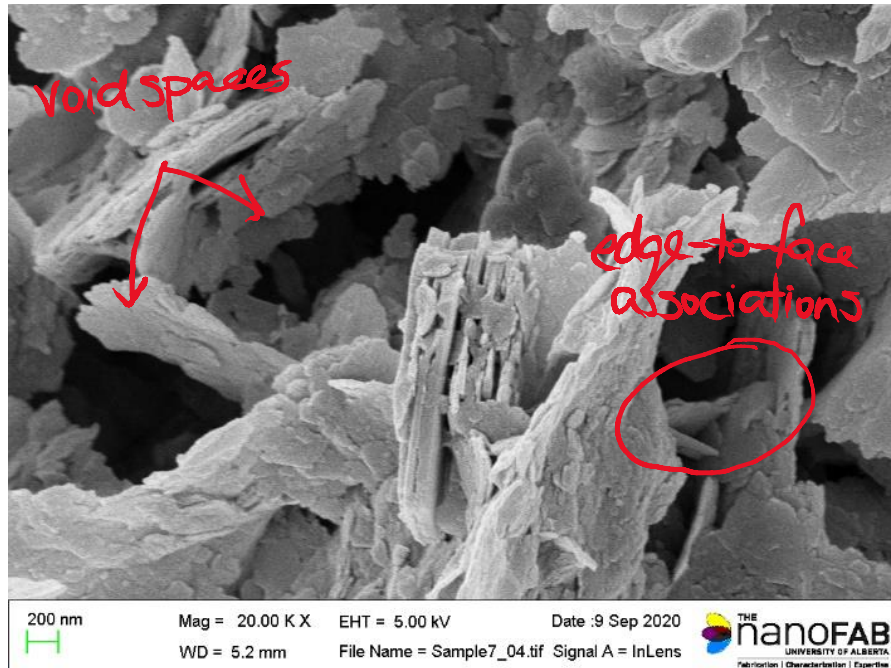
(a) 20,000x magnification; untreated



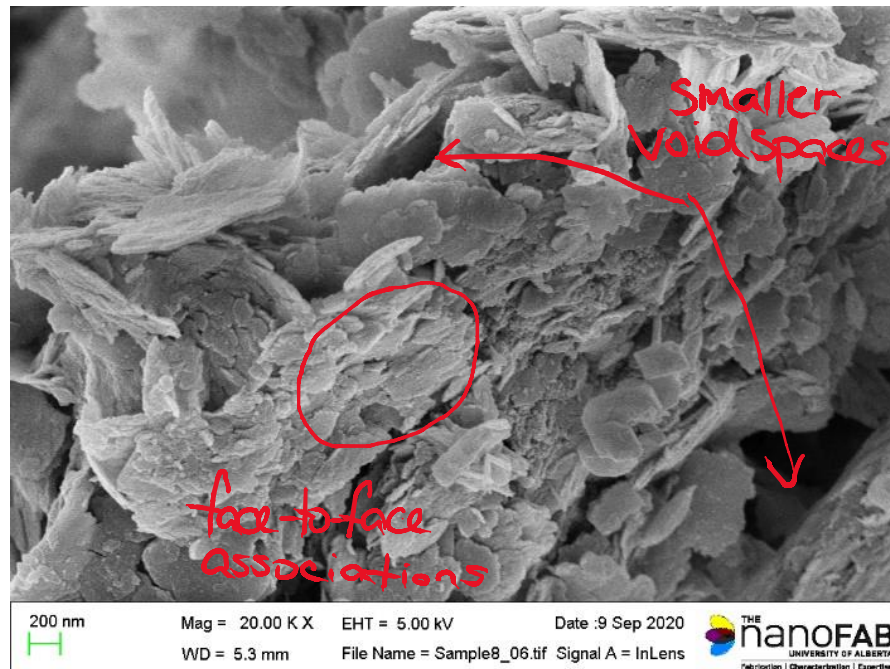
(b) heat treated

Figure 5-1: Annotated SEM of kaolinite at 20,000x magnification

Figure 4-16 shows micro and nano scale images of the higher solids content flocculated FFT sample before and after heat treatment at three different magnifications. Flocculated clay mineral platelets are visible in both the treated and untreated samples at all magnifications; however, the flocs appear to be smaller in the treated sample. Larger void spaces are seen in the untreated sample (Figure 5-2).



(a) untreated



(b) heat-treated

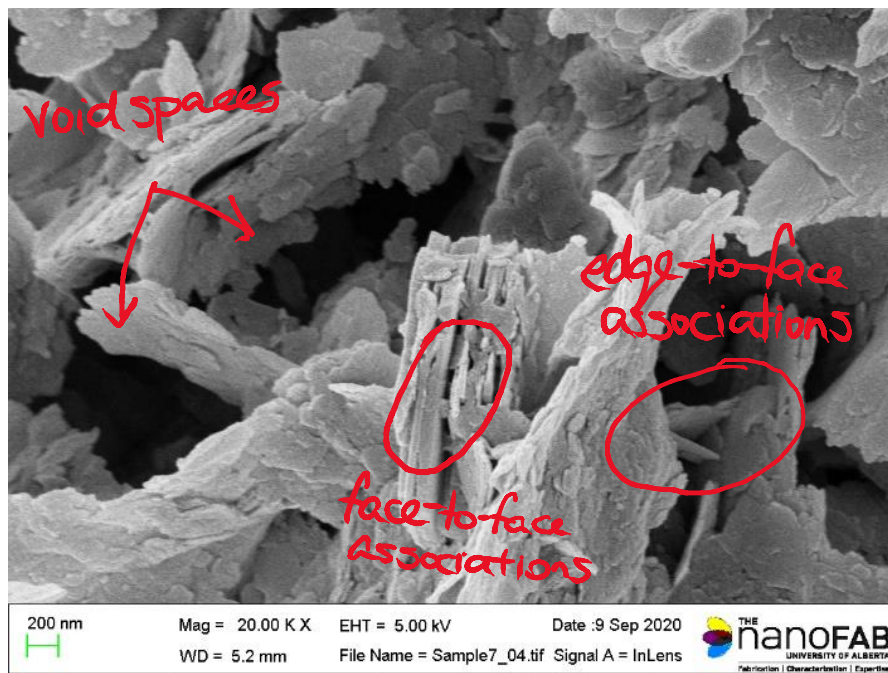
Figure 5-2: Annotated SEM image of flocculated FFT before and after heat treatment at 20,000x magnification

In the untreated sample, the flocs are formed by edge-to-edge and edge-to-face associations between clay mineral surfaces, whereas in the heat-treated sample, there appears to be more face-to-face associations. The voids in the heat-treated sample are smaller. This observation suggests that the flocs were destroyed during the heat-treatment process. From the imageJ analysis, the intensity distribution

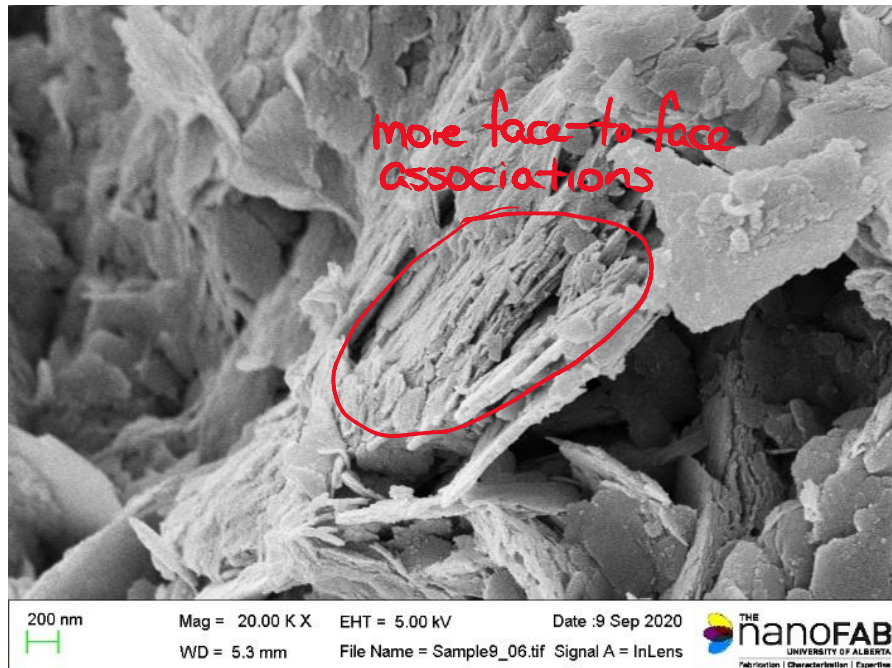
from grey image analysis differs between the samples analyzed at a magnification of 500x. The sample from before treatment has more frequent darker intensities. As the darker intensities correlate to pore spaces, this may suggest that the untreated sample has larger or more frequent pore spaces as compared to the treated sample.

### 5.3.2 Effect of Bacterial Treatment on Microstructure

Figure 4-19 shows micro and nano scale images of the higher solids content flocculated FFT sample before and after bacteria treatment at three different magnifications. Like the heat-treated samples, flocculated clay mineral platelets are visible in both the bacteria treated and untreated samples at all magnifications. More voids and the spaces appear to be larger in the untreated sample than in the bacteria treated sample. More face-to-face associations are visible in the treated sample as compared to the untreated sample.



(a) untreated



(b) bacteria treated

Figure 5-3: Annotated SEM image of flocculated FFT before and after bacteria treatment at 20,000x magnification

Similar to the imageJ results from the flocculated sample, the sample from before treatment has more frequent darker intensities.

These observations may suggest that the bacteria treatment process destroyed the polymer and the flocs collapsed. As void spaces become smaller, one would expect the saturated hydraulic conductivity to decrease. As the flocs collapse, the dewater potential would decrease. The microstructure results for the bacteria treated samples indicate a potential negative impact to the long-term strength behaviour of the bacterial treated FFT samples through reduced dewaterability potential.

## 6 Conclusions and Recommendations

### 6.1 Conclusions

It is anticipated that the synthetic flocculants will eventually degrade with time leaving only a mineral soil structure behind (Sorbie 1991). The geotechnical properties following potential degradation of the amendments is unknown. This research provided the opportunity to further understand the long-term strength behavior of polymer amended tailings deposits. Specific objectives included:

- Evaluation of potential polymer degradation methods to accelerate degradation of chemical amendments.
- Compare impact of thermal polymer degradation on geotechnical behaviour on control samples.
- Compare impact of polymer degradation on geotechnical behaviour on various chemically amended samples.

Based on the selected parameters, the following hypothesis was developed. If negative impacts to the long-term strength behaviour of polymer amended tailings occurred, the following results were expected after treatment:

- change in pH,
- decrease in yield point,
- decrease in shear strength,
- decrease in the elastic modulus,  $G'$ ,
- transition to a more fluid-like structure,
- changes in void spaces observed in SEM image, and
- increase in face-to-face associations observed in SEM images.

*Evaluation of potential polymer degradation methods to accelerate degradation of chemical amendments and compare impact of thermal polymer degradation on geotechnical behaviour on control samples.*

Two potential polymer degradation methods were evaluated – thermal and bacterial degradation. The thermal degradation pathway was selected for this research, as it is the most straightforward.

The process and experimental setup were based on previous research done by Mao and Fahey (1999). Samples of kaolinite and FFT were used as control samples to determine if the heating process was influencing the clay mineral structure.

In the control samples the following observations were made:

- 1/4 samples showed a decrease to the pH after treatment;
- 3/4 samples showed a decrease to the yield point;
- 3/4 samples showed a decrease to the shear strength;
- 3/4 samples showed a decrease to the G’;
- 3/4 samples showed a transition to a more “fluid-like” structure from oscillatory measurements; and
- no changes to structure were observed in the SEM images.

It appears that a change occurred from the heat treatment process, however it is difficult to determine whether it was a result of the change in percent solids or if the heating process was altering the mineral structure of the clay / tailings sample.

The second polymer degradation method used was bacterial degradation. This pathway was explored using a commercially available bacterium. It is sold under the name ‘Frac-Bac’ and was provided for this research by Re-Nuu Production Optimization Inc. The polymer degradation methodology was selected based on manufacture recommendations. The results suggest negative impacts to the long-term strength behaviour of polymer amended tailings, however, many of these changes to the measured parameters were low to moderate in magnitude (average 20% decrease). When comparing the two polymer degradation methodologies, less error was introduced in the bacteria treated samples and consistent negative impacts were seen in all parameters.

*Compare impact of polymer degradation on geotechnical behaviour on various chemically amended samples.*

In the heat-treated, polymer amended tailings samples the following observations were made:

- 3/3 samples showed a decrease to the pH after treatment;

- 1/3 samples showed a decrease to the to the yield point;
- 1/3 samples showed a decrease to the shear strength;
- 3/3 samples showed a decrease to the to the G’;
- 3/3 samples showed a transition to a more “fluid-like” structure from oscillatory measurements; and
- 1/1 samples showed increase in face-to-face associations in the SEM images.

In the bacteria-treated, polymer amended tailings samples the following observations were made:

- 2/3 samples showed a decrease to the pH after treatment;
- 3/3 samples showed a decrease to the to the yield point;
- 3/3 samples showed a decrease to the shear strength;
- 3/3 samples showed a decrease to the to the G’;
- 3/3 samples showed a transition to a more “fluid-like” structure from oscillatory measurements; and
- 1/1 samples showed increase in face-to-face associations in the SEM images.

While the results suggest negative impacts to the long-term strength behaviour of polymer amended tailings, many of these changes were low to moderate in magnitude (average 30% change). Errors introduced from the limitations of the heat treatment process (change in percent solids) are known to have large effects on the measured shear strength in oil sands tailings and were difficult to control in the experiment. Significant spread was also observed in the measured parameters where duplicate samples were prepared.

It appears that a change in structure occurred from the heat treatment process, however it is difficult to quantify whether it was a result of the change to percent solids or from degradation of the polymer itself. The results from the bacteria treated samples showed consistent negative impacts seen in all parameters.

## 6.2 Recommendations

It would be a benefit to further study the impact of polymer degradation on amended tailings with the following improvements:



- Additional research on the bacterial treatment process – this degradation pathway showed consistent negative impacts to the samples and introduced fewer errors
- Quantifying error in the oscillatory rheology for each tailing sample
- Improvements to the heat treatment process to ensure that moisture content / percent solids of the samples stay within defined parameters. This had the greatest impact on the higher percent solids samples.

The research showed that negative impacts occurred from the investigated treatment processes, however, the magnitude of those impacts were difficult to quantify as a result of experimental error through moisture loss and errors in the measurement. With the above improvements, it would be possible to determine the magnitude of the impacts from polymer degradation on the long-term strength behaviour of polymer amended tailings samples.

## 7 References

- Abdulnabi, A., Amoako, K., Moran, D., Vandara, K., Aldaeef, A.A., Esmailzadeh, A., Beier, N.A., Soares, J.B.P., and Simms, P. 2021. Evaluation of candidate polymers to maximize the geotechnical performance of oil sands tailings. *Canadian Geotechnical Journal*.
- AER. 2020. State of fluid tailings management for mineable oil sands, 2019. Alberta Energy Regulator, Calgary, Alberta.
- AER. 2019. Decision 2019 ABAER 006: Syncrude canada ltd. mildred lake extension project and mildred lake tailings management plan. Alberta Energy Regulator, Calgary, Alberta.
- AER. 2018. Decision 20180613A: Syncrude canada ltd.; application for aurora north tailings management plan. Alberta Energy Regulator, Calgary, Alberta.
- AER. 2017a. Decision 20171218A: Canadian natural resources limited; application for horizon oil sands processing plant and mine tailings management plan. Alberta Energy Regulator, Calgary, Alberta.
- AER. 2017b. Decision 20171025A: Suncor energy inc., application for millennium operational amendment and base plant tailings management plan. Alberta Energy Regulator, Calgary, Alberta.
- AER. 2016. Alberta's energy reserves 2015 & supply/demand outlook 2016-2025 (ST98-2016). Alberta Energy Regulator, Calgary, Alberta.

- AER. 2009. Directive 074: Tailings performance criteria and requirements for oil sands mining schemes. Alberta Energy Regulator, Calgary, Alberta.
- Ajao, V., Bruning, H., Rijnaarts, H., and Temmink, H. 2018. Natural flocculants from fresh and saline wastewater: Comparative properties and flocculation performances. *Chemical Engineering Journal*, **349**: 622-632.
- Alberta Culture and Tourism. 2018. The formation of oil sands [online]. Available from <http://www.history.alberta.ca/energyheritage/sands/origins/the-geology-of-the-oil-sands/the-formation-of-oil-sands.aspx> [cited May 2, 2018].
- Alberta Energy. 2020. Oil sands facts and statistics [online]. Available from [https://www.alberta.ca/oil-sands-facts-and-statistics.aspx#:~:text=Alberta's%20oil%20sands%20has%20the,bb1%2Fd\)%20in%202017](https://www.alberta.ca/oil-sands-facts-and-statistics.aspx#:~:text=Alberta's%20oil%20sands%20has%20the,bb1%2Fd)%20in%202017).
- Bajwa, T.M. 2015. Microstructure and macroscopic behaviour of polymer amended oil sands mature fine tailings. Carleton University, Ottawa, Ontario.
- Barnes, H.A. 1995. A review of the slip (wall depletion) of polymer solutions, emulsions and particle suspensions in viscometers: Its cause, character, and cure. *Journal of Non-Newtonian Fluid Mechanics*, **56**(3): 221-251.
- Beier, N., Wilson, W., Dunmola, A., and Segoo, D. 2013. Impact of flocculation-based dewatering on the shear strength of oil sands fine tailings. *Canadian Geotechnical Journal*, **50**(9): 1001-1007.

- BGC Engineering Inc. 2010. Oil sands tailings technology review. Oil Sands Research and Information Network, University of Alberta, School of Energy and the Environment, Edmonton, Alberta.
- Birn, K. and Khanna, P. 2010. A discussion paper on the oil sands: Challenges and opportunities. Natural Resources Canada, Ottawa, Canada.
- Boger, D., Scales, P., and Sofra, F. 2006. Rheological concepts. *In* Paste and thickened tailings: a guide *Edited by* R.J. Jewell and A.B. Fourie. Australian Centre for Geomechanics, The University of Western Australia, Nedlands, Western Australia, Australia, pp. 257.
- Broughton, P.L. 2013. Devonian salt dissolution-collapse breccias flooring the cretaceous athabasca oil sands deposit and development of lower McMurray formation sinkholes, northern alberta basin, western canada. *Sedimentary geology*, **283**: 57-82.
- Cavanagh, P. 2016. Tailings treatment approaches at kearl - an update. *In* Fifth International Oil Sands Tailings Conference, December 4-7, 2016. U of A Geotechnical Centre, Edmonton, Alberta, 2-11.
- Chalaturnyk, R.J., Don Scott, J., and Özüim, B. 2002. Management of oil sands tailings. *Petroleum Science and Technology*, **20**(9-10): 1025-1046.
- Chhabra, R.P. and Richardson, J.F. 2008. Non-newtonian flow and applied rheology – engineering applications. Elsevier: Butterworth- Heinemann, Oxford, Great Britain.

- Chmelir, M., Künschner, A., and Barthell, E. 1980. Water soluble acrylamide polymers, 2. aging and viscous flow of aqueous solutions of polyacrylamide and hydrolyzed polyacrylamide. *Die Angewandte Makromolekulare Chemie*, **89**(1): 145-165.
- CTMC. 2012. Oil sands tailings technology deployment roadmap project report – volume 1 – project summary report. Alberta Innovates - Energy and Environment Solutions and the Oil Sands Tailings Consortium (OSTC), Edmonton, Alberta.
- Das, B.M. and Sivakugan, N. 2017. Fundamentals of geotechnical engineering. Cengage Learning, Boston, MA.
- Derakhshandeh, B., Junaid, A., and Freeman, G. 2016. Effects of shearing and shearing time on dewatering and yield characteristics of oil sands flocculated fine tailings. *In Fifth International Oil Sands Tailings Conference, December 4-7, 2016*. U of A Geotechnical Centre, Edmonton, Alberta, 416-421.
- Dolinar, B. and Trauner, L. 2007. The impact of structure on the undrained shear strength of cohesive soils. *Engineering Geology*, **92**(1): 88-96.
- e Silva, M., Dutra, E.R., Mano, V., and Machado, J.C. 2000. Preparation and thermal study of polymers derived from acrylamide. *Polymer Degradation and Stability*, **67**(3): 491-495.
- Ferreira, T. and Rasband, W. 2012. Image J/fiji 1.46 user guide.
- Fisseha, B. 2020. Experimental study on consolidation behaviour and shear strength gain for saturated/unsaturated treated fluid fine tailings. University of Alberta, Edmonton, Alberta.

- Gibson, R.E., England, G.L., and Hussey, M.J.L. 1967. The theory of one-dimensional consolidation of saturated clays. I. finite non-linear consolidation of thin homogeneous layers. *17*(3): 261-273.
- Gingras, M. and Rokosh, D. 2004. A brief overview of the geology of heavy oil, bitumen and oil sand deposits. *In* 2004 CSEG National Convention, May 2004. Canadian Society of Exploration Geophysicists, Calgary, AB.
- Government of Alberta. 2015. Lower athabasca region tailings management framework for the mineable athabasca oil sands. Government of Alberta, Edmonton, Alberta.
- Gurkaynak, A., Tubert, F., Yang, J., Matyas, J., Spencer, J.L., and Gryte, C.C. 1996. High-temperature degradation of polyacrylic acid in aqueous solution. *Journal of Polymer Science, Part A: Polymer Chemistry*, **34**(3): 349-355.
- Hartman, H.L. and Mutmansky, J.M. 2002. *Introductory mining engineering*. Hoboken, N.J.: J. Wiley, c2002; 2nd ed.
- Haveroen, M.E. 2005. *Microbiological studies of polyacrylamide as a flocculant aid for oil sands tailings*. University of Alberta, Edmonton, Alberta.
- Haveroen, M.E., MacKinnon, M.D., and Fedorak, P.M. 2005. Polyacrylamide added as a nitrogen source stimulates methanogenesis in consortia from various wastewaters. *Water Research*, **39**(14): 3333-3341.
- Hogg, R. 2000. Flocculation and dewatering. *International Journal of Mineral Processing*, **58**(1): 223-236.

- Hripko, R., Vajihinejad, V., LopesMotta, F., and Soares, J.B.P. 2018. Enhanced flocculation of oil sands mature fine tailings using hydrophobically modified polyacrylamide copolymers. *Global Challenges*, **2**(3): 1700135-n/a.
- Hwang, G., Dong, T., Islam, M.S., Sheng, Z., Pérez-Estrada, L.A., Liu, Y., and Gamal El-Din, M. 2013. The impacts of ozonation on oil sands process-affected water biodegradability and biofilm formation characteristics in bioreactors. *Bioresource technology*, **130**: 269-277.
- Jarvis, P., Jefferson, B., and Parsons, S.A. 2005. Measuring floc structural characteristics. *Reviews in Environmental Science and Bio/Technology*, **4**(1/2): 1-18.
- Jarvis, P., Jefferson, B., Gregory, J., and Parsons, S.A. 2005. A review of floc strength and breakage. *Water research*, **39**(14): 3121-3137.
- Jeeravipoolvarn, S. 2010. Geotechnical behaviour of in-line thickened oil sands tailings. University of Alberta, Edmonton, Alberta.
- Jeeravipoolvarn, S. 2005. Compression behaviour of thixotropic oil sands tailings. University of Alberta, Edmonton, Alberta.
- Kabwe, L.K., Wilson, G.W., Beier, N.A., Cunningham, K.A., and Scott, J.D. 2017. Geotechnical characterization of a frozen and thawed centrifuge product *In Tailings and Mine Waste '17*, 5-8 November 2017. University of Alberta Geotechnical Center, Edmonton, Alberta, 750-759.

- Kaiser, K.L.E. and Lawrence, J. 1977. Polyelectrolytes: Potential chloroform precursors. *Science*, (4295): 1205-1206.
- Kaminsky, H. 2014. Demystifying the methylene blue index. *In* Fourth International Oil Sands Tailings Conference, 7-10 December 2014. University of Alberta Geotechnical Centre, Edmonton, Alberta, 220-230.
- Kaminsky, H. 2008. Characterization of an athabasca oil sand ore and process stream. University of Alberta, Edmonton, Alberta.
- Kasperski, K.L. and Mikula, R.J. 2011. Waste streams of mined oil sands; characteristics and remediation. *Elements*, 7(6; 6): 387-392.
- Kay-Shoemake, J., Watwood, M E, Lentz, R D, and Sojka, R E. 1998. Polyacrylamide as an organic nitrogen source for soil microorganisms with potential effects on inorganic soil nitrogen in agricultural soil. *Soil Biology and Biochemistry*, **30**(8-9): 1045-1052.
- Koppula, S.D. 1970. The consolidation of soil in two dimensions and with moving boundaries. University of Alberta, Edmonton, Alberta.
- Lee, K. 1979. An analytical and experimental study of large strain soil consolidation. University of Oxford, Oxford, United Kingdom.
- Levitt, D. and Pope, G.A. 2008. Selection and screening of polymers for enhanced-oil recovery. *In* 2008 SPE/DOE Improved Oil Recovery Symposium, 19-23 April 2008. Society of Petroleum Engineers, Tulsa, Oklahoma, USA, 18.



- Liang, L., Peng, Y., Tan, J., and Xie, G. 2015. A review of the modern characterization techniques for flocs in mineral processing. *Minerals Engineering*, **84**: 130-144.
- Lipp, D. and Kozakiewicz, J. 1993. Acrylamide polymers. in: Kroschwitz JI, howe-grant M, eds. *kirk-othmer encyclopedia of chemical technology*. Wiley, New York.
- Locat, J. and Demers, D. 1988. Viscosity, yield stress, remolded strength, and liquidity index relationships for sensitive clays. *Canadian Geotechnical Journal*, **25**(4): 799-806.
- Loganathan, K., Chelme-Ayala, P., and Gamal El-Din, M. 2015. Effects of different pretreatments on the performance of ceramic ultrafiltration membrane during the treatment of oil sands tailings pond recycle water: A pilot-scale study. *Journal of environmental management*, **151**: 540-549.
- Malkin, A.Y. and Isayev, A.I. 2006. Introduction. rheology: Subject and goals. *In Rheology - Concepts, Methods, & Applications Edited by N/A*. ChemTec Publishing, Toronto, Ontario.
- Mao, X. and Fahey, M. 1999. A method of reconstituting an aragonite soil using a synthetic flocculant. *Geotechnique*, **49**(1): 15-32.
- Masliyah, J., Zhou, Z., Xu, Z., Czarnecki, J., Hamza, H., Univ, A., Syncrude Canada, L., and Canmet. 2004. Understanding water-based bitumen extraction from athabasca oil sands. *Canadian Journal of Chemical Engineering, The*, **82**(4; 200540): 628-654.

- Masliyah, J.H., Xu, Z., Czarnecki, J.A., and Dabros, M. 2013. Handbook on theory and practice of bitumen recovery from athabasca oil sands. Kingsley Knowledge Pub., Cochrane, Alberta.
- McKenna, G., Mooder, B., Burton, B., and Jamieson, A. 2016. Shear strength and density of oil sands fine tailings for reclamation to a boreal forest landscape. *In* International Oil Sands Tailings Conference, Lake Louise, AB, 4-7 December 2016. University of Alberta Geotechnical Centre, Edmonton, Alberta, 130-153.
- Mellon, G.B., Wall, J.H., and Alberta Research Council. 1956. Geology of the McMurray formation. Research Council of Alberta, Edmonton, Alberta.
- Mewis, J. and Spaul, A.J.B. 1976. Rheology of concentrated dispersions. *Advances in Colloid and Interface Science*, **6**(3): 173-200.
- Mikula, R.J., Munoz, V.A., and Omotoso, O. 2009. Centrifugation options for production of dry stackable tailings in surface- mined oil sands tailings management. *Journal of Canadian Petroleum Technology*, **48**(09): 19-23.
- Mitchell, J.K. and Soga, K. 2005. Fundamentals of soil behavior. John Wiley & Sons, Hoboken, New Jersey, USA.
- Mizani, S., He, X., and Simms, P. 2013. Application of lubrication theory to modeling stack geometry of high density mine tailings. *Journal of Non-Newtonian Fluid Mechanics*, **198**: 59-70.

- Mizani, S. 2016. Experimental study and surface deposition modelling of amended oil sands tailings products. Carlton University, Ottawa, Ontario.
- Mizani, S., Simms, P., and Wilson, W. 2017. Rheology for deposition control of polymer-amended oil sands tailings. *Rheologica Acta*, **56**(7): 623-634.
- Mojid, M.A. 2011. Diffuse double layer (DDL). *In Encyclopedia of Agrophysics Edited by J. Gliński, J. Horabik and J. Lipiec*. Springer Netherlands, Dordrecht, pp. 213-214.
- Mpofu, P., Addai-Mensah, J., and Ralston, J. 2003. Investigation of the effect of polymer structure type on flocculation, rheology and dewatering behaviour of kaolinite dispersions. *International Journal of Mineral Processing*, **71**(1): 247-268.
- Natural Resources Canada. 2013. Oil sands processes [online]. Available from <https://www.nrcan.gc.ca/energy/oil-sands/5853> [cited May 2, 2018].
- Oil Sands Discovery Centre. 2010. Facts about alberta's oil sands and its industry [online]. Available from <https://search.proquest.com/docview/1943862193> [cited May 2, 2018].
- OSTC and COSIA. 2012. Technical guide for fluid fine tailings. Canada's Oil Sands Innovation Alliance, Calgary, Alberta.
- Owolagba, J.O. 2013. Dewatering behavior of centrifuged oil sand fine tailings for surface deposition. University of Regina, Regina, Saskatchewan.

- Reid, D. and Fourie, A. 2016. Laboratory assessment of the effects of polymer treatment on geotechnical properties of low-plasticity soil slurry. *Canadian Geotechnical Journal*, **53**(10): 1718-1730.
- Rima, U.S. and Beier, N. 2018. Evaluation of temperature and multiple freeze- thaw effects on the strength properties of centrifuged tailings. *In Geo Edmonton 2018*, September 23-26, 2018.
- Rosenqvist, I.T. 1953. Considerations on the sensitivity of norwegian quick-clays. *Géotechnique*, **3**(5): 195-200.
- Salam, A., M.Simms, P.H., and Örmeci, B. 2018. Evidence of creep & structuration in polymer amended oil sands tailings. *In 6th International Oil Sands Tailings Conference*, 9-12 December, 2018. U of A Geotechnical Centre, Edmonton, Alberta.
- Scott, J.D., Jeeravipoolvarn, S., and Chalaturnyk, R. 2008. Tests for wide range of compressibility and hydraulic conductivity of flocculated tailings. *In Sixty-first Canadian Geotechnical Conference*  
9th Joint CGS/IAH-CNC Groundwater Conference, 21-24 September 2008. Canadian Geotechnical Society, Edmonton, Alberta.
- Skempton, A.W. and Northey, R.D. 1952. The sensitivity of clays. *Geotechnique*, **III** (1).
- Small, C.C., Cho, S., Hashisho, Z., and Ulrich, A.C. 2015. Emissions from oil sands tailings ponds: Review of tailings pond parameters and emission estimates. *Journal of Petroleum Science and Engineering*, **127**: 490-501.

- SNF Floerger. 2018. Water soluble polymers. MDPI - Multidisciplinary Digital Publishing Institute, Andrézieux-Bouthéon, France.
- Somogyi, F. 1980. Large-strain consolidation of fine-grained slurries. *In* Presented at the Canadian Society for Civil Engineering, 1980. Univ of Manit, Winnipeg, Manitoba, 12p.
- Soponkanaporn, T. and Gehr, R. 1989. The degradation of polyelectrolytes in the environment: Insights provided by size exclusion chromatography measurements. *Water Science and Technology*, **21**(8-9): 857-868.
- Sorbie, K.S. 1991a. Polymer stability. *In* *Polymer-Improved Oil Recovery Edited by K.S. Sorbie*. Springer Netherlands, Dordrecht, pp. 83-125.
- Sorbie, K.S. 1991b. *Polymer-improved oil recovery*. New York: Springer Science+Business Media, New York, New York, USA.
- Sorta, A.R., Sego, D.C., and Wilson, W. 2012. Effect of thixotropy and segregation on centrifuge modelling. *International Journal of Physical Modelling in Geotechnics*, **12**(4): 143-161.
- Suthaker, N.N. and Scott, J.D. 1994. Large scale consolidation testing of oil sand fine tails. *In* 1st International Congress on Environmental Geotechnics, 10-15 July 1994. Edmonton, AB.
- Suzuki, J., Taumi, N., and Suzuki, S. 1979. Ozone treatment of water-soluble polymers. IV. ozone degradability of water-soluble polymers. *Journal of Applied Polymer Science*, **23**(11): 3281-3288.

- Swiecinski, F., Reed, P., and Andrews, W. 2016. The thermal stability of polyacrylamides in EOR applications. *In* SPE Improved Oil Recovery Conference, Tulsa, Oklahoma, USA Society of Petroleum Engineers, Tulsa, Oklahoma, USA.
- Taylor, K.C. and Nasr-El-Din, H.A. 1994. Acrylamide copolymers: A review of methods for the determination of concentration and degree of hydrolysis. *Journal of Petroleum Science and Engineering*, **12**(1): 9-23.
- Toorman, E.A. 1997. Modelling the thixotropic behaviour of dense cohesive sediment suspensions. *Rheologica acta*, **36**(1): 56-65.
- Truong, N.D., Galin, J.C., Francois, J., and Pham, Q.T. 1986. Microstructure of acrylamide acrylic-acid copolymers .1. as obtained by alkaline-hydrolysis. *Polymer*, **27**(3): 459-466.
- Vedoy, D.R.L. and Soares, J.B.P. 2015. Water-soluble polymers for oil sands tailing treatment: A review. *The Canadian Journal of Chemical Engineering*, **93**(5; 201645): 888-904.
- Wang, C., Harbottle, D., Liu, Q., and Xu, Z. 2014. Current state of fine mineral tailings treatment: A critical review on theory and practice. *Minerals Engineering*, **58**: 113-131.
- Wang, Y.H. and Siu, W.K. 2006. Structure characteristics and mechanical properties of kaolinite soils. I. surface charges and structural characterizations. *Canadian Geotechnical Journal*, **43**(6): 587-600.
- Williams, P.A. 2007. *Handbook of industrial water soluble polymers*. Blackwell Pub., Ames, Iowa, USA.

Yasuda, K., Okajima, K., and Kamide, K. 1988. Study on alkaline hydrolysis of polyacrylamide by  $^{13}\text{C}$  nmr. *Polymer Journal*, **20**(12): 1101-1107.

## Appendix A: Methods and Test Procedures

### A-1: Dean Stark Analysis Method

The bitumen content was determined using the Dean Stark extraction method with the aid of the Soxhley extractor shown in Figure A-1.



*Figure A-1: Dean Stark extraction setup*

The tailings sample is dried to remove all moisture. The remaining bitumen and tailings solids are used for the test. The apparatus typically consists of a vertical cylindrical glass tube, a boiler, and a reflux condenser. Toluene is used as a solvent, where it is boiled to create toluene vapor. The vapor rises to the siphon where the sample is held. The toluene separates the bitumen and the tailings solids. In the siphon, toluene vapor is condensed and simultaneously, water is separated into a water trap. The solids remain in place and the toluene / bitumen solution is



returned to the boiler until only bitumen remains. At the end of the extraction process, all separated components are weighed, and the percentage of bitumen is calculated.

### A-2: Water Content

Water content was determined according to the ASTM D2216-10, where it was dried at 110°C for 24 hours. The following formulas were used to calculate the water content:

$$M_{wet\ sample} = M_{container+wet\ sample} - M_{container}$$

$$M_{solids} = M_{solids+container} - M_{container}$$

$$M_{water} = M_{wet\ sample+container} - M_{solids+container}$$

$$W\% = \frac{M_{water}}{M_{solids}} \times 100$$

### A-3: Specific Gravity

Specific gravity is a vital parameter when determining other geotechnical parameters such as void ratio and dry density. It was determined according to ASTM D854-14 using vacuum deairing.

A picture of the setup is shown below in Figure A-2.

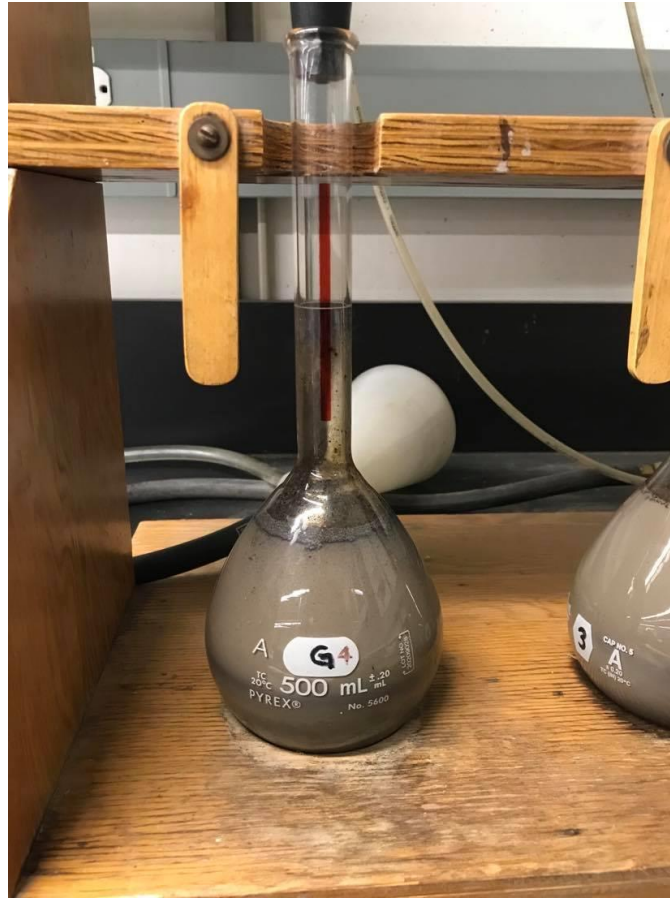


*Figure A-2: Specific gravity setup*

#### A-4: Particle Size Distribution

A grain size distribution (GSD) analysis of soils and tailings is an important aspect of geotechnical engineering and reclamation practices. It provides relevant information about the proportions of the different sized particles present in a sample. This information can be used in order to classify materials. It establishes the most basic characterizations of soils according to mass, grading, and distribution of the size of particles. The particles of the materials in question, FFT and centrifuged tailings, are expected to be in the clay-silt range as they are both types of oil sand tailings, commonly known to be very fine-grained. As such, the hydrometer test was used. This test analyzes soils with a GSD ranging from 0.075 mm to approximately 0.001 mm using a sedimentation method based on Stokes' law. This principle dictates that the velocity of the settlement of particles in water depends on grain size, shape, and mass (Das 2013). ASTM D7928 (2017) was followed for the hydrometer experiments.

# Appendix B: Material Characterization Test Data

**UNIVERSITY OF ALBERTA WO# 18C 345399 MBI RESULTS**

Lab Number	Description	Sample Weight	Methylene Blue Volume	meq/100g
		(g)	(mL)	
18A 19032	Tailings, FFT (Big Container)	2.00	25.0	7.50



2905 - 12 Street NE  
 Calgary, Alberta  
 T2E 7J2  
 Tel:(403) 299-2000  
 Fax:(403) 299-2010

**INVOICE NO. 18487333H**

**Date:** 19 Jun 2018

**GST #:** R100073238      **QST #:** 1212241632

**Calgary lab**

Customer No	WorkOrder No	Branch	Customer P.O.	Division ID	Acct Code	District	Product
3247200	18C345399	C		10		10	

Date Received	Project No/Name	AFE
May 31, 2018		

Product ID	Product Description	Quantity	Surcharge	Unit Price	Extended Price
------------	---------------------	----------	-----------	------------	----------------

**RE: FFT TAILINGS SAMPLES**

04-731	Analytical Dean Stark - Bitumen, Solids and Water Content (Small Extractor) Direct Oil Determination/sample	1		\$167.00	\$167.00
11-200	Bulk XRD Analysis	1		\$367.50	\$367.50
31-120	Methylene Blue Index for clay activity (per sample)	1		\$36.05	\$36.05
39-200	Environmentally Safe Sample Disposal	2		\$12.00	\$24.00
39-550	Invoice Administration	1		\$9.00	\$9.00
58-557	Atterberg Limits	1		\$200.00	\$200.00

Continued On Next Page...

**Corporate Office:**  
**UNIVERSITY OF ALBERTA**  
 114 STREET, 89 AVE  
 EDMONTON AB T6G2E1

**Invoice To:**  
**UNIVERSITY OF ALBERTA**  
 114 STREET, 89 AVE  
 EDMONTON AB T6G2E1  
**Attn To: Kelsey Cunningham**



2905 - 12 Street NE  
 Calgary, Alberta  
 T2E 7J2  
 Tel:(403) 299-2000  
 Fax:(403) 299-2010

**INVOICE NO. 18487333H**

Date: 19 Jun 2018

GST #: R100073238      QST #: 1212241632

Calgary lab

Customer No	WorkOrder No	Branch	Customer P.O.	Division ID	Acct Code	District	Product
3247200	18C345399	C		10		10	

Date Received	Project No/Name	AFE
May 31, 2018		

Product ID	Product Description	Quantity	Surcharge	Unit Price	Extended Price
------------	---------------------	----------	-----------	------------	----------------

RE: FFT TAILINGS SAMPLES

\* \*\*\*\*\*  
 \* Should you require any information regarding this analysis, please contact your  
 \* Client Project Manager @ (403) 299-2000  
 \*  
 \* We appreciate and welcome your feedback which can be provided by submitting a  
 \* Client Review at <http://www.agatlabs.com/resources/client-forms.cfm>  
 \* \*\*\*\*\*

Subtotal: \$803.55

GST: \$40.18

Grand Total: **\$843.73**

Terms: NET 30 DAYS. INTEREST CHARGED ON OVERDUE ACCOUNT AT THE RATE OF 2% PER MONTH (24% PER ANNUM).

**By choosing AGAT you've limited your waste disposal liability.** We assure our clients that we are committed to safe, clean, and legal sample disposal protocols. We dispose of samples according to federal and provincial environmental regulations.

**CLIENT NAME: UNIVERSITY OF ALBERTA  
114 STREET, 89 AVE  
EDMONTON, AB T6G2E1  
(403) 492-4166**

**ATTENTION TO: Kelsey Cunningham**

**PROJECT: 18C345399**

**AGAT WORK ORDER: 18C346965**

**SOIL ANALYSIS REVIEWED BY: Krystyna Krauze, Senior Analyst**

**DATE REPORTED: Jun 13, 2018**

**PAGES (INCLUDING COVER): 4**

**VERSION\*: 1**

Should you require any information regarding this analysis please contact your client services representative at (403) 735-2005

**\*NOTES**

**All samples will be disposed of within 30 days following analysis. Please contact the lab if you require additional sample storage time.**



# Certificate of Analysis

AGAT WORK ORDER: 18C346965

PROJECT: 18C345399

2910 12TH STREET NE  
CALGARY, ALBERTA  
CANADA T2E 7P7  
TEL (403)735-2005  
FAX (403)735-2771  
<http://www.agatlabs.com>

CLIENT NAME: UNIVERSITY OF ALBERTA

ATTENTION TO: Kelsey Cunningham

SAMPLING SITE:

SAMPLED BY:

## Soil Analysis - Atterberg Limits

DATE RECEIVED: 2018-06-04

DATE REPORTED: 2018-06-13

		SAMPLE DESCRIPTION: Tailings FFT		
		SAMPLE TYPE: Soil		
		DATE SAMPLED: 2018-05-30		
Parameter	Unit	G / S	RDL	9300075
Liquid Limit	%		1	52
Plastic Limit	%		1	32
Plasticity Index	%		1	20

**Comments:** RDL - Reported Detection Limit; G / S - Guideline / Standard  
9300075 Note: Oily sample.

**Certified By:**



## Quality Assurance

CLIENT NAME: UNIVERSITY OF ALBERTA

AGAT WORK ORDER: 18C346965

PROJECT: 18C345399

ATTENTION TO: Kelsey Cunningham

SAMPLING SITE:

SAMPLED BY:

Soil Analysis															
RPT Date:			DUPLICATE				Method Blank	REFERENCE MATERIAL			METHOD BLANK SPIKE		MATRIX SPIKE		
PARAMETER	Batch	Sample Id	Dup #1	Dup #2	RPD	Measured Value		Acceptable Limits		Recovery	Acceptable Limits		Recovery	Acceptable Limits	
								Lower	Upper		Lower	Upper		Lower	Upper

**Soil Analysis - Atterberg Limits**

Liquid Limit	9293537		25	25	0.0%	< 1	100%	80%	120%					
Plastic Limit	9293537		19	18	5.4%	< 1	105%	80%	120%					
Plasticity Index	9293537		6	6	0.0%	< 1	92%	80%	120%					

Comments: If the RPD value is NA, the results of the duplicates are under 5X the RDL and will not be calculated.

**Certified By:**




## Method Summary

CLIENT NAME: UNIVERSITY OF ALBERTA

AGAT WORK ORDER: 18C346965

PROJECT: 18C345399

ATTENTION TO: Kelsey Cunningham

SAMPLING SITE:

SAMPLED BY:

PARAMETER	AGAT S.O.P	LITERATURE REFERENCE	ANALYTICAL TECHNIQUE
<b>Soil Analysis</b>			
Liquid Limit	N/A	ASA 9 - 31-3	LIQUID LIMIT DEVICE
Plastic Limit	N/A	ASA 9 - 31-3	LIQUID LIMIT DEVICE
Plasticity Index	N/A	ASA 9 - 31-3	LIQUID LIMIT DEVICE



**CLIENT NAME: UNIVERSITY OF ALBERTA  
114 STREET, 89 AVE  
EDMONTON, AB T6G2E1  
(403) 492-4166**

**ATTENTION TO: Louis Kabwe**

**PROJECT:**

**AGAT WORK ORDER: 17E177119**

**SOIL ANALYSIS REVIEWED BY: Melinda Guay, Technical Reviewer**

**DATE REPORTED: Jan 16, 2017**

**PAGES (INCLUDING COVER): 7**

**VERSION\*: 1**

Should you require any information regarding this analysis please contact your client services representative at (780) 395-2525

**\*NOTES**

**All samples will be disposed of within 30 days following analysis. Please contact the lab if you require additional sample storage time.**



## Certificate of Analysis

AGAT WORK ORDER: 17E177119

PROJECT:

6310 ROPER ROAD  
EDMONTON, ALBERTA  
CANADA T6B 3P9  
TEL (780)395-2525  
FAX (780)462-2490  
<http://www.agatlabs.com>

CLIENT NAME: UNIVERSITY OF ALBERTA

ATTENTION TO: Louis Kabwe

SAMPLING SITE:

SAMPLED BY:

### Soil Analysis - Atterberg Limits

DATE RECEIVED: 2017-01-11

DATE REPORTED: 2017-01-16

Parameter	Unit	G / S	RDL	MFT Centrifuge	MFT
				Cake	Flocculated
SAMPLE DESCRIPTION:				Cake	Flocculated
SAMPLE TYPE:				Other	Other
DATE SAMPLED:				2017-01-11	2017-01-11
				8121927	8121929
Liquid Limit			1	57	79
Plastic Limit			1	26	28
Plasticity Index				31.9	50.6

Comments: RDL - Reported Detection Limit; G / S - Guideline / Standard

8121927-8121929 Plasticity Index is a calculated parameter. The calculated value is the difference between the liquid limit and the plastic limit.

**Certified By:**

## Quality Assurance

CLIENT NAME: UNIVERSITY OF ALBERTA

AGAT WORK ORDER: 17E177119

PROJECT:

ATTENTION TO: Louis Kabwe

SAMPLING SITE:

SAMPLED BY:

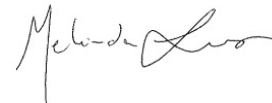
### Soil Analysis

RPT Date: Jan 16, 2017			DUPLICATE			Method Blank	REFERENCE MATERIAL			METHOD BLANK SPIKE			MATRIX SPIKE		
PARAMETER	Batch	Sample Id	Dup #1	Dup #2	RPD		Measured Value	Acceptable Limits		Recovery	Acceptable Limits		Recovery	Acceptable Limits	
								Lower	Upper		Lower	Upper		Lower	Upper

**Soil Analysis - Atterberg Limits**

Liquid Limit	13	8123002	47	47	0.0%	< 1	100%	80%	120%
Plastic Limit	13	8123002	28	28	0.0%	< 1	95%	80%	120%
Plasticity Index	13	8123002	18.8	18.6	1.1%	< 1	104%	80%	120%

Comments: \*Non-accredited test. Inquire with lab for details.

**Certified By:**




## Method Summary

CLIENT NAME: UNIVERSITY OF ALBERTA

AGAT WORK ORDER: 17E177119

PROJECT:

ATTENTION TO: Louis Kabwe

SAMPLING SITE:

SAMPLED BY:

PARAMETER	AGAT S.O.P	LITERATURE REFERENCE	ANALYTICAL TECHNIQUE
<b>Soil Analysis</b>			
Liquid Limit	INOR-171-6218	ASA 9 - 31-3	LIQUID LIMIT DEVICE
Plastic Limit	INOR-171-6218	ASA 9 - 31-3	N/A
Plasticity Index	INOR-171-6218	ASTM D4318-00	N/A



# AGAT Laboratories

2910 12 Street NE  
 Calgary, Alberta T2E 7P7  
 P: 403.735.2005 • F: 403.735.2771  
 webearth.agatlabs.com

**Laboratory Use Only**

Arrival Temperature: 19.5°C

AGAT Job Number: 17E17719

Date and Time: 17 JAN 11 13:00

## Chain of Custody Record

Emergency Support Services Hotline **1-855-AGAT 245 (1-855-242-8245)**

### Report Information

Company: U of A

Contact: Louis Kabwe

Address: Civil Eng

Phone: 780-492-2248 Fax: \_\_\_\_\_

LSD: \_\_\_\_\_

Client Project #: \_\_\_\_\_

### Report Information

1. Name: Louis Kabwe

Email: lkabwe@ualberta.ca

2. Name: \_\_\_\_\_

Email: \_\_\_\_\_

3. Name: \_\_\_\_\_

Email: \_\_\_\_\_

### Report Format

Single Sample per Page

Multiple Samples per Page

### Turnaround Time Required (TAT)

Regular TAT  5 to 7 business days

Rush TAT  Less than 24 hours

24 to 48 hours

48 to 72 hours

RUSH TAT REQUESTS UPON SELECTING A RUSH TAT, THE CLIENT ACCEPTS THAT A RUSH SURCHARGE WILL BE ADDED TO THE INVOICE. SEE BACK FOR SURCHARGE.

Date Required: \_\_\_\_\_

### Invoice To

Same  Yes / No

Company: U of A

Contact: \_\_\_\_\_

Address: \_\_\_\_\_

Phone: \_\_\_\_\_ Fax: \_\_\_\_\_

PO/AFE#: \_\_\_\_\_

### Requirements (Selection may impact detection limits)

CCME  AB Tier 1  BC CSR

Agricultural  Agricultural  AW

Industrial  Industrial  IW

Residential/Park  Residential/Park  LW

Commercial  Commercial  DW

Drinking Water  Natural Area

FWAL  AB Surface Water

Other

D50 (Drilling)  SPIGEC

LABORATORY USE (LAB ID #)	SAMPLE IDENTIFICATION	SAMPLE MATRIX	DATE/TIME SAMPLED	COMMENTS - SITE SAMPLE INFO. SAMPLE CONTAINMENT	# OF CONTAINERS	Detailed Soil Salinity (Saturated Paste)	CCME BTEX/F1-F4	Soil Metals <input type="checkbox"/> HWS-B <input type="checkbox"/> Cr <sup>6</sup> <input type="checkbox"/> Hg	Water Metals <input type="checkbox"/> Dissolved <input type="checkbox"/> Total <input type="checkbox"/> Hg <input type="checkbox"/> Cr <sup>6</sup>	Routine Water Potability	AB Class 2 Landfill	BC Landfill	D50 Detailed Soil Salinity (As Received)	Microtox	BTEXS/MPH/EPH <input type="checkbox"/> LEPH/HEPH <input type="checkbox"/>	HOLD FOR 60 DAYS	PRESERVED (Y/N)	CONTAMINATED/HAZARDOUS (Y/N)	
8121927	MFT Centrifuge Cake	Solids	11/1/17																
929	MFT Flocculated	Solids	11/1/17																

Samples Relinquished By (Print Name and Sign): <u>Chris Heregoers</u>	Date/Time: <u>11/09/17</u>	Samples Received By (Print Name and Sign): <u>Ron deGuzman</u>	Date/Time: <u>11/11/2017</u>	Pink Copy - Client	Page _____ of _____
Samples Relinquished By (Print Name and Sign): <u>Chris Heregoers</u>	Date/Time:	Samples Received By (Print Name and Sign):	Date/Time:	Yellow Copy - AGAT	N <sup>o</sup> : AB <b>031880</b>
Samples Relinquished By (Print Name and Sign):	Date/Time:	Samples Received By (Print Name and Sign):	Date/Time:	White Copy - AGAT	



# AGAT Laboratories

## SAMPLE INTEGRITY RECEIPT FORM

### RECEIVING BASICS - Shipping

Company/Consultant: U of A

Courier: prop off Prepaid Collect

Waybill# N/A

Branch  EDM  GP  FN  FM  RD  VAN  LYD  FSJ  EST Other: \_\_\_\_\_

If multiple sites were submitted at once:  Yes  No

Custody Seal Intact: Yes  No  NA

TAT: <24hr  24-48hr  48-72hr  Reg Other \_\_\_\_\_

Cooler Quantity: 2

### TIME SENSITIVE ISSUES - Shipping

ALREADY EXCEEDED HOLD TIME? Yes  No

Inorganic Tests (Please Circle): Mibi , BOD , Nitrate/Nitrite , Turbidity , Microtox , Ortho PO4 , Tedlar Bag , Residual Chlorine , Chlorophyll\* , Chloroamines\*

Earliest Expiry:                     

Hydrocarbons: Earliest Expiry                     

### SAMPLE INTEGRITY - Shipping

Hazardous Samples: YES  NO  Precaution Taken: \_\_\_\_\_

Legal Samples: Yes  No

International Samples: Yes  No

Tape Sealed: Yes  No

Coolant Used: Icepack  Bagged Ice  Free Ice  Free Water  None

Temperature (Bottles/Jars only) N/A if only Soil Bags Received

### FROZEN (Please Circle if samples received Frozen)

1 (Bottle/Jar) 19.5 + 19.5 + = 19.5 °C    2 (Bottle/Jar) \_\_\_ + \_\_\_ + \_\_\_ = \_\_\_ °C

3 (Bottle/Jar) \_\_\_ + \_\_\_ + \_\_\_ = \_\_\_ °C    4 (Bottle/Jar) \_\_\_ + \_\_\_ + \_\_\_ = \_\_\_ °C

5 (Bottle/Jar) \_\_\_ + \_\_\_ + \_\_\_ = \_\_\_ °C    6 (Bottle/Jar) \_\_\_ + \_\_\_ + \_\_\_ = \_\_\_ °C

7 (Bottle/Jar) \_\_\_ + \_\_\_ + \_\_\_ = \_\_\_ °C    8 (Bottle/Jar) \_\_\_ + \_\_\_ + \_\_\_ = \_\_\_ °C

9 (Bottle/Jar) \_\_\_ + \_\_\_ + \_\_\_ = \_\_\_ °C    10 (Bottle/Jar) \_\_\_ + \_\_\_ + \_\_\_ = \_\_\_ °C

(If more than 10 coolers are received use another sheet of paper and attach)

### LOGISTICS USE ONLY

Workorder No: 17E177119

Samples Damaged: Yes  No  If YES why?

No Bubble Wrap  Frozen  Courier

Other: \_\_\_\_\_

Account Project Manager: \_\_\_\_\_ have they been notified of the above issues: Yes  No

Whom spoken to: \_\_\_\_\_ Date/Time: \_\_\_\_\_

CPM Initial \_\_\_\_\_

General Comments: \_\_\_\_\_

\_\_\_\_\_

\_\_\_\_\_

\_\_\_\_\_

\_\_\_\_\_

\* Subcontracted Analysis (See CPM)



Dr. Louis Kabwe  
Research Associate  
University of Alberta  
Department of Civil and Environmental Engineering  
1-035 Markin/CNRL  
Edmonton, AB  
T6G 2W2  
Tel. 780 492 2248  
lkabwe@ulaberta.ca

January 11, 2017

Alvelyn Pasco, B.Sc.  
Direct: [780.395.2552](tel:780.395.2552)  
Cell: [780.243.8889](tel:780.243.8889)  
AGAT Laboratories  
6310 Roper Rd NW,  
Edmonton, AB T6B 3P9

**Samples Tests Requests**

**Sample 1: MFT Centrifuge Cake**

1. Atterberg test @ \$190.00 per sample (Liquid and Plastic Limits) –

**Sample 2: Flocculated MFT**

1. Atterberg test @ \$190.00 per sample (Liquid and Plastic Limits) –

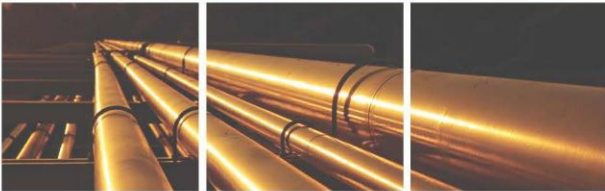
Regards,



Louis Kabwe



**BULK XRD ANALYSIS OF ONE SAMPLE OF HYDROCARBON CLEANED  
SOLIDS RECOVERED ON 'MAY 30, 2018' AND IDENTIFIED AS  
'TAILINGS, FFT'**



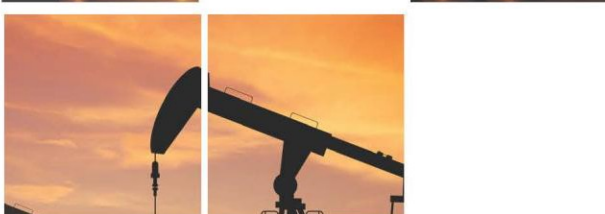
**Company: UNIVERSITY OF ALBERTA**



**Work Order No: 18A19032 [18G345399]**



**Date: June, 2018**



**AGAT Laboratories**  
**3801 – 21<sup>st</sup> Street N.E. Calgary,**  
**Alberta T2E 6T5**



**AGAT** Laboratories

Service Beyond Analysis



### **BULK XRD ANALYSIS**

One sample of hydrocarbon cleaned solids recovered on ‘**May 30, 2018** and identified as ‘**TAILINGS FFT**’ from the University of Alberta was analyzed by AGAT Laboratories Ltd. for crystalline phase(s). The sample was analyzed by X-ray diffraction (XRD) technique to determine crystalline phases. It is important to note that XRD analysis identifies crystalline material.

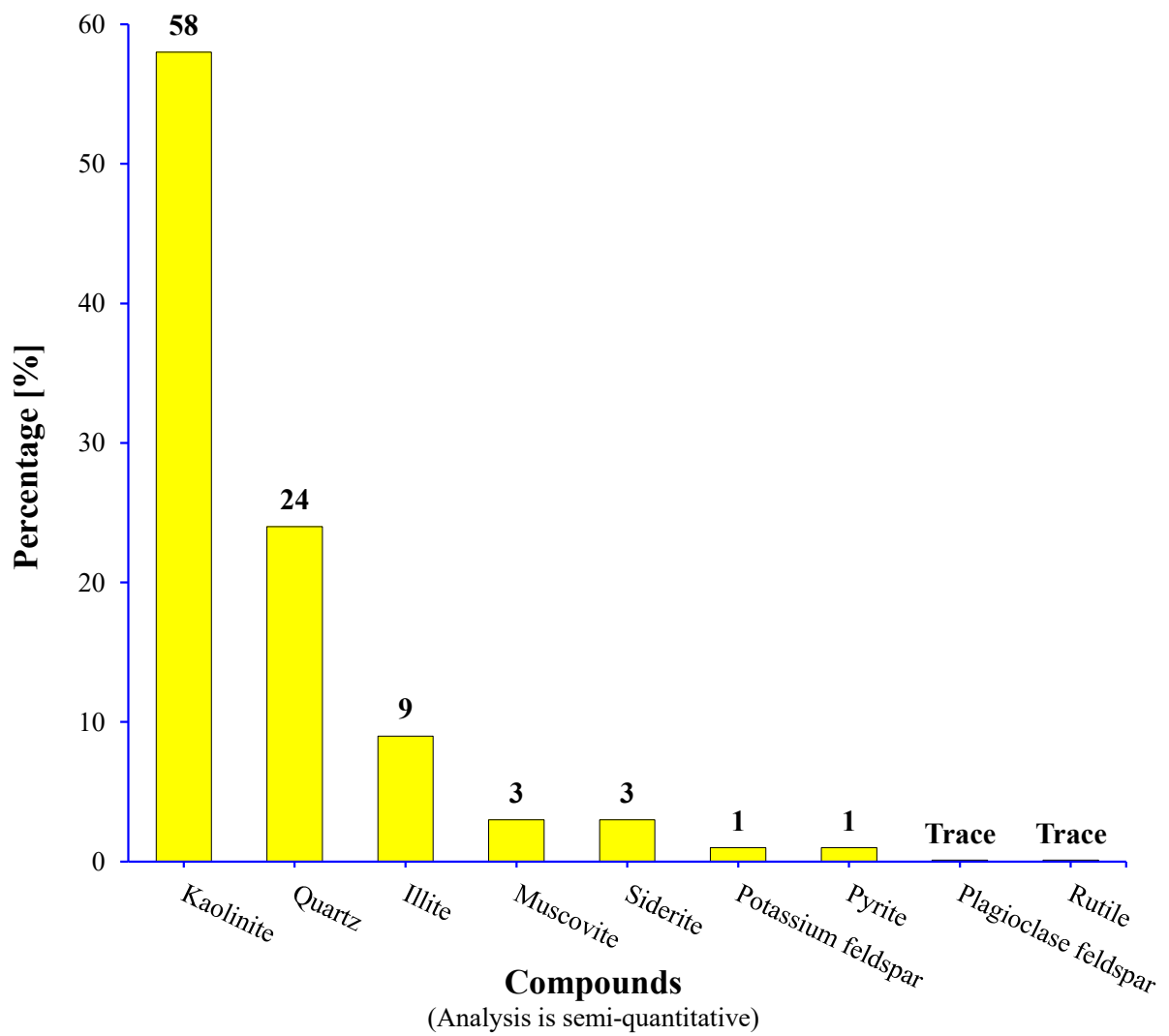
**Results:** The bulk XRD results (Figure 1) of this sample consists mainly of kaolinite (58%) [aluminum silicate hydroxide,  $\text{Al}_4\text{Si}_4\text{O}_{10}(\text{OH})_8$ ] with lesser amounts of quartz (24%) [silicon dioxide,  $\text{SiO}_2$ ] and illite (9%) [potassium aluminum silicate hydroxide,  $\text{KAl}_2(\text{OH})_2(\text{AlSi}_3(\text{O},\text{OH})_{10})$ ]. In addition, minor amounts of muscovite (3%) [potassium aluminum silicate hydroxide,  $\text{KAl}_2(\text{AlSi}_3\text{O}_{10})(\text{OH})_2$ ], siderite (3%) [iron carbonate,  $\text{FeCO}_3$ ], potassium feldspar (1%) [potassium aluminum silicate,  $\text{K}(\text{SiAl}_3\text{O}_8)$ ], and pyrite (1%) [iron sulfide,  $\text{FeS}_2$ ], plus trace amounts of plagioclase feldspar [calcium sodium aluminum silicate,  $(\text{Ca},\text{Na})(\text{Si},\text{Al})_4\text{O}_8$ ] and rutile (titanium oxide,  $\text{TiO}_2$ ) are also present in this sample.

**Remarks:** The analysis indicates the sample consists mainly of formation clays/silts/sands (kaolinite, quartz, illite, muscovite, and plagioclase/potassium feldspars). Moderate amounts of iron compounds (siderite and pyrite - diagenetic cements?) and trace amount of heavy mineral (rutile – derived from formation material?) are also present in this sample.

---

### Figure 1 XRD (X-Ray Diffraction) Analysis

Sample ID: TAILINGS, FFT  
Date Sampled: May 30, 2018



Note: XRD identifies crystalline material only

3801 – 21st Street N.E.  
 Calgary, Alberta  
 T2E 6T5  
 CANADA



**AGAT** Laboratories

TEL: (403) 299-2077  
 FAX: (403) 299-2022  
 www.agatlabs.com

Prepared for University of Alberta

SENT ON June 7 2018

Work Order	Sample #	Matrix	Date Samples	Sample Wet wt (g)	Hydrocarbons wt (g)	% Hydrocarbons	Water wt (g)	% Water	Solids Dry wt (g)	% Solids	Discrep Wt (g)	% Discrep	% Cumm	Comments
18C345399	CONT 1A	Tailings FFT	30-May-18	171.07	6.73	3.934	80.78	47.220	82.75	48.372	0.810	0.473	99.526	

**CLIENT NAME: UNIVERSITY OF ALBERTA  
EDMONTON, AB  
(403) 492-5655**

**ATTENTION TO: Louis Kabwe**

**PROJECT:**

**AGAT WORK ORDER: 17C178866**

**SOIL ANALYSIS REVIEWED BY: Krystyna Krauze, Senior Analyst**

**WATER ANALYSIS REVIEWED BY: Loan Nguyen, Senior Analyst**

**DATE REPORTED: Jan 20, 2017**

**PAGES (INCLUDING COVER): 9**

**VERSION\*: 2**

Should you require any information regarding this analysis please contact your client services representative at (403) 735-2005

**\*NOTES**

VERSION 2:CEC Added to MFT Centrifuge Cake (AGAT ID: 8162524A)

**All samples will be disposed of within 30 days following analysis. Please contact the lab if you require additional sample storage time.**



## Certificate of Analysis

AGAT WORK ORDER: 17C178866

PROJECT:

2910 12TH STREET NE  
 CALGARY, ALBERTA  
 CANADA T2E 7P7  
 TEL (403)735-2005  
 FAX (403)735-2771  
<http://www.agatlabs.com>

CLIENT NAME: UNIVERSITY OF ALBERTA

ATTENTION TO: Louis Kabwe

SAMPLING SITE:

SAMPLED BY:

### Soil Analysis - Cation Exchange Capacity (mg/kg)

DATE RECEIVED: 2017-01-16

DATE REPORTED: 2017-01-20

Parameter	Unit	MFT Centrifuge		
		G / S	RDL	8162524
Available Calcium (CEC)*	mg/kg		6	1990
Available Magnesium (CEC)*	mg/kg		8	304
Available Potassium (CEC)*	mg/kg		12	144
Available Sodium (CEC)*	mg/kg		12	994
pH, Buffer*	pH Units		N/A	7.27
Cation Exchange Capacity - CEC	meq/100g			17.4

**Comments:** RDL - Reported Detection Limit; G / S - Guideline / Standard  
 8162524 Analysis based on dry weight

**Certified By:**



## Certificate of Analysis

AGAT WORK ORDER: 17C178866

PROJECT:

2910 12TH STREET NE  
 CALGARY, ALBERTA  
 CANADA T2E 7P7  
 TEL (403)735-2005  
 FAX (403)735-2771  
<http://www.agatlabs.com>

CLIENT NAME: UNIVERSITY OF ALBERTA

ATTENTION TO: Louis Kabwe

SAMPLING SITE:

SAMPLED BY:

### Anion Scan in Water

DATE RECEIVED: 2017-01-16

DATE REPORTED: 2017-01-20

MFT Centrifuge

SAMPLE DESCRIPTION: Cake Pond

SAMPLE TYPE: Water

DATE SAMPLED: 2017-01-11

8132059

Parameter	Unit	G / S	RDL	8132059
Chloride	mg/L		1.0	777
Nitrate	mg/L		0.20	2.20
Nitrite	mg/L		0.10	<0.10
Sulfate	mg/L		0.15	69.7
Fluoride	mg/L		0.03	3.92
Bromide	mg/L		0.10	0.47

Comments: RDL - Reported Detection Limit; G / S - Guideline / Standard

Certified By:





## Certificate of Analysis

AGAT WORK ORDER: 17C178866

PROJECT:

2910 12TH STREET NE  
 CALGARY, ALBERTA  
 CANADA T2E 7P7  
 TEL (403)735-2005  
 FAX (403)735-2771  
<http://www.agatlabs.com>

CLIENT NAME: UNIVERSITY OF ALBERTA

ATTENTION TO: Louis Kabwe

SAMPLING SITE:

SAMPLED BY:

### Cation Scan in Water

DATE RECEIVED: 2017-01-16

DATE REPORTED: 2017-01-20

		MFT Centrifuge		
		SAMPLE DESCRIPTION: Cake Pond		
		SAMPLE TYPE: Water		
		DATE SAMPLED: 2017-01-11		
Parameter	Unit	G / S	RDL	8132059
Dissolved Calcium	mg/L		0.3	9.2
Dissolved Magnesium	mg/L		0.2	6.6
Dissolved Sodium	mg/L		0.6	988
Dissolved Potassium	mg/L		0.6	11.0

Comments: RDL - Reported Detection Limit; G / S - Guideline / Standard

Certified By:



## Certificate of Analysis

AGAT WORK ORDER: 17C178866

PROJECT:

2910 12TH STREET NE  
 CALGARY, ALBERTA  
 CANADA T2E 7P7  
 TEL (403)735-2005  
 FAX (403)735-2771  
<http://www.agatlabs.com>

CLIENT NAME: UNIVERSITY OF ALBERTA

ATTENTION TO: Louis Kabwe

SAMPLING SITE:

SAMPLED BY:

### Dissolved Metals Scan in Water

DATE RECEIVED: 2017-01-16

DATE REPORTED: 2017-01-20

Parameter	Unit	MFT Centrifuge	
		G / S	RDL
SAMPLE DESCRIPTION: Cake Pond			
SAMPLE TYPE: Water			
DATE SAMPLED: 2017-01-11			
		<b>8132059</b>	
Dissolved Aluminum	mg/L	0.004	0.025
Dissolved Antimony	mg/L	0.001	<0.001
Dissolved Arsenic	mg/L	0.001	0.002
Dissolved Barium	mg/L	0.05	0.15
Dissolved Beryllium	mg/L	0.0010	<0.0010
Dissolved Boron	mg/L	0.05	4.36
Dissolved Cadmium	mg/L	0.000017	0.000057
Dissolved Chromium	mg/L	0.0010	<0.0010
Dissolved Cobalt	mg/L	0.001	0.001
Dissolved Copper	mg/L	0.0008	0.0028
Dissolved Iron	mg/L	0.1	<0.1
Dissolved Lead	mg/L	0.0005	<0.0005
Dissolved Lithium	mg/L	0.001	0.179
Dissolved Manganese	mg/L	0.005	<0.005
Dissolved Molybdenum	mg/L	0.001	0.004
Dissolved Nickel	mg/L	0.003	0.008
Dissolved Selenium	mg/L	0.0005	0.0043
Dissolved Silicon	mg/L	0.032	2.39
Dissolved Silver	mg/L	0.0001	<0.0001
Dissolved Strontium	mg/L	0.001	0.405
Dissolved Thallium	mg/L	0.0001	<0.0001
Dissolved Tin	mg/L	0.0001	0.0004
Dissolved Titanium	mg/L	0.001	0.007
Dissolved Uranium	mg/L	0.001	0.002
Dissolved Vanadium	mg/L	0.001	0.008
Dissolved Zinc	mg/L	0.01	0.03

**Comments:** RDL - Reported Detection Limit; G / S - Guideline / Standard  
 8132059 < - Values refer to Method Detection Limit.

**Certified By:** 

## Quality Assurance

**CLIENT NAME: UNIVERSITY OF ALBERTA**
**AGAT WORK ORDER: 17C178866**
**PROJECT:**
**ATTENTION TO: Louis Kabwe**
**SAMPLING SITE:**
**SAMPLED BY:**

Soil Analysis															
RPT Date: Jan 20, 2017			DUPLICATE				Method Blank	REFERENCE MATERIAL			METHOD BLANK SPIKE		MATRIX SPIKE		
PARAMETER	Batch	Sample Id	Dup #1	Dup #2	RPD	Measured Value		Acceptable Limits		Recovery	Acceptable Limits		Recovery	Acceptable Limits	
								Lower	Upper		Lower	Upper		Lower	Upper

**Soil Analysis - Cation Exchange Capacity (mg/kg)**

Available Calcium (CEC)*	8162524	8162524	1990	2020	1.5%	< 6	109%	80%	120%	119%	80%	120%
Available Magnesium (CEC)*	8162524	8162524	304	308	1.3%	< 8	98%	80%	120%	101%	80%	120%
Available Potassium (CEC)*	8162524	8162524	144	148	2.7%	< 12	97%	80%	120%	112%	80%	120%
Available Sodium (CEC)*	8162524	8162524	994	1020	2.6%	< 12	99%	80%	120%	103%	80%	120%
pH, Buffer*	3187	2524	7.27	7.26	0.1%	N/A	99%	90%	110%			

Comments: If the RPD value is NA, the results of the duplicates are under 5X the RDL and will not be calculated.

\*Non-accredited test. Inquire with lab for details.

**Certified By:**




## Quality Assurance

CLIENT NAME: UNIVERSITY OF ALBERTA

AGAT WORK ORDER: 17C178866

PROJECT:

ATTENTION TO: Louis Kabwe

SAMPLING SITE:

SAMPLED BY:

### Water Analysis

RPT Date: Jan 20, 2017

#### DUPLICATE

#### REFERENCE MATERIAL

#### METHOD BLANK SPIKE

#### MATRIX SPIKE

PARAMETER	Batch	Sample Id	Dup #1	Dup #2	RPD	Method Blank	Measured Value		Acceptable Limits		Recovery		Acceptable Limits		Recovery	
							Lower	Upper	Lower	Upper	Lower	Upper	Lower	Upper		

#### Anion Scan in Water

Chloride	8130677	8130677	1.54	1.52	0.7%	< 0.03	112%	80%	120%	110%	80%	120%	110%	80%	120%
Nitrate	8130677	8130677	<0.08	<0.08	NA	< 0.08	112%	80%	120%	113%	80%	120%	113%	80%	120%
Nitrite	8130677	8130677	<0.03	<0.03	NA	< 0.03	110%	80%	120%	110%	80%	120%	109%	80%	120%
Sulfate	8130677	8130677	1.72	1.68	1.9%	< 0.03	109%	80%	120%	109%	80%	120%	107%	80%	120%
Fluoride	8130677	8130677	0.08	0.10	14.2%	< 0.01	106%	80%	120%	85%	80%	120%	118%	80%	120%
Bromide	8130677	8130677	<0.02	<0.02	NA	< 0.02	115%	80%	120%	113%	80%	120%	111%	80%	120%

Comments: If Matrix spike value is NA, the spiked analyte concentration was lower than that of the matrix contribution.  
If the RPD value is NA, the results of the duplicates are under 5X the RDL and will not be calculated.

Nitrate and Nitrite: The regulatory hold time for the analysis of nitrate and/or nitrite in water is 48 hours in Alberta and 72 hours in British Columbia.

#### Dissolved Metals Scan in Water

Dissolved Aluminum	8133424		0.156	0.164	4.8%	< 0.004	98%	80%	120%	104%	80%	120%	108%	80%	120%
Dissolved Antimony	8133424		<0.001	<0.001	NA	< 0.001	99%	80%	120%	104%	80%	120%	105%	80%	120%
Dissolved Arsenic	8133424		<0.001	<0.001	NA	< 0.001	94%	80%	120%	106%	80%	120%	104%	80%	120%
Dissolved Barium	8133424		0.13	0.13	NA	< 0.05	97%	80%	120%	106%	80%	120%	108%	80%	120%
Dissolved Beryllium	8133424		<0.0010	<0.0010	NA	< 0.0010	98%	80%	120%	109%	80%	120%	113%	80%	120%
Dissolved Boron	8133424		0.04	0.04	NA	< 0.01	102%	80%	120%	104%	80%	120%	98%	80%	120%
Dissolved Cadmium	8133424		< 0.000017	< 0.000017	NA	< 0.000017	100%	80%	120%	107%	80%	120%	106%	80%	120%
Dissolved Chromium	8133424		<0.0010	<0.0010	NA	< 0.0010	93%	80%	120%	96%	80%	120%	103%	80%	120%
Dissolved Cobalt	8133424		<0.001	<0.001	NA	< 0.001	97%	80%	120%	101%	80%	120%	104%	80%	120%
Dissolved Copper	8133424		0.0020	0.0020	NA	< 0.0008	97%	80%	120%	99%	80%	120%	101%	80%	120%
Dissolved Iron	8131827	8131827	<0.1	<0.1	NA	< 0.1	105%	80%	120%	103%	80%	120%	101%	80%	120%
Dissolved Lead	8133424		<0.0005	<0.0005	NA	< 0.0005	95%	80%	120%	98%	80%	120%	99%	80%	120%
Dissolved Lithium	8133424		0.005	0.006	5.4%	< 0.001	95%	80%	120%	96%	80%	120%	102%	80%	120%
Dissolved Manganese	8131827	8131827	<0.005	<0.005	NA	< 0.005	104%	80%	120%	103%	80%	120%	102%	80%	120%
Dissolved Molybdenum	8133424		<0.001	<0.001	NA	< 0.001	93%	80%	120%	104%	80%	120%	106%	80%	120%
Dissolved Nickel	8133424		<0.003	<0.003	NA	< 0.003	97%	80%	120%	97%	80%	120%	103%	80%	120%
Dissolved Selenium	8133424		0.0014	0.0011	NA	< 0.0005	100%	80%	120%	101%	80%	120%	116%	80%	120%
Dissolved Silicon	8131827	8131827	<0.032	<0.032	NA	< 0.032	105%	80%	120%	114%	80%	120%	113%	80%	120%
Dissolved Silver	8133424		<0.0001	<0.0001	NA	< 0.0001	85%	80%	120%	101%	80%	120%	97%	80%	120%
Dissolved Strontium	8133424		0.406	0.417	2.8%	< 0.001	89%	80%	120%	96%	80%	120%	NA	80%	120%
Dissolved Thallium	8133424		<0.0001	<0.0001	NA	< 0.0001	96%	80%	120%	99%	80%	120%	101%	80%	120%
Dissolved Tin	8133424		0.0004	0.0004	NA	< 0.0001	99%	80%	120%	103%	80%	120%	103%	80%	120%
Dissolved Titanium	8133424		0.002	0.002	NA	< 0.001	84%	80%	120%	102%	80%	120%	107%	80%	120%
Dissolved Uranium	8133424		<0.001	<0.001	NA	< 0.001	99%	80%	120%	103%	80%	120%	108%	80%	120%
Dissolved Vanadium	8133424		<0.001	<0.001	NA	< 0.001	92%	80%	120%	97%	80%	120%	105%	80%	120%
Dissolved Zinc	8133424		<0.01	<0.01	NA	< 0.01	99%	80%	120%	105%	80%	120%	107%	80%	120%



## Quality Assurance

CLIENT NAME: UNIVERSITY OF ALBERTA  
 PROJECT:  
 SAMPLING SITE:

AGAT WORK ORDER: 17C178866  
 ATTENTION TO: Louis Kabwe  
 SAMPLED BY:

### Water Analysis (Continued)

RPT Date: Jan 20, 2017			DUPLICATE				Method Blank	REFERENCE MATERIAL			METHOD BLANK SPIKE			MATRIX SPIKE		
PARAMETER	Batch	Sample Id	Dup #1	Dup #2	RPD	Measured Value		Acceptable Limits		Recovery	Acceptable Limits		Recovery	Acceptable Limits		
								Lower	Upper		Lower	Upper		Lower	Upper	

Comments: If Matrix spike value is NA, the spiked analyte concentration was lower than that of the matrix contribution.  
 If the RPD value is NA, the results of the duplicates are under 5X the RDL and will not be calculated.

#### Cation Scan in Water

Dissolved Calcium	8131827	8131827	<0.3	<0.3	NA	< 0.3	107%	80%	120%	111%	80%	120%	110%	80%	120%
Dissolved Magnesium	8131827	8131827	<0.2	<0.2	NA	< 0.2	98%	80%	120%	94%	80%	120%	94%	80%	120%
Dissolved Sodium	8131827	8131827	<0.6	<0.6	NA	< 0.6	99%	80%	120%	99%	80%	120%	97%	80%	120%
Dissolved Potassium	8131827	8131827	<0.6	<0.6	NA	< 0.6	93%	80%	120%	92%	80%	120%	91%	80%	120%

Comments: If Matrix spike value is NA, the spiked analyte concentration was lower than that of the matrix contribution.  
 If the RPD value is NA, the results of the duplicates are under 5X the RDL and will not be calculated.

**Certified By:** \_\_\_\_\_

## Method Summary

**CLIENT NAME: UNIVERSITY OF ALBERTA**
**AGAT WORK ORDER: 17C178866**
**PROJECT:**
**ATTENTION TO: Louis Kabwe**
**SAMPLING SITE:**
**SAMPLED BY:**

PARAMETER	AGAT S.O.P	LITERATURE REFERENCE	ANALYTICAL TECHNIQUE
<b>Soil Analysis</b>			
Available Calcium (CEC)*	SOIL 0210; SOIL 0110; SOIL 0120; INST 0140	HENDERSHOT 2008; SHEPPARD 2007; EATON 2005	ICP/OES
Available Magnesium (CEC)*	SOIL 0210; SOIL 0110; SOIL 0120; INST 0140	HENDERSHOT 2008; SHEPPARD 2007; EATON 2005	ICP/OES
Available Potassium (CEC)*	SOIL 0210; SOIL 0110; SOIL 0120; INST 0140	HENDERSHOT 2008; SHEPPARD 2007; EATON 2005	ICP/OES
Available Sodium (CEC)*	SOIL 0210; SOIL 0110; SOIL 0120; INST 0140	HENDERSHOT 2008; SHEPPARD 2007; EATON 2005	ICP/OES
pH, Buffer*	SOIL 0250 ; SOIL 0110; SOIL 0120	ZIADI & TRAN 2008; SHEPPARD 2007	pH METER
Cation Exchange Capacity - CEC	SOIL 0210	HENDERSHOT 2008; SHEPPARD 2007; EATON 2005	N/A
<b>Water Analysis</b>			
Chloride	INST 0150	SM 4110 B	ION CHROMATOGRAPH
Nitrate	INST 0150	SM 4110 B	ION CHROMATOGRAPH
Nitrite	INST 0150	SM 4110 B	ION CHROMATOGRAPH
Sulfate	INST 0150	SM 4110 B	ION CHROMATOGRAPH
Fluoride	INST 0150	SM 4110 B	ION CHROMATOGRAPH
Bromide	INST 0150	SM 4110 B	ION CHROMATOGRAPH
Dissolved Calcium	INST 0140	SM 3120 B	ICP/OES
Dissolved Magnesium	INST 0140	SM 3120 B	ICP/OES
Dissolved Sodium	INST 0140	SM 3120 B	ICP/OES
Dissolved Potassium	INST 0140	SM 3120 B	ICP/OES
Dissolved Aluminum	INST 0141	SM 3125 B DW	ICP-MS
Dissolved Antimony	INST 0141	SM 3125 B DW	ICP-MS
Dissolved Arsenic	INST 0141	SM 3125 B DW	ICP-MS
Dissolved Barium	INST 0141	SM 3125 B DW	ICP-MS
Dissolved Beryllium	INST 0141	SM 3125 B DW	ICP-MS
Dissolved Boron	INST 0141	SM 3125 B DW	ICP-MS
Dissolved Cadmium	INST 0141	SM 3125 B DW	ICP/MS
Dissolved Chromium	INST 0141	SM 3125 B DW	ICP-MS
Dissolved Cobalt	INST 0141	SM 3125 B DW	ICP-MS
Dissolved Copper	INST 0141	SM 3125 B DW	ICP-MS
Dissolved Iron	INST 0140	SM 3120 B DW	ICP/OES
Dissolved Lead	INST 0141	SM 3125 B DW	ICP/MS
Dissolved Lithium	INST 0141	SM 3125 B DW	ICP-MS
Dissolved Manganese	INST 0140	SM 3120 B DW	ICP/OES
Dissolved Molybdenum	INST 0141	SM 3125 B DW	ICP-MS
Dissolved Nickel	INST 0141	SM 3125 B DW	ICP-MS
Dissolved Selenium	INST 0141	SM 3125 B DW	ICP-MS
Dissolved Silicon	INST 0140	SM 3120 B DW	ICP/OES
Dissolved Silver	INST 0141	SM 3125 B DW	ICP-MS
Dissolved Strontium	INST 0141	SM 3125 B DW	ICP-MS
Dissolved Thallium	INST 0141	SM 3125 B DW	ICP-MS
Dissolved Tin	INST 0141	SM 3125 B DW	ICP-MS
Dissolved Titanium	INST 0141	SM 3125 B DW	ICP-MS
Dissolved Uranium	INST 0141	SM 3125 B DW	ICP/MS
Dissolved Vanadium	INST 0141	SM 3125 B DW	ICP-MS
Dissolved Zinc	INST 0141	SM 3125 B DW	ICP-MS

**CLIENT NAME: UNIVERSITY OF ALBERTA  
EDMONTON, AB  
(403) 492-5655**

**ATTENTION TO: Louis Kabwe**

**PROJECT: Water Sample**

**AGAT WORK ORDER: 17E183606**

**WATER ANALYSIS REVIEWED BY: Loan Nguyen, Senior Analyst**

**DATE REPORTED: Feb 06, 2017**

**PAGES (INCLUDING COVER): 8**

**VERSION\*: 1**

Should you require any information regarding this analysis please contact your client services representative at (403) 735-2005

**\*NOTES**

**All samples will be disposed of within 30 days following analysis. Please contact the lab if you require additional sample storage time.**



## Certificate of Analysis

AGAT WORK ORDER: 17E183606

PROJECT: Water Sample

2910 12TH STREET NE  
CALGARY, ALBERTA  
CANADA T2E 7P7  
TEL (403)735-2005  
FAX (403)735-2771  
<http://www.agatlabs.com>

CLIENT NAME: UNIVERSITY OF ALBERTA

ATTENTION TO: Louis Kabwe

SAMPLING SITE:

SAMPLED BY:

### Anion Scan in Water

DATE RECEIVED: 2017-01-31

DATE REPORTED: 2017-02-06

MFT Centrifuge

Cake Pond

SAMPLE DESCRIPTION: Water

SAMPLE TYPE: Water

DATE SAMPLED: 2017-01-31

Parameter	Unit	G / S	RDL	8164011
Chloride	mg/L		1.0	446
Nitrate	mg/L		0.20	0.26
Nitrite	mg/L		0.10	<0.10
Sulfate	mg/L		0.15	17.7
Fluoride	mg/L		0.03	2.47
Bromide	mg/L		0.10	0.53

Comments: RDL - Reported Detection Limit; G / S - Guideline / Standard

Certified By:





## Certificate of Analysis

AGAT WORK ORDER: 17E183606

PROJECT: Water Sample

2910 12TH STREET NE  
 CALGARY, ALBERTA  
 CANADA T2E 7P7  
 TEL (403)735-2005  
 FAX (403)735-2771  
<http://www.agatlabs.com>

CLIENT NAME: UNIVERSITY OF ALBERTA

ATTENTION TO: Louis Kabwe

SAMPLING SITE:

SAMPLED BY:

### Cation Scan in Water

DATE RECEIVED: 2017-01-31

DATE REPORTED: 2017-02-06

Parameter	Unit	MFT Centrifuge		
		G / S	RDL	8164011
SAMPLE DESCRIPTION: Cake Pond				
SAMPLE TYPE: Water				
DATE SAMPLED: 2017-01-31				
Dissolved Calcium	mg/L	0.3	36.5	
Dissolved Magnesium	mg/L	0.2	15.9	
Dissolved Sodium	mg/L	0.6	780	
Dissolved Potassium	mg/L	0.6	14.6	

Comments: RDL - Reported Detection Limit; G / S - Guideline / Standard

Certified By: \_\_\_\_\_



## Certificate of Analysis

AGAT WORK ORDER: 17E183606

PROJECT: Water Sample

2910 12TH STREET NE  
 CALGARY, ALBERTA  
 CANADA T2E 7P7  
 TEL (403)735-2005  
 FAX (403)735-2771  
<http://www.agatlabs.com>

CLIENT NAME: UNIVERSITY OF ALBERTA

ATTENTION TO: Louis Kabwe

SAMPLING SITE:

SAMPLED BY:

### Metals - Dissolved - CCME

DATE RECEIVED: 2017-01-31

DATE REPORTED: 2017-02-06

Parameter	Unit	MFT Centrifuge		
		G / S	RDL	8164011
Dissolved Aluminum	mg/L	(VARIABLE)	0.004	0.006
Dissolved Antimony	mg/L	0.006	0.001	<0.001
Dissolved Arsenic	mg/L	0.010	0.001	0.006
Dissolved Barium	mg/L	1.0	0.05	0.47
Dissolved Beryllium	mg/L		0.0010	<0.0010
Dissolved Boron	mg/L	5	0.05	3.75
Dissolved Cadmium	mg/L	0.005	0.000016	<0.000016
Dissolved Chromium	mg/L	0.05	0.0010	<0.0010
Dissolved Cobalt	mg/L		0.001	<0.001
Dissolved Copper	mg/L	(1.0)	0.0008	<0.0008
Dissolved Iron	mg/L	(0.3)	0.1	1.3
Dissolved Lead	mg/L	0.010	0.0005	<0.0005
Dissolved Manganese	mg/L	(0.05)	0.005	0.023
Dissolved Molybdenum	mg/L		0.001	0.003
Dissolved Nickel	mg/L		0.003	0.006
Dissolved Selenium	mg/L	0.05	0.0005	0.0042
Dissolved Silver	mg/L		0.00005	0.00014
Dissolved Sodium	mg/L	(200)	0.6	780
Dissolved Thallium	mg/L		0.0005	<0.0005
Dissolved Titanium	mg/L		0.001	0.028
Dissolved Uranium	mg/L	0.02	0.001	0.001
Dissolved Zinc	mg/L	(5.0)	0.01	<0.01

Comments: RDL - Reported Detection Limit; G / S - Guideline / Standard: Refers to 2014 Canadian Drinking Water Quality MAC (AO)

8164011 < - Values refer to Report Detection Limit.

Certified By: \_\_\_\_\_



## Quality Assurance

**CLIENT NAME: UNIVERSITY OF ALBERTA**
**AGAT WORK ORDER: 17E183606**
**PROJECT: Water Sample**
**ATTENTION TO: Louis Kabwe**
**SAMPLING SITE:**
**SAMPLED BY:**

### Water Analysis (Continued)

RPT Date: Feb 06, 2017			DUPLICATE				Method Blank	REFERENCE MATERIAL			METHOD BLANK SPIKE			MATRIX SPIKE		
PARAMETER	Batch	Sample Id	Dup #1	Dup #2	RPD	Measured Value		Acceptable Limits		Recovery	Acceptable Limits		Recovery	Acceptable Limits		
								Lower	Upper		Lower	Upper		Lower	Upper	
Dissolved Magnesium	8155462	8155462	17.7	17.8	0.2%	< 0.2	100%	80%	120%	98%	80%	120%	NA	80%	120%	
Dissolved Sodium	8155462	8155462	5.7	5.6	0.8%	< 0.6	99%	80%	120%	100%	80%	120%	NA	80%	120%	
Dissolved Potassium	8155462	8155462	0.9	0.8	NA	< 0.6	95%	80%	120%	97%	80%	120%	98%	80%	120%	

Comments: If Matrix spike value is NA, the spiked analyte concentration was lower than that of the matrix contribution.  
 If the RPD value is NA, the results of the duplicates are under 5X the RDL and will not be calculated.

**Certified By:**


## QA Violation

**CLIENT NAME: UNIVERSITY OF ALBERTA**
**AGAT WORK ORDER: 17E183606**
**PROJECT: Water Sample**
**ATTENTION TO: Louis Kabwe**

RPT Date: Feb 06, 2017			REFERENCE MATERIAL			METHOD BLANK SPIKE			MATRIX SPIKE		
PARAMETER	Sample Id	Sample Description	Measured Value	Acceptable Limits		Recovery	Acceptable Limits		Recovery	Acceptable Limits	
				Lower	Upper		Lower	Upper		Lower	Upper

**Metals - Dissolved - CCME**

Dissolved Beryllium	8159877	MFT Centrifuge Cake Pond Water	95%	80%	120%	98%	80%	120%	125%	80%	120%
---------------------	---------	--------------------------------	-----	-----	------	-----	-----	------	------	-----	------

Comments: If Matrix spike value is NA, the spiked analyte concentration was lower than that of the matrix contribution.  
If the RPD value is NA, the results of the duplicates are under 5X the RDL and will not be calculated.

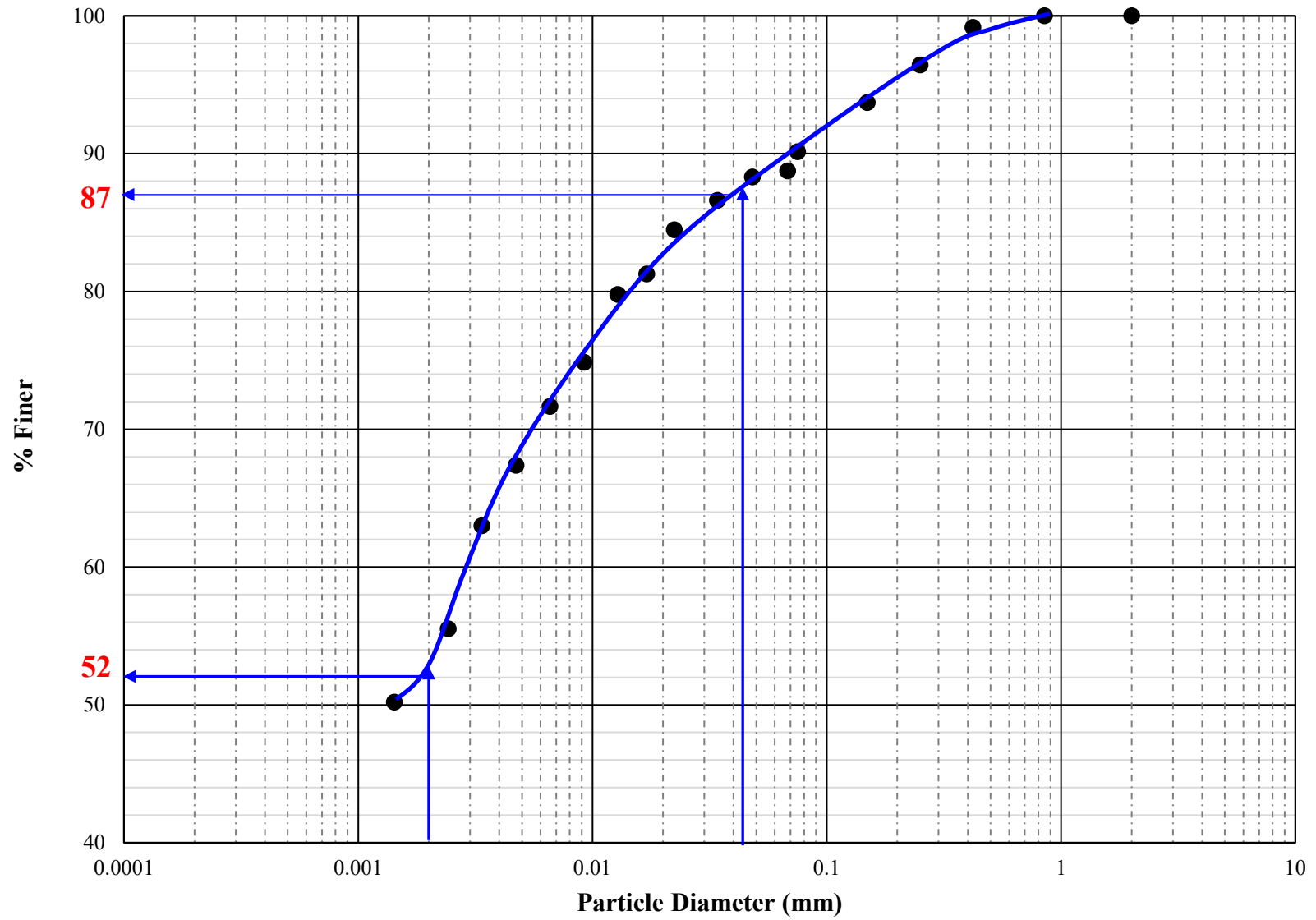
With multi element scans it is acceptable for a maximum of 10% (including non-reported elements) of each QC criteria to fail to an absolute maximum of 10%.

## Method Summary

**CLIENT NAME: UNIVERSITY OF ALBERTA**
**AGAT WORK ORDER: 17E183606**
**PROJECT: Water Sample**
**ATTENTION TO: Louis Kabwe**
**SAMPLING SITE:**
**SAMPLED BY:**

PARAMETER	AGAT S.O.P	LITERATURE REFERENCE	ANALYTICAL TECHNIQUE
<b>Water Analysis</b>			
Chloride	INST 0150	SM 4110 B	ION CHROMATOGRAPH
Nitrate	INST 0150	SM 4110 B	ION CHROMATOGRAPH
Nitrite	INST 0150	SM 4110 B	ION CHROMATOGRAPH
Sulfate	INST 0150	SM 4110 B	ION CHROMATOGRAPH
Fluoride	INST 0150	SM 4110 B	ION CHROMATOGRAPH
Bromide	INST 0150	SM 4110 B	ION CHROMATOGRAPH
Dissolved Calcium	INST 0140	SM 3120 B	ICP/OES
Dissolved Magnesium	INST 0140	SM 3120 B	ICP/OES
Dissolved Sodium	INST 0140	SM 3120 B	ICP/OES
Dissolved Potassium	INST 0140	SM 3120 B	ICP/OES
Dissolved Aluminum	INST 0141	SM 3125 B DW	ICP/MS
Dissolved Antimony	INST 0141	SM 3125 B DW	ICP/MS
Dissolved Arsenic	INST 0141	SM 3125 B DW	ICP/MS
Dissolved Barium	INST 0141	SM 3125 B DW	ICP-MS
Dissolved Beryllium	INST 0141	SM 3125 B	ICP-MS
Dissolved Boron	INST 0141	SM 3125 B DW	ICP/MS
Dissolved Cadmium	INST 0141	SM 3125 B DW	ICP/MS
Dissolved Chromium	INST 0141	SM 3125 B DW	ICP/MS
Dissolved Cobalt	INST 0141	SM 3125 B	ICP-MS
Dissolved Copper	INST 0141	SM 3125 B DW	ICP-MS
Dissolved Iron	INST 0140	SM 3120 B DW	ICP/OES
Dissolved Lead	INST 0141	SM 3125 B DW	ICP/MS
Dissolved Manganese	INST 0140	SM 3120 B DW	ICP/OES
Dissolved Molybdenum		SM 3125 B	ICP-MS
Dissolved Nickel	INST 0141	SM 3125 B DW	ICP/MS
Dissolved Selenium	INST 0141	SM 3125 B DW	ICP/MS
Dissolved Silver	INST 0141	SM 3125 B DW	ICP/MS
Dissolved Sodium	INST 0140	SM 3120 B DW	ICP/OES
Dissolved Thallium	INST 0141	SM 3125 B DW	ICP-MS
Dissolved Titanium	INST 0141	SM 3125 B	ICP-MS
Dissolved Uranium	INST 0141	SM 3125 B DW	ICP/MS
Dissolved Zinc	INST 0141	SM 3125 B DW	ICP/MS

### Grain Size Distribution Curve





## Method Summary

CLIENT NAME: UNIVERSITY OF ALBERTA

AGAT WORK ORDER: 17E177119

PROJECT:

ATTENTION TO: Louis Kabwe

SAMPLING SITE:

SAMPLED BY:

PARAMETER	AGAT S.O.P	LITERATURE REFERENCE	ANALYTICAL TECHNIQUE
<b>Soil Analysis</b>			
Liquid Limit	INOR-171-6218	ASA 9 - 31-3	LIQUID LIMIT DEVICE
Plastic Limit	INOR-171-6218	ASA 9 - 31-3	N/A
Plasticity Index	INOR-171-6218	ASTM D4318-00	N/A
Specific Gravity (S.G.) as Received*			



## Quality Assurance

CLIENT NAME: UNIVERSITY OF ALBERTA

AGAT WORK ORDER: 17E177119

PROJECT:

ATTENTION TO: Louis Kabwe

SAMPLING SITE:

SAMPLED BY:

Soil Analysis															
RPT Date: Jan 16, 2017			DUPLICATE				Method Blank	REFERENCE MATERIAL			METHOD BLANK SPIKE		MATRIX SPIKE		
PARAMETER	Batch	Sample Id	Dup #1	Dup #2	RPD	Measured Value		Acceptable Limits		Recovery	Acceptable Limits		Recovery	Acceptable Limits	
								Lower	Upper		Lower	Upper		Lower	Upper

**Soil Analysis - Atterberg Limits**

Liquid Limit	13	8123002	47	47	0.0%	< 1	100%	80%	120%
Plastic Limit	13	8123002	28	28	0.0%	< 1	95%	80%	120%
Plasticity Index	13	8123002	18.8	18.6	1.1%	< 1	104%	80%	120%

Comments: \*Non-accredited test. Inquire with lab for details.

**Soil Analysis - Spec Grav**

Specific Gravity (S.G.) as Received*	66	8232227	1.26	1.26	0.0%	< 0.01	100%	80%	120%
--------------------------------------	----	---------	------	------	------	--------	------	-----	------

Comments: N/A: Not applicable

**Certified By:**




# Certificate of Analysis

AGAT WORK ORDER: 17E177119

PROJECT:

6310 ROPER ROAD  
EDMONTON, ALBERTA  
CANADA T6B 3P9  
TEL (780)395-2525  
FAX (780)462-2490  
<http://www.agallabs.com>

CLIENT NAME: UNIVERSITY OF ALBERTA

ATTENTION TO: Louis Kabwe

SAMPLING SITE:

SAMPLED BY:

## Soil Analysis - Spec Grav

DATE RECEIVED: 2017-01-11

DATE REPORTED: 2017-01-16

Parameter	Unit	MFT Centrifuge		MFT
		G / S	RDL	Flocculated
Specific Gravity (S.G.) as Received*	NA	0.01	1.47	1.41

Comments: RDL - Reported Detection Limit; G / S - Guideline / Standard

Certified By:



**AGAT** Laboratories

### Certificate of Analysis

AGAT WORK ORDER: 17E177119

PROJECT:

6310 ROPER ROAD  
EDMONTON, ALBERTA  
CANADA T6B 3P9  
TEL (780)395-2525  
FAX (780)462-2490  
<http://www.agatlabs.com>

CLIENT NAME: UNIVERSITY OF ALBERTA

ATTENTION TO: Louis Kabwe

SAMPLING SITE:

SAMPLED BY:

#### Soil Analysis - Atterberg Limits

DATE RECEIVED: 2017-01-11

DATE REPORTED: 2017-01-16

Parameter	Unit	MFT Centrifuge		MFT
		G / S	RDL	Flocculated
SAMPLE DESCRIPTION:			Cake	Flocculated
SAMPLE TYPE:			Other	Other
DATE SAMPLED:		2017-01-11	2017-01-11	
			8121927	8121929
Liquid Limit		1	57	79
Plastic Limit		1	26	28
Plasticity Index			31.9	50.6

Comments: RDL - Reported Detection Limit; G / S - Guideline / Standard

8121927-8121929 Plasticity Index is a calculated parameter. The calculated value is the difference between the liquid limit and the plastic limit.

**Certified By:**



**CLIENT NAME: UNIVERSITY OF ALBERTA  
114 STREET, 89 AVE  
EDMONTON, AB T6G2E1  
(403) 492-4166**

**ATTENTION TO: Louis Kabwe**

**PROJECT:**

**AGAT WORK ORDER: 17E177119**

**SOIL ANALYSIS REVIEWED BY: Shanna Mills, Inorganics Manager**

**DATE REPORTED: Jan 16, 2017**

**PAGES (INCLUDING COVER): 8**

**VERSION\*: 1**

Should you require any information regarding this analysis please contact your client services representative at (780) 395-2525

**\*NOTES**

Empty rectangular box for notes.

**All samples will be disposed of within 30 days following analysis. Please contact the lab if you require additional sample storage time.**

# METHYLENE BLUE INDEX

CLIENT UNIVERSITY OF ALBERTA

AGAT FILE WO# A18340-1

Sample ID #	Weight (g)		Methylene Blue Volume (mL)	meq/100g
	Recommended	Actual		
MFT Centrifugal Cake	2.00	2.14	10.50	4.91

3801 - 21st Street N.E.  
Calgary, Alberta  
CANADA T2E 6T5



**AGAT** Laboratories

TEL: (403) 299-2077  
FAX: (403) 299-2022  
www.agatlabs.com

Prepared for University of Alberta

SENT ON JANUARY 17 2017

Work Order	Sample Wet wt (g)	Hydrocarbon wt (g)	% Hydrocarbon	Water wt (g)	% Water	Solids Dry wt (g)	% Solids	Discrep Wt (g)	% Discrep	% Cumm	Comments
A18340	154.73	8.81	5.694	67.74	43.779	77.71	50.223	0.470	0.304	99.696	



**AGAT** Laboratories

**DEAN STARK REPORT  
FOR  
UNIVERSITY OF ALBERTA**

**(1 sample) (CAKE)**

**A18340**

**By Direct Determination**

**Jan 17 2017**

**AGAT Laboratories**

**3801 - 21 Street N.E.**

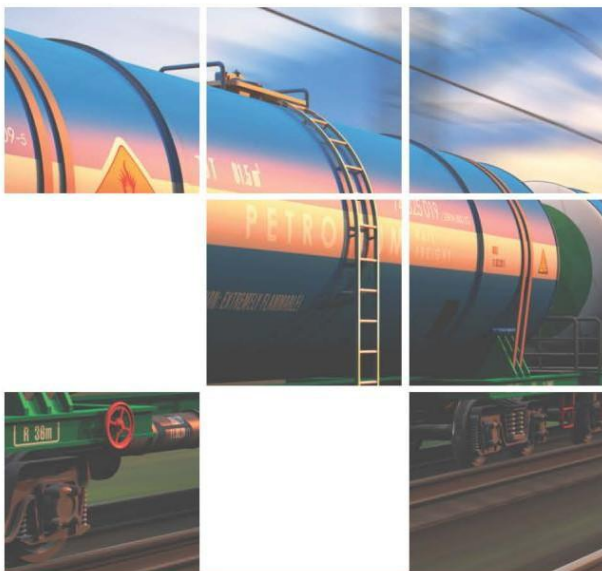
**Calgary, Alberta**

**T2E 6T5**

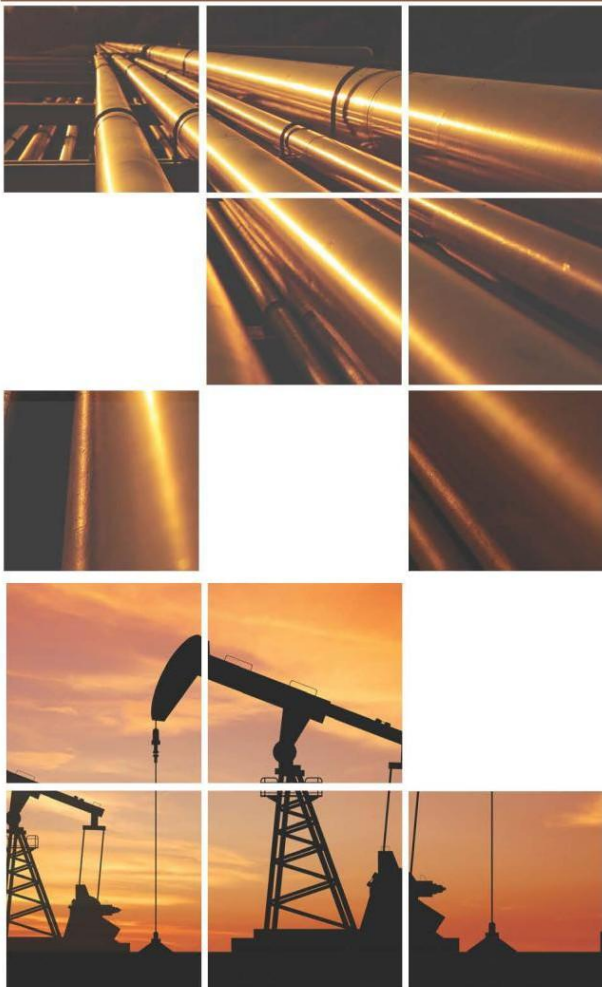
AGAT Laboratories is accredited to ISO/IEC 17025 by the Canadian Association for Laboratory Accreditation Inc. (CALA) and/or Standards Council of Canada (SCC) for specific tests listed on the scope of accreditation. Accreditations are location and parameter specific. A complete listing of parameters for each location is available from [www.cala.ca](http://www.cala.ca) and/or [www.scc.ca](http://www.scc.ca). The tests in this report may not necessarily be included in the scope of accreditation.

Member of: The Association of Professional Engineers and Geoscientists of Alberta (APEGA),  
Canadian Council of Independent Laboratories (CCIL)

*Results relate only to the items tested and to all the items tested*



*COMBINED BULK AND CLAY XRD ANALYSES OF ONE DEAN-STARK CLEANED  
SOLID SAMPLE COLLECTED ON JANUARY 11, 2017 IDENTIFIED  
AS "MFT CENTRIFUGE CAKE".*



**Company: University of Alberta**

**Work Order No: A18340**

**Date: January, 2017**

**AGAT Laboratories**  
3801 – 21<sup>st</sup> Street N.E.  
Calgary, Alberta T2E 6T5

**AGAT** Laboratories

Service Beyond Analysis





### COMBINED X-RAY DIFFRACTION ANALYSIS

One Dean-Stark cleaned sample collected on ‘**January 11, 2017**’ identified as “**MFT CENTRIFUGE CAKE**” for University Alberta was analyzed by AGAT Laboratories Ltd. for bulk and clay XRD mineralogy. The sample was examined using XRD techniques to determine mineralogical composition.

In order to separate the particles less than  $3\mu\text{m}$  in size (clay fraction) from the bulk fraction, the sample was treated in an ultrasonic bath using sodium metaphosphate as a deflocculating agent. The material was then centrifuged at different speeds, which separate the clay fraction from the bulk material. The weight fraction was measured for both bulk and clay portions of the sample.

The combined bulk and clay XRD results (Table 1) for sample 1 (MFT Centrifuge Cake) consist mainly of quartz (40%) [silicon dioxide,  $\text{SiO}_2$ ] and kaolinite (36%), [aluminum silicate hydroxide,  $\text{Al}_4\text{Si}_4\text{O}_{10}(\text{OH})_8$ ], with lesser to minor amounts of illite (15%) [potassium aluminum silicate hydroxide,  $\text{KAl}_2(\text{OH})_2[\text{AlSi}_3(\text{O},\text{OH})_{10}]$ ] and potassium feldspar (2%), [potassium aluminum silicate,  $\text{K}(\text{SiAl}_3\text{O}_8)$ ]. In addition, minor siderite (3%) [(iron carbonate,  $\text{FeCO}_3$ )], pyrite (2%) [iron sulfide,  $\text{FeS}_2$ ] and dolomite (1%), [calcium magnesium carbonate,  $\text{CaMg}(\text{CO}_3)_2$ ] were also detected.

The clay fraction ( $<3\mu\text{m}$ ) weight is 8.71% of the total rock volume. The clay fraction XRD (Table 1) results indicate that the samples consist mainly of kaolinite (80%), with lesser amounts of illite (18%). Minor amounts of quartz (1%) were also present. In addition, minor siderite (1%) was also detected.

The analysis indicate that the sample consist mainly of sands/silts/clays (quartz, kaolinite, illite and potassium feldspar - formation materials?). Minor amounts of iron compounds (siderite and pyrite - diagenetic cements?) and calcium magnesium carbonate (dolomite - diagenetic

---

cements?) are also detected. Note a portion of the illite detected in bulk XRD would also represent any mica minerals (muscovite [potassium aluminum silicate hydroxide,  $K_2Al_4[Si_6Al_2O_{20}](OH,F)_4$ ] and biotite [potassium magnesium iron titanium silicate hydroxide,  $K_2(Mg, Fe^{+2})_{6-4}(Fe^{+3}, Al, Ti)_{0-2}[Si_{6-5}Al_{2-3}O_{20}][(OH,F)_4]$ ). Biotite mica may partially explain the presence of titanium detected by EDX analysis. The presence of trace calcium in EDX suggests trace calcite precipitated from water as well. The calcite was too small quantity to be detected by XRD.

**Table 1 - Summary of XRD Analysis**

Company: University of Alberta  
 Location: MFT Centrifuge Cake

Work Order No. A18340  
 January, 2017

SAMPLE ID.	TYPE OF ANALYSIS	WEIGHT %	← CLAYS →															Total Clay
			Qtz	Plag	K-Feld	Cal	Dol	Anhy	Pyr	Musc	Bar	Sider	Kaol	Chl	Ill	ML	Smec	
1	BULK FRACTION:	91.29	43	0	2	0	2	0	3	0	0	3	32	0	15	0	0	47
	CLAY FRACTION:	8.71	1	0	0	0	0	0	0	0	0	1	80	0	18	0	0	98
	BULK & CLAY	100	40	0	2	0	1	0	2	0	0	3	36	0	15	0	0	52

## XRD LEGEND

- XRD Analysis is semi-quantitative (approx. 10% at best) and identifies only crystalline substances; amorphous (non-crystalline) substances will not be detected.
- Bulk Fraction – greater than 3 micron size fraction.
- Clay Fraction – less than 3 micron size fraction.
- Bulk and Clay – mathematical recalculation including the bulk and clay fraction representing the whole sample.
- Total Clay – sum of the clay minerals (may include authigenic and matrix clays plus clays in rock fragments).

### ABBREVIATIONS

Amp - Amphiboles	Dol - Dolomite	Marc - Marcasite	Pr - Pure (95 – 100%)
Ana - Analcime	Gyp - Gypsum	ML* - Illite-Smectite	NPr - Near Pure (90 – 95%)
Anhy- Anhydrite	Hal - Halite	ML** - Corrensite (chlorite-smectite)	Abnt - Abundant (60 – 90%)
Ank - Ankerite	Hem - Hematite	Plag - Plagioclase Feldspar	Com - Common (30 – 60%)
Apa - Apatite	Ill - Illite	Pyr - Pyrite	Mnr - Minor (10 – 30%)
Bar - Barite	Kaol - Kaolinite	Qtz - Quartz	Rre - Rare (1 – 10%)
Cal - Calcite	K-feld- Potassic Feldspar	Sider - Siderite	Tr - Trace; detectable, but not measurable (0 – 1%)
Chl - Chlorite	Mack - Mackinawite	Smec - Smectite (montmorillonite)	Unk - Unknown
Phos – Phosphate	Musc - Muscovite	Wues - Wuestite	

## APPENDIX

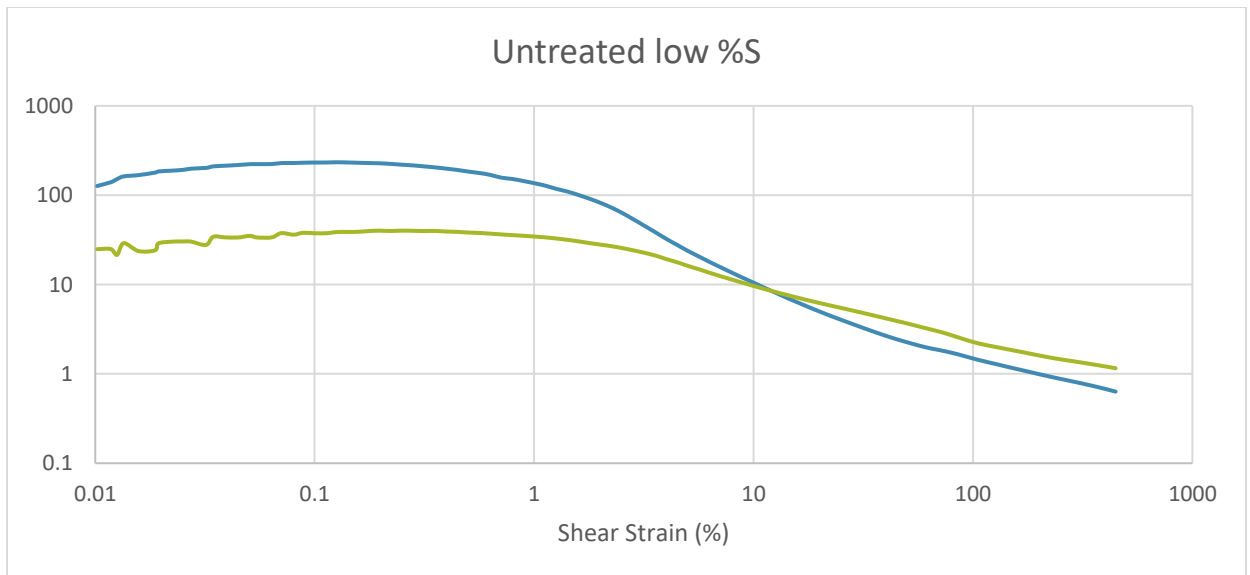
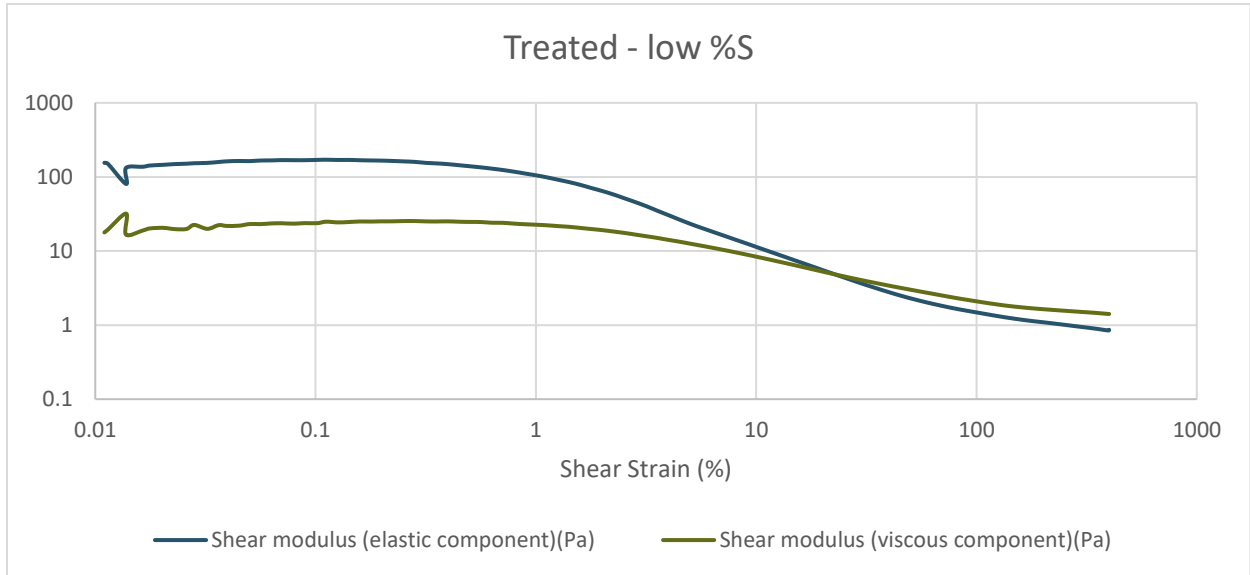
### **BULK & CLAY PROCEDURES**

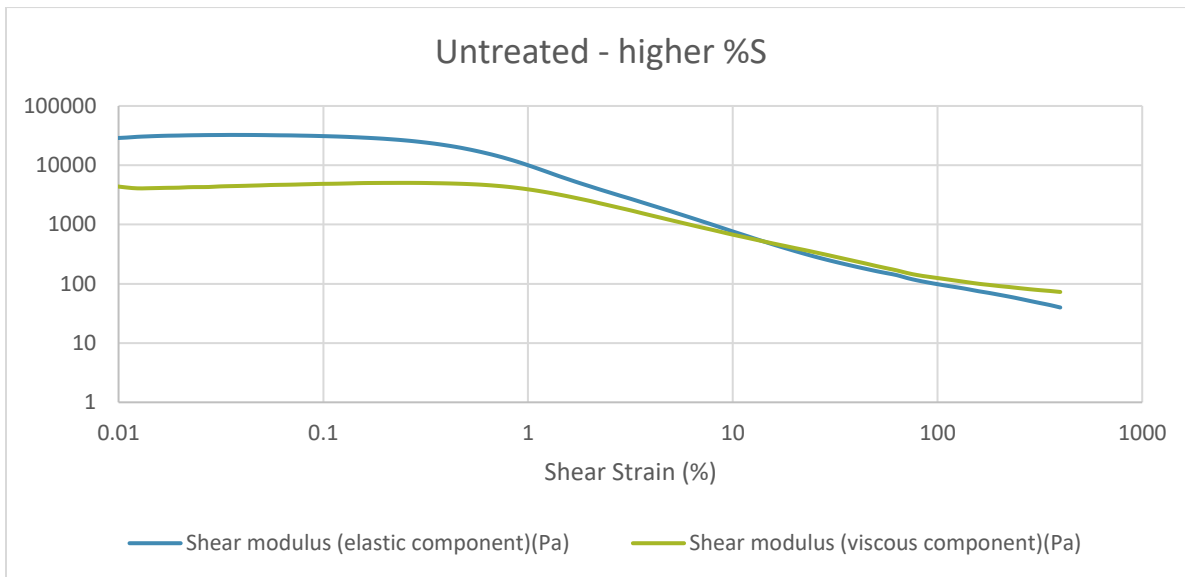
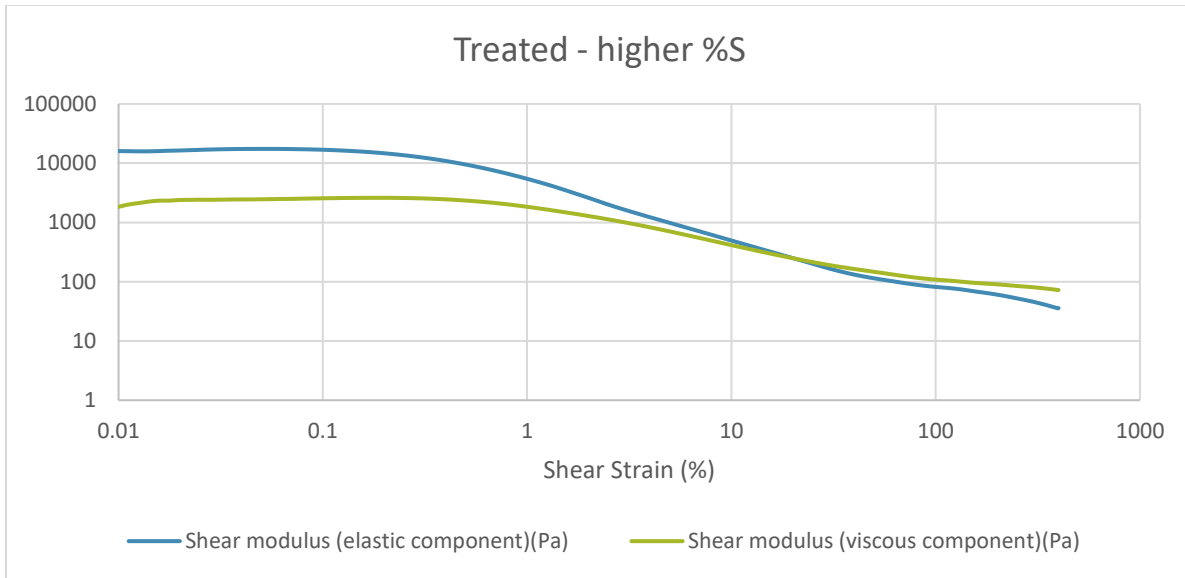
1. Crush dry rock sample until grains disintegrate completely.
2. Weigh empty beaker and put sample in it. Weigh again “total weight”. ( $\approx 3$ g of sample).
3. Add 50 mL of distilled water, plus a few drops of Sodium Metaphosphate.
4. Put in ultrasonic bath for 2 (two) hours.
5. Stir sample and pour out top portion into test tube.
6. Centrifuge for 5 minutes at 600 rpm.
7. Pour out top portion into another test tube for the clay fraction ( $< 3\mu\text{m}$ ) sample.
8. Recombine the coarser residue in the first test tube with the residue in the beaker and weight this “bulk sample” (after drying completely). Subtract this weight from the “total weight” to get the clay fraction weight.
9. Centrifuge the “clay fines” in the second test tube for 20 minutes at maximum rpms.
10. Pour out most of the water then shake test tube using Vortex Mixer.
11. Pipette onto a glass slide.
12. Put the slide on the hot plate (low) until dry then run sample in XRD.
13. Then put slide in a glycol vapour bath overnight (glycolated clay); Smectite will swell and be recognized.
14. If chlorite suspected, then treat the remaining sample in the test tube with diluted HCl and leave overnight (acidized clay). If chlorite was present in the sample this test causes it to disappear.
15. Run the “clay fraction” slide from 2-38 degrees.
16. Grind the “bulk sample” and spread the powder on an aluminum holder then run from 4-58 degrees.
17. Data acquisition and interpretation is done by PANalytical High Score software suite

## Appendix C: Rheology Data

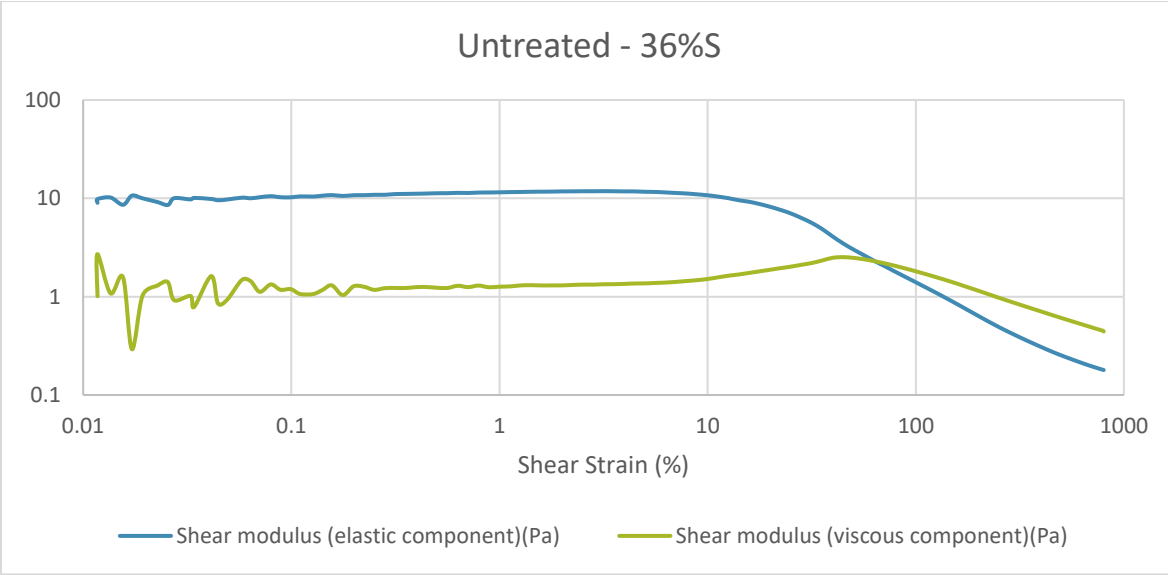
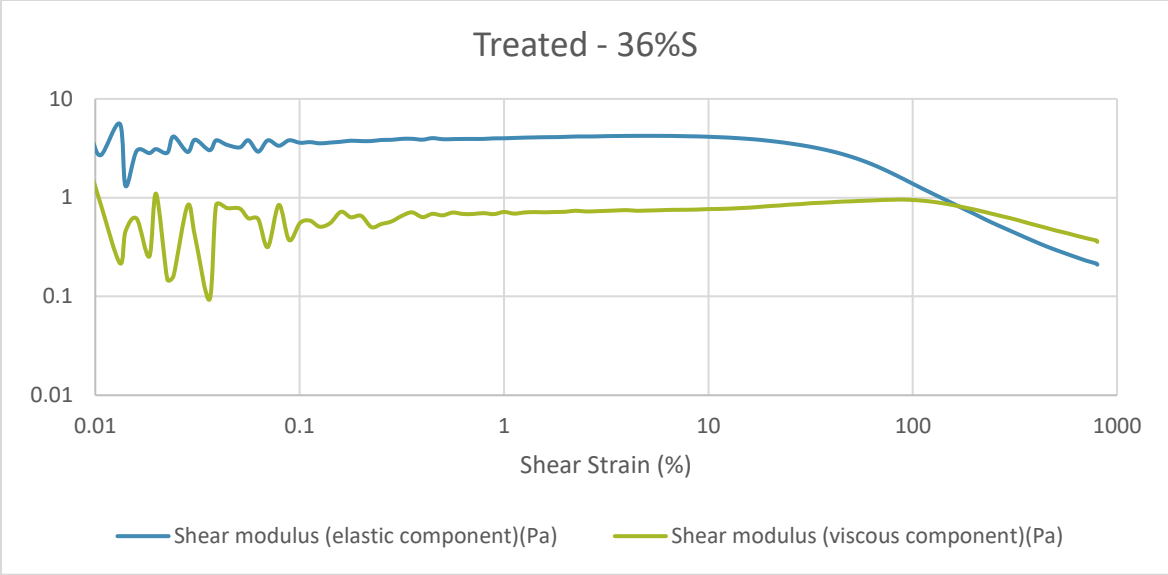
### C-1: Limit of the linear viscoelastic region (LVE) and viscoelastic character

Kaolinite – Heat Treatment

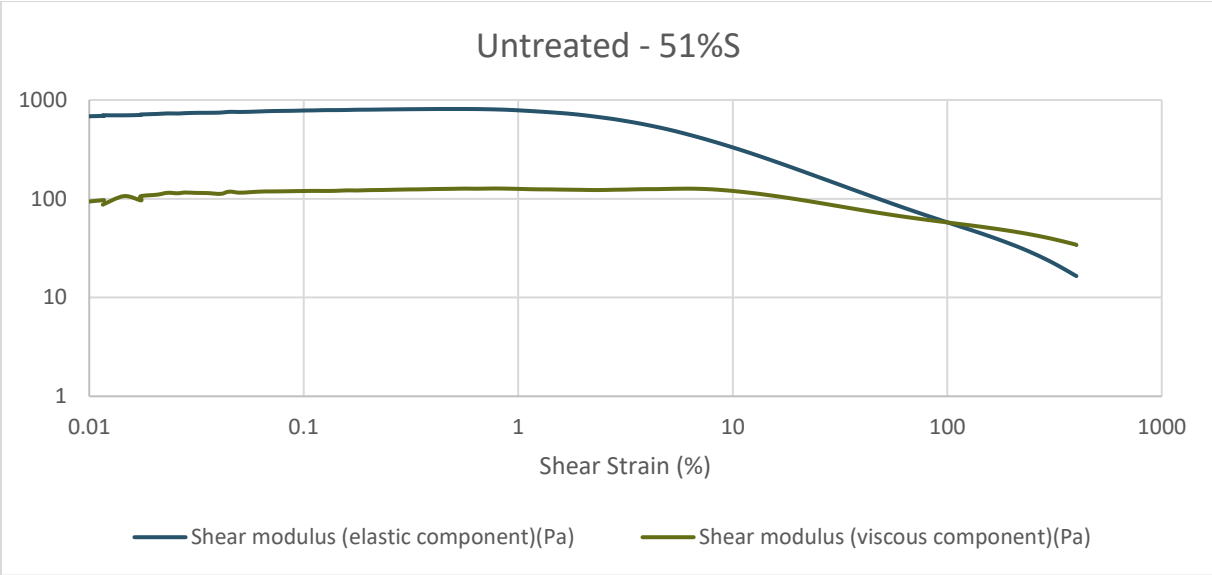
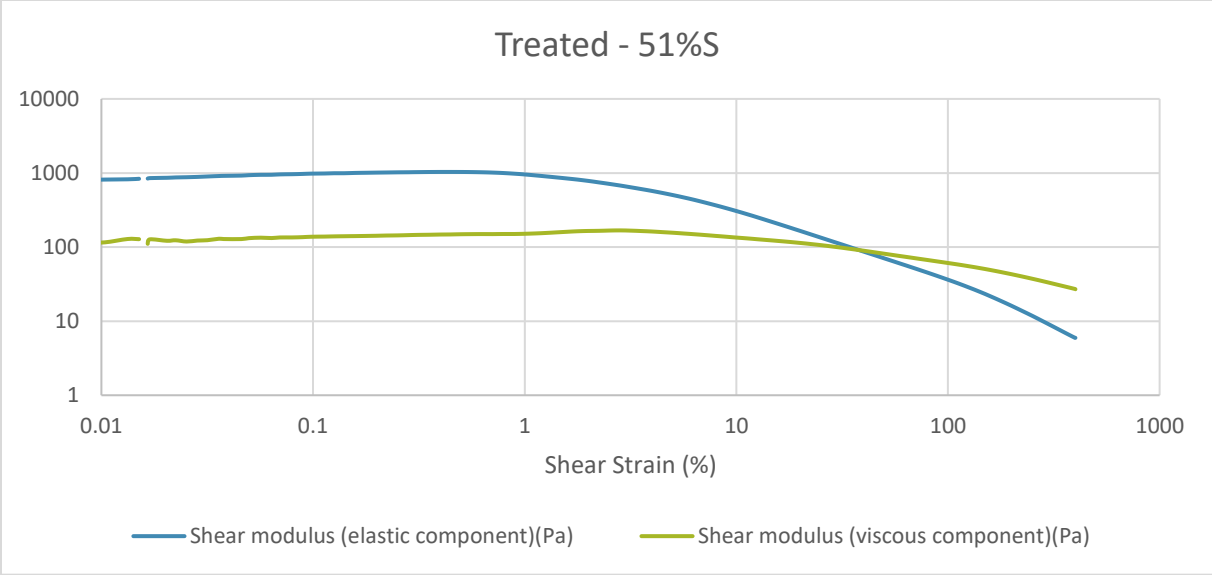




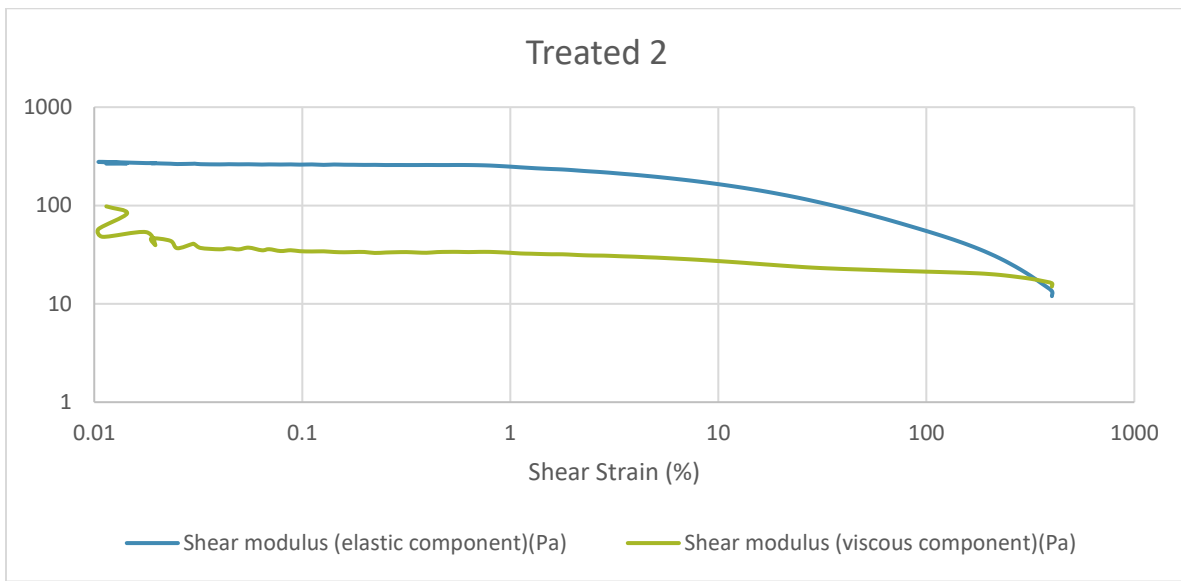
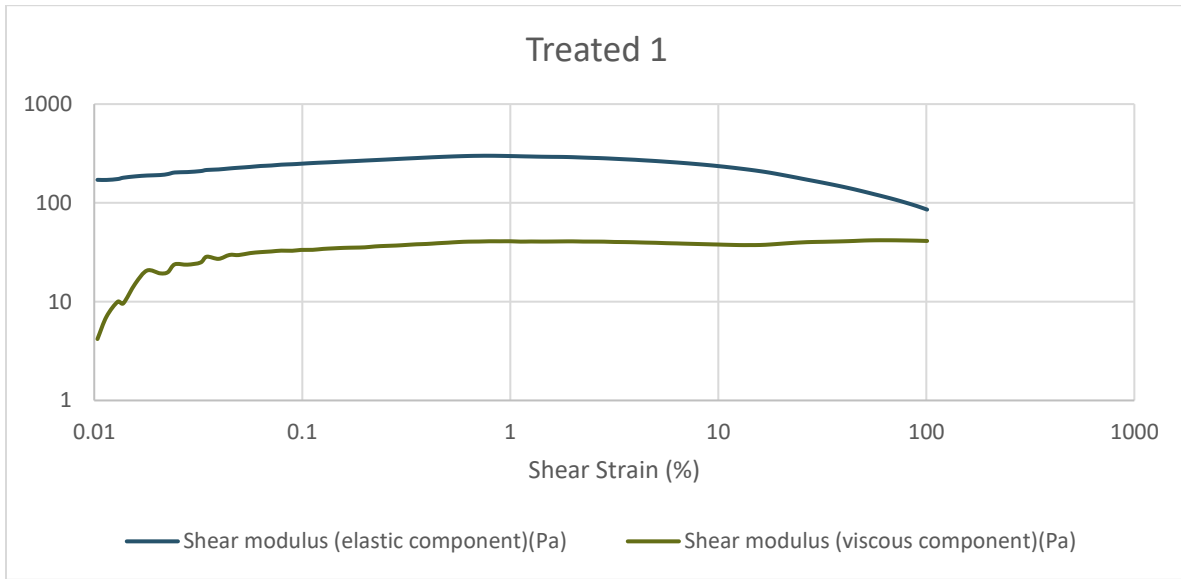
Fluid Fine Tailings

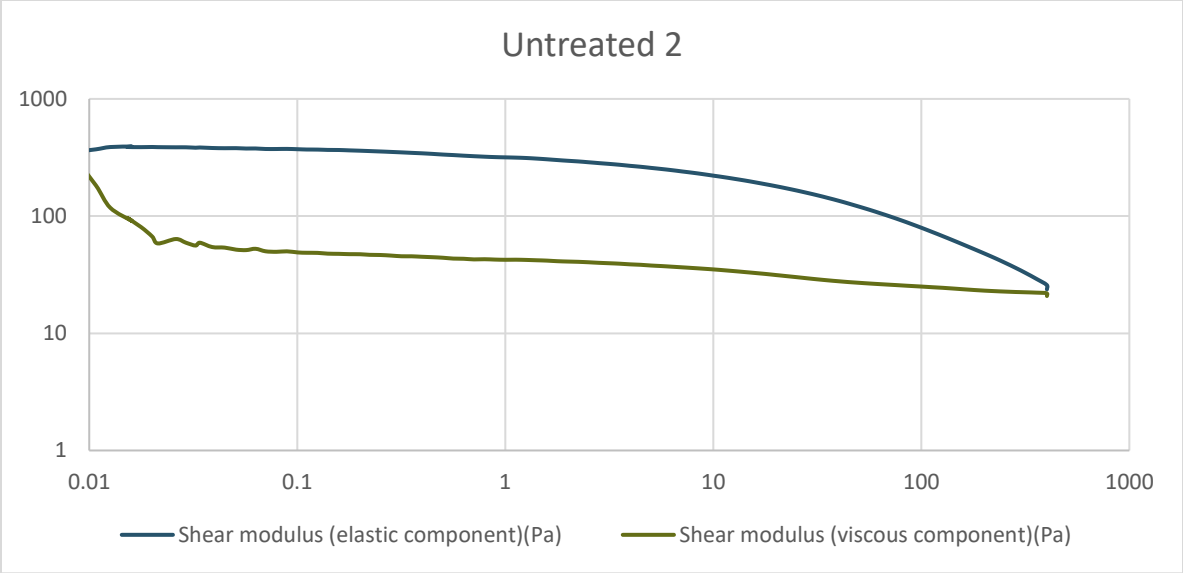




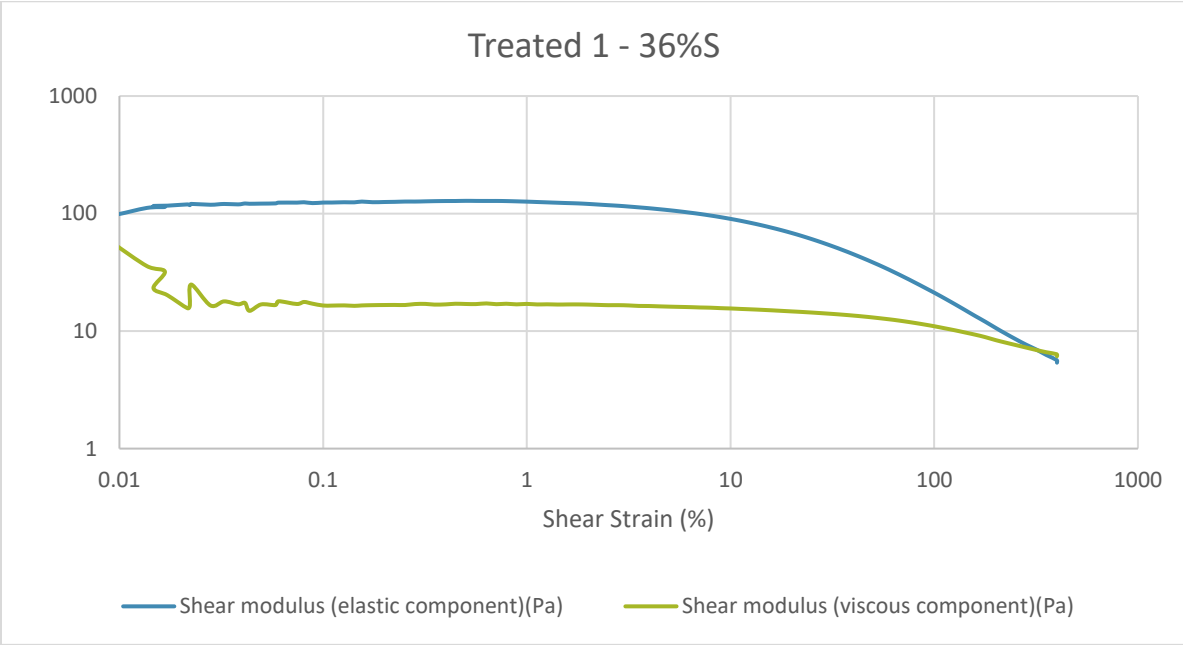


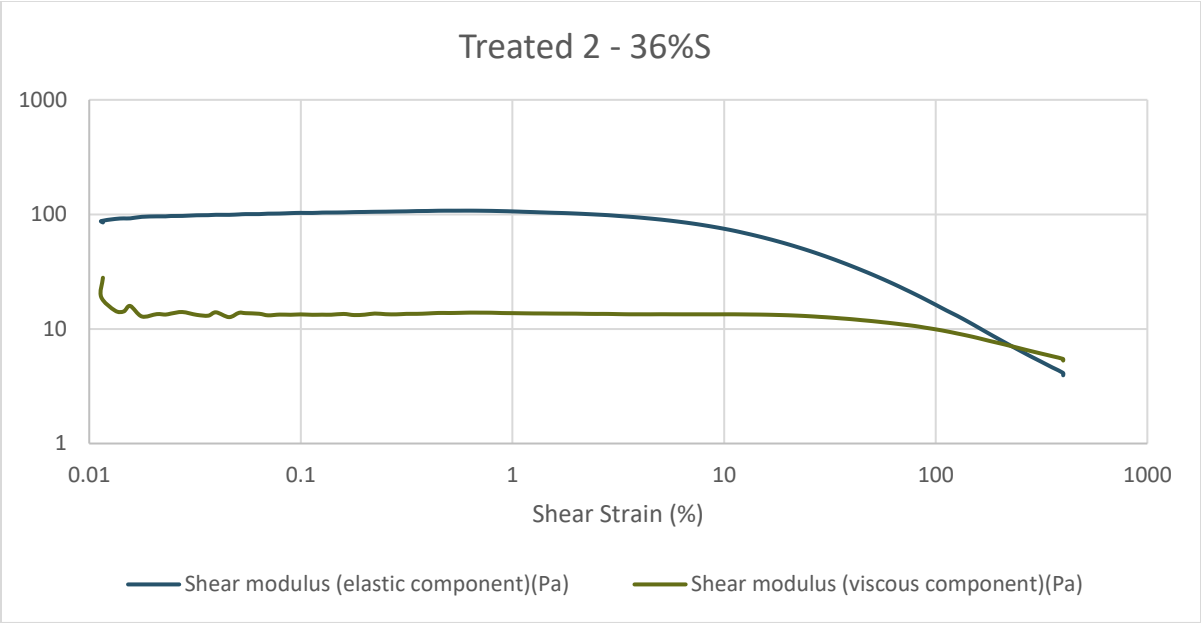
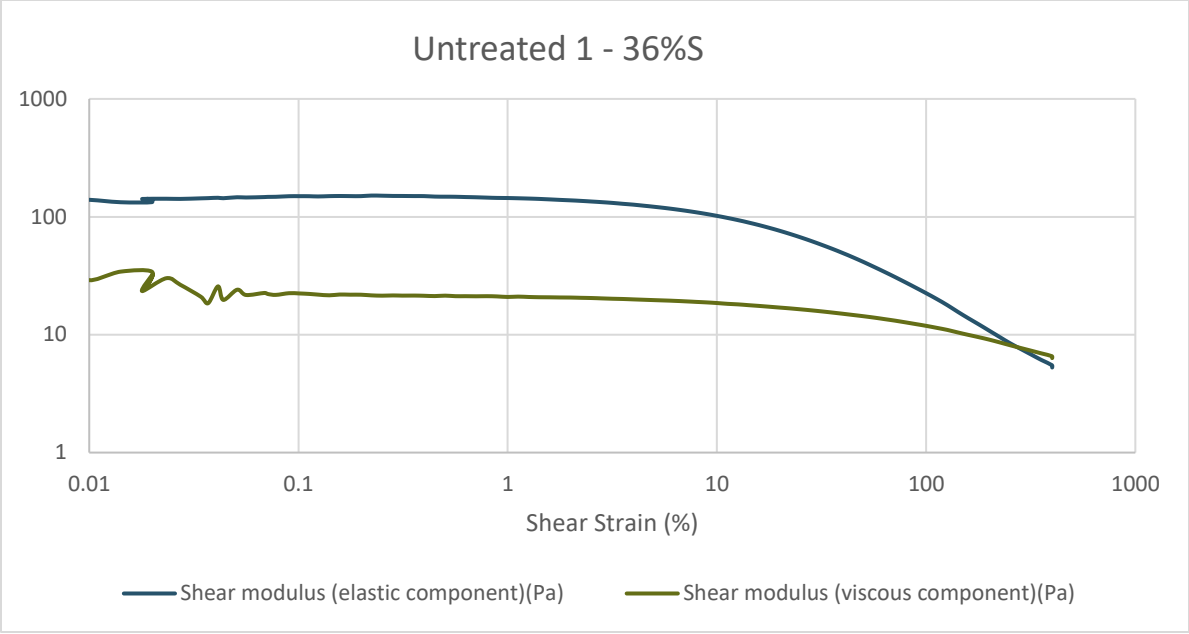
## Centrifuged Tailings

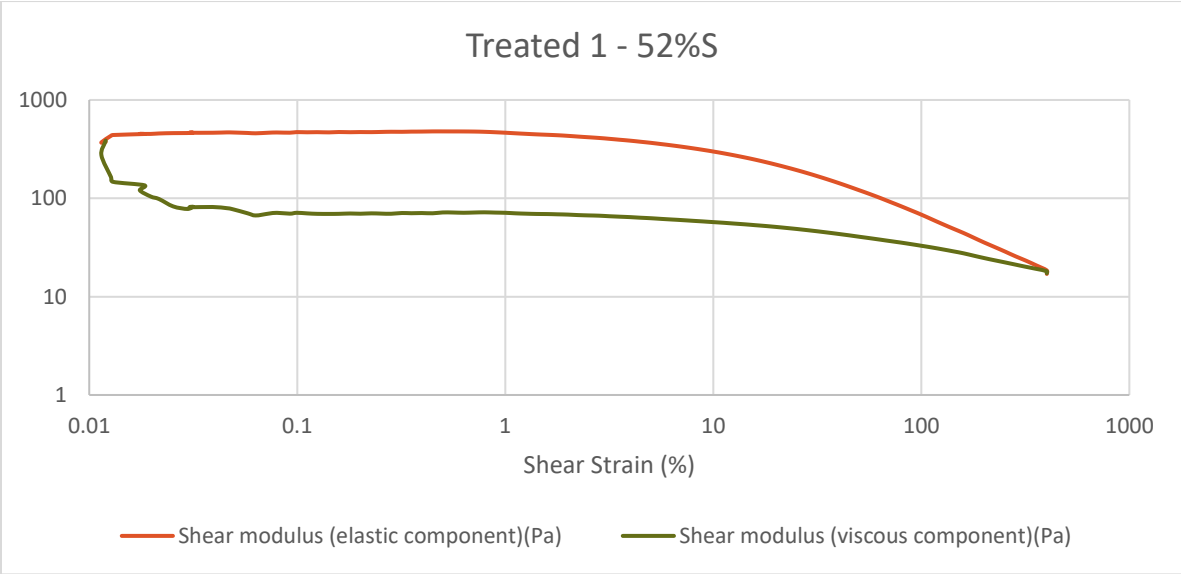
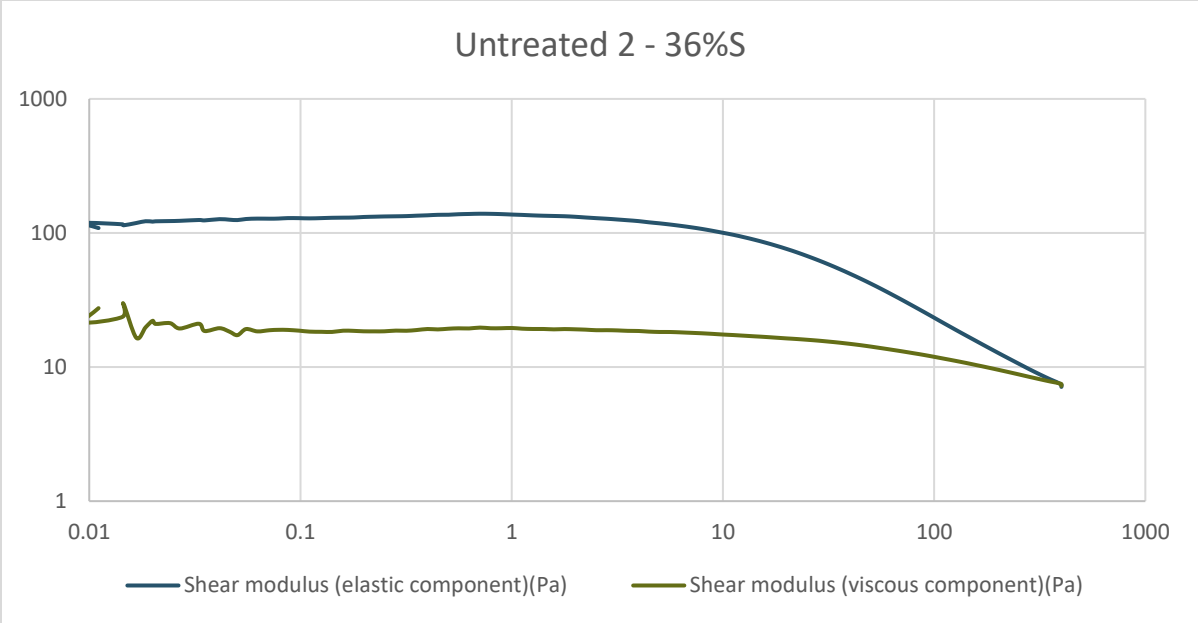


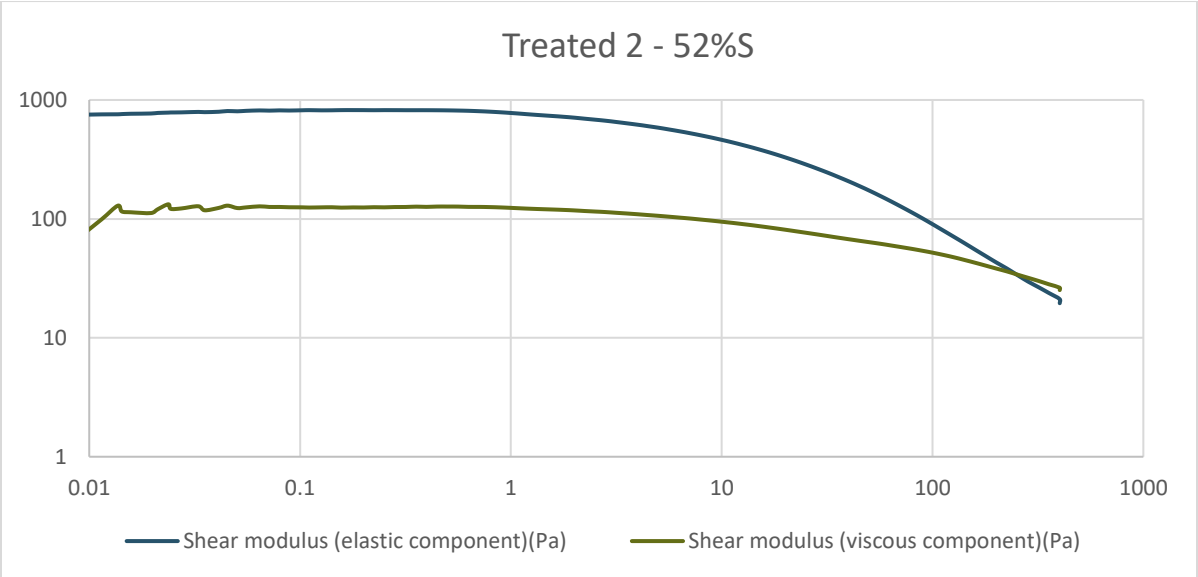
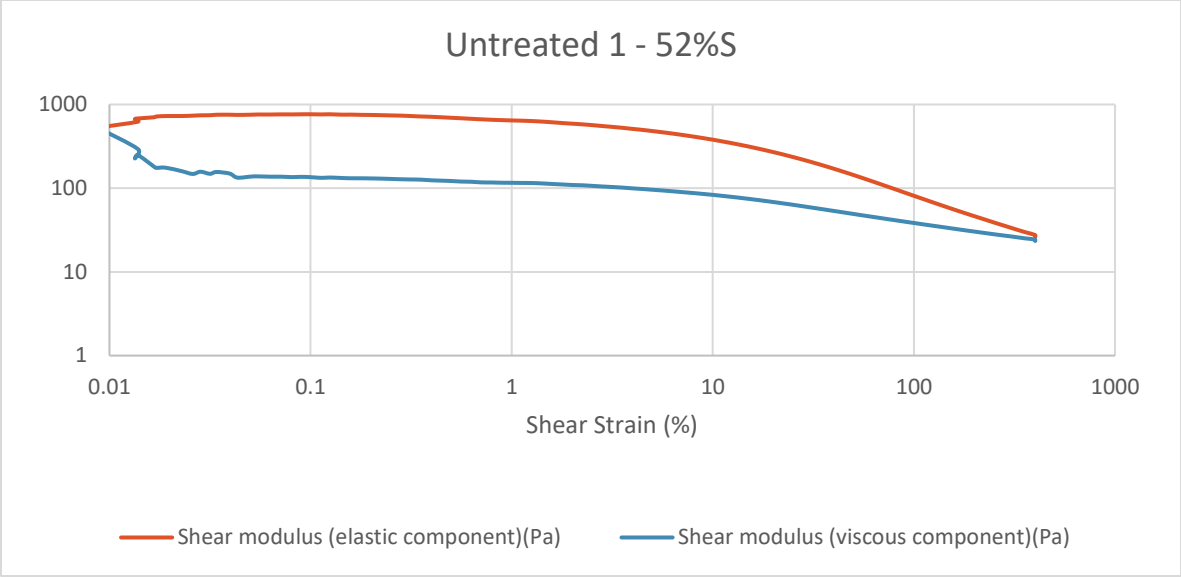


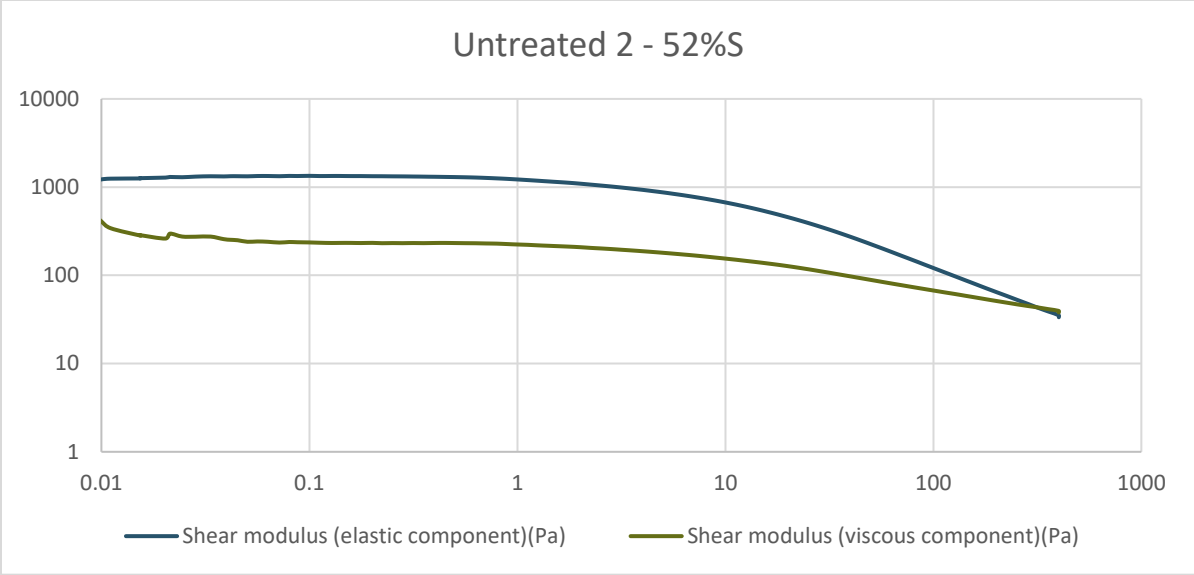
Flocculated FFT











## Appendix D: Large Strain Consolidation Data

### D-1: Raw Data

Table D-1: Large Strain consolidation of Cell 3

Load	Effective stress (kPa)	Height (mm)	$\Delta H$ (mm)	Void ratio, e
		6.70		2.07
<b>1</b>	0.13	5.93	0.77	1.72
<b>2</b>	0.28	5.70	0.23	1.61
<b>3</b>	1.48	5.44	0.26	1.49
<b>4</b>	4.00	5.19	0.26	1.38
<b>5</b>	6.60	4.94	0.24	1.27
<b>6</b>	12.00	4.72	0.22	1.16
<b>7</b>	24.00	4.46	0.26	1.04

Table D-2: Large Strain consolidation of Cell 4

Load	Effective stress (kPa)	Height (mm)	$\Delta H$ (mm)	Void ratio, e
		6.23		2.07
<b>1</b>	0.17	5.74	0.49	2.07
<b>2</b>	0.34	5.52	0.21	1.96
<b>3</b>	1.48	5.38	0.14	1.88
<b>4</b>	4.00	5.18	0.21	1.77
<b>5</b>	6.60	4.73	0.45	1.53

Table D-3: Large Strain consolidation of Cell 5

Load	Effective stress (kPa)	Height (mm)	$\Delta H$ (mm)	Void ratio, e
		6.83		2.07
<b>1</b>	0.13	6.14	0.69	2.07



<b>2</b>	0.32	5.90	0.24	1.95
<b>3</b>	1.47	5.64	0.26	1.82
<b>4</b>	4.00	5.39	0.25	1.70
<b>5</b>	6.60	5.11	0.28	1.56

## D-2: LVDT and Pore Pressure Data

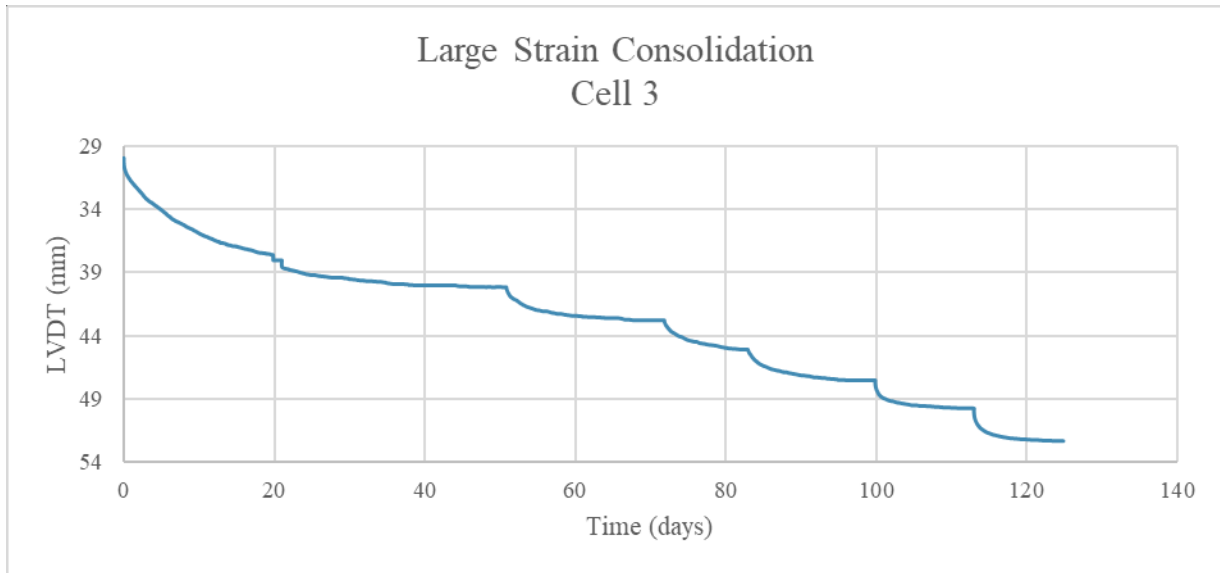


Figure D-3: Sample height versus time (Cell 3)

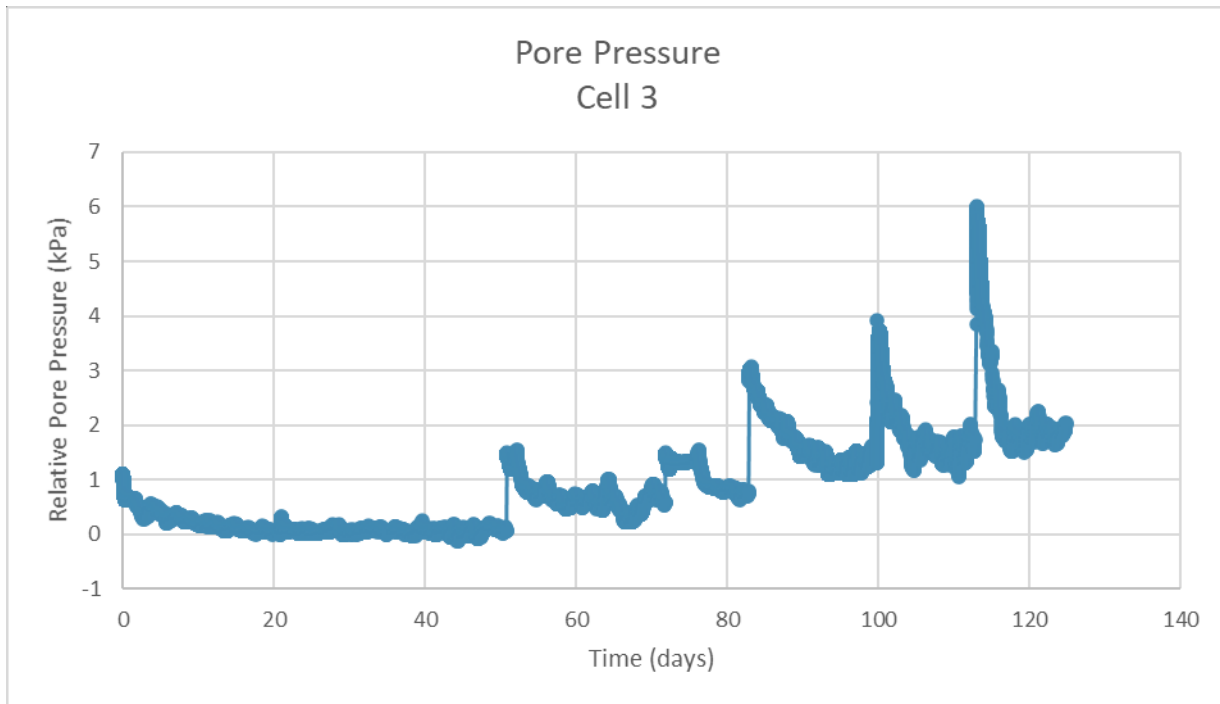


Figure D-4: Relative Pore Pressure (Cell 3)

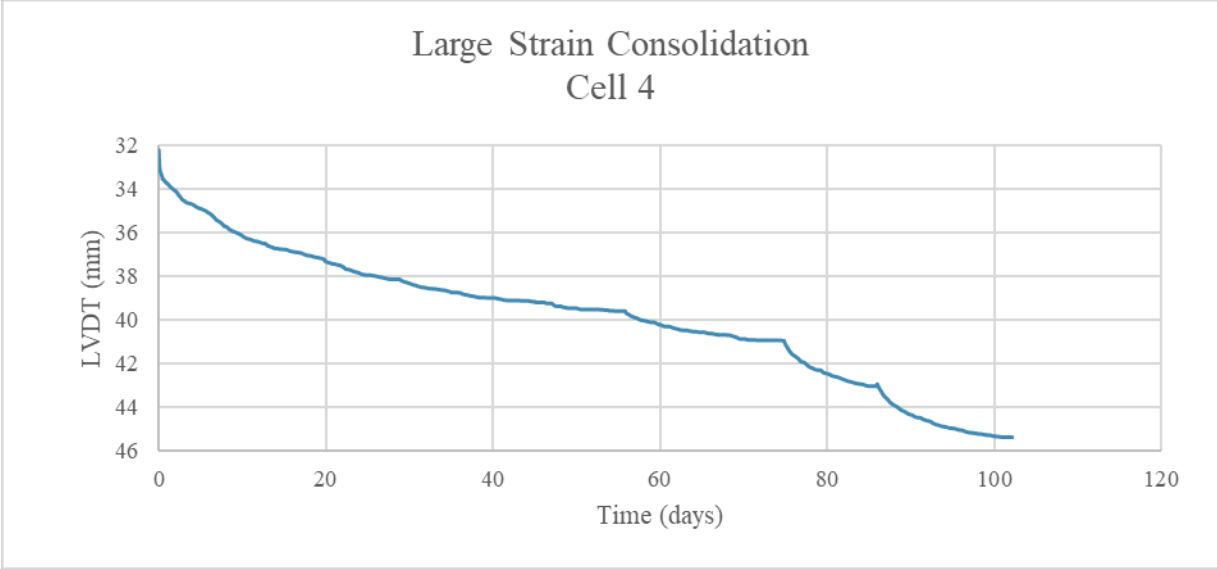


Figure D-5: Sample height versus time (Cell 4)

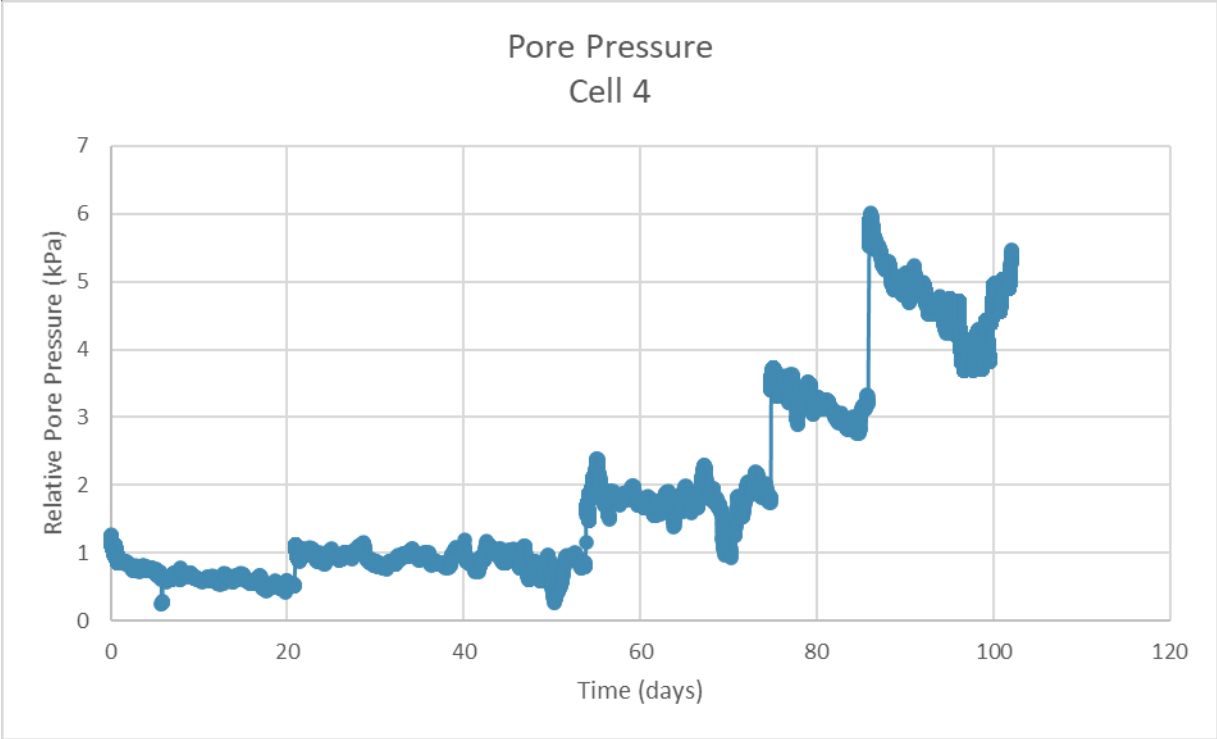


Figure D-6: Relative Pore Pressure (Cell 4)

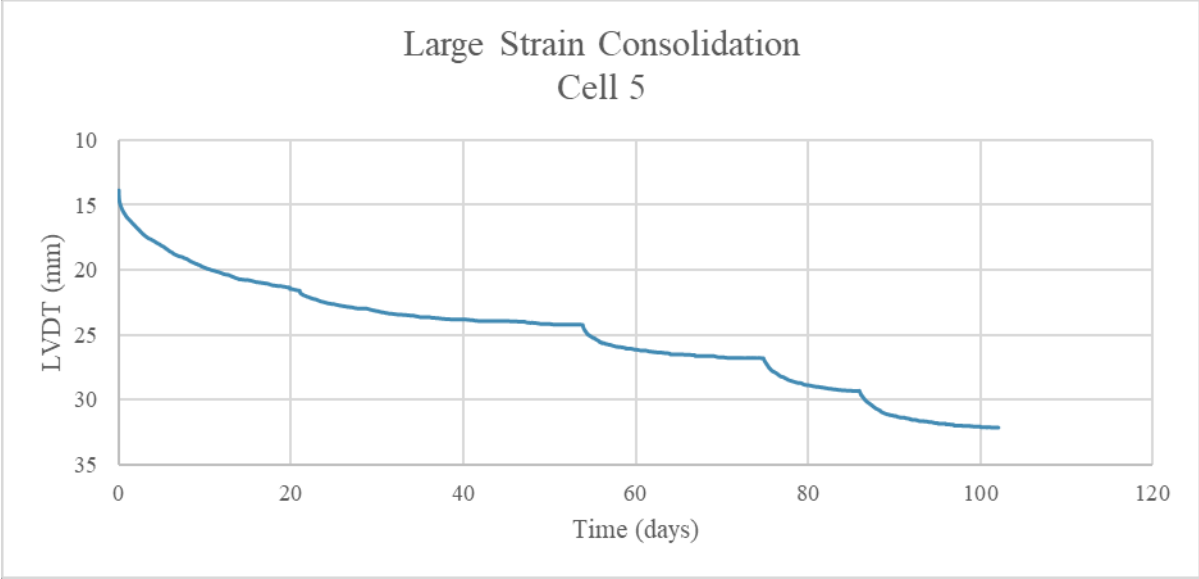


Figure D-7: Sample height versus time (Cell 5)

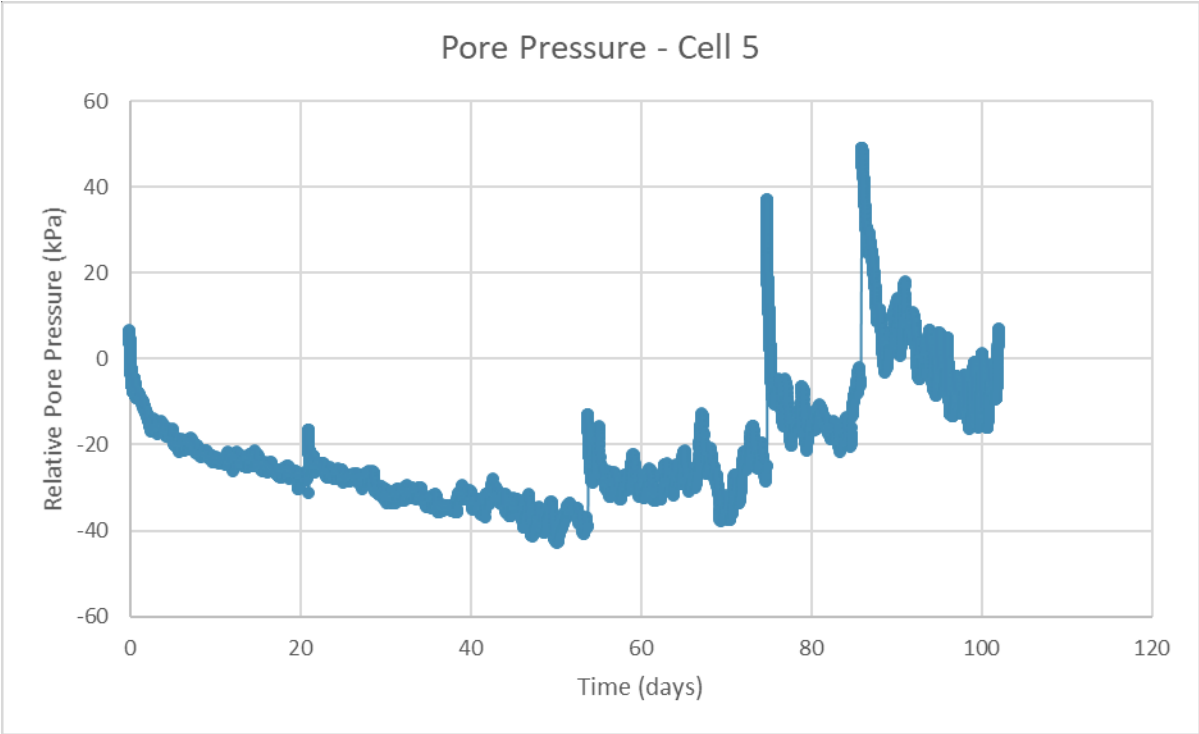


Figure D- 8: Relative Pore Pressure (Cell 5)